

Washington University in St. Louis

## Washington University Open Scholarship

---

Arts & Sciences Electronic Theses and  
Dissertations

Arts & Sciences

---

Spring 5-15-2019

### Discoidin Domain Receptor 2 as a Therapeutic Target in Breast and Ovarian Cancer

Whitney Grither

*Washington University in St. Louis*

Follow this and additional works at: [https://openscholarship.wustl.edu/art\\_sci\\_etds](https://openscholarship.wustl.edu/art_sci_etds)



Part of the [Oncology Commons](#)

---

#### Recommended Citation

Grither, Whitney, "Discoidin Domain Receptor 2 as a Therapeutic Target in Breast and Ovarian Cancer" (2019). *Arts & Sciences Electronic Theses and Dissertations*. 1783.

[https://openscholarship.wustl.edu/art\\_sci\\_etds/1783](https://openscholarship.wustl.edu/art_sci_etds/1783)

This Dissertation is brought to you for free and open access by the Arts & Sciences at Washington University Open Scholarship. It has been accepted for inclusion in Arts & Sciences Electronic Theses and Dissertations by an authorized administrator of Washington University Open Scholarship. For more information, please contact [digital@wumail.wustl.edu](mailto:digital@wumail.wustl.edu).

WASHINGTON UNIVERSITY IN ST. LOUIS  
Division of Biology and Biomedical Sciences  
Biochemistry

Dissertation Examination Committee:  
Gregory Longmore, Chair  
Kendall Blumer  
Andreas Herrlich  
Robert Mecham  
Kevin Moeller  
Audrey Odom

Discoidin Domain Receptor 2 as a Therapeutic Target in Breast and Ovarian Cancer  
by  
Whitney Rose Grither

A dissertation presented to  
The Graduate School  
of Washington University in  
partial fulfillment of the  
requirements for the degree  
of Doctor of Philosophy

May 2019  
St. Louis, Missouri

© 2019, Whitney Grither

## **Table of Contents**

List of Figures .....	iv
List of Tables .....	vii
Acknowledgments .....	viii
Abstract .....	xi
<b>Chapter 1: Introduction</b> .....	<b>1</b>
Figures .....	24
References .....	31
<b>Chapter 2: Inhibition of Tumor-Microenvironment Interactions and Metastasis by a Small-Molecule Allosteric Inhibitor of DDR2 Extracellular Domain</b> .....	<b>44</b>
Introduction .....	46
Results .....	49
Discussion .....	62
Materials and Methods .....	66
Figures .....	78
References .....	106
<b>Chapter 3: TWIST1 Induces Expression of Discoidin Domain Receptor 2 to Promote Ovarian Cancer Metastasis</b> .....	<b>113</b>
Introduction .....	115
Results .....	118
Discussion .....	126
Materials and Methods .....	130
Figures .....	138
References .....	155
<b>Chapter 4: Kinase Independent Functions of Discoidin Domain Receptor 2</b> .....	<b>161</b>
Introduction .....	162

Results .....	165
Discussion .....	170
Materials and Methods .....	173
Figures .....	178
References .....	190
<b>Chapter 5: Conclusions and Future Directions</b> .....	<b>192</b>
Figures .....	211
References .....	213

## List of Figures

### **Chapter 1**

Figure 1.1: Breast cancer progression and the metastatic cascade .....	24
Figure 1.2: The breast tumor microenvironment .....	25
Figure 1.3: Ovarian cancer metastasis.....	26
Figure 1.4: epithelial-mesenchymal transition—cell plasticity between states .....	27
Figure 1.5: Domain structure of the discoidin domain receptors .....	28
Figure 1.6: DDR2 is expressed in human invasive ductal carcinomas, but not in normal mammary epithelia .....	29
Figure 1.7: Therapeutic targeting of DDR2 .....	30

### **Chapter 2**

Figure 2.1: <i>In vitro</i> screening for active DDR2 inhibitors .....	78
Figure 2.2: Chemical structures of synthesized derivatives .....	79
Figure 2.3: Identification of WRG-28 as a potent and reversible inhibitor of DDR2 binding .....	80
Figure 2.4: WRG-28 inhibits DDR2 activation but has no effect on DDR1 activation ....	82
Figure 2.5: WRG-28 is selective towards DDR2 .....	84
Figure 2.6: WRG-28 does not affect other kinase pathways in non-DDR2 expressing MCF10A cells .....	86
Figure 2.7: DDR2 acts in a non-orthosteric manner to accelerate the dissociation of receptor-ligand complex .....	87
Figure 2.8: WRG-28 impairs clustering of the DDR2 extracellular domain .....	89
Figure 2.9: Computational prediction of WRG-28 binding site .....	91
Figure 2.10: Identification of DS-DSL domain interface residues required for DDR2-collagen binding and signaling .....	93
Figure 2.11: Evaluation of an alternatively predicted binding site .....	95

Figure 2.12: WRG-28 inhibition of DDR2 blunts tumor cell invasion and migration, but does not influence proliferation .....	96
Figure 2.13: WRG-28 blocks DDR2 mediated signaling in breast tumor cells and is effective against TKI resistant mutations.....	98
Figure 2.14: WRG-28 blocks the tumor promoting effects of DDR2 expressing CAFs ..	99
Figure 2.15: Genetic validation of DDR2 as a therapeutic target to prevent breast cancer metastasis .....	101
Figure 2.16: WRG-28 attenuates DDR2 signaling <i>in vivo</i> .....	103
Figure 2.17: WRG-28 administration reduces metastatic lung colonization of breast tumor cells .....	104
<b>Chapter 3</b>	
Figure 3.1: TWIST1 regulates DDR2 expression in Ovarian Cancer Cells .....	138
Figure 3.2: DDR2 promotes mesothelial cell clearance .....	140
Figure 3.3: DDR2 contributes to invasion and migration of ovarian cancer cells but does not influence proliferation. ....	142
Figure 3.4: DDR2 stabilizes SNAIL1 and regulates expression and activity of matrix remodeling enzymes .....	144
Figure 3.5: DDR2 contributes to fibronectin cleavage by ovarian cancer cells and promotes ovarian cancer cell spreading on fibronectin .....	146
Figure 3.6: DDR2 is critical for ovarian cancer metastasis <i>in vivo</i> .....	148
Figure 3.7: DDR2 is expressed in human ovarian carcinomas and is an indicator of poor prognosis.....	150
Figure 3.8: DDR2 expression level is correlated with increased invasion in patient derived primary ovarian cancer cells .....	152
Figure 3.9: Proposed role for DDR2 in ovarian cancer metastasis .....	154
<b>Chapter 4</b>	
Figure 4.1: Rescue of DDR2 expression with a kinase-dead DDR2 receptor.....	178
Figure 4.2: DDR2 functions independent of its kinase activity to promote Matrigel invasion .....	179

Figure 4.3: DDR2 kinase activity predominates in 3D collagen invasion ..... 180

Figure 4.4: DDR2 influences BT549 cell spreading on collagen I and fibronectin independent of kinase activity ..... 181

Figure 4.5: DDR2 influences ES2 cell spreading on fibronectin independent of kinase activity and this is blocked by WRG-28 ..... 182

## **Chapter 5**

Figure 5.1: Role of stromal DDR2 in secondary site growth and colonization ..... 211

Figure 5.2: PTK7 co-immunoprecipitation validation ..... 212

## List of Tables

### **Chapter 4**

Table 1: Putative DDR2 interacting proteins in the absence of collagen ligand..... 183

Table 2: Putative DDR2 interacting proteins in the presence of collagen ligand..... 186

## **Acknowledgments**

I'd first and foremost like to thank my mentor, Greg Longmore, for all of his support during the past five years. Greg has provided me with an environment to grow as a scientist, and guidance with experimental design, writing, and career in general. He has helped me learn to see the broader implications of a given scientific question, afforded me with an appreciation for the importance of rigorous scientific interrogation, and imparted an appreciation for a healthy level of skepticism in results. He has allowed me to work independently, while still being available for the inevitable need for advice when it arises. Perhaps most importantly, through his mentorship he has instilled in me the confidence to move forward in this career path, and for that I am very thankful. I also owe a big thanks to all of the Longmore lab members, both current and past, for providing an environment that I looked forward to coming to every day. Without their willingness to help me with new techniques, provide feedback and suggestions on my project, and just be general sounding boards for ideas, I would not have had the positive lab experience that I did. Past members Hanako Yashiro, Callie Corsa, Hira Biswas, Kun Zhang, Greg Schimizzi, and Andrew Loza, and present members Audrey Brenot, Sam Van Hove, and Craig Barcus—thank you for being great lab mates, and also great friends. A special thank you to Katherine Fuh, a former member of the Longmore group and now an investigator herself, Katherine has been a wonderful collaborator, and has been supportive of my career goals and helping me to shape my interests in science and medicine. Thank you to the members of the ICCE institute. They have been extremely helpful with advice, reagents and equipment when needed, and it has been a great experience to work in such a collaborative environment. A special thank you to

my friends, both in graduate school and outside of the science world. They have helped me to maintain my sanity by providing fun breaks that allow me to stay motivated. Thank you to all of my MSTP classmates who have made this long journey more enjoyable just by being themselves. The MSTP cohort has been such an amazing source of friendship and encouragement, as well as a sometimes much needed forum to lament about life and graduate school as we made our way through this lengthy training together. Thank you to the MSTP administration and staff—Wayne, Brian, Christy, Liz and Linda. Without all of their help the transitions would not be as smooth, the correct forms would not get filed, and I would have had many more headaches. They make the transitions between medical school and graduate school flow seamlessly, and allow us to focus on our work. I'd also like to acknowledge MSTP NIH grant 5T32GM07200 for financial support.

Next, I would like to thank all of the members of my thesis committee—Ken Blumer, Bill Frazier, Kevin Moeller, Bob Mecham, Audrey Odom, and Andreas Herrlich. They have been a helpful source of suggestions in designing experiments and offered constructive criticisms of my work. As a diverse group of investigators, they have provided unique and interesting perspectives, and have helped my project to grow and progress.

I would like to thank all of the members of my family, who have been my pillars of strength throughout this journey, and life in general. My parents, Jim and Cheryl Grither, have been a constant source of love and support. They have taught me to work hard and believe in myself, and have always supported me in the paths that I chose. They have taken on my burdens and made them their own, and I hope that they do the

same with my successes. My grandma, Audrey Schmelzle, who has been a role model of strength and determination, and a constant source of encouragement and support. My siblings, Allie and Xavier, who have always been the best friends, listeners, and supporters, and just add general fun to my life when we are together. I am thankful to Guinness and Bailey, my four-legged friends, who have been a daily source of companionship and happiness, and help me to remember to take joy in the simple facets of life. Finally, I'd like to thank Garrett Bahr, for being my partner and rock for the past few years. He has encouraged me when things were tough, been a partner in adventure, celebrated and supported my achievements, and provides perspective in my life to the world outside of science. You all have been instrumental in my success.

Whitney Grither

*Washington University in St. Louis*

*May 2019*

## ABSTRACT OF THE DISSERTATION

Discoidin Domain Receptor 2 as a Therapeutic Target in Breast and Ovarian Cancer

by

Whitney Rose Grither

Doctor of Philosophy in Biology and Biomedical Sciences

Biochemistry

Washington University in St. Louis, 2019

Professor Gregory Longmore, Chair

Discoidin Domain Receptor 2 (DDR2) is a receptor tyrosine kinase that utilizes the extracellular matrix protein collagen as its ligand. Recently, DDR2 was shown to be critical in facilitating breast cancer metastasis. DDR2 stabilizes protein levels of the epithelial-mesenchymal-transition (EMT) inducing transcription factor, SNAIL1 in basal K14<sup>+</sup> epithelial cells that are known to be important for invasive leader cell properties during collective invasion/migration. DDR2 expression is present in a majority of human invasive ductal breast carcinomas, and expression is localized to the tumor-stroma boundary. Additionally, in genetic models of breast cancer, deletion of DDR2 within the stroma (MMTV-PyMT; DDR2 fl/fl; FSP-Cre) leads to a dramatic inhibition of tumor metastasis. This indicates that DDR2 also functions within the stromal compartment to facilitate metastasis, presumably through its function in cancer-associated fibroblasts (CAFs). In CAFs DDR2 is critical for fibrillar collagen and ECM production and the organization and architecture of collagen fibers. Additionally, paracrine factors from

DDR2 expressing CAFs promote the invasion of surrounding tumor cells. Therefore, it appears that DDR2 engagement by collagen provides a means for both tumor and stromal cells to communicate with the surrounding environment to enhance metastatic potential.

Additionally, we have established the action of DDR2 as critical for metastasis of ovarian cancer. In both breast and ovarian tumor cells DDR2 expression, which is absent in normal epithelium, is induced during EMT. The mesenchymal gene program has been shown to promote the metastatic progression of ovarian cancer; however, specific proteins induced by this program that lead to these metastatic behaviors have not been identified. We found that the EMT transcription factor TWIST1 drives expression of DDR2 upon EMT induction. In ovarian cancer, the expression and action of DDR2 was critical for mesothelial cell clearance, invasion and migration in ovarian tumor cells. It does so, in part, by upregulating expression and activity of matrix remodeling enzymes that lead to increased cleavage of fibronectin and spreading of tumor cells. *In vivo* studies demonstrated that the presence of DDR2 promotes ovarian cancer metastasis. These findings indicate the critical importance of DDR2 for multiple steps of ovarian cancer progression to metastasis, and thus, identifies DDR2 as a potential new target for the treatment of metastatic ovarian cancer.

As such, DDR2 is a novel RTK target for the treatment of cancer metastasis, leading us to hypothesize that the development of small molecule inhibitors to target DDR2 function in both the tumor and stromal cells could provide a means of blunting cancer metastasis. Using an *in vitro* binding assay, followed by medicinal chemistry optimization of lead compounds, we identified potent and selective small molecule

inhibitors of DDR2. The developed inhibitors have nanomolar potency at blocking DDR2 activation. Unlike traditional tyrosine kinase inhibitors (TKIs) that target the intracellular kinase domain, these inhibitors act on the extracellular domain (ECD) of DDR2, and disrupt DDR2 signaling by accelerating the disassembly of DDR2-collagen complexes, potentially by disrupting oligomerization of the receptor ECD. Therefore, these inhibitors have a unique mode of action and are able to attenuate DDR2 signaling both in cell culture, as well as *in vivo* as demonstrated by using a Snail1-clic beetle green reporter in a xenograft transplant model. In co-culture assays, treating CAFs with the developed inhibitors reduces the paracrine effect on invading tumor organoids. Furthermore, using mouse models of late stage breast tumor metastasis, we have shown that these inhibitors reduce metastatic burden in the lungs of mice, to a level comparable of that of genetic knockdown of DDR2. Together these data support further investigation of this novel class of DDR2 inhibitors as anti-metastasis agents, potentially for use in combination with standard of care therapy to halt cancer progression and prevent relapse. Further, it will be important to study the role of these inhibitors in other cancers where DDR2 expression has been shown to promote metastasis, including, but not limited to, ovarian, head and neck, and non-small cell lung carcinoma.

**Chapter 1**  
**Introduction**

## **Breast Cancer and metastasis**

In the United States, breast cancer is the most common type of cancer in women and the second leading cause of cancer related death among women. It is estimated that in 2017 there will be 252,710 newly diagnosed cases of breast cancer, and 40,610 deaths from the disease<sup>1</sup>. Breast cancer development follows a stepwise model, beginning with epithelial hyperplasia and transitioning to ductal carcinoma in situ (DCIS). DCIS is the premalignant proliferation of neoplastic epithelial cells contained within the lumen of mammary ducts, and is considered the precursor of invasive ductal carcinomas (IDC)<sup>2</sup>. IDC is characterized by the invasion of tumor cells through the layer of myoepithelial cells surrounding the mammary duct, and then breaching the basement membrane<sup>2</sup>. At this stage, the cancer can then further spread to distant organs, giving rise to metastasis. The vast majority of breast cancer deaths are due to metastasis, which accounts for over 90% of disease related mortality<sup>3</sup>. The molecular and genetic underpinnings of how breast cancer cells progress from DCIS to IDC to metastasis are poorly understood, thereby posing difficulty in predicting which lesions will progress to the next stage of development in patients. These insights are desperately needed, as the median patient survival once disease has disseminated is only 2-3 years<sup>4</sup>.

Epithelial cells accumulate somatic mutations in a stochastic manner over their lifetime. Breast cancer arises when the epithelial cells of the mammary gland accumulate mutations that affect their cell growth and survival, allowing for aberrant cell growth and evasion of the growth suppressive pathways that are in place in the normal epithelium<sup>5</sup>. This random acquisition of mutations leads to tumors that are heterogeneous at the molecular, cellular and patient levels. Commonly used

chemotherapeutics target this highly proliferative behavior, irrespective of tumor specific mutations. This non-specific targeting, while effective to some degree, carries inherent toxicity to healthy cells as well as the risk of leaving behind resistant sub-populations.

In addition to uncontrolled cell growth and proliferation, the cells must also acquire the ability to evade the body's immune system, stimulate growth of new blood vessels, and invade surrounding tissues<sup>5</sup>. While all of these characteristics are crucial to the survival of the cancer cell, perhaps the most detrimental from a clinical perspective is the ability of the cancer cell to invade and migrate. A confined breast tumor, or DCIS, is amenable to multiple treatment options, and prognosis is generally favorable. However, once tumor cells have invaded surrounding basement membrane, now considered an IDC, there is a large reduction in overall survival and limited additional treatment options, as the molecular basis of this transition is poorly understood<sup>6</sup>.

The process of metastasis involves multiple distinct steps, each orchestrated by distinct molecular pathways. As mentioned, the IDC must first invade the confining myoepithelial lumen and basement membrane. The cell then invades through the surrounding extracellular matrix (ECM) to reach nearby blood vessels, at which time it must intravasate into the circulatory or lymphatic system, survive transport, and then extravasate into the tissue at a distant site<sup>7</sup>. Once there, the cancer cell must survive in this foreign environment and eventually proliferate to generate macroscopic metastases capable of compromising organ function (Figure 1.1)<sup>5</sup>. While this process is rife with inefficiency, and the majority of cells that escape from the primary site do not survive, the impact of the few surviving cells on patient survival is significant. A great deal of

research has focused on identifying molecular targets of the DCIS to IDC progression, however these have failed to identify tumor stage specific gene expression profiles<sup>8</sup>, and a better understanding is imperative to improve treatment options for breast cancer patients at risk of developing invasive disease.

### **Breast tumor microenvironment**

While there remains a lack of understanding at the progression of breast tumor cells from benign to invasive, research in the field of tumor metastasis has led to the establishment of new concepts regarding the motility, dormancy, and establishment of tumors at distant locations<sup>9</sup>. It is now appreciated that crosstalk between the tumor cells and the surrounding cellular, chemical, and physical microenvironment influences tumor development, progression, metastasis, and response to treatment<sup>10, 11</sup>. In breast tumors these stromal components differ from their normal tissue counterparts in composition, architecture, and function (Figure 1.2). Furthermore, given the critical role the supporting environment plays in tumor progression, this opens the door to new strategies for therapeutic intervention that are often more consistent across different tumors.

Non-neoplastic cells of the breast tumor microenvironment in the preinvasive stages include myoepithelial and inflammatory cells. The players in the invasive stage of progression become more numerous, and include fibroblasts, myofibroblasts, adipocytes, inflammatory cells and endothelial cells (Figure 1.2)<sup>12,13</sup>. Significant differences in gene expression in the cells of the tumor microenvironment has been documented, both when comparing normal to DCIS-associated stroma, as well as

differences between DCIS to IDC transition<sup>8,14</sup>. Importantly, interactions between carcinoma cells and these non-neoplastic stromal cells are crucial at every step of the invasion-metastasis cascade<sup>3</sup>.

Additionally, the physical microenvironment is known to play a part in promoting invasion and metastasis. This includes the various extracellular matrix (ECM) proteins of the stroma, as well as the organizational arrangement of those components. Studies have shown that in contact with basement membrane, malignant mammary cells are fairly indolent in their invasiveness, but when placed in collagen I, those same tumor cells show increased invasion<sup>15</sup>. Data such as this indicates that cell-ECM contacts are critical in promoting migration of tumor cells. Collagen fibers are the most abundant protein within the extracellular matrix (ECM) of breast tumor stroma, and play a key role in breast cancer development and progression<sup>16</sup>. Increased collagen deposition contributes to breast density, and women with dense breasts have increased risk for developing breast cancer, with the resulting cases tending to be more aggressive<sup>17</sup>. Modulation of ECM stiffness, via collagen crosslinking, enhances breast carcinoma progression, in part via altered integrin signaling<sup>18</sup>. Additionally, increased tumor stiffness results in the development of both tissue stress and interstitial fluid pressure, which can alter many aspects of cell behavior<sup>19</sup>. It is not just an increase in these fibers, but also the orientation that can influence the behavior of tumor cells. Stromal collagen surrounding mammary tumors is frequently aligned and reoriented perpendicular to the tumor boundary, and this alignment is correlated with poor prognosis<sup>20</sup>. Alignment of collagen matrix can enhance invasion by increasing directional persistence of tumor protrusion, and increasing the efficiency of the migrating cell<sup>21</sup>.

Determining effective ways to halt cancer metastasis remains an elusive goal. A proposed reason for the limited success of current molecular therapies in the metastatic setting is the lack of modulating both tumor cells and the tumor microenvironment<sup>22</sup>. This points towards the need for therapeutic strategies that target both tumor cells and the surrounding stroma as a more effective means to stop metastatic spread.

### **Ovarian cancer and metastasis**

Ovarian cancer is the most lethal gynecologic malignancy, in part due to the poorly understood origin and pathogenesis of the disease. In 2017 it is estimated that there will be 22,440 newly diagnosed cases in the United States, and 14,080 deaths, making it one of the most lethal cancers in the U.S.<sup>1</sup>. The diverse array of ovarian tumors are broadly categorized into two groups based on morphologic and molecular genetic features. Type I tumors are composed of low-grade serous, low-grade endometrioid, clear cell, mucinous and transitional (Brenner) carcinomas. These are generally indolent and confined to the ovary at presentation. In contrast, type II tumors, which represent approximately 75% of all ovarian carcinomas and are responsible for 90% of ovarian cancer deaths, include conventional high-grade serous carcinoma (HGSOC), undifferentiated carcinoma and malignant mixed mesodermal tumors (carcinosarcoma). These type II tumors are highly aggressive and almost always present in advanced stage. Genetically, type II tumors display *TP53* mutations in over 80% of cases<sup>23,24</sup>.

Recently, it has been proposed that HGSOC actually arise from the implantation of tissue derived from the fallopian tube epithelium, rather than ovarian surface

epithelium<sup>25,26</sup>. These serous intraepithelial tubal carcinomas (STIC) arise in the fimbriated end of the fallopian tube and resemble high grade ovarian serous carcinoma both morphologically and molecularly<sup>25</sup>. Additional studies have confirmed that STIC possess most of the genomic aberrations present in advanced cancers, supporting STIC as a precursor lesion. However, that same study identified STIC as metastasis in a number of patients, indicating that they can also represent intraepithelial metastasis to the fallopian tube rather than the origin of HGSOc<sup>27</sup>. With a lack of early detection and screening strategies, and limited treatment options, in order to improve prognosis for patients with HGSOc a better understanding of the origin and spread of the tumor is needed.

While other malignancies of epithelial origin utilize hematogenous or lymphatogenous routes to metastasize, ovarian cancer is unique in that the metastatic cascade of ovarian tumors most commonly occurs via the peritoneal circulation. While metastasis of epithelial ovarian cancer can occur via the lymphatic or circulatory systems, transcoelomic metastasis is the most common. This results in the majority of metastases being confined within the abdominal peritoneal cavity<sup>28</sup>, which contributes substantially to the morbidity and mortality associated with the disease due to the frequency, ability to affect multiple vital organs, and development of malignant ascites<sup>29</sup>. At diagnosis, two thirds of the patients with ovarian cancer have already developed peritoneal metastasis.<sup>30</sup>

After tumor cell detachment from the primary site in the ovary, tumor cells are transported throughout the peritoneal cavity by intraperitoneal fluid, and must evade immune surveillance. Upon reaching the secondary site, the tumor cells encounter a

unique cell type of the ovarian microenvironment—a continuous mesothelial cell monolayer that covers the surfaces within the peritoneal cavity(Figure 1.3). This protective monolayer is the first contact site for ovarian cancer cells that have disseminated from their site of origin. It is thought to act as barrier to ovarian tumor metastasis, as mesothelial cells markedly inhibit the initial attachment of ovarian cancer cells<sup>31</sup>.

The tumor cells therefore must adopt mechanisms to attach to the mesothelial cells covering the peritoneal and pleural organs, then clear the mesothelial layer to invade through the underlying basement membrane and extracellular matrix (ECM) to form metastatic implants(Figure 1.3)<sup>32</sup>. This involves both adhesion to, and remodeling of, the surrounding ECM by the ovarian cancer cell for efficient metastasis to occur<sup>33,34</sup>. The mesothelial cells themselves secrete the ECM protein fibronectin, and ovarian tumor cells have been shown to adhere to and remodel this fibronectin network to invade within the peritoneal cavity<sup>34,35</sup>. Further, once the mesothelial cells are cleared, and underlying basement membrane is breached, ovarian tumor cells reach a thick network of collagen I fibers that are entwined with stromal fibroblasts(Figure 1.3). Both of these microenvironment components have shown to be important for ovarian cancer progression and invasion. Collagen I is a strong adhesive substrate for ovarian tumor cells<sup>31,36</sup> and has been shown to be upregulated in ovarian metastatic lesions. Stromal fibroblasts have been shown to enhance the invasiveness of ovarian cancer cells, via both direct contact and secreted factors<sup>31</sup>. Additionally, activated fibroblasts secrete and remodel ECM within the microenvironment, with this desmoplastic stroma providing a feed forward loop to invading tumor cells<sup>37</sup>. Identifying cellular and molecular targets

important for one or more of these steps of metastasis could have tremendous clinical impact by enabling the development of therapeutics that block these critical steps.

### **Epithelial-to-Mesenchymal Transition**

Epithelial to mesenchymal transition (EMT) is the transdifferentiation of epithelial cells into motile, mesenchymal cells. This process is integral to development, and the program is reactivated in pathologic states such as wound healing, fibrosis, and cancer progression<sup>38</sup>. This switch in cell differentiation is initiated by a number of diverse signals, which tend to be cell type or tissue type specific. Major developmental signaling pathways, such as TGF- $\beta$ , Wnt, Notch and growth factor receptor signaling have been implicated in EMT. Additionally, inflammatory cytokines and hypoxia in the tumor microenvironment have been shown to promote EMT<sup>39</sup>.

Regardless of the signal, these effector pathways converge on three core groups of transcriptional regulators that are regarded as the master regulators of EMT. The first group is the Snail zinc finger family (Snail1 and Snail2), which directly bind to the E-boxes of target epithelial genes to repress their expression. The second group is the zinc finger E-box binding homeobox family of proteins (Zeb1 and Zeb2). These proteins often recruit a C-terminal binding protein co-repressor to exert their action. The third group is the basic helix-loop-helix family of transcription factors (Twist1, Twist2, and E12/E47)<sup>38,39</sup>. The end result of expression of these master EMT regulators is the repression of epithelial genes (i.e. E-Cadherin, occludin), and the activation of mesenchymal gene expression (i.e. N-cadherin, vimentin, fibronectin, CD44<sup>40</sup>). The end product of these transcriptional changes results in the dissolution of cell-cell junctions,

loss of apical-basal polarity, reorganization of the cytoskeleton, and increased cell protrusions and motility(Figure 1.4)<sup>38</sup>.

In breast cancer, a cooperation of the various EMT transcription factors to induce and sustain EMT is critical for metastasis. For example, it has been shown that SNAIL1 is required for EMT initiation, while TWIST1 is required to maintain EMT in those cells<sup>41</sup>. Deletion of SNAIL1 in mouse models of breast cancer (MMTV-PyMT) in both early and late stages of primary tumor development led to a decrease in lung metastasis<sup>42</sup>. There is strong clinical and experimental evidence supporting a role for SNAIL1 in breast cancer metastasis<sup>43-45</sup>. SNAIL1 protein has a very short half-life and when cytosolic is rapidly degraded by the ubiquitin-proteasome system. While EMT-stimulating signals are able to induce SNAIL1 transcription, other modes of post-transcriptional and post-translational regulation influence SNAIL1 stability and subcellular localization, which is critical for its capacity to sustain cancer EMT<sup>46-48</sup>. In tumor samples, expression of SNAIL1 protein and mRNA are discordant; SNAIL1 mRNA is present in most cells within the tumor, but SNAIL1 protein is only detected in tumor cells at the tumor/ECM boundary and in mesenchymal cells within the tumor associated stroma<sup>49</sup>. This suggests that SNAIL1 protein levels are regulated post-transcriptionally by a uniquely localized signal. A human kinome/phosphatome RNAi screen identified the receptor tyrosine kinase (RTK) Discoidin Domain Receptor 2 (DDR2) as an indirect post-transcriptional regulator of SNAIL1 protein levels<sup>48</sup>, indicating that upstream regulation of these transcription factors plays a critical role in maintaining their expression in cells.

In ovary, studies have suggested that ovarian surface epithelium can undergo epithelial-to-mesenchymal transition (EMT) in response to regenerative stimuli (such as

ovulatory rupture) in order to repair the surface after ovulation<sup>51</sup>. While under normal conditions EMT likely confers advantages during postovulatory repair, the ability of ovarian cancer cells to adopt a mesenchymal gene program has been shown to promote ovarian cancer metastasis<sup>52</sup>. Induction of epithelial-to-mesenchymal transition (EMT) in ovarian cancer cells through expression of EMT transcription factors TWIST1, SNAIL1, or ZEB1 promotes mesothelial cell clearance<sup>52</sup>. These factors also promote the ability of an ovarian cancer cell to invade the basement membrane and extracellular matrix, and form metastatic implants<sup>53,54</sup>. While these EMT transcription factors induce a mesenchymal program crucial for ovarian cancer metastasis, the specific proteins whose expression is regulated during EMT that functionally mediate mesothelial cell attachment, clearance, and tumor cell invasion are not fully appreciated.

EMT is appreciated to be critical for localized carcinoma to gain invasive potential, thus giving rise to metastatic tumor cells<sup>44</sup>. EMT in a tumor cell bestows the cell with the ability to invade through the basement membrane and migrate along the extracellular matrix network<sup>43,44</sup>. Furthermore, in the context of cancer, many cells express both epithelial and mesenchymal markers, concurrently. This is likely a reflection of EMT not existing as a binary switch, but rather, a continuum along which the cancer cell progresses in either direction depending on the various cues within its surrounding environment(Figure 1.4)<sup>39,55</sup>. Additionally, while EMT seems to facilitate the metastatic dissemination of tumor cells, to establish a metastatic colony, the disseminated cell must again become epithelial in nature and proliferate. This requires the notion is EMT is itself transient in nature, and the cancer cells undergo a mesenchymal-to-epithelial transition when they reach the secondary site (Figure 1.4)<sup>56</sup>.

Indeed, if SNAIL1 is continuously overexpressed in the primary breast tumors of MMTV-NeuNT mice, there is decrease in lung metastasis despite an increase in dissemination of tumor cells<sup>42</sup>, indicating that the cells must be able to revert upon reaching a secondary site. This notion is also supported by recent *in vivo*, live imaging data illustrating that cells undergoing EMT are the migratory cells within a tumor, and that once arriving at the secondary site, cells convert to the epithelial state within one or two divisions<sup>57</sup>. Further studies into the various cues that control these EMT and MET switches, as well as EMT effector pathways that drive these behaviors may provide insight into more effective approaches to treating or preventing metastatic disease.

### **Receptor tyrosine kinases in the cancer setting**

Receptor tyrosine kinases (RTKs) are a diverse family of membrane spanning proteins with intrinsic phosphotyrosine kinase activity. In humans there are 58 members that can be divided into 20 different subfamilies. One canonical feature of all RTKs is the presence of an extracellular ligand binding domain (Lemmon and Schlessinger, 2010). The ligands that activate these receptors are typically polypeptide growth factors (i.e. IGF, EGFR, FGF, PDGF) or cytokines, with one distinct exception—the Discoidin Domain Receptor family that utilizes collagen, a structural protein, as ligand (Vogel W, 1997, Shrivastava A, 1997). When these ligands bind to their cognate receptors, this catalyzes phosphorylation of select tyrosine residues in target proteins, and this modification is a pivotal component of cellular communication and signaling. The phosphorylated tyrosine residues serve as docking sites for cytoplasmic signaling proteins containing Src homology-2 and protein tyrosine binding domains, which then assemble signaling complexes to activate a cascade of intracellular biochemical signals

that define a response to a given external signal<sup>58</sup>. This signal transduction plays key roles in cellular processes such as growth, differentiation, metabolism, and motility<sup>59</sup>.

RTKs exist in their active form as dimers, and ligand binding to the extracellular domain either promotes this dimerization, or stabilizes the formation of an active dimer conformation and subsequent activation<sup>60</sup>. Furthermore, studies have provided evidence that receptor oligomerization increases the local concentration of RTKs, leading to more efficient transphosphorylation of tyrosine residues in the active loop<sup>58</sup>, or an increase in affinity to ligand<sup>61,62</sup>. It appears that activation of certain RTKs may be dependent on the formation of larger oligomers<sup>59</sup>.

In addition to self-catalyzed phosphorylation in response to cognate ligand, crosstalk between RTKs also exists at the receptor level. For instance, an RTK can induce activation of a structurally unrelated RTK. This can occur by direct heterodimerization of the distinct RTKs, such as the case for c-Met/ErbB or EGFR/ErbB2. Another mechanism is whereby a transactivation is mediated by a cytoplasmic tyrosine kinase such as Src being activated by one receptor and then binding to and phosphorylating a member of the heterodimeric pair, such as with IGF-1R and EGFR<sup>63,64</sup>.

In addition to the functions of RTKs mediated by their kinase activity, evidence suggests that a number of non-catalytic properties are also essential for their function. These roles include acting as scaffolds for protein complexes, allosteric effects on other enzymes, and DNA binding<sup>65</sup>. For example, EGFR has been shown to interact with and stabilize the sodium/glucose cotransporter SGLT1. This stabilization occurs

independent of EGFR kinase activity, and promotes glucose uptake into the cancer cell to maintain intracellular glucose levels<sup>66</sup>. In the case of the ErbB4 receptor, cleavage of its ectodomain leads to a C-terminal fragment that translocates to the nucleus to affect the transcription of target genes. The C-terminal fragment of ErbB4 is able to activate transcription by associating with YAP2 transcription factor, and this occurs even when the fragment is lacking the kinase domain, suggesting this function may be independent of kinase activity of ErbB4<sup>65,67</sup>. In the developing neuron, EphB2 receptors influence depotentiation and long term potentiation independent of kinase signaling<sup>68</sup>. Therefore, the possibility of non-catalytic function of a given RTK must be taken into consideration when evaluating its function.

### **Therapeutic targeting of RTKs**

Given their critical roles in cell signaling, RTKs are well appreciated therapeutic targets for the treatment of cancer (Gschwind et al., 2004). Cancer is hallmarked by aberrant cell growth, evasion of apoptosis, and increased invasion, and many of these signals are regulated by the activity of RTKs<sup>69</sup>. Oncogenic activation of RTKs is achieved in numerous ways. This includes mutations within the extracellular domain of the protein leading to constitutive activation, mutations within the kinase domain leading to uncontrolled activation, aberrant overexpression of the receptor, or overexpression of an RTK ligand<sup>58</sup>.

Most drugs targeting RTKs are of two classes—antibodies that block ligand binding, receptor dimerization, or alter receptor internalization; or small molecule

tyrosine kinase inhibitors (TKIs) that interact with the intracellular kinase domain of the proteins<sup>70-73</sup>

A number of different strategies have been employed using monoclonal antibodies (mAbs) to target RTKs. For example, mAbs such as cetuximab bind the extracellular domain of the EGFR receptor and block dimerization that is necessary for activation. There are also mAbs that bind to RTKs and orthosterically block ligand binding, such as icrucumab for VEGFR1 or olaratumab for PDGFRa. Several IGF1R antibodies have been developed that bind to the receptor and cause internalization, thereby preventing binding to ligand. Ligand trapping, such as that achieved with the anti-VEGF mAb bevacizumab, represents yet another strategy utilized to target RTK signaling<sup>74</sup>. While efficacious in some settings, several therapeutic antibodies that bind to receptors do not inhibit the activity of oncogenic RTKs that harbor activating mutations in their kinase domains<sup>59</sup>.

As the ATP-binding site of RTKs is highly conserved, small molecule TKIs tend to affect many tyrosine kinases in addition to their intended target. For example, Gleevec (imatinib) which is used clinically to inhibit constitutive tyrosine kinase activation of a Bcr-Abl fusion in chronic myeloid leukemia, was actually identified in the development of PDGFR inhibitors<sup>59</sup>. While many of these drugs have shown success clinically, effective and lasting use of traditional TKI strategies have been hampered by the emergence of drug resistance<sup>73</sup>. This resistance is commonly achieved through the acquisition of gatekeeper mutations that stabilize a “hydrophobic spine” characteristic of the active state of several kinases<sup>75</sup>. Additionally, the growing body of literature demonstrating kinase independent functions of RTKs suggest that the use of TKIs to inhibit these

receptors may be short-sighted, as non-catalytic functions of the receptors may prevent the efficacy of such inhibition strategies.

Therefore, development of inhibitors of RTKs with alternative mechanisms of action could be highly advantageous. Recently, a small molecule inhibitor targeting the extracellular domain of the fibroblast growth factor receptor (FGFR) was described (Bono et al., 2013, Herbert et al., 2013). This compound inhibits the signaling linked to receptor internalization in an allosteric manner. Non-classical small molecule inhibitors that disrupt protein complexes have been reported (He et al., 2005, Berg, 2003), but no such inhibitors have been identified for any RTK. These types of non-classical or allosteric inhibitors remain an elusive goal for drug development as they offer therapeutic advantages such as increased selectivity and safety (Christopoulos, 2002, Wenthur et al., 2014).

### **Discoidin Domain Receptors**

The human discoidin domain receptors, DDR1 and DDR2, are members of the receptor tyrosine kinase (RTK) family. DDR1 is present in epithelial cells, whereas DDR2 is expressed primarily in mesenchymal cells. Unlike typical RTKs, the DDRs are not activated by soluble growth factors. Rather, various forms of the extracellular matrix protein collagen act as ligands for DDRs<sup>76,77</sup>. The DDRs are composed of an extracellular region, a transmembrane domain, a cytosolic juxtamembrane domain, and a C-terminal tyrosine kinase domain. The extracellular region consists of a collagen binding discoidin (DS) domain, an accessory discoidin-like (DSL) domain, and a small juxtamembrane domain (Figure 1.5)<sup>78</sup>. NMR<sup>79</sup> and X-ray<sup>80,81</sup> crystallographic studies

have revealed the three dimensional structure of the extracellular discoidin domain of DDRs--a jelly roll motif<sup>82</sup> where five loops comprise the top of the barrel, three of which are involved in binding to fibrillar collagen<sup>83</sup>. These three loops form an amphiphilic trench which accommodates the collagen triple helix and contains the central collagen-binding residues of DDR2<sup>79,80</sup>. Collagen binding by this region within the DS domain leads to slow and prolonged activation of the receptors, a unique feature of the DDRs<sup>76</sup>.

The DDRs are activated by collagen only when it is in its native, triple-helical form, as heat denatured collagen fails to induce kinase activity<sup>84</sup>. Both DDR1 and DDR2 bind to and are activated by fibrillar collagens, including collagens I-III and V, which are the collagens common to the extracellular matrix (ECM) surrounding tumors. The two receptors recognize a GVMGFO motif present in fibrillar collagens<sup>85</sup>. Notably, this is distinct from the GFOGER motif within collagen that serves as the high affinity binding site for collagen binding integrins the well-studied family of transmembrane collagen receptors known to contribute to breast cancer metastasis<sup>85-87</sup>. Interestingly, while DDR1 also binds to collagen IV, which is present in the basement membrane (BM)<sup>76,77</sup>, DDR2 does not bind and recognize this non-fibrillar collagen. This difference in collagen IV recognition has been mapped to a small patch of non-conserved residues near the binding pocket<sup>88</sup>. At the cell surface, DDRs exist as dimers in the absence of ligand<sup>84,89,90</sup>. How exactly ligand binding produces changes within these DDR dimers to mediate activation of the receptor remains unknown. Given the prolonged activation kinetics of this class of receptors it is likely that there is a unique mechanism at play. Studies on DDR1 have illustrated that receptor oligomerization and internalization occurs at timescales much shorter than receptor activation<sup>89</sup>, and DDR1 extracellular

domain plays a crucial role in receptor oligomerization that mediates high affinity interactions with collagen ligand<sup>61,62</sup>.

The cellular functions of the DDRs have gained increased attention in recent years, and are still being explored<sup>91</sup>. Genetic deletion of DDR1 or DDR2 in mice causes dwarfism<sup>92,93</sup>. In DDR2 mice this phenotype has been shown to be caused by a reduced proliferation of chondrocytes<sup>93</sup>. This defect is manifested in humans with spondylo-meta-epiphyseal dysplasia (SMED-SL), a rare genetic condition caused by a mutation in DDR2 that leads to short stature and limbs, and bone abnormalities<sup>94</sup>. While DDR1 null mice exhibit defective mammary gland development<sup>92</sup>, no mammary gland phenotype has been documented for DDR2. DDR2 null mice are infertile due to defects in spermatogenesis and ovulation<sup>95</sup>. DDR2 is required for the migration of fibroblasts and neutrophils in 3D matrices<sup>96,97</sup>, in part by regulating the activity of matrix metalloproteinases (MMPs), a family of zinc-dependent proteases that degrade the ECM. The DDRs play pivotal roles in regulating the expression and activity of several MMPs, and aberrant activity of many MMPs have been shown to contribute to the pathology of a number of diseases<sup>91</sup>.

### **DDR2 in cancer**

Genomic analysis and histologic evaluation of human tumor samples reveal that in a significant number of different human tumors expression of both DDR1 and DDR2 is either present or increased<sup>98</sup>. DDR2 expression is associated with cancer metastasis in a number of different human cancers types. These include breast<sup>50,99,100</sup>, prostate<sup>101</sup>, papillary thyroid<sup>102</sup>, nasopharyngeal<sup>103</sup>, hepatocellular<sup>104</sup>, lung squamous

cell<sup>105</sup>, and head and neck squamous cell<sup>106</sup> carcinomas. In invasive breast cancer, for example, over 70% of tumors, across all clinical subtypes expressed DDR2, while normal breast epithelium does not express DDR2 (Figure 1.6)<sup>50 107</sup>. DDR2 expression has also been detected in tumor associated stromal cells such as cancer associated fibroblasts (CAFs)<sup>50</sup>, endothelial cells<sup>108</sup>, and myeloid cells<sup>96</sup>. This highlights a possible cancer role for DDR2 in the tumor microenvironment as well as tumor cells. While DDR2 expression in tumors is well documented, mutations in DDR2 are much less common. In 3.8% of squamous cell lung carcinomas mutations in DDR2 were found and these occurred throughout the entire coding region<sup>109</sup>. Some mutations resulted in gain-of-function phenotypes (proliferation) when expressed in cell lines. In the breast cancer TCGA project, 5% of patients exhibited amplified expression of DDR2, for unclear reasons, and these patients have decreased survival<sup>50</sup>.

In multiple different tumor cell *ex vivo* cell-based studies DDR2 has been shown to exhibit pro- and anti-proliferative effects, positively cell-ECM adhesion, and positively influence tumor cell invasion and migration<sup>98</sup>. DDR expression has been found to correlate with both developmental and cancer EMT. During EMT induced by many different environmental signals (e.g., TGF- $\beta$ , hypoxia, collagen I) and in different epithelial and tumor cell lines, DDR1 expression decreases and DDR2 expression increases as cells become less epithelial and more mesenchymal in nature. A number of cell-based studies have implicated DDRs as important regulators of cancer EMT. In renal tubule epithelial cells and lung cancer cells RNAi-mediated deletion of DDR2 inhibited TGF- $\beta$ -mediated EMT<sup>110</sup>. Hypoxia induced EMT was inhibited in breast cancer cell lines transduced with DDR2 shRNAi<sup>100</sup>. Forcing cells to undergo EMT by

overexpression of the EMT inducing factor SNAIL2 led to DDR switching from DDR1 in parental MDCK cells, to DDR2 expression in SNAIL2-MDCK cells<sup>111</sup>. When breast epithelial cell lines that do not express SNAIL1 are induced to undergo TGF- $\beta$ -mediated EMT, DDR1 levels decrease and DDR2 levels increase, but DDR2 expression was not necessary for EMT induction<sup>50</sup>.

In regards to breast cancer, the function of DDR2 in both the tumor<sup>50,100</sup> and tumor stroma<sup>99</sup> has been shown to play a critical role in metastasis. While not expressed in normal breast epithelium, DDR2 is expressed in the majority of human invasive ductal carcinomas, and contributes to enhanced or sustained invasion and migration of K14<sup>+</sup> leader cells by maintaining the cellular levels and activity of the EMT transcription factor SNAIL1(Figure 1.6)<sup>50,99</sup>. In the breast tumor stroma, the action of DDR2 in cancer associated fibroblasts (CAFs) influences extracellular matrix (ECM) synthesis and remodeling<sup>99,112</sup> leading to the production of a more invasive collagen organization within tumors. Additionally, the action of DDR2 in CAFs influences the collective invasiveness of surrounding breast tumor cells in a paracrine manner<sup>99</sup>.

### **DDR2 in other pathologic states**

In addition to its role in cancer progression and metastasis, DDR2 also plays a role in other pathologic states. Perhaps not surprisingly, most evidence for DDR2 related pathogenesis has been illustrated in the context of pro-fibrotic diseases.

### **DDRs and Arthritis**

Osteoarthritis (OA) involves degeneration of articular cartilage. Injury results in activation of MMP13 that degrades collagen II, the major collagen present in articular

cartilage. Since collagen II is a ligand for DDR2 several studies have explored possible roles for DDR2 in the pathogenesis of OA. DDR2 expression is increased in chondrocytes of OA patients and mouse models of OA<sup>113 114</sup>. Activation of DDR2 in chondrocytes leads to MMP13 upregulation<sup>114</sup>. Overexpression of DDR2 alone in chondrocytes does not result in OA in normal mice, likely because normal articular chondrocytes are not directly exposed to collagen II<sup>115</sup>. However, injury can expose chondrocytes to collagen II and the development of OA<sup>115</sup>. Genetically reducing DDR2 levels in mouse genetic models and injury models of OA attenuates OA progression<sup>116 117</sup>.

Whether DDRs contributes to rheumatoid arthritis has not been experimentally tested but DDR2 is highly expressed in synovial fibroblasts from patients with RA<sup>118,119</sup>, and may act as one of the stimulators of the over-expression of MMP-1 in RA synovial fibroblasts<sup>120</sup>, and may also stimulate other pathways that contribute to RA pathogenesis<sup>119</sup>.

### **DDRs and Fibrosis**

In lung fibrosis, DDR2 has been shown to play a role in the induction of fibrosis and angiogenesis. DDR2 null mice were shown to be refractory to bleomycin induced lung fibrosis, and *in vitro*, DDR2 was shown to stimulate myofibroblastic changes in lung fibroblasts<sup>121</sup>. For DDR2 there are conflicting reports about its role in liver fibrosis. DDR2<sup>-/-</sup> mice exhibit increased liver inflammation and fibrosis in response to carbon tetrachloride injury<sup>122</sup>. But the same group has previously shown that DDR2 is important for hepatic stellate cell activation – a profibrotic state<sup>123</sup>. In rats, RNAi

deletion of DDR2 in liver stellate cells protects against alcohol-induced liver injury and fibrosis<sup>124</sup>. Since Snail1 expression in liver hepatocytes has been shown to be important for liver fibrosis in response to injury<sup>125</sup>, and DDR2 stabilizes Snail1, this suggests that a DDR2-Snail1 signaling pathway could be critical for pathologic fibrosis.

### **DDR2 Therapeutic targeting**

As a major contributor to fibrotic diseases and cancer progression, this implies that blocking the actions of DDR2 might represent a promising therapeutic strategy (Figure 1.7). Thus far, identification of small molecule antagonists of DDR2 activity have been limited to pharmacological agents directed against the kinase domain of DDR2<sup>126,127</sup> or uncharacterized, low-potency inhibitors of DDR2-collagen binding<sup>128</sup>. Antibodies that target the DS-like domain of DDR1 and inhibit activation have been developed<sup>81</sup>, however no such antibodies have been reported for DDR2. While progress has been made towards the development of traditional TKI agents for DDR2, these compounds exhibit only a preference for DDR2 inhibition and still show significant inhibitory profiles towards other kinases<sup>126,127,129</sup>. Furthermore, effective and lasting use of traditional TKI strategies have been hampered by the emergence of drug resistance, and acquired gatekeeper mutations in DDR2 treated with TKIs have already been reported<sup>130</sup>.

## **Summary and thesis objectives**

The goal of this thesis was to address the role of DDR2 as a therapeutic target in the setting of metastasis. In breast cancer, we asked whether DDR2 was a candidate therapeutic target for metastasis by temporally depleting *Ddr2* in early stage tumors in MMTV-PyMT mice. We developed small molecule inhibitors of DDR2 that target the extracellular domain of the receptor to inhibit ligand binding in a non-orthosteric manner. These compounds actively inhibit DDR2 activation and downstream signaling in response to collagen in both breast tumor cells and *in vivo*. We also elucidated a region at the interface of the two DDR2 extracellular domains that is important for receptor binding and activation. Furthermore, we have documented kinase independent functions of the DDR2 receptor, and identified putative interacting partners of the protein in breast cancer cells. In ovarian cancer, we established DDR2 as critical for metastasis. Additionally, we detailed a pathway whereby DDR2 expression is regulated in invasive tumor cells. Upon induction of EMT, the EMT transcription factor TWIST1 drives the expression of DDR2, which in turn stabilizes the transcription factor SNAIL1 to sustain EMT. DDR2 in ovarian cells drives the cleavage and remodeling of fibronectin, which promotes mesothelial cell clearance by the cancer cell.

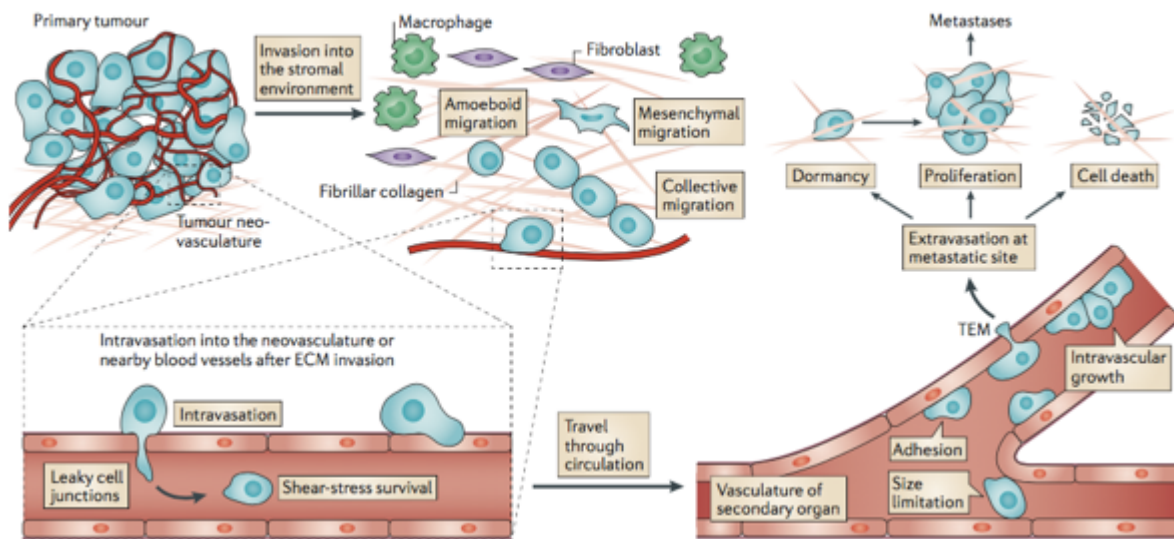


**Figure 1.1: Breast cancer progression and the metastatic cascade**

Breast cancer is initiated by the accumulation of genetic mutations in the epithelial cells of the mammary gland. Invasive cells must breach the basement membrane and traverse the microenvironment to reach the vasculature. This microenvironment is also changed in the context of malignancy, and fibroblasts become activated, immune cells infiltrate, and the extracellular matrix is remodeled. After migrating through this altered environment, cells intravasate into the blood stream, survive in the circulation, extravasate at the metastatic site, and reinitiate proliferative programs to form detectable metastasis. Adapted from Reymond, Borda d'Agua, and Ridley 2013.

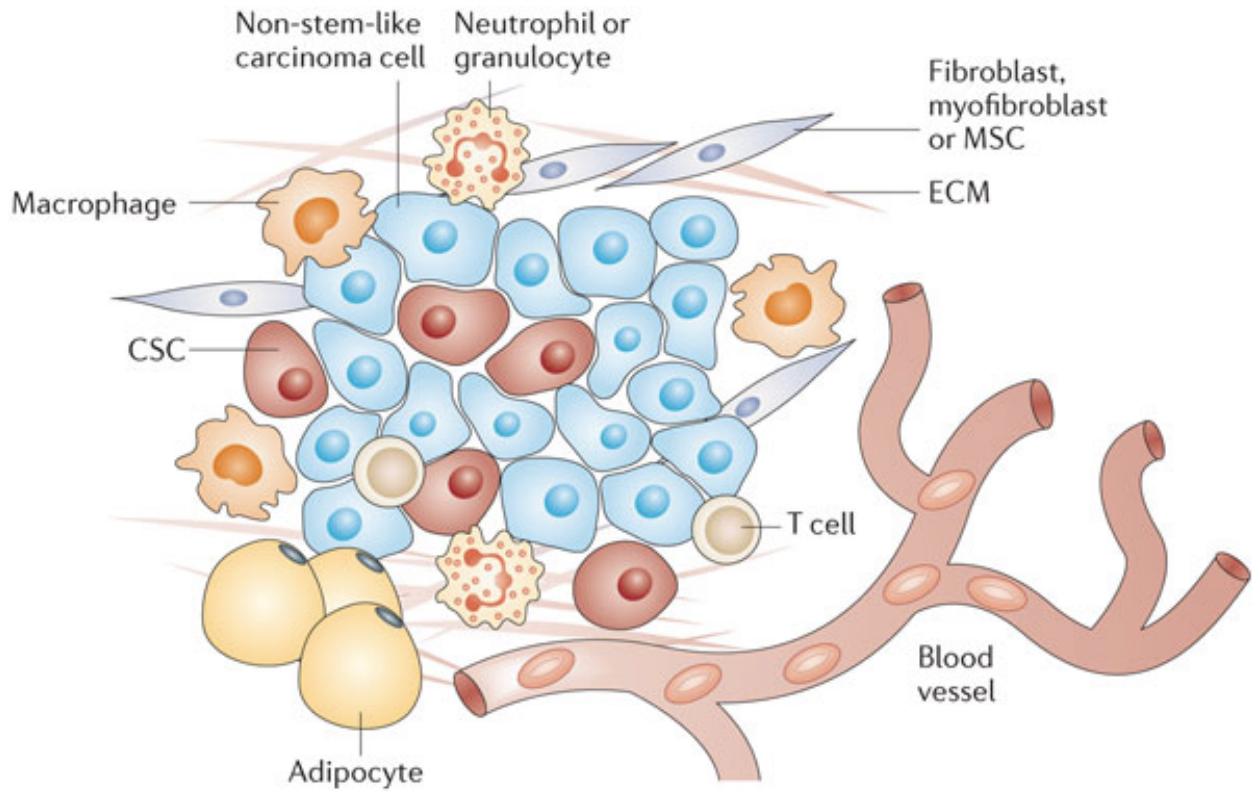


**Figure 1.2: The breast tumor microenvironment**

During tumor development, mammary epithelial cells begin to divide uncontrollably and lose polarity. Tumor angiogenesis increases the bloodflow to the malignant cells. Fibroblasts within the stroma become activated, and secrete increased amounts of extracellular matrix proteins and remodel the existing matrix, leading to a more fibrotic environment. Adipocytes secrete growth factors, resident immune cells become activated, and non-resident immune cells infiltrate into the tumor and surrounding tissue. Adapted from Pattabiraman and Weinberg 2014.

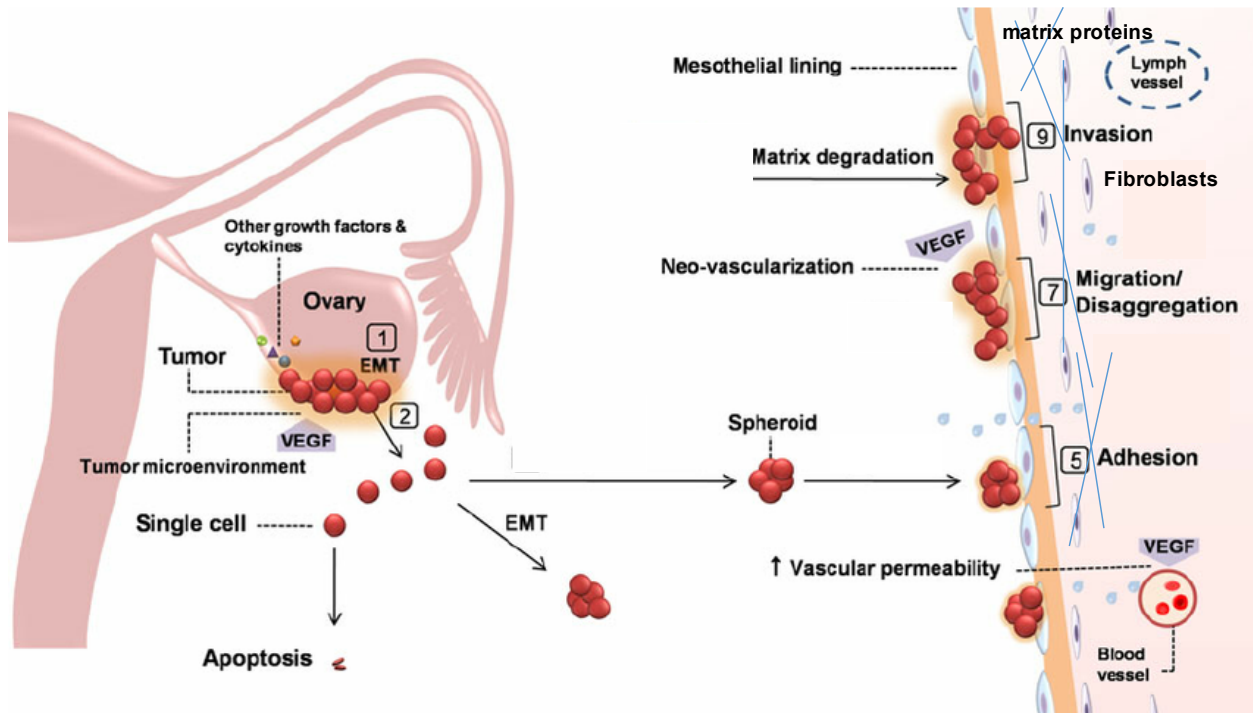


**Figure1.3: Ovarian cancer metastasis**

Ovarian cells undergo transcoelomic metastasis, where they are transported throughout the peritoneal cavity. Potential secondary sites of metastasis are covered in a monolayer of mesothelial cells, a barrier the ovarian cancer cell must clear before reaching the stroma of the secondary site to establish metastasis. Adapted from Masoumi Moghaddam et al. 2011.

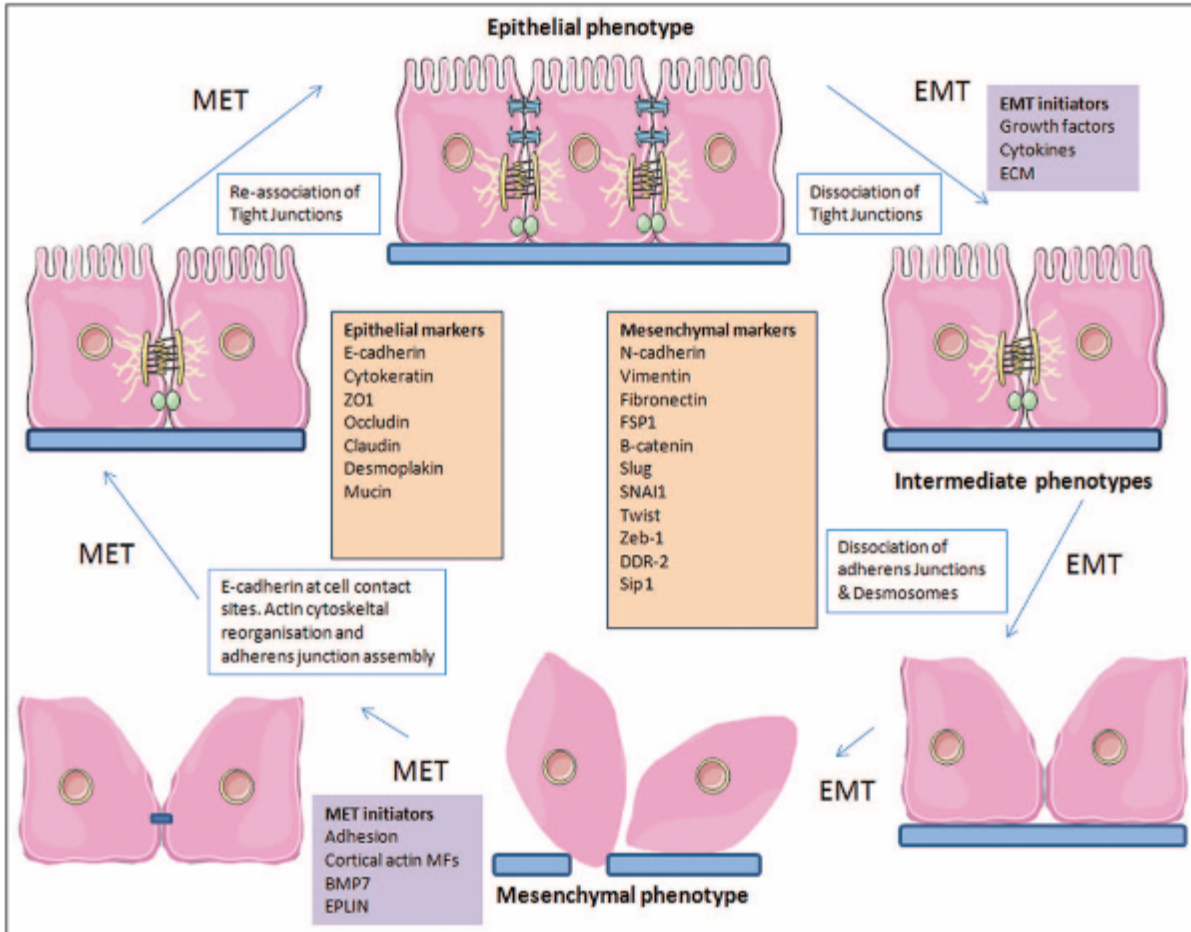


**Figure 1.4: epithelial-mesenchymal transition—cell plasticity between states**

Features of epithelial and mesenchymal cells, and signals that initiate EMT and MET. Epithelial cells are polarized and adhere tightly to one another. As epithelial cell proliferated , EMT contributes to a loss of polarity and detachment of cells to one another. These elongated mesenchymal cells have invasive properties that promote migration out of the primary tumor, through the stroma, and into the bloodstream. Once reaching the secondary site, the cell must undergo the reverse process, MET, to re-establish growth and form macrometastasis. Adapted from Martin et al. 2012.

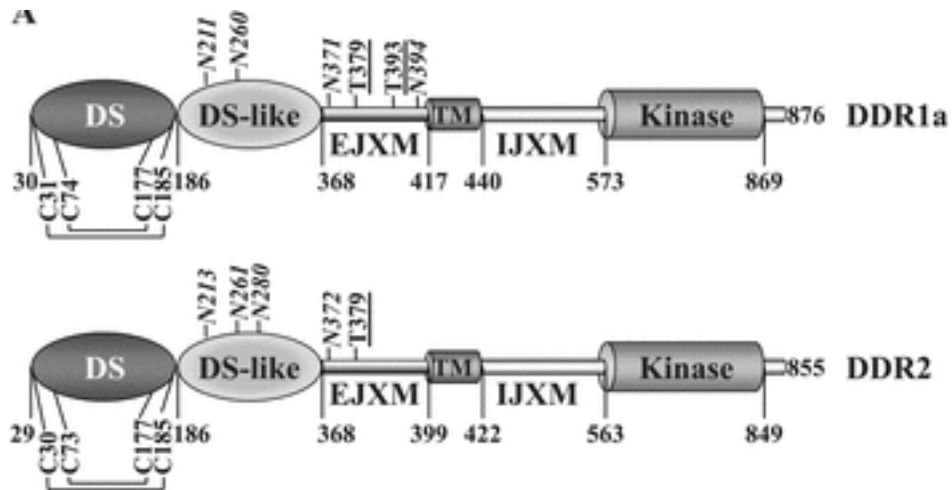
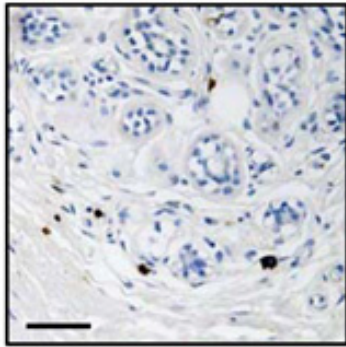
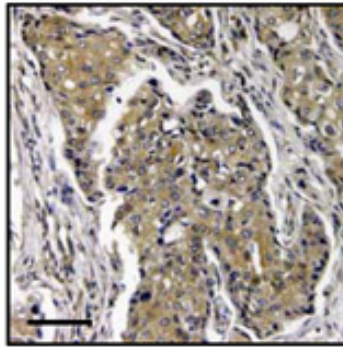


**Figure 1.5: Domain structure of the discoidin domain receptors**

The discoidin domain receptors are type I transmembrane receptor proteins that contain a discoidin (DS) ligand binding domain, a discoidin-like domain (DS-like), an extracellular juxtamembrane region, transmembrane domain, intracellular juxtamembrane domain, and intracellular kinase domain. Amino acid residue numbers delineating these domains are pictured, as well as N- and O- glycosylation sites. Adapted from Fu et al. 2013.



CA assoc. nl breast



Invasive ductal CA

**Figure 1.6: DDR2 is expressed in human invasive ductal carcinomas, but not in normal mammary epithelia**

Immunohistochemical staining of DDR2 in human invasive ductal carcinoma or cancer associated normal breast tissue. Both epithelial tumor cells and adjacent stromal fibroblasts show DDR2 expression in the invasive ductal carcinoma. Adapted from Zhang et al. 2013.

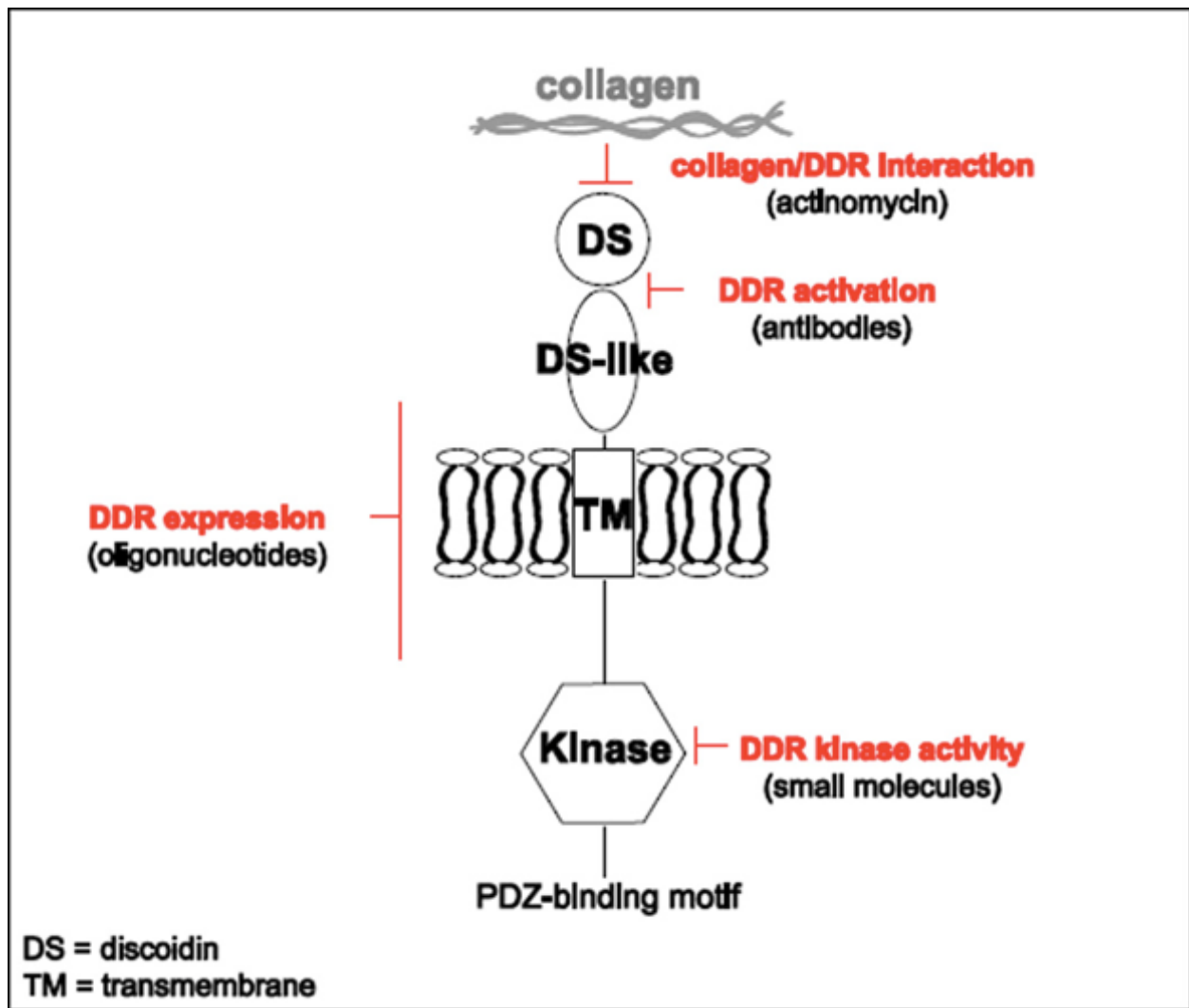


**Figure 1.7: Therapeutic targeting of DDR2**

Diagram depicting of DDR2 expression/activation can be targeted therapeutically. This includes targeting of the extracellular domain to inhibit collagen binding, inhibiting activation with antibodies, and traditional tyrosine kinase inhibitors. Adapted from Borza and Pozzi 2014.

## References

1. Siegel, R.L., Miller, K.D. & Jemal, A. Cancer Statistics, 2017. *CA: a cancer journal for clinicians* **67**, 7-30 (2017).
2. Cowell, C.F., *et al.* Progression from ductal carcinoma in situ to invasive breast cancer: revisited. *Molecular oncology* **7**, 859-869 (2013).
3. Valastyan, S. & Weinberg, R.A. Tumor metastasis: molecular insights and evolving paradigms. *Cell* **147**, 275-292 (2011).
4. Montero AJ, E.S., Gorin B, Adler P. The economic burden of metastatic breast cancer: a US managed care perspective. *Breast Cancer Res Treat* **134**, 815-822 (2012).
5. Hanahan, D. & Weinberg, R.A. Hallmarks of cancer: the next generation. *Cell* **144**, 646-674 (2011).
6. Groen, E.J., *et al.* Finding the balance between over- and under-treatment of ductal carcinoma in situ (DCIS). *Breast* **31**, 274-283 (2017).
7. Reymond, N., d'Agua, B.B. & Ridley, A.J. Crossing the endothelial barrier during metastasis. *Nature reviews. Cancer* **13**, 858-870 (2013).
8. Hu, M., *et al.* Regulation of in situ to invasive breast carcinoma transition. *Cancer Cell* **13**, 394-406 (2008).
9. Coghlin, M.C.a.G. Current and emerging concepts in tumour metastasis. *J Pathol* **222**, 1-15 (2010).
10. McAllister, S.S. & Weinberg, R.A. Tumor-host interactions: a far-reaching relationship. *Journal of clinical oncology : official journal of the American Society of Clinical Oncology* **28**, 4022-4028 (2010).

11. Hanahan, D. & Coussens, L.M. Accessories to the crime: functions of cells recruited to the tumor microenvironment. *Cancer Cell* **21**, 309-322 (2012).
12. Bombonati, A. & Sgroi, D.C. The molecular pathology of breast cancer progression. *J Pathol* **223**, 307-317 (2011).
13. Pattabiraman, D.R. & Weinberg, R.A. Tackling the cancer stem cells - what challenges do they pose? *Nature reviews. Drug discovery* **13**, 497-512 (2014).
14. Ma, X.J., Dahiya, S., Richardson, E., Erlander, M. & Sgroi, D.C. Gene expression profiling of the tumor microenvironment during breast cancer progression. *Breast cancer research : BCR* **11**, R7 (2009).
15. Nguyen-Ngoc, K.V., *et al.* ECM microenvironment regulates collective migration and local dissemination in normal and malignant mammary epithelium. *Proceedings of the National Academy of Sciences of the United States of America* **109**, E2595-2604 (2012).
16. Provenzano, P.P., *et al.* Collagen density promotes mammary tumor initiation and progression. *BMC medicine* **6**, 11 (2008).
17. Tice, J.A., *et al.* Benign breast disease, mammographic breast density, and the risk of breast cancer. *Journal of the National Cancer Institute* **105**, 1043-1049 (2013).
18. Levental, K.R., *et al.* Matrix crosslinking forces tumor progression by enhancing integrin signaling. *Cell* **139**, 891-906 (2009).
19. Ivey, J.W., Bonakdar, M., Kanitkar, A., Davalos, R.V. & Verbridge, S.S. Improving cancer therapies by targeting the physical and chemical hallmarks of the tumor microenvironment. *Cancer letters* **380**, 330-339 (2016).
20. Conklin, M.W., *et al.* Aligned collagen is a prognostic signature for survival in human breast carcinoma. *The American journal of pathology* **178**, 1221-1232 (2011).
21. Riching, K.M., *et al.* 3D collagen alignment limits protrusions to enhance breast cancer cell persistence. *Biophys J* **107**, 2546-2558 (2014).

22. Swartz, M.A., *et al.* Tumor microenvironment complexity: emerging roles in cancer therapy. *Cancer research* **72**, 2473-2480 (2012).
23. Kurman, R.J. & Shih Ie, M. The origin and pathogenesis of epithelial ovarian cancer: a proposed unifying theory. *Am J Surg Pathol* **34**, 433-443 (2010).
24. Guth, U., *et al.* Metastatic patterns at autopsy in patients with ovarian carcinoma. *Cancer* **110**, 1272-1280 (2007).
25. Lee, Y., *et al.* A candidate precursor to serous carcinoma that originates in the distal fallopian tube. *J Pathol* **211**, 26-35 (2007).
26. Marquez, R.T., *et al.* Patterns of gene expression in different histotypes of epithelial ovarian cancer correlate with those in normal fallopian tube, endometrium, and colon. *Clinical cancer research : an official journal of the American Association for Cancer Research* **11**, 6116-6126 (2005).
27. Eckert, M.A., *et al.* Genomics of Ovarian Cancer Progression Reveals Diverse Metastatic Trajectories Including Intraepithelial Metastasis to the Fallopian Tube. *Cancer Discov* **6**, 1342-1351 (2016).
28. Yeung, T.L., *et al.* Cellular and molecular processes in ovarian cancer metastasis. A Review in the Theme: Cell and Molecular Processes in Cancer Metastasis. *American journal of physiology. Cell physiology* **309**, C444-456 (2015).
29. Tan, D.S., Agarwal, R. & Kaye, S.B. Mechanisms of transcoelomic metastasis in ovarian cancer. *Lancet Oncol* **7**, 925-934 (2006).
30. Masoumi Moghaddam, S., Amini, A., Morris, D.L. & Pourgholami, M.H. Significance of vascular endothelial growth factor in growth and peritoneal dissemination of ovarian cancer. *Cancer metastasis reviews* **31**, 143-162 (2012).
31. Kenny, H.A., Krausz, T., Yamada, S.D. & Lengyel, E. Use of a novel 3D culture model to elucidate the role of mesothelial cells, fibroblasts and extra-cellular matrices on adhesion and invasion of ovarian cancer cells to the omentum. *International journal of cancer* **121**, 1463-1472 (2007).

32. Iwanicki, M.P., *et al.* Ovarian cancer spheroids use myosin-generated force to clear the mesothelium. *Cancer Discov* **1**, 144-157 (2011).
33. Cho, A., Howell, V.M. & Colvin, E.K. The Extracellular Matrix in Epithelial Ovarian Cancer - A Piece of a Puzzle. *Frontiers in oncology* **5**, 245 (2015).
34. Kenny, H.A., Kaur, S., Coussens, L.M. & Lengyel, E. The initial steps of ovarian cancer cell metastasis are mediated by MMP-2 cleavage of vitronectin and fibronectin. *The Journal of clinical investigation* **118**, 1367-1379 (2008).
35. Kenny, H.A., *et al.* Mesothelial cells promote early ovarian cancer metastasis through fibronectin secretion. *The Journal of clinical investigation* **124**, 4614-4628 (2014).
36. Moser, T.L., Pizzo, S.V., Bafetti, L.M., Fishman, D.A. & Stack, M.S. Evidence for preferential adhesion of ovarian epithelial carcinoma cells to type I collagen mediated by the alpha2beta1 integrin. *International journal of cancer* **67**, 695-701 (1996).
37. Schauer, I.G., Sood, A.K., Mok, S. & Liu, J. Cancer-associated fibroblasts and their putative role in potentiating the initiation and development of epithelial ovarian cancer. *Neoplasia* **13**, 393-405 (2011).
38. Lamouille, S., Xu, J. & Derynck, R. Molecular mechanisms of epithelial-mesenchymal transition. *Nature reviews. Molecular cell biology* **15**, 178-196 (2014).
39. Tsai, J.H. & Yang, J. Epithelial-mesenchymal plasticity in carcinoma metastasis. *Genes Dev* **27**, 2192-2206 (2013).
40. Tracey A. Martin, L.Y., Andrew J. Sanders, Jane Lane and Wen G. Jiang. *Cancer Invasion and Metastasis: Molecular and Cellular Perspective*, (Landes Bioscience., 2012).
41. Tran, D.D., Corsa, C.A., Biswas, H., Aft, R.L. & Longmore, G.D. Temporal and spatial cooperation of Snail1 and Twist1 during epithelial-mesenchymal transition predicts for human breast cancer recurrence. *Molecular cancer research : MCR* **9**, 1644-1657 (2011).

42. Tran, H.D., *et al.* Transient SNAIL1 expression is necessary for metastatic competence in breast cancer. *Cancer research* **74**, 6330-6340 (2014).
43. Perou, C. Molecular stratification of triple-negative breast cancers. *Oncologist* **15**, 39-48 (2010).
44. Thiery JP, A.H., Huang RY, Nieto MA. Epithelial-mesenchymal transitions in development and disease. *Cell* **139**, 871-890 (2009).
45. Moody, S.E., *et al.* The transcriptional repressor Snail promotes mammary tumor recurrence. *Cancer Cell* **8**, 197-209 (2005).
46. Zhou BP, D.J., Xia W, Xu J, Li YM, Gunduz M, Hung MC. Dual regulation of Snail by GSK-3beta-mediated phosphorylation in control of epithelial-mesenchymal transition. *Nat. Cell Biol* **6**, 931-940 (2004).
47. Yook JI, L.X., Ota I, Hu C, Kim HS, Kim NH, Cha SY, Ryu JK, Choi YJ, Kim J, Fearon ER, Weiss SJ. A Wnt-Axin2-GSK3beta cascade regulates Snail1 activity in breast cancer cells. *Nat. Cell Biol. EMBO J.*(2006).
48. Zhang, K., *et al.* Lats2 kinase potentiates Snail1 activity by promoting nuclear retention upon phosphorylation. *The EMBO journal* **31**, 29-43 (2012).
49. Francí C, T.M., Dave N, Alameda F, Gómez S, Rodríguez R, Escrivà M, Montserrat-Sentís B, Baró T, Garrido M, Bonilla F, Virtanen I, García de Herreros A. Expression of Snail protein in the tumor-stroma interface. *Oncogene* **25**, 5134-5144 (2006).
50. Zhang, K., *et al.* The collagen receptor discoidin domain receptor 2 stabilizes SNAIL1 to facilitate breast cancer metastasis. *Nature cell biology* **15**, 677-687 (2013).
51. Auersperg, N., Wong, A.S., Choi, K.C., Kang, S.K. & Leung, P.C. Ovarian surface epithelium: biology, endocrinology, and pathology. *Endocr Rev* **22**, 255-288 (2001).
52. Davidowitz, R.A., *et al.* Mesenchymal gene program-expressing ovarian cancer spheroids exhibit enhanced mesothelial clearance. *The Journal of clinical investigation* **124**, 2611-2625 (2014).

53. Terauchi, M., *et al.* Possible involvement of TWIST in enhanced peritoneal metastasis of epithelial ovarian carcinoma. *Clinical & experimental metastasis* **24**, 329-339 (2007).
54. Wang, Y.L., *et al.* Snail promotes epithelial-mesenchymal transition and invasiveness in human ovarian cancer cells. *International journal of clinical and experimental medicine* **8**, 7388-7393 (2015).
55. Grigore, A.D., Jolly, M.K., Jia, D., Farach-Carson, M.C. & Levine, H. Tumor Budding: The Name is EMT. Partial EMT. *J Clin Med* **5**(2016).
56. Kalluri, R. & Weinberg, R.A. The basics of epithelial-mesenchymal transition. *The Journal of clinical investigation* **119**, 1420-1428 (2009).
57. Beerling, E., *et al.* Plasticity between Epithelial and Mesenchymal States Unlinks EMT from Metastasis-Enhancing Stem Cell Capacity. *Cell reports* **14**, 2281-2288 (2016).
58. Paul, M.K. & Mukhopadhyay, A.K. Tyrosine kinase - Role and significance in Cancer. *Int J Med Sci* **1**, 101-115 (2004).
59. Lemmon, M.A. & Schlessinger, J. Cell signaling by receptor tyrosine kinases. *Cell* **141**, 1117-1134 (2010).
60. Maruyama, I.N. Mechanisms of activation of receptor tyrosine kinases: monomers or dimers. *Cells* **3**, 304-330 (2014).
61. Yeung, D., Chmielewski, D., Mihai, C. & Agarwal, G. Oligomerization of DDR1 ECD affects receptor-ligand binding. *J Struct Biol* **183**, 495-500 (2013).
62. Coelho, N.M., *et al.* Discoidin Domain Receptor 1 Mediates Myosin-Dependent Collagen Contraction. *Cell reports* **18**, 1774-1790 (2017).
63. Volinsky, N. & Kholodenko, B.N. Complexity of receptor tyrosine kinase signal processing. *Cold Spring Harb Perspect Biol* **5**, a009043 (2013).
64. Schlessinger, J. Cell signaling by receptor tyrosine kinases. *Cell* **103**, 211-225 (2000).

65. Rauch, J., Volinsky, N., Romano, D. & Kolch, W. The secret life of kinases: functions beyond catalysis. *Cell communication and signaling : CCS* **9**, 23 (2011).
66. Weihua, Z., *et al.* Survival of cancer cells is maintained by EGFR independent of its kinase activity. *Cancer Cell* **13**, 385-393 (2008).
67. Aqeilan, R.I., *et al.* WW domain-containing proteins, WWOX and YAP, compete for interaction with ErbB-4 and modulate its transcriptional function. *Cancer research* **65**, 6764-6772 (2005).
68. Grunwald, I.C., *et al.* Kinase-independent requirement of EphB2 receptors in hippocampal synaptic plasticity. *Neuron* **32**, 1027-1040 (2001).
69. Sangwan, V. & Park, M. Receptor tyrosine kinases: role in cancer progression. *Curr Oncol* **13**, 191-193 (2006).
70. Arteaga, C.L. & Engelman, J.A. ERBB receptors: from oncogene discovery to basic science to mechanism-based cancer therapeutics. *Cancer Cell* **25**, 282-303 (2014).
71. Arora, A. & Scholar, E.M. Role of tyrosine kinase inhibitors in cancer therapy. *The Journal of pharmacology and experimental therapeutics* **315**, 971-979 (2005).
72. Tvorogov, D., *et al.* Effective suppression of vascular network formation by combination of antibodies blocking VEGFR ligand binding and receptor dimerization. *Cancer Cell* **18**, 630-640 (2010).
73. Sierra, J.R., Cepero, V. & Giordano, S. Molecular mechanisms of acquired resistance to tyrosine kinase targeted therapy. *Molecular cancer* **9**, 75 (2010).
74. Fauvel, B. & Yasri, A. Antibodies directed against receptor tyrosine kinases: current and future strategies to fight cancer. *MAbs* **6**, 838-851 (2014).
75. Azam, M., Seeliger, M.A., Gray, N.S., Kuriyan, J. & Daley, G.Q. Activation of tyrosine kinases by mutation of the gatekeeper threonine. *Nat Struct Mol Biol* **15**, 1109-1118 (2008).

76. Vogel, W., Gish, G.D., Alves, F. & Pawson, T. The discoidin domain receptor tyrosine kinases are activated by collagen. *Molecular cell* **1**, 13-23 (1997).
77. Shrivastava A, R.C., Campbell E, Kovac L, McGlynn M, Ryan TE, Davis S, Goldfarb MP, Glass DJ, Lemke G, Yancopoulos GD. An Orphan Receptor Tyrosine Kinase Family Whose Members Serve as Nonintegrin Collagen Receptors. *Mol. Cell* **1**, 25-34 (1997).
78. Fu, H.L., *et al.* Discoidin domain receptors: unique receptor tyrosine kinases in collagen-mediated signaling. *The Journal of biological chemistry* **288**, 7430-7437 (2013).
79. Ichikawa, O., *et al.* Structural basis of the collagen-binding mode of discoidin domain receptor 2. *The EMBO journal* **26**, 4168-4176 (2007).
80. Carafoli, F., *et al.* Crystallographic insight into collagen recognition by discoidin domain receptor 2. *Structure* **17**, 1573-1581 (2009).
81. Carafoli, F., *et al.* Structure of the discoidin domain receptor 1 extracellular region bound to an inhibitory Fab fragment reveals features important for signaling. *Structure* **20**, 688-697 (2012).
82. Baumgartner, S., Hofmann, K., Chiquet-Ehrismann, R. & Bucher, P. The discoidin domain family revisited: new members from prokaryotes and a homology-based fold prediction. *Protein Sci* **7**, 1626-1631 (1998).
83. Leitinger, B. Molecular Analysis of Collagen Binding by the Human Discoidin Domain Receptors, DDR1 and DDR2. *The Journal of biological chemistry* **278**, 16761-16769 (2003).
84. Vogel, W.F., Abdulhusein, R. & Ford, C.E. Sensing extracellular matrix: an update on discoidin domain receptor function. *Cell Signal* **18**, 1108-1116 (2006).
85. Konitsiotis, A.D., *et al.* Characterization of high affinity binding motifs for the discoidin domain receptor DDR2 in collagen. *The Journal of biological chemistry* **283**, 6861-6868 (2008).

86. H. Kato, Z.L., J. Mitsios, HY Wang, E. Deryugina, J Varner, J Quigley, S.Shattil. The Primacy of Beta1 Integrin Activation in the Metastatic Cascade. *PLOS One* **7**, e46576 (2012).
87. Knight, C.G., *et al.* The collagen-binding A-domains of integrins alpha(1)beta(1) and alpha(2)beta(1) recognize the same specific amino acid sequence, GFOGER, in native (triple-helical) collagens. *The Journal of biological chemistry* **275**, 35-40 (2000).
88. Xu H, R.N., Stathopoulos S, Myllyharju J, Farndale RW, Leitinger B. Collagen binding specificity of the discoidin domain receptors: Binding sites on collagens II and III and molecular determinants for collagen IV recognition by DDR1. *Matrix Biology* **30**, 16-26 (2011).
89. Mihai, C., Chotani, M., Elton, T.S. & Agarwal, G. Mapping of DDR1 distribution and oligomerization on the cell surface by FRET microscopy. *Journal of molecular biology* **385**, 432-445 (2009).
90. Noordeen, N.A., Carafoli, F., Hohenester, E., Horton, M.A. & Leitinger, B. A transmembrane leucine zipper is required for activation of the dimeric receptor tyrosine kinase DDR1. *The Journal of biological chemistry* **281**, 22744-22751 (2006).
91. Leitinger, B. Discoidin domain receptor functions in physiological and pathological conditions. *International review of cell and molecular biology* **310**, 39-87 (2014).
92. Vogel, W.F., Aszodi, A., Alves, F. & Pawson, T. Discoidin domain receptor 1 tyrosine kinase has an essential role in mammary gland development. *Mol Cell Biol* **21**, 2906-2917 (2001).
93. Labrador JP, A.V., Tuckermann J, Lin C, Olaso E, Mañes S, Brückner K, Goergen JL, Lemke G, Yancopoulos G, Angel P, Martínez C, Klein R. The collagen receptor DDR2 regulates proliferation and its elimination leads to dwarfism. *EMBO Reports* **2**, 446-452 (2001).
94. Bargal, R., *et al.* Mutations in DDR2 gene cause SMED with short limbs and abnormal calcifications. *Am J Hum Genet* **84**, 80-84 (2009).

95. Kano, K., *et al.* A novel dwarfism with gonadal dysfunction due to loss-of-function allele of the collagen receptor gene, Ddr2, in the mouse. *Mol Endocrinol* **22**, 1866-1880 (2008).
96. Afonso, P.V., McCann, C.P., Kapnick, S.M. & Parent, C.A. Discoidin domain receptor 2 regulates neutrophil chemotaxis in 3D collagen matrices. *Blood* **121**, 1644-1650 (2013).
97. Olaso, E., *et al.* Discoidin domain receptor 2 regulates fibroblast proliferation and migration through the extracellular matrix in association with transcriptional activation of matrix metalloproteinase-2. *The Journal of biological chemistry* **277**, 3606-3613 (2002).
98. Valiathan, R.R., Marco, M., Leitinger, B., Kleer, C.G. & Fridman, R. Discoidin domain receptor tyrosine kinases: new players in cancer progression. *Cancer metastasis reviews* **31**, 295-321 (2012).
99. Corsa, C.A., *et al.* The Action of Discoidin Domain Receptor 2 in Basal Tumor Cells and Stromal Cancer-Associated Fibroblasts Is Critical for Breast Cancer Metastasis. *Cell reports* **15**, 2510-2523 (2016).
100. Ren, T., *et al.* Discoidin domain receptor 2 (DDR2) promotes breast cancer cell metastasis and the mechanism implicates epithelial-mesenchymal transition programme under hypoxia. *J Pathol* **234**, 526-537 (2014).
101. Yan, Z., *et al.* Discoidin domain receptor 2 facilitates prostate cancer bone metastasis via regulating parathyroid hormone-related protein. *Biochimica et biophysica acta* **1842**, 1350-1363 (2014).
102. Rodrigues, R., *et al.* Comparative genomic hybridization, BRAF, RAS, RET, and oligo-array analysis in aneuploid papillary thyroid carcinomas. *Oncol Rep* **18**, 917-926 (2007).
103. Chua, H.H., *et al.* Upregulation of discoidin domain receptor 2 in nasopharyngeal carcinoma. *Head & neck* **30**, 427-436 (2008).
104. Xie, B., *et al.* DDR2 facilitates hepatocellular carcinoma invasion and metastasis via activating ERK signaling and stabilizing SNAIL1. *Journal of experimental & clinical cancer research : CR* **34**, 101 (2015).

105. Hammerman PS, S.M., Ramos AH, et al. Mutations in the DDR2 Kinase Gene Identify a Novel Therapeutic Target in Squamous Cell Lung Cancer. *Cancer Discovery* **1**, 78-89 (2011).
106. Xu, J., et al. Overexpression of DDR2 contributes to cell invasion and migration in head and neck squamous cell carcinoma. *Cancer biology & therapy* **15**, 612-622 (2014).
107. Ren, T., Zhang, J., Zhang, J., Liu, X. & Yao, L. Increased expression of discoidin domain receptor 2 (DDR2): a novel independent prognostic marker of worse outcome in breast cancer patients. *Medical oncology* **30**, 397 (2013).
108. Zhang, S., et al. A host deficiency of discoidin domain receptor 2 (DDR2) inhibits both tumour angiogenesis and metastasis. *J Pathol* **232**, 436-448 (2014).
109. Hammerman, P.S., et al. Mutations in the DDR2 kinase gene identify a novel therapeutic target in squamous cell lung cancer. *Cancer discovery* **1**, 78-89 (2011).
110. Walsh, L.A., Nawshad, A. & Medici, D. Discoidin domain receptor 2 is a critical regulator of epithelial-mesenchymal transition. *Matrix biology : journal of the International Society for Matrix Biology* **30**, 243-247 (2011).
111. Maeyama, M., et al. Switching in discoid domain receptor expressions in SLUG-induced epithelial-mesenchymal transition. *Cancer* **113**, 2823-2831 (2008).
112. Sivakumar, L. & Agarwal, G. The influence of discoidin domain receptor 2 on the persistence length of collagen type I fibers. *Biomaterials* **31**, 4802-4808 (2010).
113. Xu, L., et al. Activation of the discoidin domain receptor 2 induces expression of matrix metalloproteinase 13 associated with osteoarthritis in mice. *The Journal of biological chemistry* **280**, 548-555 (2005).
114. Xu, L., et al. Increased expression of the collagen receptor discoidin domain receptor 2 in articular cartilage as a key event in the pathogenesis of osteoarthritis. *Arthritis and rheumatism* **56**, 2663-2673 (2007).

115. Xu, L., *et al.* Intact pericellular matrix of articular cartilage is required for unactivated discoidin domain receptor 2 in the mouse model. *The American journal of pathology* **179**, 1338-1346 (2011).
116. Xu, L., *et al.* Attenuation of osteoarthritis progression by reduction of discoidin domain receptor 2 in mice. *Arthritis and rheumatism* **62**, 2736-2744 (2010).
117. Salazar, A., Polur, I., Servais, J.M., Li, Y. & Xu, L. Delayed progression of condylar cartilage degeneration, by reduction of the discoidin domain receptor 2, in the temporomandibular joints of osteoarthritic mouse models. *Journal of oral pathology & medicine : official publication of the International Association of Oral Pathologists and the American Academy of Oral Pathology* **43**, 317-321 (2014).
118. Su, J., *et al.* Discoidin domain receptor 2 is associated with the increased expression of matrix metalloproteinase-13 in synovial fibroblasts of rheumatoid arthritis. *Molecular and cellular biochemistry* **330**, 141-152 (2009).
119. Huang, T.L., *et al.* DDR2-CYR61-MMP1 Signaling Pathway Promotes Bone Erosion in Rheumatoid Arthritis Through Regulating Migration and Invasion of Fibroblast-Like Synoviocytes. *Journal of bone and mineral research : the official journal of the American Society for Bone and Mineral Research* **32**, 407-418 (2017).
120. Wang, J., *et al.* Functional analysis of discoidin domain receptor 2 in synovial fibroblasts in rheumatoid arthritis. *J Autoimmun* **19**, 161-168 (2002).
121. Zhao, H., *et al.* Targeting of Discoidin Domain Receptor 2 (DDR2) Prevents Myofibroblast Activation and Neovessel Formation During Pulmonary Fibrosis. *Molecular therapy : the journal of the American Society of Gene Therapy* (2016).
122. Olaso, E., Arteta, B., Benedicto, A., Crende, O. & Friedman, S.L. Loss of discoidin domain receptor 2 promotes hepatic fibrosis after chronic carbon tetrachloride through altered paracrine interactions between hepatic stellate cells and liver-associated macrophages. *The American journal of pathology* **179**, 2894-2904 (2011).
123. Olaso, E., *et al.* DDR2 receptor promotes MMP-2-mediated proliferation and invasion by hepatic stellate cells. *The Journal of clinical investigation* **108**, 1369-1378 (2001).

124. Luo, Z., *et al.* RNA interference against discoidin domain receptor 2 ameliorates alcoholic liver disease in rats. *PloS one* **8**, e55860 (2013).
125. Rowe, R.G., *et al.* Hepatocyte-derived Snail1 propagates liver fibrosis progression. *Molecular and cellular biology* **31**, 2392-2403 (2011).
126. Richters, A., *et al.* Identification of type II and III DDR2 inhibitors. *Journal of medicinal chemistry* **57**, 4252-4262 (2014).
127. Terai, H., *et al.* Characterization of DDR2 Inhibitors for the Treatment of DDR2 Mutated Non-small Cell Lung Cancer. *ACS chemical biology* **10**, 2687-2696 (2015).
128. Siddiqui, K., *et al.* Actinomycin D identified as an inhibitor of discoidin domain receptor 2 interaction with collagen through an insect cell based screening of a drug compound library. *Biological & pharmaceutical bulletin* **32**, 136-141 (2009).
129. Borza, C.M. & Pozzi, A. Discoidin domain receptors in disease. *Matrix biology : journal of the International Society for Matrix Biology* **34**, 185-192 (2014).
130. Beauchamp, E.M., *et al.* Acquired resistance to dasatinib in lung cancer cell lines conferred by DDR2 gatekeeper mutation and NF1 loss. *Molecular cancer therapeutics* **13**, 475-482 (2014).

## **Chapter 2**

### **Inhibition of Tumor-Microenvironment Interactions and Metastasis by a Small-Molecule Allosteric Inhibitor of DDR2 Extracellular Domain**

This chapter has been adapted from a submitted manuscript and also contains unpublished data.

The citation for the submitted manuscript is:

Whitney R. Grither and Gregory D. Longmore. Inhibition of Tumor-Microenvironment Interactions and Metastasis by a Small-Molecule Allosteric Inhibitor of DDR2 Extracellular Domain. In revision, 2017.

## **Introduction**

With advances in the management of local breast cancers, metastatic spread is now responsible for greater than 90% of breast cancer-related deaths. Crosstalk between tumor cells and their surrounding cellular, chemical, and physical microenvironment is now appreciated to influence breast tumor development, progression, metastasis, and response to treatment<sup>1,2</sup>. In breast tumors, these stromal components differ from their normal tissue counterparts in composition, architecture, and function. Therefore, a proposed reason for the limited success of current therapies in the metastatic setting is the lack of modulating both tumor cells and the tumor microenvironment<sup>3</sup>.

Collagen fibers are the most abundant protein within the extracellular matrix (ECM) of breast tumor stroma and play key roles in breast cancer development and progression<sup>4</sup>. Increased collagen deposition contributes to breast density and women with dense breasts have an increased risk for developing aggressive breast cancers<sup>5</sup>. Excessive collagen deposition, altered collagen fiber organization, and the resulting alterations in mechanical properties of the breast tumor stroma are all correlated with more aggressive disease and poor outcome<sup>6</sup>.

Receptor Tyrosine Kinases (RTKs) are well appreciated therapeutic targets for the treatment of cancer<sup>7</sup>. A defining feature of all RTKs is the presence of an extracellular ligand binding domain<sup>8</sup>. The ligands that activate these receptors are typically polypeptide growth factors or cytokines, with one distinct exception - the Discoidin Domain Receptor family. Their ligand is fibrillar collagen, a structural

protein<sup>9,10</sup>. Recent human clinical data and preclinical mouse genetic models have established Discoidin Domain Receptor 2 (DDR2) as a potential therapeutic target for the treatment of cancer metastasis. DDR2 expression is associated with cancer metastasis in a number of different human cancers types including: breast<sup>11-14</sup>, prostate<sup>15</sup>, papillary thyroid<sup>16</sup>, nasopharyngeal<sup>17</sup>, hepatocellular<sup>18</sup>, lung squamous cell<sup>19</sup>, and head and neck squamous cell<sup>20</sup> carcinomas. In regards to breast cancer, the function of DDR2 in both tumor cells<sup>11,13</sup> and tumor stroma cells<sup>14</sup> has been shown to play a role in metastasis.

While not expressed in normal breast epithelium, DDR2 expression is induced in the majority of human invasive ductal carcinomas. In breast tumor cells the action of DDR2 sustains their invasive and migratory capacity by maintaining the cellular level and activity of SNAIL1, an epithelial mesenchymal transition (EMT) inducer important for breast cancer metastasis<sup>11,21-23</sup>. In the breast tumor stroma, the action of DDR2 in cancer associated fibroblasts (CAFs) influences extracellular matrix (ECM) synthesis and remodeling<sup>14,24</sup> leading to a more pro-invasive collagen organization<sup>14</sup>. DDR2 action in CAFs also influences the invasiveness of breast tumor cells, through a paracrine function<sup>14</sup>. Together, these data suggest that DDR2 could be an important target for the development of inhibitors capable of modulating both the tumor cell and microenvironment, concurrently.

Most drugs targeting RTKs are of two classes. The first are receptor antibodies that block ligand binding, receptor dimerization, or alter receptor internalization<sup>25,26</sup>. Second, small molecule tyrosine kinase inhibitors (TKIs) that interact with the intracellular kinase domain have been developed<sup>27,28</sup>. While TKIs inhibiting DDR2 have

been identified, these compounds exhibit only a preference for DDR2 inhibition and show significant inhibitory profiles towards other kinases<sup>29,30</sup>. Effective and lasting use of traditional TKI strategies have also been hampered by the emergence of drug resistance<sup>28</sup>. Indeed, acquired gatekeeper mutations in DDR2 treated with TKIs have already been reported<sup>31</sup>. Therefore, development of inhibitors of DDR2 with alternative mechanisms of action could be highly advantageous.

Although allosteric modulators for ligand-gated ion channels and G protein-coupled receptors have been identified, only recently has a small molecule allosteric regulator that targets the extracellular domain of an RTK been described<sup>32,33</sup>. Non-classical small molecule inhibitors that disrupt protein complexes have been reported<sup>34,35</sup>, but no such inhibitors exist for RTKs. Allosteric or non-classical small molecule inhibitors of RTKs offer significant therapeutic advantages, such as increased selectivity and safety<sup>36,37</sup>. Here we describe the identification and characterization of an extracellularly acting small molecule inhibitor of DDR2 that functions in an allosteric manner to disrupt DDR2 receptor-collagen ligand interaction.

## **Results**

### **Identification of a selective, small molecule inhibitor of DDR2 binding to collagen I and receptor activation by collagen I**

In a high-throughput *in vitro* screen for inhibitors of DDR2 binding to type I collagen, the natural antibiotic Actinomycin D was identified as a weak inhibitor<sup>38</sup>. We confirmed this (Figure 2.1A). Due to its low potency and high toxicity profile<sup>39</sup>, Actinomycin D would not be considered a clinically suitable inhibitor of DDR2. Therefore, we asked whether deconstruction of Actinomycin D to various component chemical scaffolds might identify the active portion, allowing for further derivatization to develop lower toxicity, higher potency inhibitors.

To do so, we adapted a DDR2 binding assay<sup>40</sup>. Dimeric DDR2 extracellular domain, consisting of the discoidin (DS) and discoidin-like (DSL) domain with a C-terminal myc and his tag (DDR2-his), was shown to bind a DDR2-selective collagen II triple helical peptide with high affinity<sup>41,42</sup> (Figure 2.1B). We then tested compounds that contained elements of structural overlap with Actinomycin D and found that the scaffold 7-hydroxy-phenoxazin-3-one inhibited DDR2 binding with an IC<sub>50</sub> of 16μM (Figures 2.1A and 2.3A). Medicinal chemistry based optimization was performed to generate a library of lead compounds (Figure 2.2) with higher inhibitory activity towards DDR2-ligand binding (Figure 2.3A). One of these, WRG-28 (Figures 2.2 and 2.3B), showed moderate potency as an antagonist of DDR2-ligand binding (IC<sub>50</sub> 230±75nM) (Figures 2.1A and 2.3A) and was chosen for further study. We further confirmed that WRG-28 was not irreversibly modifying DDR2 by incubating recombinant DDR2-his protein with WRG-28,

followed 2 rounds of dialysis, and then the dialyzed protein was subjected to binding in the in vitro assay. After dialysis to remove the compound, the protein was once again able to bind collagen, indicating an irreversible mechanism was not at play (Figure 2.3C). Further, to rule out a redox based mechanism of action, we performed the in vitro binding assay in the presence of 1mM glutathione as a redox trap. The presence of glutathione did not substantially affect the inhibitory ability of WRG-28 (Figure 2.3D), suggesting that a redox mediated mechanism of action is not likely.

WRG-28 also blunted collagen I-mediated DDR2 activation (tyrosine phosphorylation) in HEK293 cells expressing DDR2 (HEK-DDR2) (Figure 2.4A). Activation of DDR2 by collagen I can lead to increased SNAIL1 protein level in cells via an ERK2 mediated pathway<sup>11</sup>. When HEK-DDR2 cells were stimulated with collagen I, phospho-ERK2 levels increased, and treatment with 1 $\mu$ M WRG-28 inhibited phosphorylation of ERK2 and reduced SNAIL1 protein level (Figure 2.4B). WRG-28 was not nonspecifically toxic to cells, as treatment (1 $\mu$ M) of non-DDR2 expressing, normal mammary epithelial MCF10A cells did not affect their proliferation or survival (Figure 2.4C).

To determine if the inhibitory activity of WRG-28 was selective for DDR2, we asked whether it inhibited collagen mediated activation of the homologous family member DDR1. DDR1 tyrosine phosphorylation in HEK293 cells expressing DDR1 was unaffected by the presence of WRG-28 (Figure 2.4D). Furthermore, using biolayer interferometry (BLI) when biotinylated DDR2 or DDR1 was immobilized on a streptavidin-coated BLI pin, dose dependent association of WRG-28 was seen for DDR2, but not DDR1 (Figure 2.5A-C). Additionally, in an analogous solid phase binding

assay as that used for DDR2, WRG-28 did not inhibit the unrelated collagen I receptor  $\alpha 1\beta 1$  integrin extracellular domain from binding to its high affinity collagen I triple helical peptide<sup>43</sup> (Figure 2.5D). WRG-28 treatment did not affect phosphorylation of other unrelated RTKs, as determined by a PathScan RTK signaling array (Figure 2.6A).

In summary, in *in vitro* binding and cell-based assays WRG-28 appeared to be a potent and selective small molecule inhibitor of DDR2 extracellular domain binding to collagen I, and inhibited collagen I mediated DDR2 activation in cells.

### **WRG-28 inhibits DDR2-Collagen I interaction in an allosteric manner**

Since no extracellular domain inhibitors of DDR2 have been described, we sought to determine the mode of inhibition of WRG-28. First, we asked whether a classical competitive mechanism was utilized. Using a fluorescein conjugated analog of the collagen II binding peptide for DDR2, we confirmed that when increasing amounts of collagen II peptide were added to plates, increased peptide was adsorbed onto the plates (Figure 2.7A). In the range of substrate concentrations examined, linear adsorption of the DDR2 binding collagen II peptide was observed, and was not reduced upon washing (Figure 2.7A). Fluorescein conjugation did not alter DDR2 binding to collagen II peptide (Figure 2.7B). Using the amount of collagen II peptide plated as a measure of available ligand, the availability of increasing concentration of collagen II peptide did not outcompete the inhibitory effects of WRG-28 (Figure 2.7C). This result suggested that WRG-28 was likely not acting as a strong orthosteric inhibitor of collagen binding.

Next, we asked whether WRG-28 could displace DDR2 from pre-bound DDR2-collagen II peptide ligand complex. After allowing the receptor-ligand complex to reach equilibrium, the complex was treated with buffer containing WRG-28 or control DMSO. In the absence of inhibitor there was very little dissociation of DDR2 over the 90 minutes assayed (Figure 2.7D). However, in the presence of WRG-28, there was a dramatic acceleration of DDR2 dissociation in a dose dependent manner (Figure 2.7D).

Previous reports using similar solid phase assays showed that for DDR2 to bind collagen it must exist as at least a dimer<sup>40</sup> or possibly higher order multimers<sup>44</sup>. Therefore, we asked whether WRG-28 effects on DDR2 ligand binding and signaling resulted from an impairment or disruption of receptor dimerization or multimerization. To do so, we made use of a DDR2 extracellular domain protein where dimerization is covalently fused by the addition of an Fc tag to the C-terminus of the DS-like domain (DDR2-Fc)<sup>45</sup>. In the solid phase binding assay, the ability of WRG-28 to inhibit DDR2-Fc binding to collagen II peptide was dramatically reduced (Figure 2.7E), suggesting that inhibition by WRG-28 could be due to DDR2 dimer or multimer disruption.

To further test this possibility, we analyzed the organization of the DDR2 extracellular domain in the presence or absence of WRG-28 by size exclusion chromatography. Consistent with previous reports, in solution ~20% of the DDR2 extracellular domain (DS-DSL) eluted as an oligomer, while the majority existed as dimers, with very little monomer present (Figure 2.8A). To assign peaks, elution fractions were concentrated, run on a native gel, and compared to the DDR2 protein solution added to the column (Figure 2.8B). When the DDR2 protein solution was treated with 1 $\mu$ M of WRG-28, the oligomer fraction was significantly reduced (Figures 2.8A and

2.8C). There also appeared to be an increase in the monomeric state, however as the monomer often appeared as a shoulder of the dimer peak and was not well resolved, it could not be accurately quantified (Figure 2.8E). Additionally, the DDR2 oligomeric and dimeric peaks were collected, protein concentration normalized, and subjected to *in vitro* binding analysis using the solid phase assay (Figure 2.8D). In this assay, the oligomeric species bound to the collagen II peptide with nearly three fold affinity, illustrating the functional relevance of this higher order species.

In another approach, we performed chemical cross-linking experiments of HEK293-DDR2 cells with the membrane-impermeable cross-linker BS<sup>3</sup>. Consistent with previous reports, full length DDR2 existed as dimers on the cell surface in the absence of collagen (Figure 2.8F)<sup>46</sup>. When HEK293-DDR2 cells were treated with WRG-28, we did not detect significant disruption of cell surface DDR2 dimerization (Figure 2.8F). This could be due to the fact that in cells DDR dimerization is strongly influenced by the transmembrane domain<sup>46</sup>. While inhibition of extracellular domain clustering by WRG-28 appeared to be sufficient to blunt receptor activation (Figure 2.4A), WRG-28 was not capable of complete disruption of full-length, cell surface dimers.

In sum, these results were consistent with non-active site receptor modulation by WRG-28 as contributing to its inhibitory action on the DDR2-collagen interaction. This is consistent with allosteric regulation of DDR2 activity by WRG-28, potentially due to impairment in clustering of the extracellular domain.

## Identification of DS-DSL domain interface residues required for DDR2-collagen binding and signaling

The extracellular portion of the DDR proteins consists of 3 domains—the N-terminal collagen binding discoidin (DS) domain, a DDR unique discoidin-like (DSL) domain, and a short membrane proximal juxtamembrane domain. The collagen binding motif is in the DS domain and highly conserved between DDR1 and DDR2<sup>47</sup>. To gain further insight into the structural determinants of DDR2 inhibition by WRG-28, we employed *in silico* modeling. SWISS-MODEL<sup>48-50</sup> was used to construct a homology model of the three-dimensional structure of the DDR2 extracellular domain, using the existing crystal structure of the DDR1 extracellular domain. This structure and the resulting model contain the DS and DS-like domains but lack the juxtamembrane domain (PDB: 4AG4)<sup>51</sup>. In order to identify putative WRG-28 binding sites, *in silico* docking analysis with AutoDock Vina<sup>52</sup> was performed against the homology model of the DDR2. Of the top 9 WRG-28 binding solutions to arise from these studies, 5 low energy conformations clustered around a similar site located at the DS-DSL domains interface region (Figure 2.9A-D). Such interface binding can be a common mode of action of allosteric inhibitors<sup>53,54</sup>, as conformational changes along interfaces are often needed for proper receptor function<sup>55</sup>.

In the lowest energy configuration, several key interactions were suggested (Figure 2.9D). These included polar contacts with Arg135, Glu247, Thr98, and hydrophobic interactions with Phe96, Trp187. Residues within the interdomain region have been shown to make important interdomain contacts in the crystallized structure of DDR1<sup>51</sup>. WRG-28 did not show inhibitory activity against the highly homologous family

member DDR1, despite 53% sequence identity shared between the extracellular domains of the two proteins. Among the interface region, two key potential interacting residues, Phe96 and Thr98, are not conserved between DDR2 and DDR1 (DDR1: Leu96 and Ala98, respectively). Assuming similar modes of activation between DDR2 and DDR1 this divergence could correspond to functional importance for WRG-28 action against DDR2.

Single F96A or T98A point mutations in DDR2 showed no appreciable effect on DDR2 binding to collagen *in vitro*, phosphorylation in cells, or inhibition by WRG-28 (Figures 2.10A-C). However, when we produced the extracellular domain of a DDR2<sup>F96A/T98A</sup> double mutant as a recombinant protein, it no longer bound to the collagen II peptide at concentrations of peptide where binding was saturated for the wild type DDR2 receptor (Figure 2.10D). Interestingly, when DDR2<sup>F96A/T98A</sup> was analyzed by size exclusion chromatography it existed only as a dimer fraction with virtually no higher order oligomers in solution (Figure 2.10E). This further suggested that receptor clustering may be important for receptor binding to collagen ligand in solid phase assays. DDR2<sup>F96A/T98A</sup> expressed as a full length receptor in HEK293 cells was present at the cell surface and dimerized (Figures 2.10G and 2.10H). However, collagen mediated DDR2<sup>F96A/T98A</sup> receptor activation in cells was dramatically reduced compared to wild type receptor (Figure 2.10F).

As these two residues are not conserved between DDR1 and DDR2, and the inhibitory action of WRG-28 is selective for DDR2, we asked whether we could confer inhibition by WRG-28 on DDR1 by replacing Leu96 and Ala98 residues in DDR1 with the key interacting residues of the DDR2 counterpart (Phe and Thr, respectively). When

a DDR1<sup>L96F/A98T</sup> mutant was expressed in HEK293 cells and subjected to treatment with WRG-28, unlike wild type DDR1 (2.4D), DDR1<sup>L96F/A98T</sup> exhibited diminished phosphorylation in response to collagen in the presence of WRG-28 (Figure 2.10I).

Mutants made within an alternative, lower probability WRG-28 binding site (Site 3, Figure 2.9A) within DDR2 did not affect collagen II peptide binding, collagen-induced receptor phosphorylation, or WRG-28 inhibitory activity (Figures 2.11A-E).

In sum, these modeling studies coupled with *in vitro* and cell based experiments of putative WRG-28 interacting receptor mutants, suggested that Phe96 and Thr98 residues in DDR2 are critical for sustained receptor interaction with collagen *in vitro*, and receptor activation in cells. Moreover, by introducing these two residues into DDR1, they appeared, in part, to be responsible for directing WRG-28 inhibition of DDR2.

### **WRG-28 inhibition of DDR2 blunts tumor cell invasion and migration**

Previous genetic studies in cell lines and *in vivo* have shown that the action of DDR2 in breast tumor cells is critical for invasion and migration, without affecting tumor proliferation<sup>11,13,14</sup>. Treatment of BT549 human breast cancer cells (endogenous DDR2 expression) with WRG-28 inhibited their invasion/migration in 3D collagen I matrices to an extent comparable to BT549 cells RNAi-depleted of DDR2 (Figure 2.12A and 2.12B). Treatment of BT549 cells with WRG-28 did not affect their proliferation (Figure 2.12C). WRG-28 also inhibited invasion of BT549 human breast cancer cells and 4T1 murine breast cancer cells through Matrigel (Figure 2.12D-F) to an extent comparable to that of DDR2 RNAi-depletion controls. In BT549 cells and 4T1 murine breast cancer cells,

WRG-28 treatment also inhibited SNAIL1 protein stabilization in response to exposure to collagen (Figure 2.13A and 2.13B)

### **WRG-28 shows efficacy against DDR2 gatekeeper mutations**

One of the most common setbacks to canonical TKIs is the eventual development of resistance mutations<sup>28</sup>. Within the RTK family, gatekeeper mutations are a common mode of resistance, and these have been documented in DDR2 as well<sup>31</sup>. To test whether WRG-28 maintained efficacy against DDR2 gatekeeper mutations, a DDR2 mutant containing a T654I mutation (documented gatekeeper mutation in DDR2<sup>31</sup>) was expressed in HEK293 cells. Consistent with conferring its inhibitory action via the extracellular domain, WRG-28 inhibited phosphorylation of the DDR2<sup>T654I</sup> mutant in response to collagen I (Figure 2.13C). This result suggested the potential utility of WRG-28 as an alternative to kinase directed inhibition or in cases where resistance to TKIs have been acquired through gatekeeper mutations to DDR2.

### **Targeting DDR2 with WRG-28 blocks tumor promoting effects of the microenvironment**

In addition to tumor cell intrinsic prometastatic roles, the action of DDR2 in tumor stromal cells also plays an important role in regulation of metastasis<sup>14</sup>. In particular, the action of DDR2 in cancer associated fibroblasts (CAFs) influences their tumor promoting function by regulating tumor ECM production and remodeling, as well as

mediating paracrine signals that enhance the collective invasiveness of tumor cells<sup>14</sup>. To assess the ability of WRG-28 to modulate such CAF effects, primary MMTV-PyMT; *Ddr2*<sup>+/+</sup>; ROSA-LSL-TdTomato or MMTV-PyMT; *Ddr2*<sup>-/-</sup>; ROSA-LSL-TdTomato breast mouse tumor organoids were plated in a 3D collagen I matrix with mouse CAFs derived from MMTV-PyMT; *Ddr2*<sup>+/+</sup> or MMTV-PyMT; *Ddr2*<sup>-/-</sup> breast tumors, in the presence or absence of WRG-28 and the number of invasive organoids scored. Treatment of *Ddr2*<sup>+/+</sup> tumor organoids alone with WRG-28 reduced the number of invasive tumor organoids to a level comparable to that seen with *Ddr2*<sup>-/-</sup> tumor organoids (Figure 6.14A-E, quantified in 6.14F). Addition of *Ddr2*<sup>+/+</sup> CAFs to *Ddr2*<sup>+/+</sup> tumor organoids increased the number of invasive organoids present, as anticipated<sup>14</sup> (Figure 6.14A-E, quantified in 6.14F). WRG-28 treatment potently reduced the number of invasive tumor organoids, to a level equivalent to that observed when *Ddr2*<sup>-/-</sup> breast tumor organoids and *Ddr2*<sup>-/-</sup> CAFs were co-cultured (Figure 6.14A-E, quantified in 6.14F). Expression of Tomato was used to confirm that invasive foci were composed of invading tumor cells and not CAFs that had migrated to the tumors (Figure 6.14G). PI/annexin V staining confirmed that the reduction in invasion was not due to toxic effects of WRG-28 (Figure 6.14H and 6.14I). These data indicated that not only did WRG-28 inhibit 3D collagen tumor organoid invasion but also the activity of DDR2 in CAFs to support invasion of tumor organoids. Thus, WRG-28 inhibited DDR2 action in both breast tumor cells as well as breast tumor stroma CAFs, in these culture systems.

Additionally, DDR2 has been reported to promote the migratory ability of fibroblasts<sup>56,57</sup>. We therefore tested the ability of the developed inhibitor to influence migration of normal mouse fibroblasts, or mouse tumor derived CAFs in a scratch

wound assay. WRG-28 showed inhibitory effect on the migratory ability of these fibroblasts at 24 hours (Figure 6.14J), indicating that inhibition of DDR2 dependent migratory effects in fibroblasts could also be attenuated with the compound.

### **Validation of DDR2 as a therapeutic target to prevent breast cancer metastasis**

Ubiquitous deletion of *Ddr2* or select deletion of *Ddr2* in K14 basal epithelial cells in the MMTV-PyMT mouse model of metastatic breast cancer significantly blunts the extent of lung metastases<sup>14</sup>. While these genetic studies establish the importance of DDR2 in facilitating breast cancer metastasis, *Ddr2* was deleted from birth or shortly thereafter in such models. Therefore, the potential to target DDR2 therapeutically after cancer has developed to inhibit or treat metastatic disease was still unknown. To determine whether DDR2 could serve as a therapeutic target for the treatment of metastasis, we made use of a mouse model of metastatic breast cancer where genetic deletion of *Ddr2* could be temporally controlled. Mice containing a conditional *Ddr2*<sup>fl/fl</sup> allele<sup>14</sup> were crossed to mice containing the ROSA-CreER<sup>T2</sup> allele to allow for temporal deletion of *Ddr2*<sup>fl/fl</sup> upon treatment with tamoxifen.

To confirm efficient Cre expression following tamoxifen administration, experimental *Ddr2*<sup>fl/fl</sup>; ROSA-CreER<sup>T2</sup>; ROSA-LSL-TdTomato; MMTV-PyMT and control *Ddr2*<sup>+/+</sup>; ROSA-CreER<sup>T2</sup>; ROSA-LSL-TdTomato; MMTV-PyMT mice were allowed to develop primary breast tumors. In the MMTV-PyMT model, malignant transition occurs between 8 to 12 weeks of age, with evidence for stromal invasion by tumor cells and a reactive stroma<sup>58</sup>. Histologic examination of lungs at this stage showed no evidence for

metastases (data not shown). At 8 weeks of age, mice were administered tamoxifen-supplemented dry feed for 2 weeks. Tomato fluorescence in tissues was used to document Cre activity. In mice not treated with tamoxifen, minimal tomato fluorescence was detected (Figure 2.15A). In mice treated with tamoxifen, the majority of cells in the breast and lung showed Tomato fluorescence, confirming ubiquitous and efficient induction of Cre activity under these treatment conditions (Figure 2.15A). In experimental mice deletion of *Ddr2* in the tumor was confirmed by PCR (Figure 2.15B). In experimental and control mice there was no difference in latency of primary tumor formation (time to reach maximum size (2cm)) (Figure 2.15C), or total primary tumor burden per mouse (Figure 2.15D). However, there was a significant reduction in the number of lung metastases in mice where *Ddr2* was deleted during cancer progression (Figures 2.15E and 2.15F). These genetic data supported therapeutic targeting of DDR2 in the setting of early stage breast cancer to prevent metastasis.

### **WRG-28 inhibits DDR2 signaling *in vivo***

Finally, we asked whether WRG-28 inhibited DDR2 action in breast tumors, *in vivo*. Since DDR2 activation by collagen leads to increased SNAIL1 protein level in breast tumor cells<sup>11</sup>, we made use of breast tumor cells that contain a SNAIL1-clic beetle green (SNAIL1.CBG) bioluminescent fusion protein that serves as a surrogate bioluminescent reporter of SNAIL1 protein level<sup>59</sup>. 4T1 mouse breast tumor cells stably expressing SNAIL1.CBG were surgically implanted into the breast tissue of syngeneic BALB/cJ mice and 1cm tumors allowed to form. Bioluminescence imaging of mice was

conducted at baseline, and then mice were given a single IV administration of WRG-28 (10mg/kg), and imaged 4 hours later. Compared to control mice (implanted with 4T1-SNAIL1.CBG cells and treated with saline) mice treated with WRG-28 exhibited, on average, a 60% reduction in SNAIL1.CBG level within the tumor as compared to pretreatment levels (Figures 2.16A and 2.16B). These data indicated that IV administration of WRG-28 attenuated biochemical signaling of DDR2 in breast tumors *in vivo*.

### **WRG-28 administration reduces metastatic lung colonization of breast tumor cells**

To determine whether WRG-28 has the potential to inhibit metastasis *in vivo*, we employed an experimental metastasis model. DDR2-expressing 4T1 mouse breast tumor cells expressing GFP/luciferase (4T1 GFP/luc) were injected into syngeneic BALB/cJ mice via tail vein, and metastatic colonization and growth within the lung was followed by bioluminescence imaging and confirmed histologically. Genetic depletion (shRNAi) of DDR2 in 4T1 cells significantly reduced lung metastatic colonization in this model (Figures 2.17A,B and 2.17E). IV administration of WRG-28 (10mg/kg/day) reduced lung metastasis to a comparable level (Figures 2.17A,B and 2.17E). Histologic analysis of GFP+ tumors in the lungs isolated at termination (7 days) confirmed the bioluminescent results (Figure 2.17C,D and 2.17F). These data indicated that WRG-28 had the potential to inhibit colonization of the lung by metastatic breast tumor cells *in vivo*.

## Discussion

We have identified a potent and selective small molecule inhibitor of DDR2. In contrast to other inhibitors of DDR2, WRG-28 acts via the extracellular domain of the receptor to inhibit receptor activation in an allosteric manner, potentially by disrupting receptor clustering. In support of the proposed allosteric mode of action, WRG-28 was not a strong orthosteric inhibitor of ligand binding, was highly selective, dissociated preformed DDR2-collagen complexes, disrupted receptor clustering in solution, and inhibited kinase-independent receptor function.

Computational modeling followed by directed mutagenesis analysis of receptor function and WRG-28 action *in vitro* and in cells suggest that a region at the interface of the two extracellular domains (DS and DS-like) could be the binding site of WRG-28. The short extracellular juxtamembrane region of DDR2 is absent from the current structural model, so this could not be assessed as a potential binding site for WRG-28. In the absence of structural data, we cannot definitively confirm the predicted binding site. However, when key residues within the highest probability WRG-28 interacting site are mutated (DDR2<sup>F96A/T98A</sup>), collagen binding and DDR2 activation are abrogated, implying that F96 and T98 in DDR2 are important for receptor function. Perhaps the most compelling evidence for this region being involved in WRG-28 binding is when these key interacting residues found in DDR2 were substituted into DDR1 (DDR1<sup>L96F/A98T</sup> mutant, Figure 2.10I), sensitivity of DDR1 to inhibition by WRG-28 was conferred. Since WRG-28 appears to interfere with receptor clustering, there also remains the possibility that the WRG-28 binding site could be a composite site formed by two or more interacting protomers.

Previous studies have suggested that receptor clustering is critical for DDR2 binding to collagen<sup>44</sup>, and recent work has demonstrated DDR1 clustering enhances activation and strengthens DDR1 binding to collagen<sup>60,61</sup>. If DDR2 oligomerization is required for efficient collagen binding and receptor activation, the inability of the inactive DDR2<sup>F96A/T98A</sup> mutant to form higher order clusters would provide a straightforward explanation for its lack of binding and activation. We can not exclude the possibility that this region could function allosterically to regulate the collagen binding site from a distance. Such regions exist among matrix protein binding integrins, and are common among receptors<sup>62,63</sup>. Alternatively, these residues might contribute to conformational changes necessary for ligand binding and receptor activation, if residues within the DS-DS-like domain interface region act to position two DDR2 protomers for binding and subsequent activation.

The type of inhibitor described here is among the first extracellularly acting small molecule RTK inhibitor. To our knowledge there is only one other example of a similar small molecule inhibition strategy targeting the extracellular domain of a RTK (FGFR)<sup>32,33</sup>. That compound inhibits signaling linked to receptor internalization in an allosteric manner, without affecting orthosteric ligand binding. Our data suggests that WRG-28 is able to disrupt preformed DDR2-collagen complexes (Figure 2.8A). Although non-classical small molecular inhibitors that disrupt protein complexes or multimerization of receptors have been reported<sup>34,35</sup>, to our knowledge no such inhibitors have been identified for any RTK. These types of non-classical or allosteric inhibitors remain an elusive goal for drug development as they offer a number of favorable attributes from a therapeutic perspective, such as increased selectivity and

safety<sup>36,37</sup>. Allosteric inhibitors are typically more selective as their interaction sites in target proteins are not conserved between related proteins<sup>37</sup>. Indeed, neither the homologous family member DDR1, nor the unrelated collagen receptor  $\alpha 1\beta 1$  integrin are inhibited by WRG-28 (Figure 2.4D and 2.5D). Allosteric modulators often leave a baseline residual level of signaling downstream of their targets that may allow for maintained cellular homeostasis and minimize undesired responses<sup>36</sup>. In our limited *in vivo* treatment (1 week) we did not observe any untoward effects in WRG-28 treated mice. Additionally, WRG-28 also maintains efficacy against “gatekeeper mutants” of DDR2, further illustrating its utility as an alternative to canonical TKIs.

Rather than blocking receptor-ligand binding, WRG-28 has the potential to engage and disrupt preformed receptor complexes. This may be important for its *in vivo* efficacy, where the ligand (fibrillar collagen) is in great excess. WRG-28 binding to DDR2-collagen complexes appears to accelerate the intrinsically slow dissociation of the complex (Figure 2.7D). Extrapolation of this *in vitro* data would suggest that *in vivo* the DDR2-collagen interaction equilibrium lies strongly in favor of receptor-ligand complex. Therefore, this mode of inhibition may be poised as advantageous over blockage of ligand binding with an orthosteric inhibitor, where an empty receptor would be needed for drug binding.

In spontaneous mouse tumor models, genetic evidence has shown that DDR2 promotes the metastasis of breast cancer through its function in both the tumor cells, as well as cancer associated fibroblasts within the tumor microenvironment. Therefore, in the context of a DDR2 inhibitor, it becomes possible to target both the invasive tumor cell, as well as stromal cells concurrently. While we have studied DDR2 inhibition in the

context of breast cancer metastasis, DDR2 activation has also been implicated in the progression of multiple other cancer types<sup>20,64</sup> as well as other disease states such as osteoarthritis<sup>65,66</sup>, and cardiac<sup>67</sup> and pulmonary<sup>68</sup> fibrosis. It will be important to determine whether DDR2 inhibition with WRG-28 or derivatives would be a useful therapeutic strategy in those settings. In the context of cancer, it is important to note that we, and others, have shown that genetic depletion of *Ddr2* or selective pharmacologic inhibition of the receptor activation does not affect primary tumor growth<sup>11,13,14</sup>. Thus, in the patient setting, treatment with such an anti-metastasis agent capable of inhibiting cell invasion and migration would likely need to be administered as an adjuvant therapy along with standard chemotherapeutic agents that reduce tumor cell proliferation.

## Materials and Methods

### Synthesis and Chemical features of WRG-28

4-(bromomethyl)-*N*-ethylbenzenesulfonamide.

Adapted from <sup>69</sup>. To ethylamine HCl (120mg, 1.5 mmol) and triethyl amine (0.3mL, 2.2mmol) in CH<sub>2</sub>Cl<sub>2</sub> (15mL) under inert gas at 0°C, 4-bromomethyl benzene sulfonyl chloride (300mg, 1.1mmol) dissolved in CH<sub>2</sub>Cl<sub>2</sub> was added dropwise. Reaction brought to room temperature and stirred overnight. An additional 15mL CH<sub>2</sub>Cl<sub>2</sub> was added, and washed with water (3 x 25mL), brine (1x25mL), and dried over Na<sub>2</sub>SO<sub>4</sub>. Solvent was removed under reduced pressure, and the resulting 4-(bromomethyl)-*N*-ethylbenzenesulfonamide used without further purification.

*N*-ethyl-4-(((3-oxo-5a,10a-dihydro-3*H*-phenoxazin-7-yl)oxy)methyl)benzenesulfonamide

4-(bromomethyl)-*N*-ethylbenzenesulfonamide (50mg, 0.2mmol), resorufin sodium salt (42mg, 0.2mmol), and CsCO<sub>3</sub> (88mg, 0.27mmol) in DMF (15mL) were heated to 100°C overnight with stirring. EtOAc (50mL) was added and resulting organic solution washed extensively with water. After drying over Na<sub>2</sub>SO<sub>4</sub>, solvent was removed under reduced pressure. Resulting product was purified by silica chromatography (hexane:EtOAc) to afford *N*-ethyl-4-(((3-oxo-5a,10a-dihydro-3*H*-phenoxazin-7-yl)oxy)methyl)benzenesulfonamide as an orange solid. <sup>1</sup>HNMR (400 MHz, CDCl<sub>3</sub>): δ 7.94 ppm (dd, 2H), 7.76 (dd 1H), 7.62 (dd 2H), 7.45 (dd, 1H), 7.05 (t, 1H), 6.9-6.85 (m,

2H), 6.35 (s, 1H), 5.27 (s, 2H), 4.38 (s, 1H), 3.08 (q, 2H), 1.16 (t, 3H). HRMS for  $C_{21}H_{18}N_2O_5S_1$   $[M+H]^+$ :  $m/z = 411.2$

### **Cell culture and viral infections**

HEK293, HEKEBNA and HEK293T cells were from ATCC. MCF-10A cells were provided by L. Michel (Washington University in St Louis, USA). BT549 cells were provided by J. Weber (Washington University in St. Louis, USA). 4T1- Luc-GFP cells were described previously<sup>11</sup>. Production of lentiviruses and infection of target cells were described previously<sup>59</sup>. To make stable cell lines of BT549 and 4T1 cells selection was carried out in 3  $\mu$ g/ml puromycin.

### **Plasmids, shRNAi lentiviruses**

pFLR DDR2-Flag and pFLR SNAIL1.CBG plasmids and DDR2 shRNAis were previously described<sup>11</sup>. pCEP-His-DDR2, pc-DDR1-Fc and pc-DS2-Fc plasmids were provided by Birgit Leitinger<sup>40,45</sup> (Imperial College London, UK). pcDNA3.1 DDR1-myc was provided by Rafael Fridman (Wayne State University, USA). For mutation studies of full length receptor, the cDNA of DDR2 was subcloned into pcDNA3.1-myc plasmid. Overlapping PCR was used to introduce point mutations and then subcloned back into pcDNA3.1. Plasmids for recombinant DDR2 protein were constructed by removing the N-terminal His and Myc tags from pCEP-His-DDR2 ECD and using PCR to introduce a C-terminal His tag to DDR2 (amino acids Lys<sup>22</sup> to Thr<sup>398</sup>). BM-40 signal sequence was maintained at the N-terminus. For point mutants, overlapping PCR was used to introduce point mutations and then subcloned back into the pCEP-pu vector. For DDR2<sup>K608E</sup> plasmid, overlapping PCR was used to introduce the point mutation, and

then subcloned into the pFLRu vector<sup>70</sup> with a YFP tag. All mutations and cloning were verified by sequencing. shRNAs were subcloned into the pFLRu vector. shRNA target sequences are as follows: SCR control sequence 5'- CCTAAGGTTAAGTCGCCCTCGCTC-3', shDDR2 5'- GCCAGATTTGTCCGGTTCATT-3'. For rescue experiments, a shDDR2 directed at the 3' UTR with sequence 5' - GCCCATGCCTATGCCACTCCAT-3' was used to allow for expression of rescue construct.

## Reagents

Triple helical collagen binding peptides GPC(GPP)<sub>5</sub>-GPRGQOGVNIeGFO-(GPP)<sub>5</sub>GPC-NH<sub>2</sub> and GPC(GPP)<sub>5</sub>-GFOGER-(GPP)<sub>5</sub>GPC-NH<sub>2</sub> were purchased from Richard Farndale (University of Cambridge, UK).  $\alpha$ 1 $\beta$ 1 integrin, DDR1-Fc and DDR2-myc/His were purchased from R&D systems. DDR2-Fc was purchased from Creative Biomart.

## Production and Purification of Recombinant Proteins

The production and purification of recombinant DDR proteins was performed as previously described by others (Leitinger, 2003). A C-terminal His-tagged DDR2 extracellular domain protein (DDR2-His) and DDR2 point mutants were produced from episomally transfected HEK293-EBNA cells.

## Solid Phase Collagen Binding experiments

Collagens or collagen peptides (100uL) were diluted in 0.01 N acetic acid coated onto Immulon 2 HB 96-well plates (Fisher Scientific) overnight at 4°C. Collagen binding peptides have been previously validated and described in detail<sup>41,71</sup>. For DDR proteins, the collagen peptide included the binding sequence GPRGQOGVNleGFO. For integrin  $\alpha 1\beta 1$ , the collagen peptide included the binding sequence GFOGER. Wells were then blocked for 1 h at room temperature with 1 mg/ml bovine serum albumin in phosphate-buffered saline plus 0.05% Tween 20. Recombinant proteins, diluted in incubation buffer (0.5 mg/ml bovine serum albumin in phosphate-buffered saline plus 0.05% Tween 20), were added for 3 h at room temperature. Wells were washed with incubation buffer between all incubation steps. Bound DDR2-His protein or  $\alpha 1\beta 1$ -His were detected with anti-His conjugated HRP monoclonal antibody (1:2500 dilution), added for 1 h at room temperature. Bound DDR1-Fc or DS2-Fc protein were detected with goat anti-human Fc coupled to horseradish peroxidase (1:2500 dilution), added for 1 h at room temperature. Detection was achieved using o-phenylenediamine dihydrochloride (Sigma), added for 3–5 min. The reaction was stopped with 3M H<sub>2</sub>SO<sub>4</sub>, and plates were read in a 96-well plate reader at 492 nm.  $\alpha 1\beta 1$  integrin assay was performed as described<sup>43</sup>, but with anti-His conjugated HRP used for detection.

### **DDR2-ligand dissociation assay**

Immulon 2HB plates were coated overnight with 0.5 $\mu$ g/mL collagen peptide ligand. Coat solution was removed and wells were washed once with PBS, and then blocked for 1h at room temperature with 1mg/ml bovine serum albumin in phosphate-buffered saline plus 0.05% Tween 20. 25nM DDR2 was plated allowed to bind to equilibrium (2 hours). At that point, the protein solution was removed and a maximal

volume of incubation buffer that contained indicated concentrations of WRG-28 or control DMSO was added. At indicated time points, wash off solution was removed, and incubated with 1:5000 anti-His-HRP for 60 minutes to detect remaining bound DDR2. Detection was achieved as indicated for the solid phase collagen binding experiments.

### **Peptide labeling**

NHS-fluorescein (Thermo scientific) was used to label collagen toolkit peptide. Labeling was carried out at a 5 fold molar excess of labeling reagent to peptide on ice for 2 hours. Non-reacted NHS-fluorescein was removed by dialysis, and the resulting labeled peptide lyophilized and then resuspended. Solid phase assay was used to confirm there was no loss of DDR2 binding upon conjugation of the peptide.

### **Peptide plating quantification**

Increasing amounts of fluorescein conjugated collagen peptide were plated in triplicate into wells of a Immulon 2HB plate. Plating was carried out overnight at 4°C. At that time, fluorescence intensity of each well was detected using a Tecan Infinite 200 PRO plate reader. Wells were then washed 3 times with PBS, and post wash fluorescence intensity was measured to determine the portion of the plated peptide that was adsorbed onto the plate.

### **Size exclusion chromatography**

Size exclusion chromatography was carried out at 4°C using a BioRad Biologic Duoflow system equipped with a Superdex 200 Increase 10/300 GL column (GE).

Experiments were run using PBS at a 0.5mL/min flow rate and elution monitored at UV absorbance 280nm. 25µg of protein were incubated in solution with 1µM WRG-28 or DMSO for 1 hour, then injected, and 1mL fractions were collected upon elution. Composition of fractions was assessed by concentration using Vivaspin 500 centrifugal concentrators (10K MWCO), and concentrated fractions run on 10% gel under non-reducing conditions. For assessment of collegen binding of different multimeric states, 1mL fractions of the indicated multimer were immediately spin concentrated. Protein concentration was then measured using Bradford Assay, and concentration across samples normalized. Multimer samples were then subjected to binding in the solid phase plate assay.

### **Biolayer Interferometry**

Biolayer Interferometry (BLI) with an Octet (ForteBio, Menlo Park, CA) instrument was used to assess WRG-28 binding to various protein constructs. DDR2 was randomly biotinylated *in vitro* using EZ-link NHS-PEG4-Biotin (Thermo Scientific) at a 1:2 molar ratio (protein: reagent). Streptavidin-coated biosensors (ForteBio) were used to capture biotinylated DDR2 onto the surface of the sensor. After reaching baseline, sensors were moved to association step for 600 s and then dissociation for 300 s. Curves were corrected by referencing technique using both biotin-coated pins dipped into the experimental wells. The binding buffer was identical to that of the solid phase assay.

### **Cell Surface Biotinylation**

Cell surface biotinylation was used to confirm cell surface expression of protein

constructs. HEK293 cells expressing the indicated constructs were incubated with cell impermeable EZ-link NHS-PEG4-Biotin in PBS for 30 minutes on ice. Cells were then washed twice with 100mM glycine in PBS to quench reaction. Cells were lysed, and the expressed constructs immunoprecipitated using the indicated protein tag. Lysates were run and analyzed by SDS-PAGE, blotting with Streptavidin-HRP to detect biotin. Blots were stripped and reprobed for the indicated protein to confirm band identity. Non-biotin treated lysates were run as a control.

### **Assessment of receptor dimerization**

Dimerization was assessed by chemical cross linking analysis. HEK293 cells expressing the indicated constructs were treated with 0.1M BS<sup>3</sup> (Thermo Scientific) in PBS for 30min at room temperature, after which the reaction was quenched with 15mM glycine. Cells were then lysed and lysates analyzed by SDS-PAGE.

### **Immunoprecipitation and western blots.**

For collagen dependent phosphorylation, indicated concentrations of collagen I in 0.01N acetic acid were plated for 1hr at 37°C. plates were washed twice with PBS, and cells then plated in culture medium. Cells were lysed with a non-denaturing lysis buffer as described previously<sup>11</sup>. Five hundred micrograms of whole-cell lysate, as determined by Bradford analysis (BioRad), was used for immunoprecipitation. Blots were probed with indicated antibodies, followed by corresponding horseradish peroxidase-conjugated secondary antibodies. Detection was performed using SuperSignal Chemiluminescent substrate (Thermo Scientific) on a ChemiDoc XRS+(BioRad). Integrated relative densities of individual bands were quantified using ImageLab software. All

quantification was performed under conditions of linear signal response.

### **RTK Signaling Array**

MCF10A cells were starved overnight, and then stimulated with media containing 20% horse serum + EGF for 5, 15, or 60 minutes in the presence or absence of 500nM WRG-28. Another derivative, WRG-11, was also compared at 15minutes. Cells were lysed, and lysates were assayed using PathScan RTK signaling array (Cell Signaling). Following detection on a ChemiDoc XRS+(BioRad), integrated relative densities of individual dot blots were quantified using ImageLab software, and normalized to positive blot controls. All quantification was performed under conditions of linear signal response.

### **Cell proliferation analysis**

Cells were seeded at  $3 \times 10^4$  cells per well in triplicate in 24 well plates in 500 $\mu$ L growth medium on day 0. Cells were trypsinized, resuspended in a total volume of 500 $\mu$ L of medium and counted with a haemocytometer at the intervals shown.

### **Migration and invasion assays.**

Migration assays through matrigel and 3D collagen I invasion assays were performed as described previously<sup>11</sup>, For 3D cell migration assays,  $10^5$  cells were embedded in 20 $\mu$ l of type I collagen gel (2.0mg/mL) extracted from rat tail (BD Biosciences). After gelling, the plug was embedded in a cell-free collagen gel (2.0 mg/mL) within a 24-well plate. After allowing the surrounding collagen matrix to gel (1 h at 37°C), 0.5 mL of culture medium was added on the top of the gel and cultured for

another 2 days. Invasion distance from the inner collagen plug into the outer collagen gel was quantified. For invasion assays, Transwell cell invasion assays were performed using either 24-well polycarbonate membrane (Corning) with 8- $\mu$ m pore size, or 24-well FluoroBlok Transwell insert (BD) with 8- $\mu$ m pore size. Inserts were prepared by coating the upper surface with 1 mg/mL of Matrigel (BD Biosciences) for 4–6 h at 37°C in a 5% CO<sub>2</sub> incubator.  $5 \times 10^4$  BT549 or 4T1-Luc cells in DMEM containing 1% FBS were seeded into the upper chamber of the insert. The bottom chamber contained DMEM with 10% FBS. After 24 or 48 hr, Membranes were processed. Polycarbonate membranes were stained with HEMA3 staining kit (Fisher) and then mounted and enumerated based on number of cells per 20x high power field, 5 fields per insert. For FluoroBlok transwells, luminescence intensity was measured using a FluoStar Optima microplate reader (BMG Labtech) for 10 individual fields on the bottom of each insert.

### **Tumor Organoid and CAF coculture**

Isolation of tumor organoids and CAFs was described previously<sup>14</sup>. Primary tumor organoids (30–50, each 200–1,000 cells) with or without CAFs (750 cells) were cultured in 50mL droplets of 3mg/mL acid-solubilized rat-tail collagen I (BD Biosciences), and number of invasive organoids were enumerated daily for 4 days. Organoids were scored as invasive if they contained  $\geq 1$  protrusive projection.

### **Organoid Apoptosis Staining**

Organoids derived from MMTV-PyMT tumor bearing mice were grown in 3D collagen culture as indicated in experimental methods. Organoids were grown in the presence of control DMSO or 1 $\mu$ M WRG-28. On day 4, positive control wells were

treated with 1uM doxorubicin for 4 hours to induce apoptosis. Organoids were then stained using an annexin V-FITC/PI apoptosis detection kit (Abcam), and imaged. 10 organoids/condition were imaged, and percent of organoids staining positive for annexin V was quantified using ImageJ software.

### **Molecular docking**

The homology model of the DDR2 extracellular domain was created by using SWISS-MODEL protein structure homology modeling server<sup>48-50</sup>. PDB 4AG4 was used as a template. For docking studies, PyRx using the AutoDock Vina Wizard<sup>52</sup> was used. For molecular visualization, docking poses generated by Autodock Vina were loaded into Pymol.

### **Animal studies**

All procedures and care of animals were done in accordance with a protocol approved by the Washington University Institutional Animal Care and Use Committee (St. Louis, MO), and were performed in accordance with institutional and national guidelines.

Temporal deletion of Ddr2. Ddr2<sup>fl/fl</sup>; ROSA-LSL-TdTomato or Ddr2<sup>+/+</sup>; ROSA-LSL-TdTomato mice were crossed to MMTV-PyMT; ROSA-CreER<sup>T2</sup> mice. At 8 weeks, experimental and control mice were switched to 400 citrate tamoxifen-supplemented non-pelleted dry feed (Envigo) for 2 weeks. The tumor bearing mice were monitored weekly and euthanized when the largest tumor reached 2 cm in diameter. Lungs were fixed overnight in 10% formalin, cryopreserved in 30% sucrose overnight, and finally embedded in OCT and frozen in a dry ice/ethanol bath. Frozen specimens were

sectioned with a cryostat (6  $\mu\text{m}$ ) and analyzed by fluorescence microscopy for tomato expression or stained with haematoxylin and eosin for histological analysis. For analysis of lung metastasis, microscopically visible metastatic foci were counted from three H&E stained sections taken 200 $\mu\text{m}$  apart and reported as the total number of metastases in those three sections.

Breast implant in vivo assay. Eight-week old female BALB/cJ mice (Jackson Labs) were anaesthetized with a ketamine/xylazine cocktail (90 mg/kg ketamine and 13 mg/kg xylazine, intraperitoneal injection) and the abdomen was sterilized using povidone–iodine (Betadine) solution and ethanol. A small Y-shaped incision was made in the lower abdominal skin to expose the fourth mammary gland using surgical scissors and bleeding vessels were cauterized. 4T1-Snail.CBG cells ( $1 \times 10^6$ ) in 50  $\mu\text{l}$  DMEM were injected into the fourth mammary gland using a 29-gauge needle. The skin flaps were replaced and closed using 9 mm wound clips, and the surgical site was swabbed with triple-antibiotic cream. When tumors were 1cm in diameter, in vivo biochemical response studies were conducted by bioluminescence imaging (BLI) at baseline, followed by IV lateral tail vein injection of either control saline, or indicated doses of WRG-28 in saline/DMSO, and BLI at indicated time points. The baseline BLI signal for each mouse served as its own control.

For lung metastasis formation assay,  $5 \times 10^5$  cells in 100 $\mu\text{L}$  DMEM were injected into the lateral tail vein of BALB/cJ mice. Beginning on day 0, mice were treated with either control saline, or 10mg/kg WRG-28 in saline/DMSO daily for 7 days, and BLI imaging used to follow tumor growth at time points indicated. After 7 days, mice were euthanized and lungs removed and fixed in 10% formalin for 24 h, cryopreserved in

30% sucrose overnight, and finally embedded in OCT and frozen in a dry ice/ethanol bath. Frozen specimens were sectioned with a cryostat (6  $\mu\text{m}$ ) and analyzed by fluorescence microscopy for GFP expression or stained with haematoxylin and eosin for histological analysis.

For all BLI, mice were anaesthetized with isoflurane and imaged using the IVIS 100 bioluminescent imaging system (Perkin Elmer) following an intraperitoneal injection of d-luciferin (150 mg/kg).

### **Statistics**

All data represent the mean  $\pm$  SEM of the indicated number of experiments. Statistical parameters and  $\text{IC}_{50}$  values were calculated using Prism. Statistical significance was calculated by the indicated test, considering  $p < 0.05$  as statistically significant.

## Figures

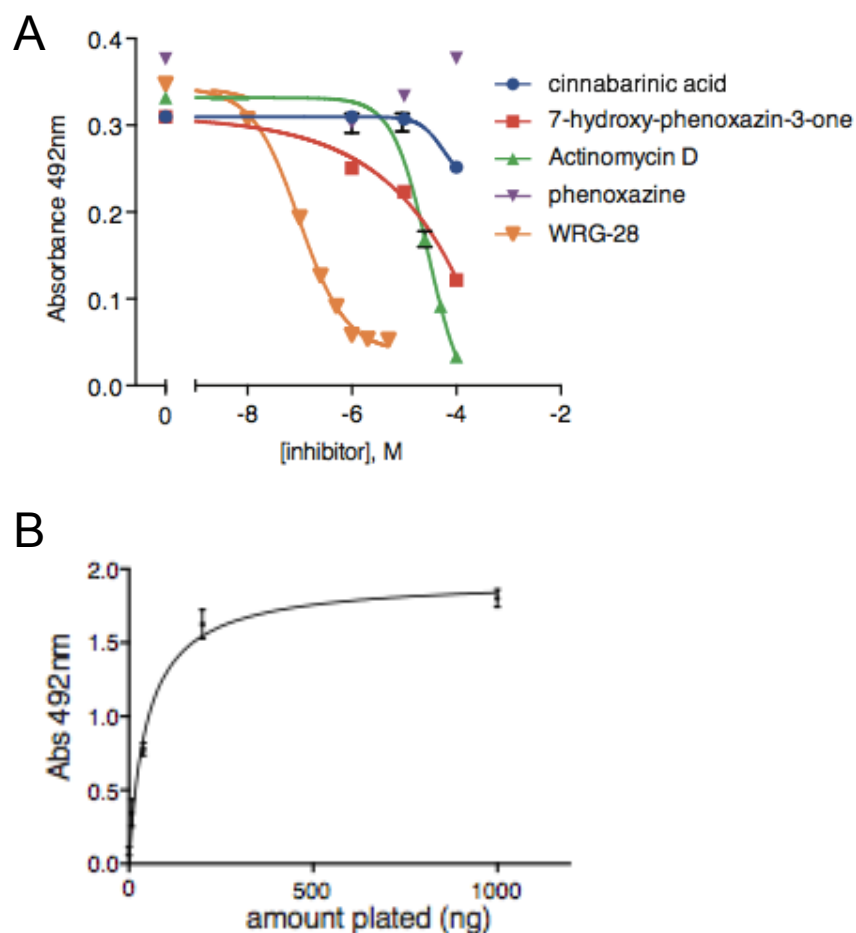
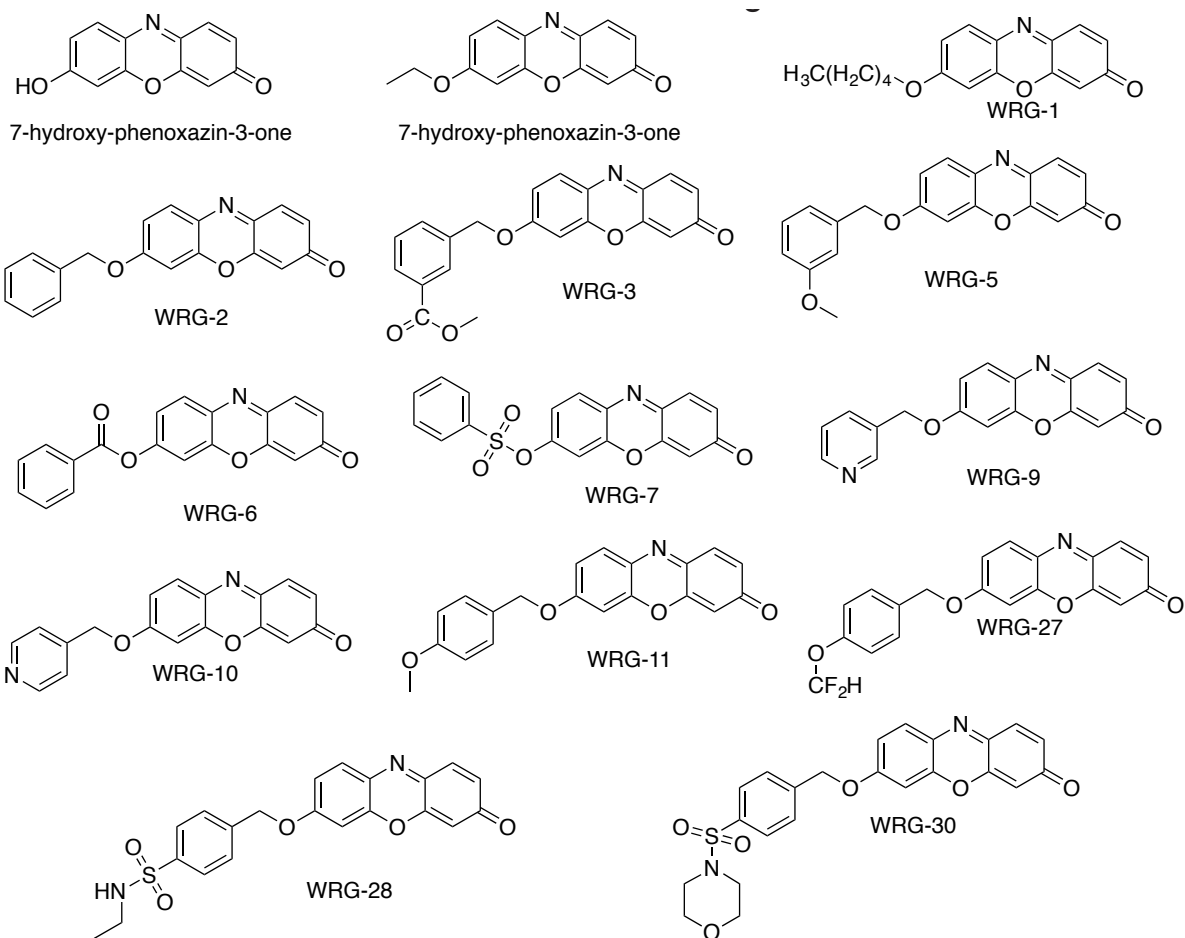


### Figure 2.1: *In vitro* screening for active DDR2 inhibitors

(A) Effect of various organic compounds on DDR2-His extracellular domain binding. Inhibitory curves as measured by solid phase binding assay of 25nM DDR2-His binding, 500ng immobilized ligand. Cinnabarinic acid (blue), 7-hydroxy-phenoxazin-3-one (red), Actinomycin D (green), phenoxazine (purple), WRG-28 (orange). Graph shows mean  $\pm$  SEM from a single experiment representative of at least three independent experiments, three replicates per treatment per experiment.

(B) Solid phase binding assay of 25nM recombinant DDR2-His to the high affinity collagen II DDR2 binding peptide. Graph shows mean  $\pm$  SEM from a single experiment representative of at least three independent experiments, three replicates per concentration per experiment.



### Inactive Derivatives

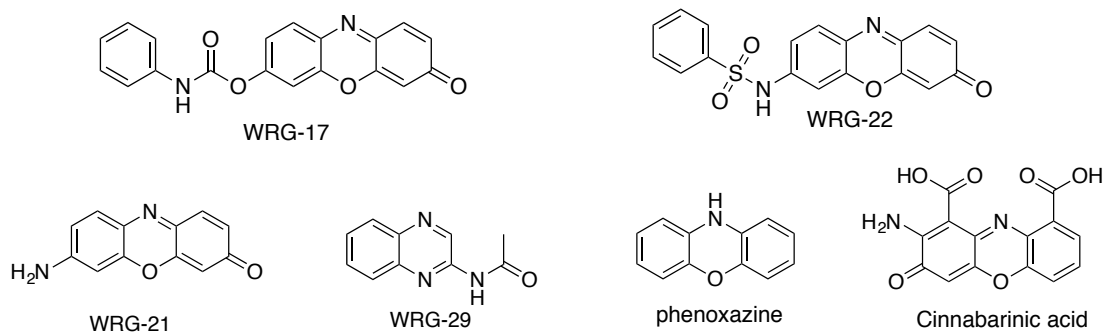


**Figure 2.2: Chemical structures of synthesized derivatives**

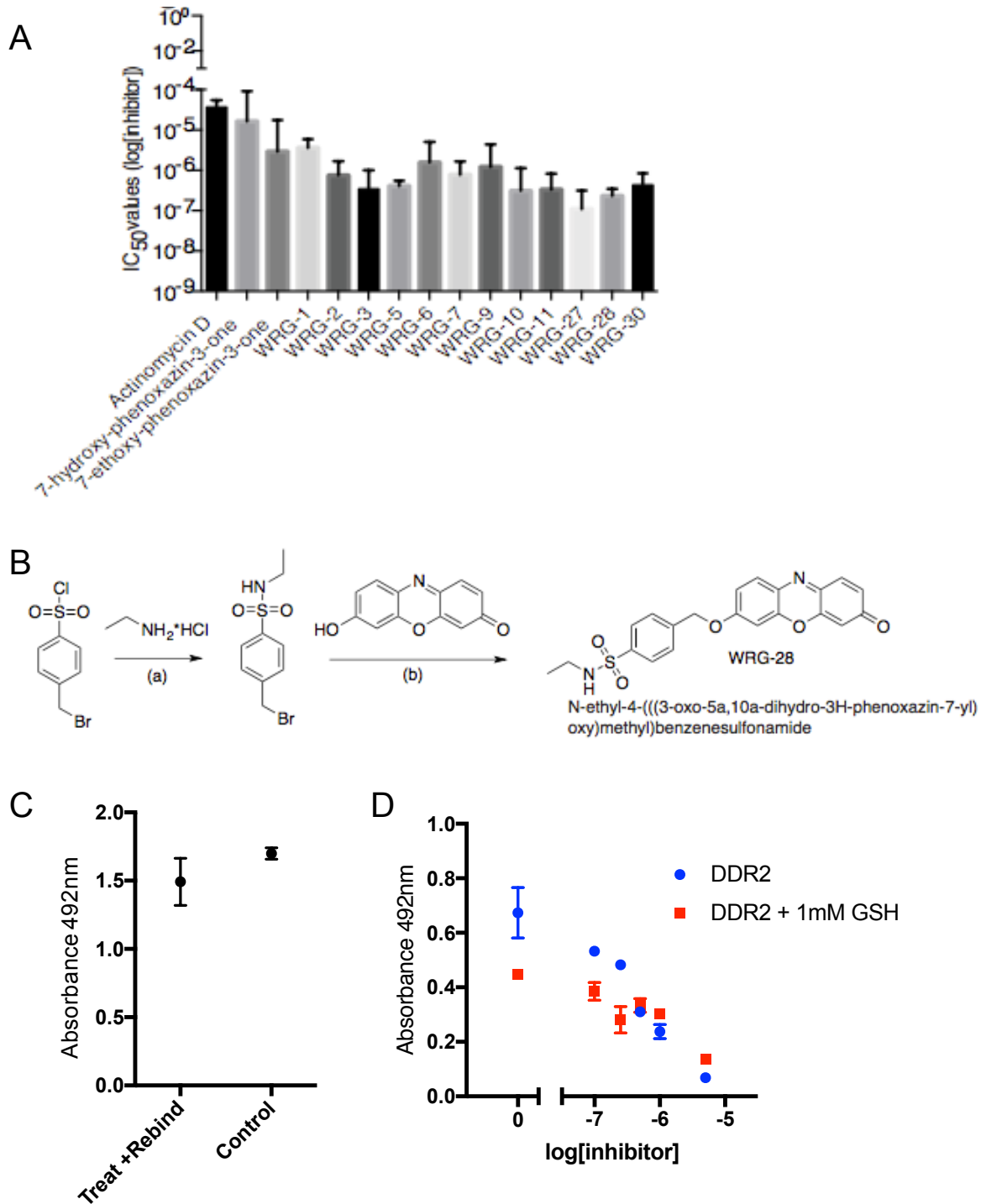


**Figure 2.3: Identification of WRG-28 as a potent and reversible inhibitor of DDR2 binding**

(A) SAR study of the 7-hydroxy-phenoxazin-3-one derivatives and their inhibitory ability as tested by solid phase binding assay of 25nM recombinant DDR2-His to the high affinity collagen II DDR2 binding peptide. Data are mean  $\pm$  SEM. IC<sub>50</sub> values as determined by 3 independent experiments (n=3).

- (B) Synthetic route of WRG-28 (a)  $\text{NET}_3/\text{CH}_2\text{Cl}_2$ ; (b)  $\text{CsCO}_3/\text{DMF}$
- (C) Treatment of DDR2-his protein with  $1\mu\text{M}$  WRG-28 in solution, followed by dialysis. Protein was then allowed to bind in the in vitro assay as compared to a non-treated, dialyzed control sample.
- (D) Effect of WRG-28 on DDR2-His extracellular domain binding in the presence of  $1\text{mM}$  glutathione. Inhibitory curves as measured by solid phase binding assay of  $25\text{nM}$  DDR2-His binding,  $500\text{ng}$  immobilized ligand. Graph shows mean  $\pm$  SEM three replicates per treatment.

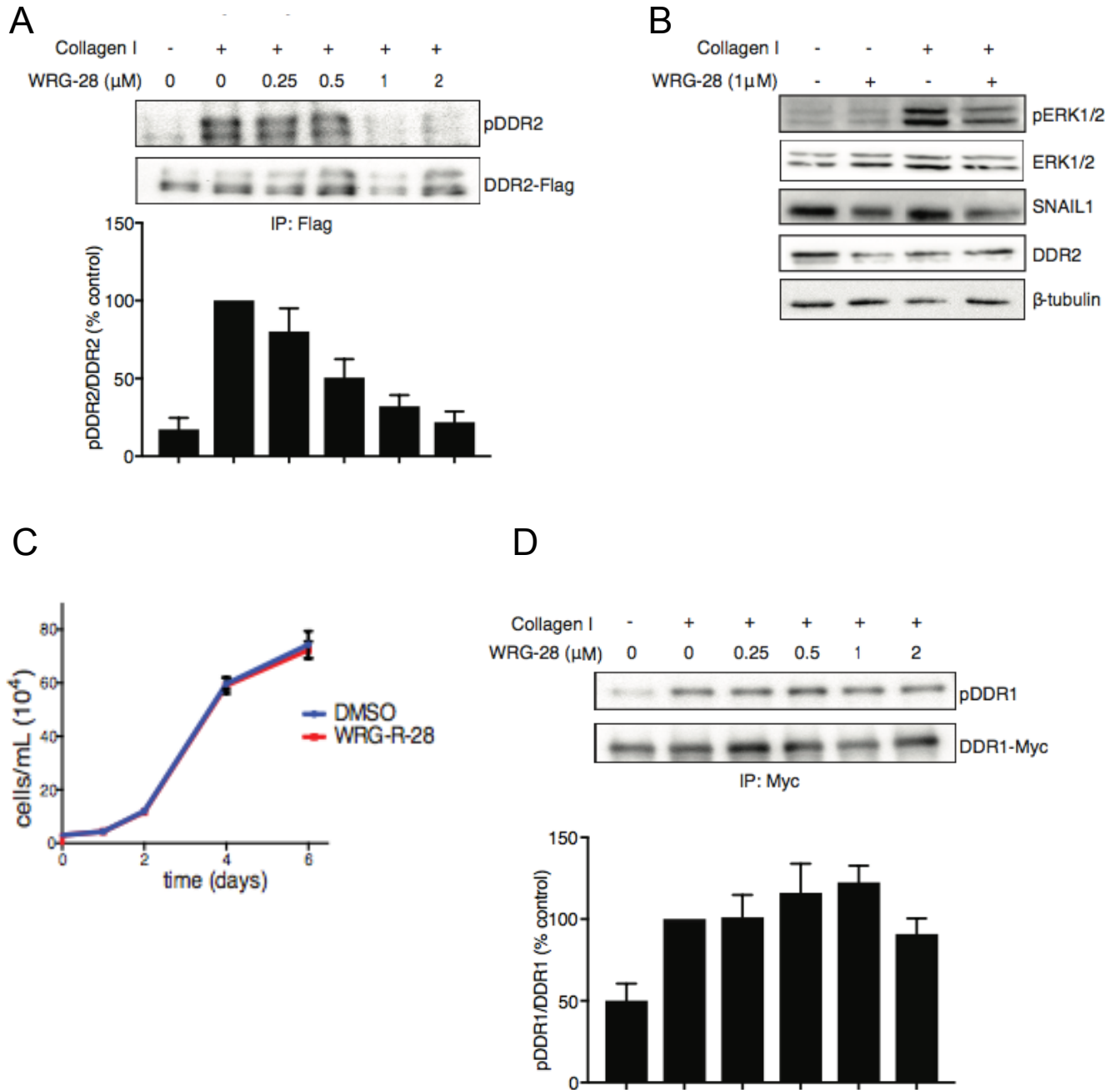


**Figure 2.4: WRG-28 inhibits DDR2 activation but has no effect on DDR1 activation**

(A) HEK293 cells transfected with DDR2-Flag were added to plates coated with 30 $\mu\text{g}/\text{mL}$  collagen I for 4 hours in the presence of various concentrations of WRG-28. DDR2 was immunoprecipitated with Flag antibody and bound products western blotted with pTyr mAb 4G10 and reprobbed with anti-DDR2 antibodies. Densitometric quantification used to assess effect of WRG-28 on collagen-induced phosphorylation of DDR2. Representative blot shown, quantification of 5 independent experiments represented as mean  $\pm$  SEM.

(B) HEK293 cells stably expressing DDR2-Flag were added to plates coated with 30µg/mL collagen I for 7 hours in the presence or absence of WRG-28. Western blots were performed.

(C) MCF10A cell proliferation curve of DMSO control or 1µM WRG-28 treated cells. Means ± SEM. Three replicates per treatment per experiment.

(D) HEK293 cells transfected with DDR1-Myc were added to plates coated with 30µg/mL collagen I for 4 hours in the presence of various concentrations of WRG-28. DDR1 was immunoprecipitated with Myc antibody and bound products western blotted with pTyr mAb 4G10 and reprobbed with Myc antibodies. Densitometric quantification used to assess effect of WRG-28 on collagen-induced phosphorylation of DDR1. Representative blot shown, quantification of 4 independent experiments represented as mean ± SEM.

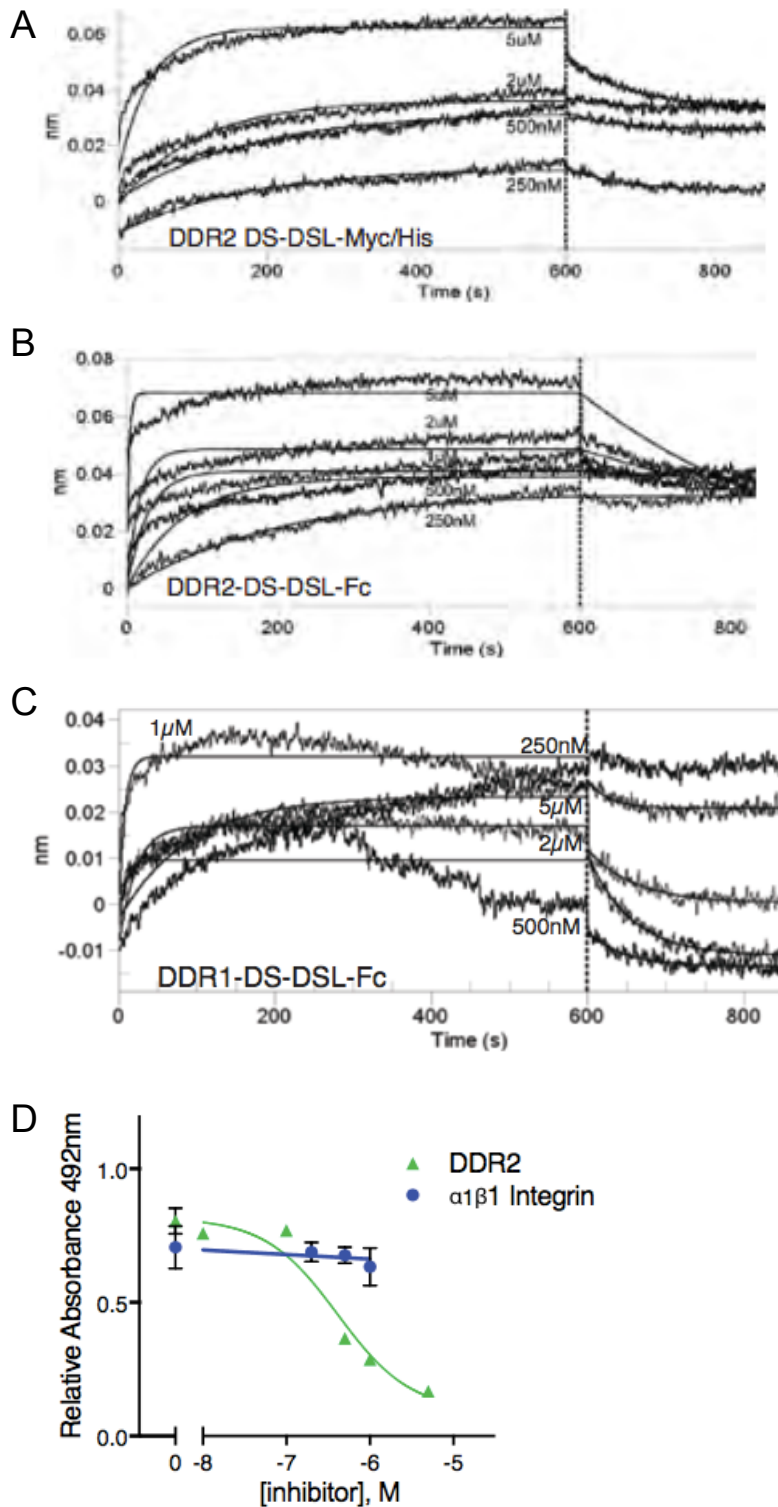


**Figure 2.5: WRG-28 is selective towards DDR2**

(A-C) Bi-layer interferometry analysis of WRG-28 binding to (A) DDR2-His, (B) DDR2-Fc, (C) DDR1-Fc. Data are shown as black lines representing increasing concentration of WRG-28, with global kinetic fits overlaid.

(D) Solid phase binding assays of either 25nM  $\alpha 1\beta 1$  integrin (blue) or 25nM DDR2(green) showing the relative inhibition of binding of each protein to its respective high-affinity triple helical collagen peptide in response to WRG-28. Graph shows mean  $\pm$  SEM from a single experiment representative of at least three independent experiments, three replicates per treatment per experiment.

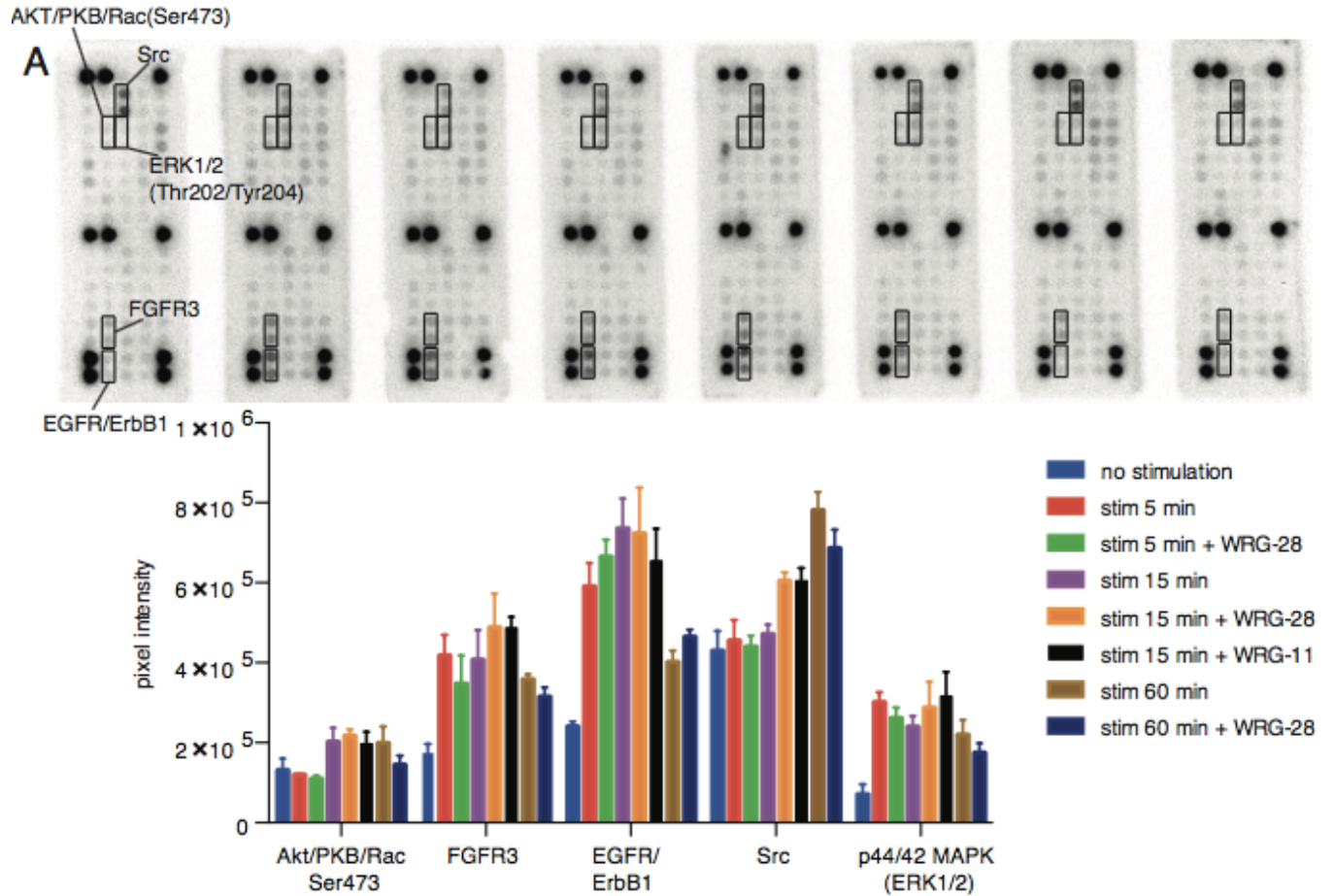


**Figure 2.6: WRG-28 does not affect other kinase pathways in non-DDR2 expressing MCF10A cells**

(A) MCF10A cells were stimulated with 20% horse serum + EGF for indicated time period in the presence or absence of 500nM WRG-28 and cells lysed. Lysates were assayed using Cell Signaling PathScan RTK signaling array. Phosphoarray of RTK signaling pathways highlighting various responsive RTKs in MCF10A cells and densitometry used to quantify changes.

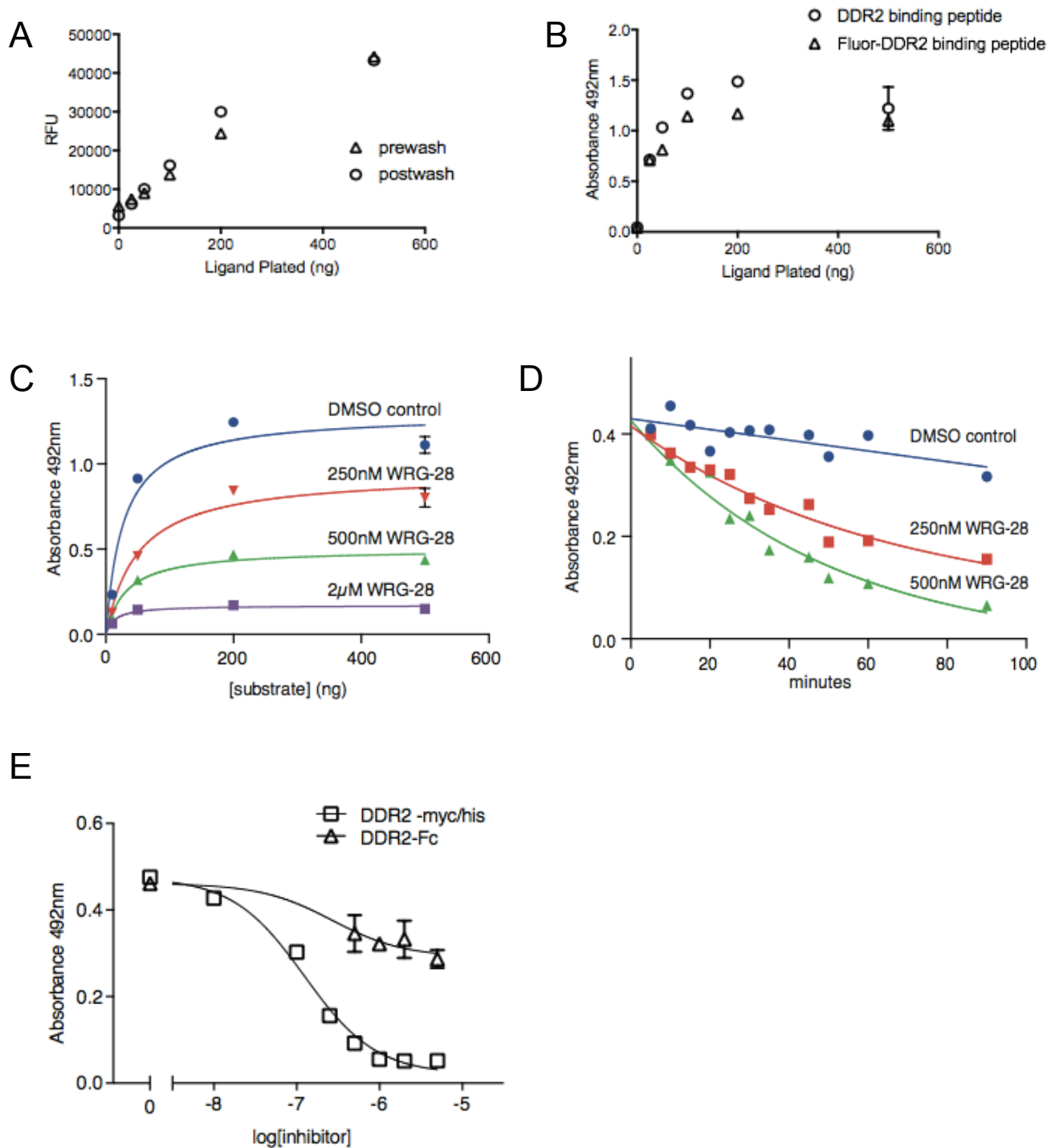


**Figure 2.7: DDR2 acts in a non-orthosteric manner to accelerate the dissociation of receptor-ligand complex**

(A) Fluorescein conjugated collagen II binding peptide was plated at known amounts overnight at 4°C. Fluorescence of wells was measured (prewash) and then plating solution washed and fluorescence again measured (postwash) to assess proportion of plated peptide that remained adsorbed to the plate. Graph showing linear adsorption of

peptide in the range assessed, with similar fluorescence pre- and post-wash. 3 measurements/plating concentration were taken.

(B) Solid phase binding assay of 25nM DR2-His to either high affinity collagen II DDR2 binding peptide unlabeled or fluorescein conjugated, plated at indicated concentrations. Graph shows mean  $\pm$  SEM, three replicates per concentration per experiment.

(C) 25nM DDR2-His binding in the presence of increasing concentration of collagen peptide at varying concentrations of WRG-28. DMSO control (blue), 250nM WRG-28 (red), 500nM WRG-28 (green), 2 $\mu$ M WRG-28 (purple). Data are means  $\pm$  SEM from a single experiment representative of at least 3 independent experiments, 3 replicates/treatment per experiment.

(D) 25nM DDR2 bound to immobilized collagen II peptide in solid phase binding assay at equilibrium was exposed to a titration of compound. Graph showing dissociation of DDR2 ECD from ligand after exposure to compound at indicated concentrations for time indicated. DMSO control (blue), 250nM WRG-28 (red), 500nM WRG-28 (green). Data are independent time points from a single experiment representative of at least three independent experiments.

(E) Effect of WRG-28 on 25ng DDR2-His or DDR2-Fc extracellular domain binding. Inhibitory curves as measured by solid phase binding assay. Graph shows mean  $\pm$  SEM from a single experiment representative of at least three independent experiments, three replicates per treatment per experiment.

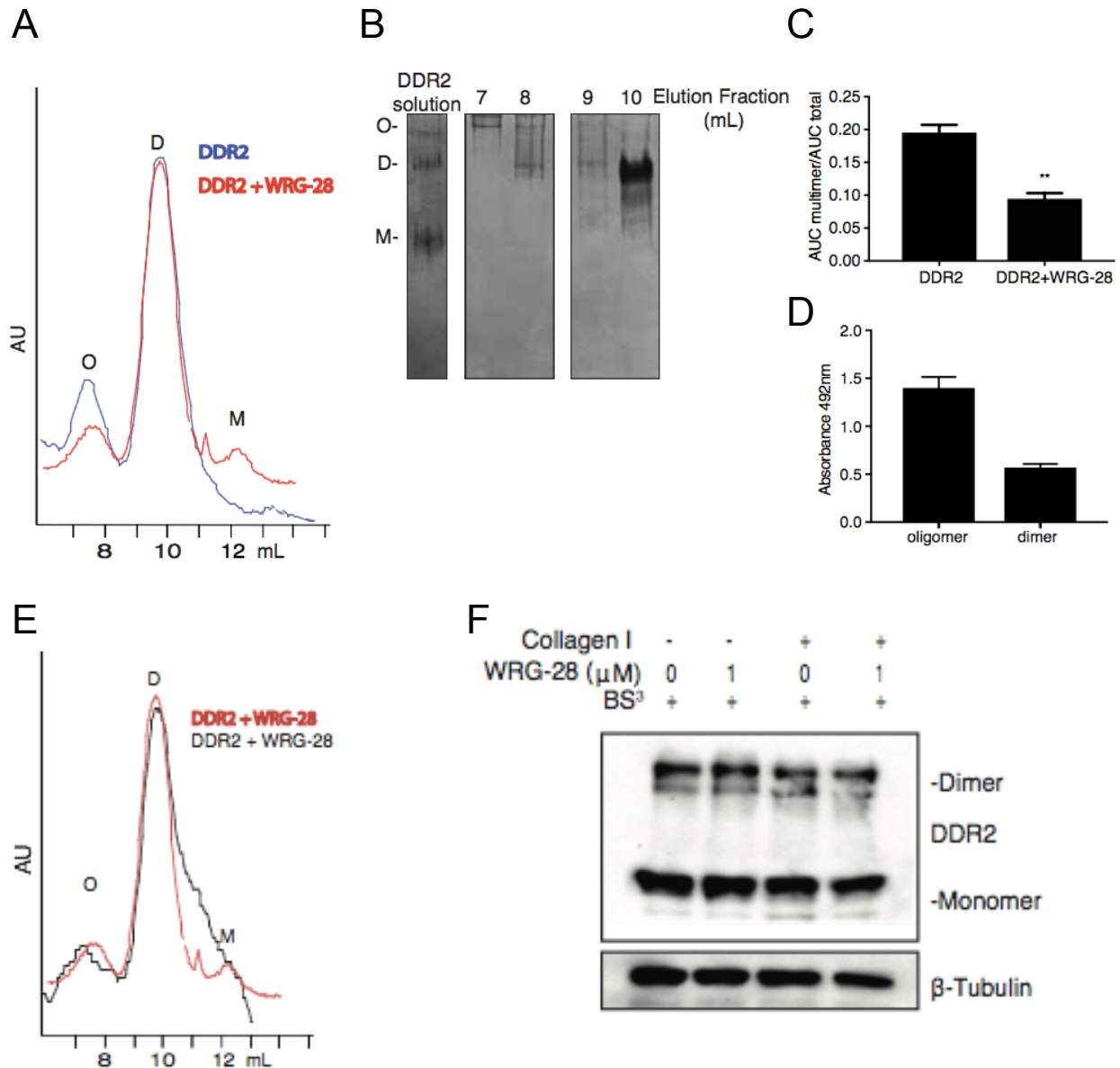


**Figure 2.8: WRG-28 impairs clustering of the DDR2 extracellular domain**

(A) Size exclusion chromatography. Representative elution profile of DDR2-His in the presence or absence of 1 $\mu$ M WRG-28 on a Superdex 200 Increase 10/300 GL column. Oligomer (O), dimer (D), monomer (M).

(B) Native gel fraction analysis. Indicated elution fractions were concentrated and resolved by native PAGE on a 10% gel, followed by silver staining.

(C) Area under the curve used to quantify fraction of DDR2 multimer (oligomer) as compared to total DDR2. Three independent runs of each condition were quantified, data represented as mean  $\pm$  SEM.

(D) Protein concentration of dimer or oligomer fractions was normalized, and the given multimeric species subjected to binding in the in vitro binding assay. Three replicates of each condition were tested, data represented as mean  $\pm$  SEM.

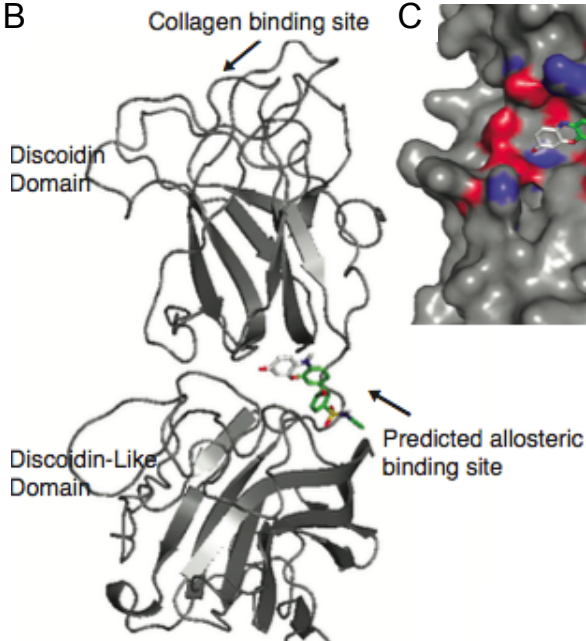
(E) Two independent size exclusion chromatography traces of DDR2-His treated with WRG-28, illustrating the peak shouldering commonly seen.

(F) HEK293 cells transfected with DDR2-Flag added to plates and stimulated with collagen I in the presence or absence of 1 $\mu$ M WRG-28 for 4 hours. Cells were then treated with 0.1M BS<sup>3</sup> in PBS. Samples were western blotted with Myc antibodies.  $\beta$ -tubulin used as a loading control.

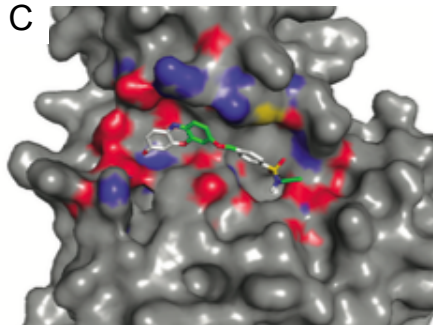
A

Ligand Binding Site	Binding Affinity (kcal/mol)
<b>1</b>	<b>-7.8</b>
<b>2</b>	<b>-7.4</b>
3	-7.4
<b>4</b>	<b>-7.3</b>
5	-7.2
<b>6</b>	<b>-7.2</b>
7	-7.2
<b>8</b>	<b>-7.1</b>
9	-6.8

B



C



D

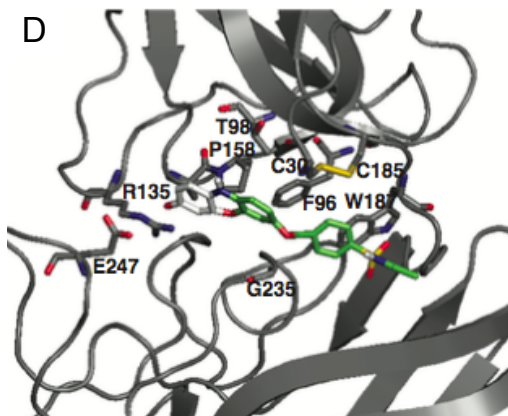


**Figure 2.9: Computational prediction of WRG-28 binding site**

(A) Autodock calculated binding affinities of top 9 computationally predicted binding sites for WRG-28. Sites highlighted in red represent those clustered within the same site at the DS-DSL interface region.

(B) Overall view of the DDR2 extracellular domain structure depicting WRG-28 in its putative binding site

(C) View of WRG-28 oriented in predicted cleft using surface representation of DDR2. For protein and inhibitor atom colors rendered as follows: nitrogen (blue), oxygen (red), sulfur (yellow). For inhibitor, carbon rendered green.

(D) Detailed view of the predicted interactions of WRG-28

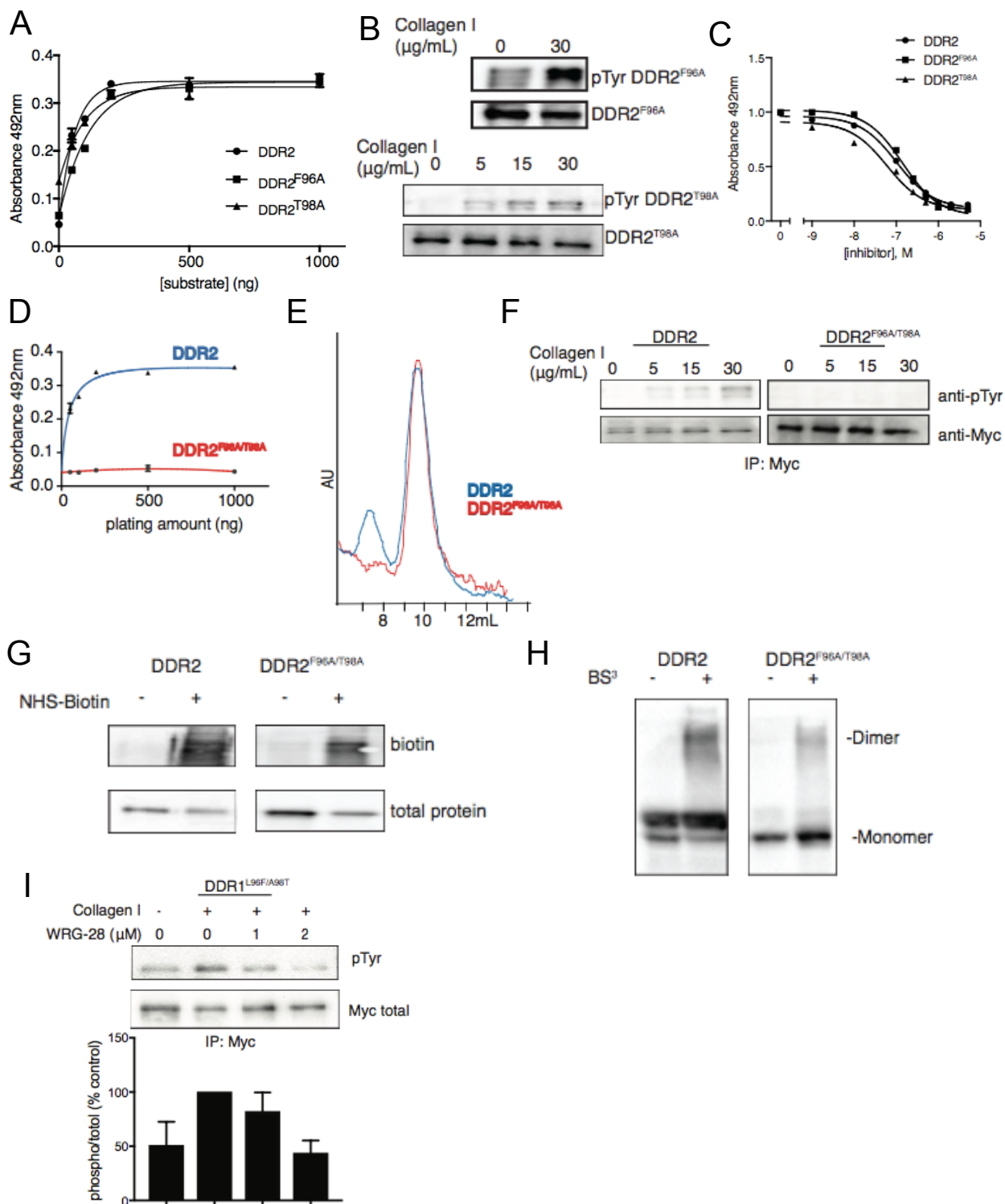


**Figure 2.10: Identification of DS-DSL domain interface residues required for DDR2-collagen binding and signaling**

(A) Solid phase binding assay of 25nM recombinant DDR2-His, DDR2<sup>F96A</sup>-His, or DDR2<sup>T98A</sup>-His binding to the high affinity collagen II DDR2 binding peptide.

- (B) HEK293 cells transfected with DDR2F96A-Myc or DDR2T98A-Myc were added to plates and stimulated with indicated concentrations of collagen I for 4 hours. Tagged proteins were immunoprecipitated with Myc antibody and bound products western blotted with pTyr 4G10 and then stripped and reprobed with Myc antibodies.
- (C) Inhibition by WRG-28 of DDR2-His or single point mutants DDR2F96A or DDR2T98A binding. Inhibitory curves as measured by solid phase binding assay of DDR2-His or point mutant binding (25nM). Graph shows mean  $\pm$  SEM from a single experiment representative of at least three independent experiments, three replicates per treatment per experiment.
- (D) Solid phase binding assay of 25nM recombinant DDR2-His or DDR2<sup>F96A/T98A</sup>-His binding to the high-affinity collagen II DDR2 binding peptide.
- (E) Size exclusion chromatography. Representative elution profile of DDR2-His or DDR2<sup>F96A/T98A</sup>-His on a Superdex 200 Increase 10/300 GL column
- (F) HEK293 cells transfected with DDR2-Myc or DDR2<sup>F96A/T98A</sup>-Myc were added to plates and stimulated with indicated concentrations of collagen I for 4 hours. Tagged proteins were immunoprecipitated with Myc antibody and bound products western blotted with pTyr 4G10 or Myc antibodies.
- (G) Surface biotinylation. Cell surface expression of DDR2-Myc or DDR2F96A/T98A-Myc was confirmed using a biotinylation assay. HEK293 cells expressing indicated constructs were biotinylated using EZ-link NHS-PEG4-Biotin. Proteins were immunoprecipitated using Myc antibody, and then western blotted with Streptavidin-HRP.
- (H) Cross linking to determine ability of DDR2 constructs to homodimerize. HEK293 cells transfected with DDR2-Myc or DDR2F96A/T98A-Myc were treated with 0.1M BS3 in PBS and analyzed by Western blotting with anti-DDR2 antibody.
- (I) HEK293 cells transfected with DDR1<sup>L96F/A98T</sup>-Myc were added to plates coated with 30 $\mu$ g/mL collagen I for 4 hours in the presence indicated concentrations of WRG-28. Tagged proteins were immunoprecipitated with Myc antibody and bound products western blotted with pTyr mAb 4G10 and reprobed with Myc antibodies. Representative blot shown, quantification of 3 independent experiments represented as mean  $\pm$  SEM.

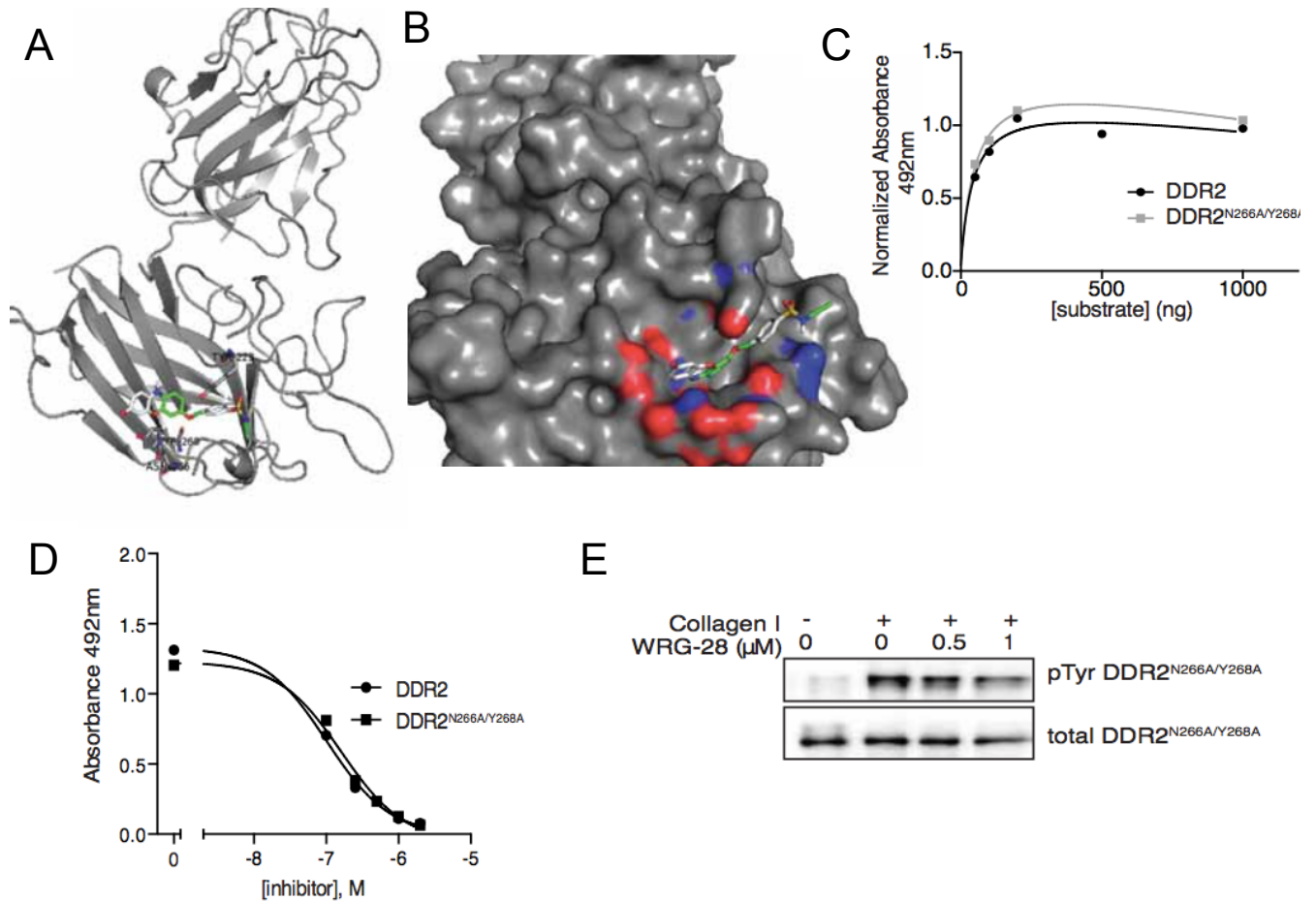


**Figure 2.11: Evaluation of an alternatively predicted binding site**

(A) Overall view of the DDR2 extracellular domain structure depicting WRG-28 in alternative binding site (Site 3 from S4A)

(B) View of WRG-28 oriented in predicted cleft using surface representation of DDR2. For protein and inhibitor atom colors rendered as follows: nitrogen (blue), oxygen (red), sulfur (yellow). For inhibitor, carbon rendered green.

(C) Solid phase binding assay of 25nM recombinant DDR2-His or DDR2<sup>N266A/Y268A</sup>-His binding to the high affinity collagen II DDR2 binding peptide.

(D) Effect of WRG-28 on DDR2 or DDR2<sup>N266A/Y268A</sup> extracellular domain binding. Inhibitory curves as measured by solid phase binding assay of DDR2 extracellular domain binding (25nM protein). Graph shows mean  $\pm$  SEM from a single experiment representative of at least three independent experiments, three replicates per treatment per experiment.

(E) HEK293 cells transfected with DDR2<sup>N266A/Y268A</sup>-Myc were added to plates coated with 30 $\mu$ g/mL collagen I for 4 hours in the presence of various concentrations of WRG-28. DDR2 was immunoprecipitated with Myc antibody and bound products western blotted with pTyr 4G10 or Myc antibodies.

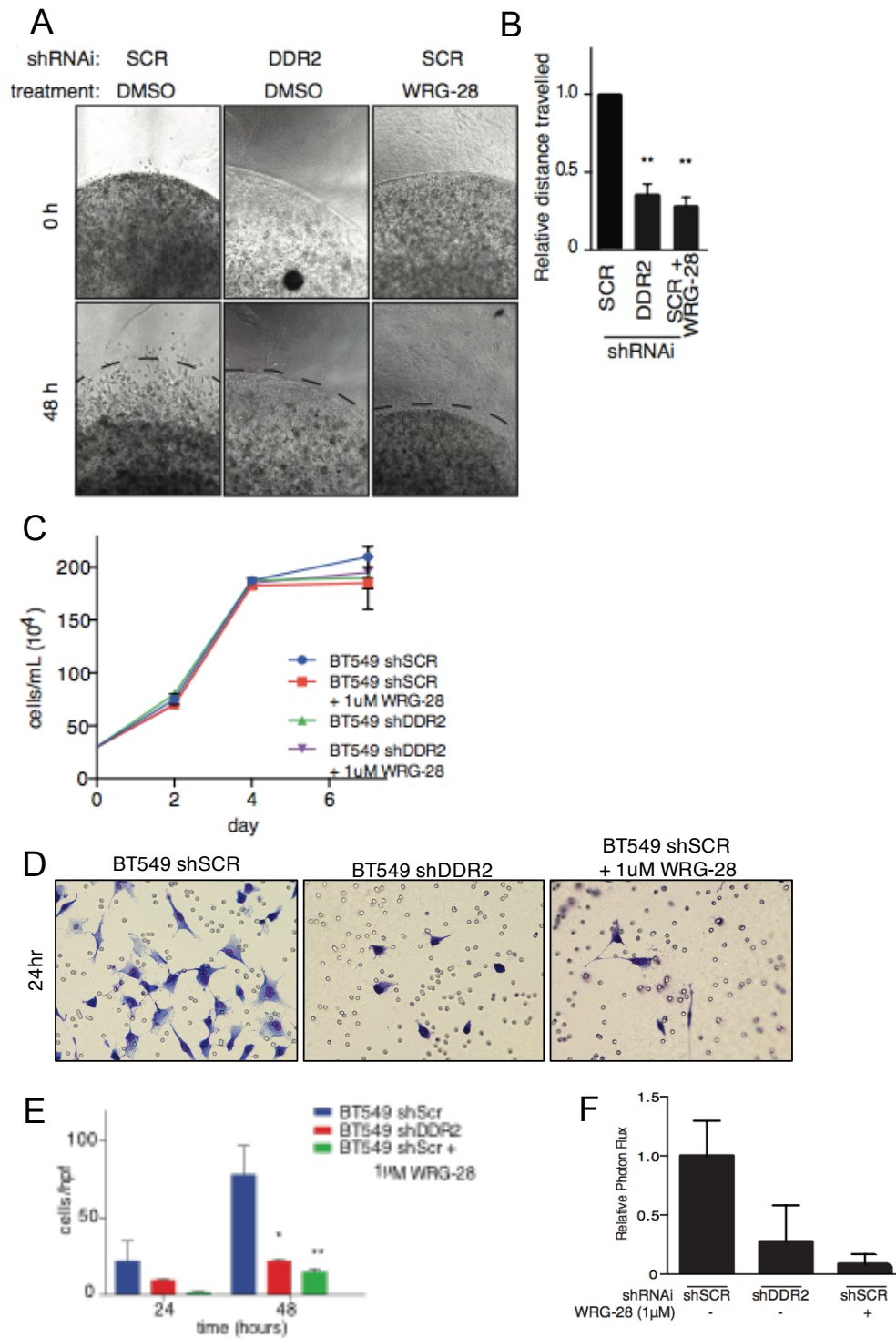


**Figure 2.12: WRG-28 inhibition of DDR2 blunts tumor cell invasion and migration, but does not influence proliferation**

(A) Cell migration in 3D collagen I gels of BT549 cells treated with 1μM WRG-28 or control, as compared to cells depleted of DDR2. Representative images shown. Dashed line delineates invasive front.

- (B) Quantification of experiment described in (A). Distance traveled relative to control cells was determined at 48hrs. (\*\*P<0.01, ANOVA, n=4 per condition)
- (C) Proliferation of BT549 control or shDDR2 depleted cells in the presence or absence of 1 $\mu$ M WRG-28.
- (D) Matrigel invasion of BT549 cell lines treated with 1 $\mu$ M WRG-28 or control as compared to cells depleted of DDR2 at 48 hours. Representative images of H&E stained inserts
- (E) Quantification of experiment described in (D). BT549 shSCR (blue), shDDR2 (red), or shSCR WRG-28 treated cells (green) (\*p<0.05, \*\*p<0.01, ANOVA, n=3 inserts per condition. Experiment was preformed 3 independent times with similar results).
- (F) Matrigel invasion of 4T1-GFP-luc cell lines treated with 1 $\mu$ M WRG-28 or control as compared to depleted of DDR2 at 48 hours. Invasion measured by bioluminescence of cells on fluoroblock transwell inserts. Mean  $\pm$  SEM. (n=3 per condition)

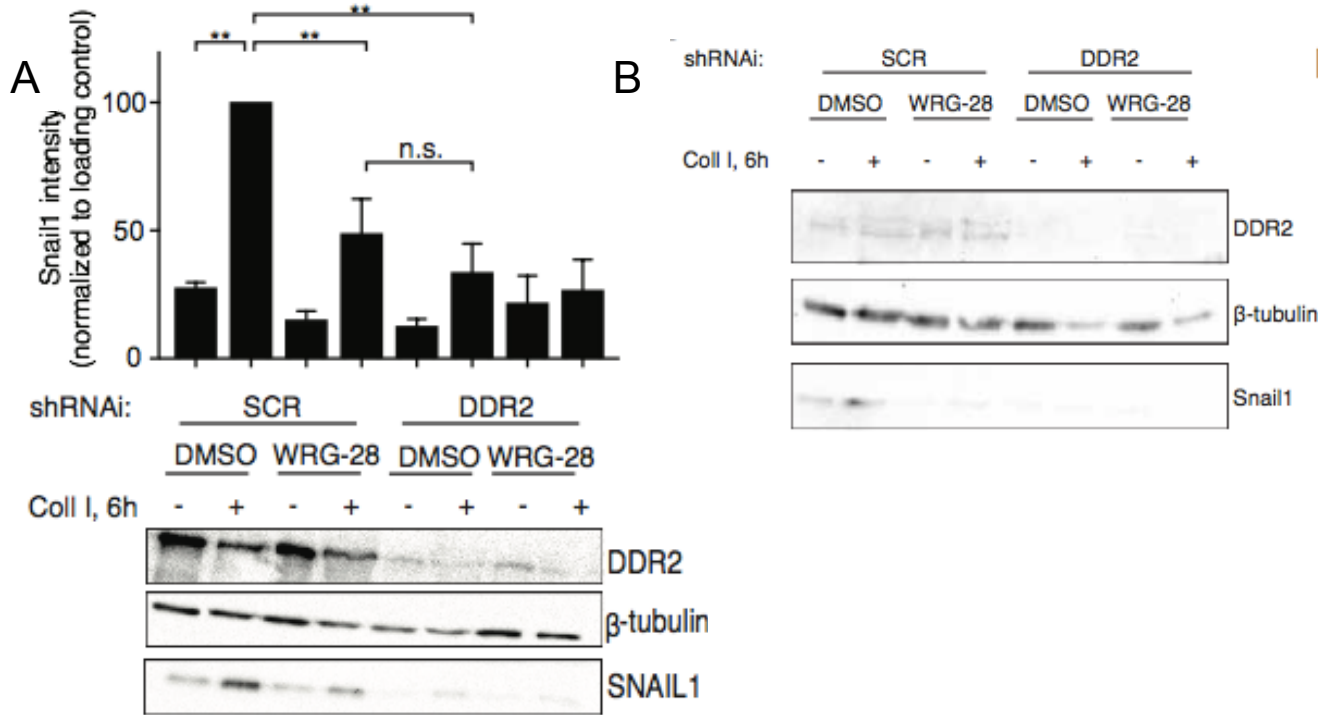


**Figure 2.13: WRG-28 blocks DDR2 mediated signaling in breast tumor cells and is effective against TKI resistant mutations**

(A) BT549 cells added to collagen I coated (2mg/mL) or uncoated plates in the presence of WRG-28 (1μM) or DMSO for 6 hours. Western blots were performed for analysis of SNAIL1 stabilization. Representative blot shown. Quantification by densitometric analysis of 3 independent experiments represented as mean ± SEM (\*\*P<0.01, n.s.=not significant, ANOVA.)

(B) 4T1 cells added to collagen I coated (2mg/mL) or uncoated plates in the presence of WRG-28 (1μM) or DMSO for 6 hours. Western blots were performed for analysis of SNAIL1 stabilization.

(C) HEK293 cells transfected with DDR2<sup>T654I</sup>-Myc were added to plates and stimulated with 30μg/mL collagen I for 4 hours in the presence of various concentrations of WRG-28. DDR2 was immunoprecipitated with Myc antibody and bound products western blotted with pTyr 4G10 or DDR2 antibodies.

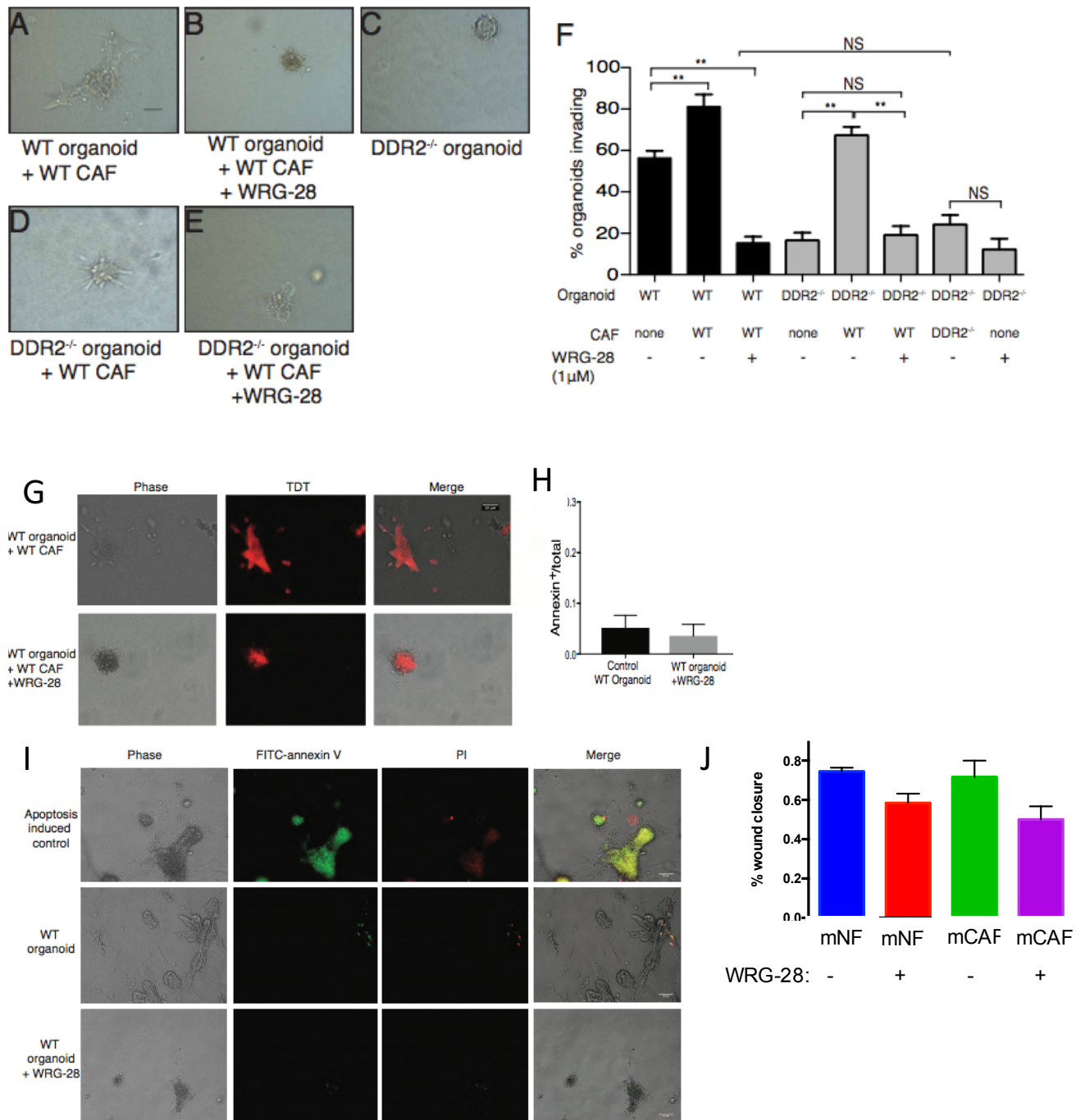


**Figure 2.14: WRG-28 blocks the tumor promoting effects of DDR2 expressing CAFs**

(A-E) Representative images of tumor organoids scored. A. invasive WT organoid cultured in the presence of WT breast CAFs B. WT organoid cultured in the presence of WT breast CAFs, 1μM WRG-28 C. *Ddr2*<sup>-/-</sup> organoid, non-invasive D. *Ddr2*<sup>-/-</sup> organoids cultured in the presence of WT breast CAFs, invasive E. *Ddr2*<sup>-/-</sup> organoid cultured in the presence of WT breast CAFs, 1μM WRG-28. Scale bar=100μm

(F) Quantification of number of invasive tumor organoids as a percent of total organoids scored after 4 days. 30 organoids per condition were scored. WT, wild type. Data are mean  $\pm$  SEM from a single experiment representative of three independent experiments. NS, not significant, \* $p < 0.05$ , \*\* $p < 0.01$  one-way ANOVA

(G) Phase contrast image, Tomato fluorescence of MMTV-PyMT; *Ddr2*<sup>+/+</sup>; ROSA-LSL-TdTomato tumor organoids, and merged image confirming that invasive foci contain migrating tumor cells. Scale bar = 50 $\mu$ m.

(H) Quantification of positive annexin V staining as compared to total organoid area for control WT organoids or WT organoids treated with 1 $\mu$ M WRG-28.

(I) Representative images of phase, PI staining, and annexin V staining of organoids quantified in (H). Doxorubicin induced apoptosis was used as a positive control of staining. Scale bar = 50 $\mu$ m

(J) Scratch wound assay of fibroblasts in the presence or absence of 1 $\mu$ M WRG-28. Distance was measured at baseline and again at 24hrs, data representing mean  $\pm$  SEM, each condition preformed in triplicate. mNF=mouse normal fibroblast. mCAF=PyMT tumor derived mouse fibroblast.

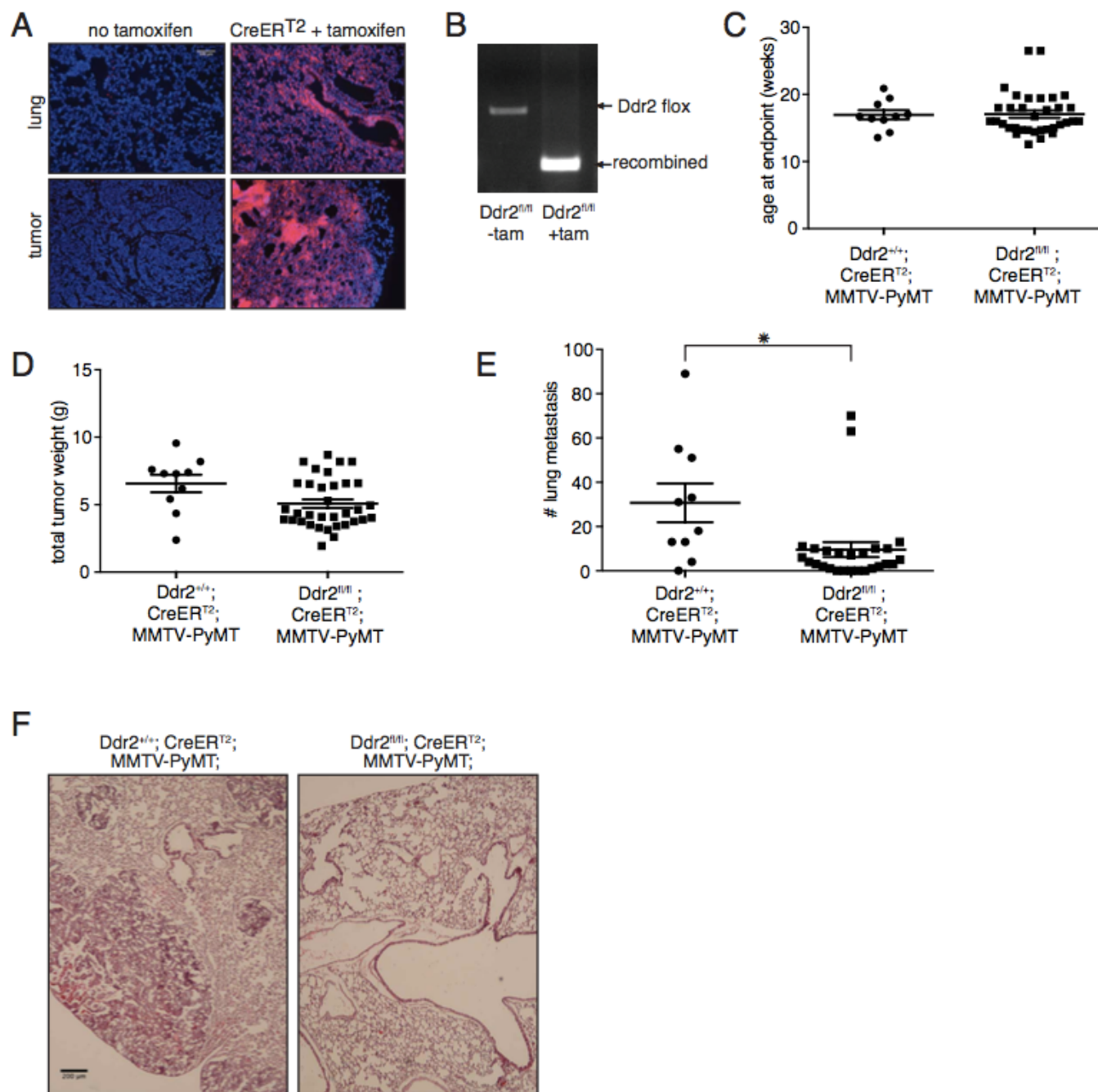


**Figure 2.15: Genetic validation of DDR2 as a therapeutic target to prevent breast cancer metastasis**

(A) Tomato (red) staining of mammary tumor/lung sections from *Ddr2<sup>fl/fl</sup>*; CreER<sup>T2</sup>; MMTV-PyMT mice ± tamoxifen administration. DAPI (blue) staining of nuclei. Scale bar=100µm.

(B) PCR for detection of the floxed and recombined DDR2 allele for a mouse prior to tamoxifen (tail) or after tamoxifen administration (tumor at endpoint). Tam=tamoxifen

(C) Primary tumor growth rates of *Ddr2*<sup>+/+</sup>; CreER<sup>T2</sup>; MMTV-PyMT (control) and *Ddr2*<sup>fl/fl</sup>; CreER<sup>T2</sup>; MMTV-PyMT (deletion at 8 weeks) mice determined by the age at which the largest tumor reached 2 cm in diameter. n=10-26 mice per group. Data are presented as mean ± SEM.

(D) Total tumor burden of *Ddr2*<sup>+/+</sup>; CreER<sup>T2</sup>; MMTV-PyMT (control) and *Ddr2*<sup>fl/fl</sup>; CreER<sup>T2</sup>; MMTV-PyMT (deletion at 8 weeks) mice determined by the sum of the weight of all tumors for each mouse when the largest tumor reached 2 cm in diameter. n=10-26 mice per group. Data are presented as mean ± SEM.

(E) Quantification of lung metastases in *Ddr2*<sup>+/+</sup>; CreER<sup>T2</sup>; MMTV-PyMT (control) and *Ddr2*<sup>fl/fl</sup>; CreER<sup>T2</sup>; MMTV-PyMT (deletion at 8 weeks) mice, calculated by the number of microscopically visible metastases counted from three H&E stained sections of lung from each mouse taken >200µm apart, normalized to the total lung area. \*p < 0.05, two tailed unpaired t-test; n=10-26 mice per group. Data are presented as mean ± SEM.

(F) Representative images of lungs quantified in E. Scale bar=200µm.

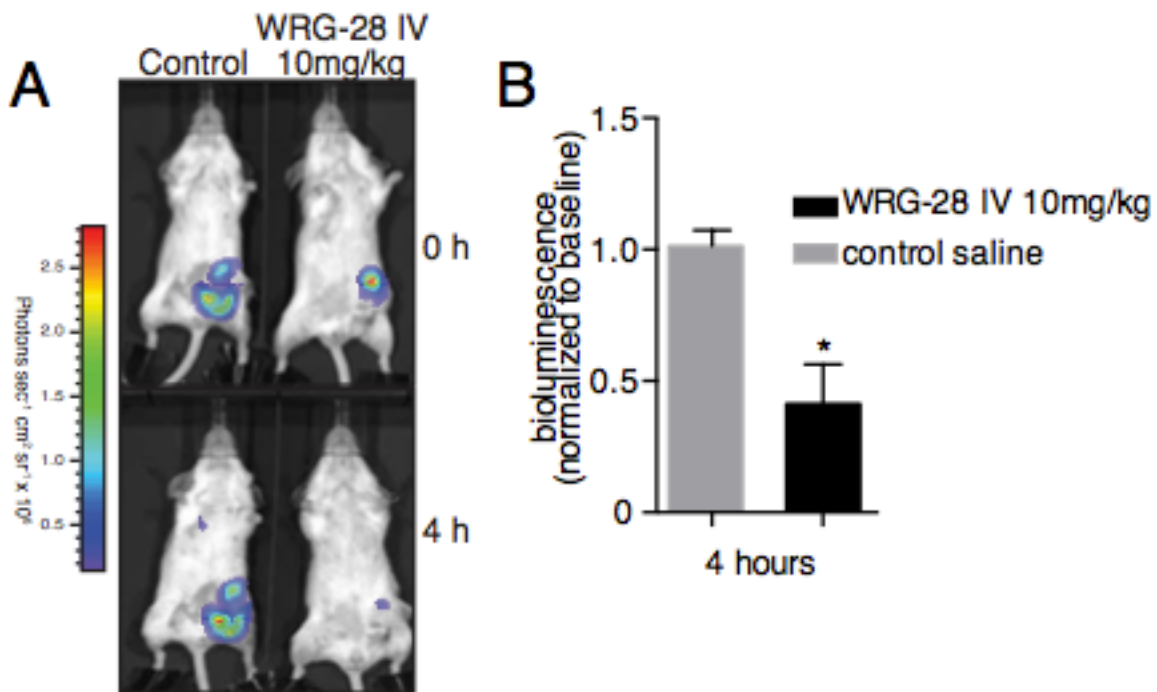


**Figure 2.16: WRG-28 attenuates DDR2 signaling *in vivo***

(A) Representative images of bioluminescence of 4T1-Snail-CBG tumor bearing mice at 4 hours following treatment with WRG-28 or saline control, as compared to their pre-treatment baseline.

(B) Quantification of relative bioluminescence of 4T1-Snail-CBG tumor bearing mice at 4 hours following treatment with WRG-28 or saline control, as compared to their pre-treatment baseline. Mean  $\pm$  SEM \* $p < 0.05$  (n=3 controls, n=8 treatment group)

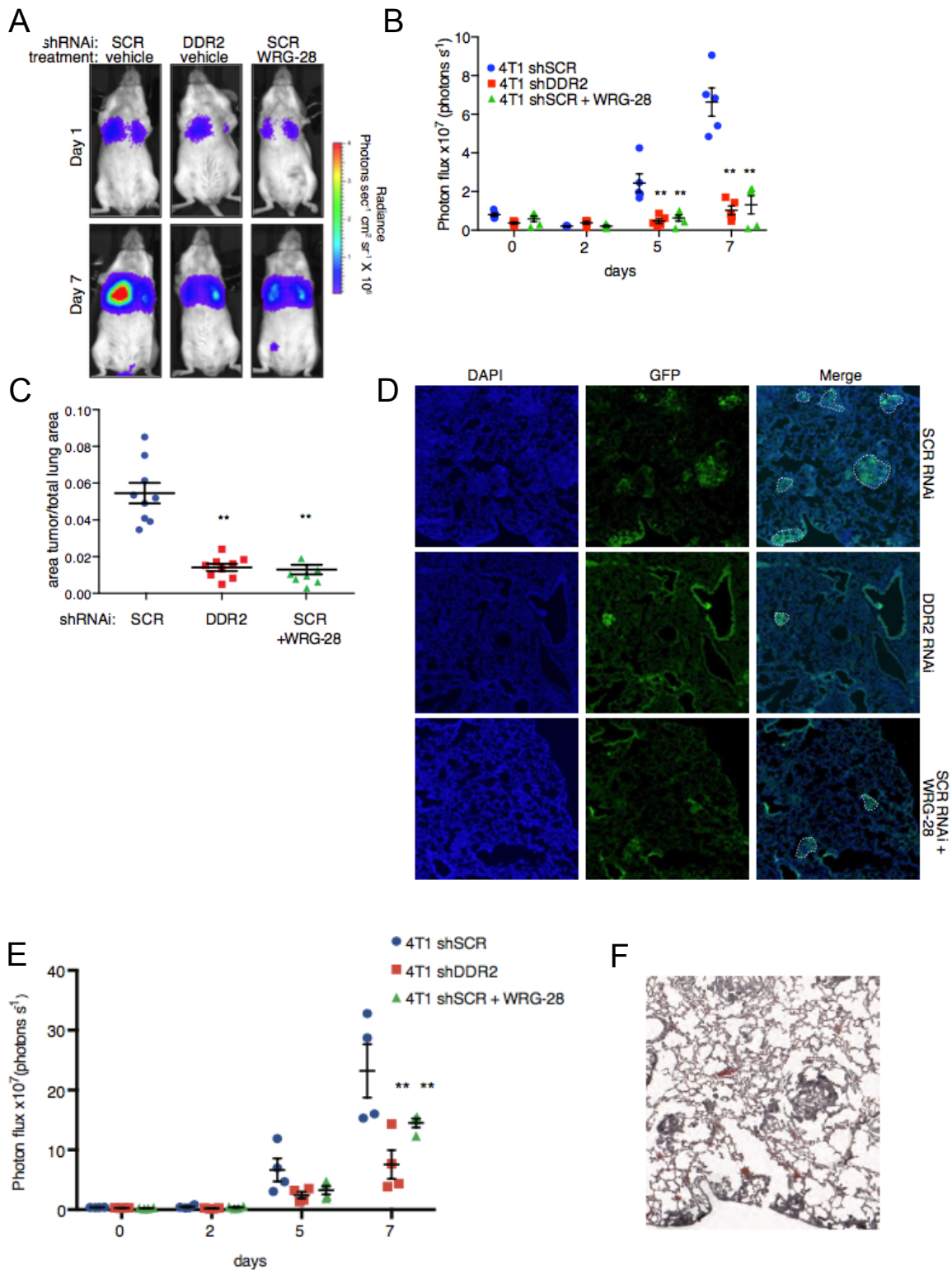


**Figure 2.17: WRG-28 administration reduces metastatic lung colonization of breast tumor cells**

(A) Tail vein metastasis assay where BALB/cJ mice are injected by tail vein with  $5 \times 10^5$  4T1-GFP-luc expressing cells and lungs evaluated for the presence of metastatic

tumors, comparing control, WRG-28 treated and shDDR2 depleted conditions. Representative images of BALB/cJ mice at baseline after injection and after 7 days for each of the various experimental groups.

(B) Quantification of experiment in (A) comparing control (blue circles), WRG-28 treated (green triangles) and shDDR2 depleted (red squares) conditions. Means  $\pm$  SEM; data derived from one experiment of five mice per condition. \*\* $p < 0.01$  two way ANOVA

(C) Quantification of images in (D), showing percentage of GFP-tumor positive areas in the lung. 2 sections through each of five lobes per animal quantified. Data derived from 2 experiments,  $n=9$  mice for each condition. Means  $\pm$  SEM. \*\* $p < 0.001$ , one way ANOVA.

(D) Representative images of histologic analysis for GFP expressing tumor nodules in lungs of mice from (A), comparing WRG-28 treated to control or DDR2 depleted tumor cells. Dashed white line delineating GFP positive tumor foci that were included in quantification.

(E) Bioluminescence quantification from second cohort of tail vein metastasis assay, BALB/cJ mice injected with 4T1 GFP-luc expressing cells. Means  $\pm$  SEM; data derived from one experiment of four mice per condition. \*\* $p < 0.01$ , two way ANOVA.

(F) H&E staining of a serial section of SCR RNAi in (D) illustrating consistency between GFP signal and tumor foci.

## References

1. McAllister, S.S. & Weinberg, R.A. Tumor-host interactions: a far-reaching relationship. *Journal of clinical oncology : official journal of the American Society of Clinical Oncology* **28**, 4022-4028 (2010).
2. Hanahan, D. & Coussens, L.M. Accessories to the crime: functions of cells recruited to the tumor microenvironment. *Cancer Cell* **21**, 309-322 (2012).
3. Swartz, M.A., *et al.* Tumor microenvironment complexity: emerging roles in cancer therapy. *Cancer research* **72**, 2473-2480 (2012).
4. Provenzano, P.P., *et al.* Collagen density promotes mammary tumor initiation and progression. *BMC medicine* **6**, 11 (2008).
5. Tice, J.A., *et al.* Benign breast disease, mammographic breast density, and the risk of breast cancer. *Journal of the National Cancer Institute* **105**, 1043-1049 (2013).
6. Conklin, M.W., *et al.* Aligned collagen is a prognostic signature for survival in human breast carcinoma. *The American journal of pathology* **178**, 1221-1232 (2011).
7. Gschwind, A., Fischer, O.M. & Ullrich, A. The discovery of receptor tyrosine kinases: targets for cancer therapy. *Nature reviews. Cancer* **4**, 361-370 (2004).
8. Lemmon, M.A. & Schlessinger, J. Cell signaling by receptor tyrosine kinases. *Cell* **141**, 1117-1134 (2010).
9. Vogel W, G.G., Alves F, Pawson T. The Discoidin Domain Receptor Tyrosine Kinases are Activated by Collagen. *Mol. Cell* **1**, 13-23 (1997).
10. Shrivastava A, R.C., Campbell E, Kovac L, McGlynn M, Ryan TE, Davis S, Goldfarb MP, Glass DJ, Lemke G, Yancopoulos GD. An Orphan Receptor Tyrosine Kinase Family Whose Members Serve as Nonintegrin Collagen Receptors. *Mol. Cell* **1**, 25-34 (1997).

11. Zhang, K., *et al.* The collagen receptor discoidin domain receptor 2 stabilizes SNAIL1 to facilitate breast cancer metastasis. *Nature cell biology* **15**, 677-687 (2013).
12. Ren, T., Zhang, J., Zhang, J., Liu, X. & Yao, L. Increased expression of discoidin domain receptor 2 (DDR2): a novel independent prognostic marker of worse outcome in breast cancer patients. *Medical oncology* **30**, 397 (2013).
13. Ren, T., *et al.* Discoidin domain receptor 2 (DDR2) promotes breast cancer cell metastasis and the mechanism implicates epithelial-mesenchymal transition programme under hypoxia. *J Pathol* **234**, 526-537 (2014).
14. Corsa, C.A., *et al.* The Action of Discoidin Domain Receptor 2 in Basal Tumor Cells and Stromal Cancer-Associated Fibroblasts Is Critical for Breast Cancer Metastasis. *Cell reports* **15**, 2510-2523 (2016).
15. Yan, Z., *et al.* Discoidin domain receptor 2 facilitates prostate cancer bone metastasis via regulating parathyroid hormone-related protein. *Biochimica et biophysica acta* **1842**, 1350-1363 (2014).
16. Rodrigues, R., *et al.* Comparative genomic hybridization, BRAF, RAS, RET, and oligo-array analysis in aneuploid papillary thyroid carcinomas. *Oncol Rep* **18**, 917-926 (2007).
17. Chua, H.H., *et al.* Upregulation of discoidin domain receptor 2 in nasopharyngeal carcinoma. *Head & neck* **30**, 427-436 (2008).
18. Xie, B., *et al.* DDR2 facilitates hepatocellular carcinoma invasion and metastasis via activating ERK signaling and stabilizing SNAIL1. *Journal of experimental & clinical cancer research : CR* **34**, 101 (2015).
19. Hammerman PS, S.M., Ramos AH, *et al.* Mutations in the DDR2 Kinase Gene Identify a Novel Therapeutic Target in Squamous Cell Lung Cancer. *Cancer Discovery* **1**, 78-89 (2011).
20. Xu, J., *et al.* Overexpression of DDR2 contributes to cell invasion and migration in head and neck squamous cell carcinoma. *Cancer biology & therapy* **15**, 612-622 (2014).

21. Toy, K.A., *et al.* Tyrosine kinase discoidin domain receptors DDR1 and DDR2 are coordinately deregulated in triple-negative breast cancer. *Breast Cancer Res Treat* **150**, 9-18 (2015).
22. Moody, S.E., *et al.* The transcriptional repressor Snail promotes mammary tumor recurrence. *Cancer Cell* **8**, 197-209 (2005).
23. Tran, H.D., *et al.* Transient SNAIL1 expression is necessary for metastatic competence in breast cancer. *Cancer research* **74**, 6330-6340 (2014).
24. Sivakumar, L. & Agarwal, G. The influence of discoidin domain receptor 2 on the persistence length of collagen type I fibers. *Biomaterials* **31**, 4802-4808 (2010).
25. Arteaga, C.L. & Engelman, J.A. ERBB receptors: from oncogene discovery to basic science to mechanism-based cancer therapeutics. *Cancer Cell* **25**, 282-303 (2014).
26. Tvorogov, D., *et al.* Effective suppression of vascular network formation by combination of antibodies blocking VEGFR ligand binding and receptor dimerization. *Cancer Cell* **18**, 630-640 (2010).
27. Arora, A. & Scholar, E.M. Role of tyrosine kinase inhibitors in cancer therapy. *The Journal of pharmacology and experimental therapeutics* **315**, 971-979 (2005).
28. Sierra, J.R., Cepero, V. & Giordano, S. Molecular mechanisms of acquired resistance to tyrosine kinase targeted therapy. *Molecular cancer* **9**, 75 (2010).
29. Terai, H., *et al.* Characterization of DDR2 Inhibitors for the Treatment of DDR2 Mutated Nonsmall Cell Lung Cancer. *ACS chemical biology* **10**, 2687-2696 (2015).
30. Richters, A., *et al.* Identification of type II and III DDR2 inhibitors. *Journal of medicinal chemistry* **57**, 4252-4262 (2014).
31. Beauchamp, E.M., *et al.* Acquired resistance to dasatinib in lung cancer cell lines conferred by DDR2 gatekeeper mutation and NF1 loss. *Molecular cancer therapeutics* **13**, 475-482 (2014).

32. Bono, F., *et al.* Inhibition of tumor angiogenesis and growth by a small-molecule multi-FGF receptor blocker with allosteric properties. *Cancer Cell* **23**, 477-488 (2013).
33. Herbert, C., *et al.* Molecular mechanism of SSR128129E, an extracellularly acting, small-molecule, allosteric inhibitor of FGF receptor signaling. *Cancer Cell* **23**, 489-501 (2013).
34. He, M.M., *et al.* Small-molecule inhibition of TNF-alpha. *Science* **310**, 1022-1025 (2005).
35. Berg, T. Modulation of protein-protein interactions with small organic molecules. *Angew Chem Int Ed Engl* **42**, 2462-2481 (2003).
36. Christopoulos, A. Allosteric binding sites on cell-surface receptors: novel targets for drug discovery. *Nature reviews. Drug discovery* **1**, 198-210 (2002).
37. Wenthur, C.J., Gentry, P.R., Mathews, T.P. & Lindsley, C.W. Drugs for allosteric sites on receptors. *Annual review of pharmacology and toxicology* **54**, 165-184 (2014).
38. Siddiqui, K., *et al.* Actinomycin D identified as an inhibitor of discoidin domain receptor 2 interaction with collagen through an insect cell based screening of a drug compound library. *Biological & pharmaceutical bulletin* **32**, 136-141 (2009).
39. Phillips FS, S.H., Sternberg SS, Tan CTC. The toxicity of actinomycin D. *ANnals of the NY Academy of Sciences* **89**, 348-360 (1960).
40. Leitinger, B. Molecular Analysis of Collagen Binding by the Human Discoidin Domain Receptors, DDR1 and DDR2. *The Journal of biological chemistry* **278**, 16761-16769 (2003).
41. Carafoli, F., *et al.* Crystallographic insight into collagen recognition by discoidin domain receptor 2. *Structure* **17**, 1573-1581 (2009).
42. Konitsiotis, A.D., *et al.* Characterization of high affinity binding motifs for the discoidin domain receptor DDR2 in collagen. *J Biol Chem* **283**, 6861-6868 (2008).

43. Knight, C.G., *et al.* The collagen-binding A-domains of integrins alpha(1)beta(1) and alpha(2)beta(1) recognize the same specific amino acid sequence, GFOGER, in native (triple-helical) collagens. *The Journal of biological chemistry* **275**, 35-40 (2000).
44. Agarwal, G., Kovac, L., Radziejewski, C. & Samuelsson, S.J. Binding of discoidin domain receptor 2 to collagen I: an atomic force microscopy investigation. *Biochemistry* **41**, 11091-11098 (2002).
45. Xu H, R.N., Stathopoulos S, Myllyharju J, Farndale RW, Leitinger B. Collagen binding specificity of the discoidin domain receptors: Binding sites on collagens II and III and molecular determinants for collagen IV recognition by DDR1. *Matrix Biology* **30**, 16-26 (2011).
46. Noordeen, N.A., Carafoli, F., Hohenester, E., Horton, M.A. & Leitinger, B. A transmembrane leucine zipper is required for activation of the dimeric receptor tyrosine kinase DDR1. *The Journal of biological chemistry* **281**, 22744-22751 (2006).
47. Fu, H.L., *et al.* Discoidin domain receptors: unique receptor tyrosine kinases in collagen-mediated signaling. *The Journal of biological chemistry* **288**, 7430-7437 (2013).
48. Arnold, K., Bordoli, L., Kopp, J. & Schwede, T. The SWISS-MODEL workspace: a web-based environment for protein structure homology modelling. *Bioinformatics* **22**, 195-201 (2006).
49. Guex, N., Peitsch, M.C. & Schwede, T. Automated comparative protein structure modeling with SWISS-MODEL and Swiss-PdbViewer: a historical perspective. *Electrophoresis* **30 Suppl 1**, S162-173 (2009).
50. Schwede, T., Kopp, J., Guex, N. & Peitsch, M.C. SWISS-MODEL: An automated protein homology-modeling server. *Nucleic acids research* **31**, 3381-3385 (2003).
51. Carafoli, F., *et al.* Structure of the discoidin domain receptor 1 extracellular region bound to an inhibitory Fab fragment reveals features important for signaling. *Structure* **20**, 688-697 (2012).

52. Trott, O. & Olson, A.J. AutoDock Vina: improving the speed and accuracy of docking with a new scoring function, efficient optimization, and multithreading. *Journal of computational chemistry* **31**, 455-461 (2010).
53. Chen, Y.N., *et al.* Allosteric inhibition of SHP2 phosphatase inhibits cancers driven by receptor tyrosine kinases. *Nature* **535**, 148-152 (2016).
54. Calleja, V., Laguerre, M., Parker, P.J. & Larijani, B. Role of a novel PH-kinase domain interface in PKB/Akt regulation: structural mechanism for allosteric inhibition. *PLoS biology* **7**, e17 (2009).
55. Amemiya, T., Koike, R., Fuchigami, S., Ikeguchi, M. & Kidera, A. Classification and annotation of the relationship between protein structural change and ligand binding. *Journal of molecular biology* **408**, 568-584 (2011).
56. Olaso, E., *et al.* Discoidin domain receptor 2 regulates fibroblast proliferation and migration through the extracellular matrix in association with transcriptional activation of matrix metalloproteinase-2. *The Journal of biological chemistry* **277**, 3606-3613 (2002).
57. Herrera-Herrera, M.L. & Quezada-Calvillo, R. DDR2 plays a role in fibroblast migration independent of adhesion ligand and collagen activated DDR2 tyrosine kinase. *Biochemical and biophysical research communications* **429**, 39-44 (2012).
58. Lin, E.Y., *et al.* Progression to malignancy in the polyoma middle T oncoprotein mouse breast cancer model provides a reliable model for human diseases. *The American journal of pathology* **163**, 2113-2126 (2003).
59. Zhang, K., *et al.* Lats2 kinase potentiates Snail1 activity by promoting nuclear retention upon phosphorylation. *The EMBO journal* **31**, 29-43 (2012).
60. Coelho, N.M., *et al.* Discoidin Domain Receptor 1 Mediates Myosin-Dependent Collagen Contraction. *Cell reports* **18**, 1774-1790 (2017).
61. Yeung, D., Chmielewski, D., Mihai, C. & Agarwal, G. Oligomerization of DDR1 ECD affects receptor-ligand binding. *J Struct Biol* **183**, 495-500 (2013).

62. Changeux, J.P. & Christopoulos, A. Allosteric Modulation as a Unifying Mechanism for Receptor Function and Regulation. *Cell* **166**, 1084-1102 (2016).
63. Arnaout, M.A., Mahalingam, B. & Xiong, J.P. Integrin structure, allostery, and bidirectional signaling. *Annual review of cell and developmental biology* **21**, 381-410 (2005).
64. Valiathan, R.R., Marco, M., Leitinger, B., Kleer, C.G. & Fridman, R. Discoidin domain receptor tyrosine kinases: new players in cancer progression. *Cancer metastasis reviews* **31**, 295-321 (2012).
65. Manning, L.B., Li, Y., Chickmagalur, N.S., Li, X. & Xu, L. Discoidin Domain Receptor 2 as a Potential Therapeutic Target for Development of Disease-Modifying Osteoarthritis Drugs. *The American journal of pathology* (2016).
66. Xu, L., *et al.* Activation of the discoidin domain receptor 2 induces expression of matrix metalloproteinase 13 associated with osteoarthritis in mice. *The Journal of biological chemistry* **280**, 548-555 (2005).
67. George, M., Vijayakumar, A., Dhanesh, S.B., James, J. & Shivakumar, K. Molecular basis and functional significance of Angiotensin II-induced increase in Discoidin Domain Receptor 2 gene expression in cardiac fibroblasts. *Journal of molecular and cellular cardiology* **90**, 59-69 (2016).
68. Zhao, H., *et al.* Targeting of Discoidin Domain Receptor 2 (DDR2) Prevents Myofibroblast Activation and Neovessel Formation During Pulmonary Fibrosis. *Molecular therapy : the journal of the American Society of Gene Therapy* (2016).
69. Zidar, N., *et al.* New 5-benzylidenethiazolidin-4-one inhibitors of bacterial MurD ligase: design, synthesis, crystal structures, and biological evaluation. *European journal of medicinal chemistry* **46**, 5512-5523 (2011).
70. Feng, Y., *et al.* A multifunctional lentiviral-based gene knockdown with concurrent rescue that controls for off-target effects of RNAi. *Genomics, proteomics & bioinformatics* **8**, 238-245 (2010).
71. Raynal, N., *et al.* Use of synthetic peptides to locate novel integrin alpha2beta1-binding motifs in human collagen III. *The Journal of biological chemistry* **281**, 3821-3831 (2006).

## **Chapter 3**

# **TWIST1 induces expression of Discoidin Domain Receptor 2 to Promote Ovarian Cancer Metastasis**

This chapter has been adapted from a submitted manuscript and also contains unpublished data.

The citation for the submitted manuscript is:

TWIST1 induces expression of Discoidin Domain Receptor2 (DDR2) to Promote Ovarian Cancer Metastasis. Whitney R. Grither, Laura M. Divine, Daniel J. Wilke, Riva A. Desai, Andrew J. Loza, Anne K. Lohrey, Eric Meller, Gregory D. Longmore, Katherine C. Fuh. In review, 2017.

## **Introduction**

Unique from other malignancies of epithelial origin, the metastatic cascade of ovarian tumors commonly occurs via the peritoneal circulation, and the majority of metastases are confined within the abdominal peritoneal cavity<sup>1</sup>. After tumor cell detachment from the primary site in the ovary, tumor cells must attach to the mesothelial cells covering the peritoneal and pleural organs, then clear the mesothelial layer to invade through the underlying basement membrane and extracellular matrix (ECM) to form metastatic implants<sup>2</sup>. Thus, for efficient metastasis, ovarian tumor cell interaction with the surrounding ECM and subsequent remodeling of the ECM is critical<sup>3,4</sup>. Identifying cellular and molecular targets important for one or more of these steps could have tremendous clinical impact by enabling the development of therapeutics that block these critical steps.

The ability of ovarian cancer cells to adopt a mesenchymal gene program has been shown to promote ovarian cancer metastasis<sup>5</sup>. Induction of epithelial-to-mesenchymal transition (EMT) in ovarian cancer cells through expression of EMT transcription factors TWIST1, SNAIL1, or ZEB1 promotes mesothelial cell clearance<sup>5</sup>. These factors also promote the ability of an ovarian cancer cell to invade the basement membrane and extracellular matrix, and form metastatic implants<sup>6-8</sup>. While these EMT transcription factors induce a mesenchymal program crucial for ovarian cancer metastasis, the specific proteins whose expression is regulated during EMT that functionally mediate mesothelial cell attachment, clearance, and tumor cell invasion are not fully appreciated.

Mesenchymal properties of the developing cranial mesoderm are regulated by Twist1 transcriptional targets that influence cell-matrix interactions. Among the

mesenchymal genes transcriptionally regulated by TWIST1 in this developing tissue is Discoidin Domain receptor 2<sup>9</sup>. TWIST1 binds to the 5'-regulatory region of *Ddr2* inducing its expression in this tissue. Discoidin domain receptor 2 (DDR2) is a unique receptor tyrosine kinase (RTK) that has been shown to promote the metastasis of multiple cancers<sup>10-18</sup>. Unlike most RTKs that utilize soluble growth factors as ligands, fibrillar collagens serve as the ligand for DDR2<sup>19,20</sup>. This provides for unique cell-ECM interactions. Fibrillar type I collagen is the major structural element of the ovarian stroma and has been shown to increase four-fold in ovarian cancer<sup>21</sup>. DDR2 is a mesenchymal gene not typically expressed by normal epithelium<sup>22</sup>, however, its expression is activated in many cancer cells of epithelial origin as they progress to invasive and metastatic cancers<sup>23</sup>. DDR2 has been shown to stabilize the EMT transcription factor SNAIL1 in tumor cells that have undergone EMT, thereby maintaining mesenchymal cell behaviors, including invasion and migration<sup>11,12,16</sup>.

In orthotopic transplant and spontaneous genetic models, depletion or deletion of *Ddr2* in tumor cells prevents metastasis *in vivo* in breast<sup>10,11</sup> and prostate<sup>13</sup> cancer models. The role of DDR2 in promoting invasion and metastasis has been ascribed to its regulation of a number of different molecular effectors, including upregulation of MT1-MMP activity via a SNAIL1 mediated pathway<sup>11,16</sup>. In addition, the expression and activity of various matrix remodeling enzymes, such as matrix metalloproteinases (MMPs) and lysyl oxidases is influenced by the presence and activation of DDR2<sup>10,24</sup>. Furthermore, while DDR2 itself does not mediate strong adhesive contacts, it has been shown to have an adhesion promoting role through enhancement of integrin activation state<sup>25</sup>. Whether DDR2 contributes to ovarian cancer metastasis is not known.

In this study, we show that TWIST1 regulates DDR2 expression in ovarian cancer cells. We find that the presence of DDR2 in ovarian tumor cells is critical for mesothelial cell clearance, and tumor cell invasion and migration, in part through promotion of ECM remodeling. We also demonstrate that the action of DDR2 in ovarian tumor cells is critical for ovarian tumor metastasis *in vivo*. As such, DDR2 represents a potential therapeutic target to modulate numerous pathways critical for metastatic ovarian tumor progression.

## **Results**

### **TWIST1 regulates DDR2 Expression in Ovarian Cancer Cells**

The EMT transcription factor TWIST1 has been shown to transcriptionally induce expression of Ddr2 in developing mesenchymal neural tissue<sup>9</sup>. Ovarian cancer cells have been shown to adopt a mesenchymal program during tumor progression, which influences tumor cell-matrix interactions and remodeling that promote metastasis<sup>26</sup>. Therefore, we asked whether the TWIST1-DDR2 pathway was present in ovarian cancer cells. In a collection of ovarian cancer cell lines the expression of DDR2 and TWIST1 was highly correlated, particularly in cell lines with metastatic potential (Figure 3.1A). To determine if TWIST1 regulated DDR2 expression in these ovarian cancer cells, TWIST1 expression was depleted using shRNA. In A2780 and ES2 ovarian tumor cells this resulted in decreased DDR2 mRNA (Figure 3.1C) and protein level (Figure 3.1B). In contrast, depletion of DDR2 had no effect on TWIST1 level (Figure 3.1B).

TWIST1 expression is induced during TGF- $\beta$ -induced EMT<sup>27</sup>. Therefore, we asked whether TGF- $\beta$ -induced TWIST1 expression in ovarian tumor cells resulted in DDR2 expression. Treatment of epithelial OVCAR3 ovarian cancer cells (which do not express TWIST1 or DDR2 at baseline) with 2 ng/mL of TGF- $\beta$  induced EMT, as assessed by expression of  $\alpha$ -SMA (Figure 3.1D). Both TWIST1 and DDR2 expression were induced as well (Figure 3.1D) and maintained under continuous exposure to TGF- $\beta$ .

In OVCAR3 cells, shRNA-mediated TWIST1 depletion did not affect EMT induction in response to TGF- $\beta$ , as seen by expression of  $\alpha$ -SMA (Figure 3.1E). However, in the absence of TWIST1, DDR2 was not expressed (Figure 3.1E). These data indicate that

as ovarian cancer cells progress to more invasive, mesenchymal phenotypes, TWIST1 promotes DDR2 expression.

### **DDR2 Promotes Mesothelial Cell Clearance**

Upon detachment of ovarian tumor cells from the primary site, the layer of mesothelial cells lining the peritoneal cavity must be cleared by the tumor cell for successful attachment<sup>2</sup>. Constitutive TWIST1 overexpression in ovarian tumor cells promotes their capacity for mesothelial cell clearance<sup>5</sup>. Therefore, we asked whether expression of DDR2, induced by TWIST1, could be responsible for mediating mesothelial cell clearance. We adapted an ovarian tumor spheroid mesothelial cell clearance assay<sup>28</sup> and confirmed that ES2 cells readily clear the mesothelial monolayer, as previously reported<sup>5</sup> (Figure 3.2A and 3.2B). Genetic depletion of DDR2 in ES2 cells significantly reduced their mesothelial cell clearance ability (Figure 3.2A and 3.2B) to an extent similar to that observed when TWIST1 was depleted<sup>5</sup> (Figure 3.2C and 3.2D).

These results indicated that the action of DDR2 in ovarian tumor cells that have adopted an invasive, mesenchymal phenotype, is largely responsible for their capacity to clear mesothelial cells.

### **DDR2 Contributes to Invasion and Migration of Ovarian Cancer Cells**

Subsequent to clearing the mesothelial layer, ovarian cancer cells must invade and migrate through the underlying basement membrane (BM) and extracellular matrix (ECM)

for successful metastases. As TWIST1 mediated EMT is known to contribute to these behaviors in other cancers<sup>29-32</sup>, we sought to determine whether the action of DDR2 in ovarian tumor cells contributed to these tumor cell functions. Matrigel has been used extensively as a BM surrogate and DDR2 depleted cells were significantly impaired in their ability to invade through Matrigel coated transwells (Figure 3.3A and 3.3B). To assess ECM invasion/migration ovarian tumor cells were embedded in 3D Collagen I gels. DDR2 depleted cells were significantly impaired in their ability to invade 3D type I collagen (Figure 3.3C and 3.3D). There were no differences in proliferation between control and DDR2-depleted ovarian tumor cells (Figure 3.3E and 3.3F). In sum these results indicated that the action of DDR2 in ovarian tumor cells contributed to critical tumor cell functions within the metastatic cascade, such as mesothelial cell clearance, BM invasion and ECM invasion/migration, but did not influence tumor cell proliferation.

### **DDR2 activation leads to increased SNAIL1 protein level in ovarian cancer cells**

We have shown that DDR2 is a transcriptional target of TWIST1 in ovarian cancer cells, and its activity serves to mediate many of the pro-metastatic phenotypes associated with the TWIST1 mesenchymal program. DDR2 activation in response to collagen I stimulation has also been shown to stabilize the EMT transcription factor SNAIL1 in multiple cancer cell types, thereby sustaining mesenchymal cell features and tumor cell invasion and migration<sup>11,12,16,33</sup>. Moreover, constitutive SNAIL1 expression can promote mesothelial clearance in ovarian cancer<sup>5</sup>. Therefore, we asked whether DDR2 regulated SNAIL1 levels in human ovarian cancer cells, and in addition to carrying out TWIST1

mediated functions, could contribute to maintaining a mesenchymal phenotype. When ES2 or A2780 ovarian tumor cells were added to Collagen I coated plates, SNAIL1 protein was increased (Figure 3.4A and 3.4B). This was dependent upon the presence of DDR2 signaling, as DDR2 depletion in those same cells abrogated the increase in SNAIL1 following collagen I stimulation (Figure 3.4A and 3.4B). These data indicated that DDR2 activation by collagen I serves to stabilize SNAIL1 protein levels in ovarian cancer cells.

### **DDR2 regulates expression and activity of extracellular matrix remodeling enzymes**

Matrix remodeling enzymes such as matrix metalloproteinases (MMPs) and lysyl oxidases (LOX) are known to be key contributors to ovarian tumor cell invasion and progression, as well as mesothelial clearance<sup>3,4,34</sup>. Multiple reports have linked DDR2 activity with increased MMP and LOX expression<sup>10,35-37</sup>. Furthermore, DDR2 has been shown to influence expression of the MMP activating enzyme, MT1-MMP (MMP14), downstream of SNAIL1 stabilization<sup>11</sup>. As collagen I induced DDR2 activation led to increased SNAIL1 protein in ovarian cancer cells (Figure 3.4A and 3.4B), we asked whether the level and activity of matrix remodeling enzymes in ovarian tumor cells was dependent upon the action of DDR2. Quantitative RT-PCR analysis of select matrix remodeling enzymes showed that overall there was a reduction in the expression of these enzymes in ES2 and A2780 ovarian tumor cells depleted of DDR2, even though the expression profile of matrix remodeling enzymes differed between the tumor cell lines (Figure 3.4C). In ES2 cells, DDR2 depletion led to decreased MMP2, MMP7, MMP13,

and LOXL2 mRNA level (Figure 3.4C). In A2780 cells, MMP1, MMP3, and LOXL2 mRNA levels were reduced in DDR2 depleted cells (Figure 3.4D). Although mRNA level of MT1-MMP (MMP14) was not influenced by the presence of DDR2 in unstimulated cells, Western blot analysis of ES2 and A2780 cells showed that active MT1-MMP protein level increased in response to collagen I stimulation (Figure 3.4A and 3.4B) and this increase was abolished when DDR2 was depleted (Figure 3.4A and 3.4B). Finally, in the ES2 cell line gelatin zymography showed that MMP-2 level and activity was reduced in DDR2-depleted cells compared to control ES2 cells (Figure 3.4C and 3.4E).

These results indicated that DDR2 activation in ovarian tumor cells regulated expression and activity of matrix remodeling enzymes. These enzymes could facilitate migration, invasion, and mesothelial cell clearance.

### **DDR2 contributes to Fibronectin cleavage by ovarian cancer cells and promotes ovarian cancer cell spreading on Fibronectin**

Fibronectin (FN) cleavage and remodeling has been shown to be important for the ability of ovarian cancer cells to clear the mesothelial cell layer covering the peritoneum during the early stages of metastasis<sup>2,3</sup>. As MMPs are efficient at FN cleavage<sup>3,38</sup>, and DDR2 modulates expression and activity of MMPs in ovarian cancer cells (Figure 3.4), we asked whether the presence of DDR2 in ovarian tumor cells led to more efficient cleavage of FN. Cell free media from collagen stimulated ES2 or A2780 shSCRM cells was capable of rapid cleavage of human FN (Figure 3.5A-C). When DDR2 was depleted in these cells there was a delay in the cleavage of FN, as quantified by the amount of

remaining full length FN (Figure 3.5A-C). These data demonstrated that DDR2 activity in ovarian tumor cells promotes efficient cleavage of FN, and as such, may contribute to the enhanced mesothelial clearance by DDR2 expressing cells.

MMP cleavage of FN has been shown to enhance peritoneal adhesion of ovarian cancer cells<sup>3</sup>. Additionally, while DDR2 itself does not bind FN, its presence has been shown to promote adhesion and spreading of cells via integrin activation<sup>25</sup>. We therefore sought to determine if depletion of DDR2 in ovarian cancer cells led to differential adhesion and spreading of these cells on FN. Polyacrylamide hydrogels were functionalized with FN. When plated on these FN coated hydrogels, ES2 shSCRM control cells appeared maximally spread at 3 hours, while DDR2 depleted ES2 cells showed a dramatic reduction in cell spreading (Figure 3.5D and 3.5E). These results indicate that DDR2 promotes the ability of ovarian cancer cells to adhere and spread on FN.

### **DDR2 is critical for ovarian tumor metastasis in vivo**

To determine whether DDR2 influenced ovarian cancer cell metastasis *in vivo*, we compared the ability of control scrambled shRNA (shSCRM) and shDDR2 (ES2 and A2780) (Figure 3.6A and 3.6E) to form metastasis in a peritoneal xenograft model of ovarian cancer. Mice were sacrificed and the tumor burden determined by measuring tumor weight and/or counting number of tumor nodules. For both cell lines, DDR2-depleted tumor-bearing mice showed less total tumor weight (Figure 3.6B and 3.6F-G). Consistent with human disease, much of the peritoneal tumor burden in these mice consisted of lesions attached to the mesentery and omentum (Figure 3.6C-D and 3.6H),

and DDR2 reduced the tumor burden on these organs. These results indicated that the action of DDR2 in ovarian tumor cells is critical for the establishment of ovarian tumor metastasis *in vivo*.

### **DDR2 is expressed in human ovarian carcinomas and is an indicator of poor prognosis**

To determine if DDR2 expression in human ovarian tumors is associated with clinical outcome, we first analyzed gene-expression data from a previously described cohort of ovarian cancer patients with advanced stage, high-grade serous cancer<sup>39</sup>. Univariate survival analysis showed that stratification of patients into “DDR2 high” and “DDR2 low” groups based on an optimum threshold revealed that high DDR2 mRNA expression levels were associated with shorter overall survival ( $p=0.02$ ) (Figure 3.7A). Next, we determined DDR2 expression, by IHC, in ovarian surface epithelium taken from patients with benign ovarian disease, primary tumors, and metastatic lesions. Although some benign ovarian disease exhibited low level DDR2 expression, 0% (0/9) of the specimens exhibited high DDR2 expression (3+) (Figure 3.7B and 3.7C). High level of DDR2 expression appeared to correlate with stage of the patient, as 44% (79/179) of early stage and 74% (28/38),  $p<0.0001$ , of advanced stage specimens show high levels of DDR2 expression (Figure 3.7B and 3.7C). Notably, 100% (12/12) of the metastatic tumor samples showed high levels of DDR2 expression (Figure 3.7B and C). These findings are consistent with a previous report<sup>40</sup> and demonstrated that DDR2 expression was induced in aggressive ovarian tumors.

## **DDR2 expression level is correlated with increased invasion in patient derived primary ovarian cancer cells**

The mesenchymal gene program correlates with increased metastatic behavior in the primary tumors of ovarian cancer patients<sup>5</sup>. We therefore assayed a number of primary ovarian cancer (POV) cells derived from the abdominal ascites of patients with advanced stage, high grade ovarian cancer for expression of mesenchymal proteins, including DDR2. All POV cells expressed at least one of the mesenchymal markers assayed (Figure 3.8A). Additionally, although variable in level, all POV cells exhibited some degree of DDR2 expression. To determine whether correlations between invasiveness and DDR2 expression could be observed in POV cells, we utilized an *ex vivo* assay in which the Matrigel invasion capacity was examined. A subset of the POV cells (POV1, 9, 10, 12) with similar proliferation rates (Figure 3.8D), but with varying expression profiles of mesenchymal proteins, were subjected to the assay (Figure 3.8B and 3.8C). Notably, POV9, which displayed the lowest expression of DDR2 among the cells assayed, was least invasive. These data are consistent with results from the established ovarian cell lines, and further implicate DDR2 action as critical for the invasive capacity of ovarian cancer cells, and its potential utility as a therapeutic in the ovarian cancer setting.

## **Discussion**

In summary, these studies have shown that the collagen receptor DDR2 contributes to the mesothelial clearance, invasion, and metastasis of ovarian cancer cells. Our working model (Figure 3.9) posits that upon EMT induction by tumor environmental signals, EMT transcription factors, including TWIST1, are expressed. During the transition to the mesenchymal state, TWIST1 induces DDR2 expression. DDR2 then modulates the expression and activity of matrix remodeling enzymes, including MMPs and LOXL2. Additionally, DDR2 enhances the ability of ovarian tumor cells to cleave fibronectin, and adhere to and spread on fibronectin substrate. This could contribute to increased mesothelial cell clearance and invasion by ovarian tumor cells. Upon reaching the collagen I-rich stromal matrix DDR2 activity maintains SNAIL1 levels, thereby serving a central role in maintaining the mesenchymal phenotype of metastatic ovarian tumor cells.

DDR2 expression led to increased adhesion to fibronectin, yet DDR2 does not directly bind fibronectin<sup>19</sup>. We have shown that DDR2 expressing cells are able to more efficiently cleave FN. Cleavage of FN is necessary to expose high affinity sites for  $\alpha 5\beta 1$  and  $\alpha \nu\beta 3$  integrin binding, leading to enhanced adhesion of ovarian cancer cells<sup>3,41</sup>. DDR2 has been shown to influence adhesion and spreading of cells by collagen binding  $\alpha 1\beta 1$  and  $\alpha 2\beta 1$  integrins<sup>25</sup>. This raises that possibility that DDR2, as a signaling receptor, could also influence the adhesive activity of integrins. As it was not determined in that study, how exactly DDR2 influences collagen and/or fibronectin integrin adhesion remains of interest.

Whereas other epithelial tumors, including ovarian cancer, have been shown to use hematogenous or lymphatogenous routes to metastasize, ovarian cancer is unique in that cells within the ascites fluid reach distant sites within the peritoneal cavity<sup>1,42</sup>. This leads to the requirement of ovarian tumor cells to clear and invade the mesothelial layer that covers the peritoneal organs in order for metastatic implants to arise<sup>43</sup>. Our findings demonstrate that DDR2 expression is associated with worse prognosis in high-grade serous cancers (Figure 3.7). Additionally, molecular profiling of the ES2 cell line used for many of our cell-based assays by The Cancer Cell Line Encyclopedia has shown the line to have a TP53 mutation. Therefore, although the ES2 cell line is classically thought of as a clear cell tumor derivative, it more likely high-grade serous<sup>44</sup>. The A2780 cell line used in our assays does not have a TP53 mutation and is unlikely of high-grade serous histology with PIK3CA, PTEN, and ARID1A mutations. However the results from this cell line adds to the potential generalizability of our findings. We have shown that DDR2 plays a critical role in mediating mesothelial cell clearance. While this could be due, simply, to the increased ability of DDR2 expressing cells to adhere and spread, there are other intriguing possibilities that warrant further study. Recently, DDR1, the other member of the discoidin domain family, was demonstrated to mediate myosin-dependent collagen contraction via association with non-muscle myosin IIA (NM-IIA)<sup>45</sup>. It has been demonstrated that ovarian cancer spheroids exert force on the mesothelial cell-associated ECM protein FN via  $\alpha 5\beta 1$  integrin in a NM-IIA dependent manner to clear the mesothelium<sup>2</sup>. As there is a rich network of collagen fibers just below the mesothelium in sites of ovarian cancer metastasis<sup>46</sup>, it would interesting to determine if a DDR2-NM-IIA

mechanism of force generation exists, and if so, whether it contributes to enhanced clearance and invasion by ovarian cancer cells.

Our findings also suggest that stabilization of SNAIL1 and regulation of MMPs may be an important component of DDR2 signaling contributing to ovarian tumor metastasis. Other studies have shown that TWIST1 and SNAIL1 promote mesothelial clearance by ovarian cancer cells, and suggest that inhibiting the pathways that drive mesenchymal programs may suppress tumor cell invasion<sup>5</sup>. As transcription factors such as TWIST1 and SNAIL1 can be difficult to target therapeutically<sup>47</sup>, modulating the activity of proteins whose expression they regulate (e.g., DDR2) or upstream regulators that stimulate or maintain their expression (e.g., DDR2) could be a more practical approach. In the case of ovarian cancer metastasis, targeting DDR2 could allow for intervention at both such levels. In human samples, advanced and metastatic ovarian tumor cells have increased DDR2 expression, and this high expression is associated with poor prognosis of ovarian cancer patients. While other authors have recently shown this association<sup>40</sup>, here we provide functional data that DDR2 expression leads to mesothelial cell clearance, and increased invasion and migration by ovarian tumor cells. Furthermore, we have demonstrated that these enhanced cellular functions translate to DDR2 promoting ovarian cancer metastasis *in vivo*. Since DDR2 is upregulated in ovarian cancer cells, but relatively undetectable in surrounding normal tissues, DDR2 could be a highly specific therapeutic target with minimal toxicity to normal cells.

In conclusion, in metastatic ovarian tumor cells DDR2 expression is a product of the mesenchymal program induced by TWIST1, and serves to maintain the mesenchymal phenotype through SNAIL1 stabilization. Our *in vitro*, *in vivo*, and *ex vivo* results confirm

that DDR2 is one of the critical factors contributing to the steps of ovarian cancer metastasis. Therapeutic modulation of DDR2 could provide a means of improving treatment for patients with advanced ovarian cancer.

## **Materials and Methods**

### **Antibodies**

The antibodies and sources were as follows: DDR2 (for IHC, R&D Systems), DDR2 (for Western Blot, Cell Signaling Technologies), MT1-MMP (Millipore), Snail1 (Cell Signaling Technologies), Twist1 (AbCam),  $\beta$ -Actin (Sigma),  $\beta$ -Tubulin (Sigma), N-cadherin (BD), E-Cadherin (BD),  $\alpha$ -SMA (sigma), Zeb1 (Santa Cruz).

### **Cell culture**

Established ovarian cancer cell lines A2780 (purchased from ATCC), SKOV3.ip1 (gift from Dr. Gordon Mills, M.D. Anderson Cancer Center, Houston, TX), OVCAR3 (purchased from ATCC), OVCAR4 (purchased from National Cancer Institute-Frederick DCTD tumor cell line repository), and OVCAR5 (National Cancer Institute-Frederick DCTD tumor cell line repository) were maintained in RPMI Medium (GIBCO) supplemented with 10% heat inactivated fetal bovine serum and 1% penicillin and streptomycin. Ovarian ES2 cells were maintained in McCoy's 5A (modified) medium (Life Technologies) supplemented with 10% heat inactivated fetal bovine serum and 1% penicillin and streptomycin. All cell lines were maintained at 37°C in a 5% CO<sub>2</sub> incubator. To authenticate our cell lines, we use IDEXX Bioresearch which performs short tandem repeat (STR) profile and interspecies contamination testing. Mycoplasma testing was also performed using MycoAlert Mycoplasma Detection Kit prior to performing experiments (Lonza).

For TGF-B induction of EMT, OVCAR3 cells were treated with 2ng/mL TGFB1 (Sigma) for the indicated time points. During treatment, media was replenished every 48 hours. For collagen I stimulation of DDR2, cells were serum starved overnight, and then plated on 2mg/mL collagen I (BD) for 6 hours.

### **Primary Ovarian Cancer Cell Culture**

Ascites from patients with ovarian cancer (POV) was obtained and plated in a 1:1 ratio in RPMI 20% FBS, 1% pen-strep. After 7-14 days, attached and proliferating cells were passaged and used for experiments. POV 1, 9, 10, and 12 were all obtained from patients with advanced stage, high-grade serous ovarian or fallopian tube cancer. Immunohistochemistry was performed with CK8 to confirm epithelial origin of these cells. All the patients who participated in this study provided written informed consent for the collection and research use of their materials, and the use of these samples was approved by the Washington University Institutional Review Board (IRB 201309050).

### **Plasmids and shRNA Constructs**

TWIST1 shRNA, 5'-CCTGAGCAACAGCGAGGAAGA-3' in the pLKO vector (Sigma) was used. Two previously validated oligos for DDR2 shRNA and shSCRM control sequence were used<sup>11</sup>. The oligos for human DDR2 shRNA, 5'-GCCAGATTTGTCCGGTTCATT-3' and 5'-GCCAAGTGATTCTAGCATGTT-3', and scramble control, 5'-CCTAAGGTAAAGTCGCCCTCGCTC-3', were cloned into the pLKO vector and infected

cells were selected in puromycin (Sigma). For all hairpins, polyclonal populations were tested for decreased DDR2 expression levels by western blot analysis.

### **Western blot analysis**

Cultured cell lysates were prepared using a 9M Urea, 0.075 M Tris buffer (pH7.6). Protein lysates were quantified using the Bradford assay, and 50-100µg of protein was subjected to reducing SDS/PAGE using standard methods.

### **Gelatin Zymography**

$3 \times 10^6$  cells were plated on plastic or 2mg/mL collagen in serum-free media. At 24hrs, supernatant was collected and run on a 10% gelatin gel under non-denaturing conditions. Gel was developed, coomassie stained, and destained until bands were visible. After harvesting supernatant, cells were trypsinized and counted to ensure there were no proliferation differences among the groups tested.

### **Immunohistochemical analysis using human tissue microarrays**

Ovarian human tissue microarrays were obtained from US Biomax (208, 2084t) which contained a majority of early stage and a smaller number of advanced stage ovarian cancers. Slides were deparaffinized with xylene, rehydrated and unmasked following standard immunohistochemical methods. The DDR2 primary antibody (R&D

Systems, MAB2538) was used at a 1:500 dilution. Negative controls for all samples were done using the secondary antibody alone. Antigen-antibody complexes were visualized using the VECTASTAIN ABC system (Vector Laboratories) and DAB Substrate Kit for Peroxidase (Vector Laboratories) following the manufacturer's protocol. Slides were counterstained in hematoxylin. DDR2 staining on the membrane of tumor cells was scored microscopically according to the percentage of cells positive for DDR2 expression both by intensity and percentage of cells with expression (0 for absent, 1 for 1%-40%, 2 for 40-60%, and 3 for > 60%).

### **Invasion and Migration Assays**

Matrigel invasion assays were performed according to the manufacturer's protocol (Corning). Briefly, cells were serum starved for 24 hours and 25,000 cells were plated in media containing 1% FBS onto Matrigel coated boyden (8um pore size) chambers. Media containing 10% FBS and 5ug/mL fibronectin was placed in the lower chamber as chemoattractant. Invasion assays were stained and analyzed after 48 hours. Migration assays were performed in a similar fashion, in uncoated Boyden chambers. Invaded cells were quantified by counting the number of invading cells per high powered field, 4 high powered fields per insert, and 3 inserts per condition were quantified.

Collagen I invasion assays were performed where cells were mixed with 2mg/mL collagen and plated in 48 well format. After polymerization, media was added and cells were monitored for invasive branching over 7 days.

## Proliferation Assay

Cells were plated at densities of 4,000 cells per well into four 96-well plates in medium as described previously. Using an 2,3-bis[2-methoxy-4-nitro-5-sulfo-phenyl]-2H-tetrazolium-5-carboxanilide inner salt (XTT)-based assay (Roche Molecular Biochemicals) as previously described<sup>48</sup>, proliferation was measured at 24, 48, 72 and 96 hours.

Real-time PCR with reverse transcription.

Real-time PCR reactions were done using the SYBR Green PCR Master Mix (Applied Biosystems) in the ABI detection system (Applied Biosystems). The thermal cycling conditions were composed of 50 °C for 2 min followed by an initial denaturation step at 95 °C for 20 s, 40 cycles at 95 °C for 3 s, and 60 °C for 30 s. The experiments were carried out in triplicate for each data point. The relative quantification in gene expression was determined using the  $2^{-\Delta\Delta C_t}$  method as described previously<sup>49</sup>. Primers used for PCR with reverse transcription and real-time PCR with reverse transcription are listed in Supplemental table.

ES2 or A2780 shRNAi-depleted of DDR2 or transduced with scrambled control (SCRM) were cultured for 6 hours under serum free conditions on 2mg/mL of collagen I, and cell free, conditioned media was collected and incubated with 4ug human Fibronectin (BD). Extent of cleavage was measured at time intervals of 0.25, 1, and 16 hours by SDS Page followed by coomassie staining. Amount of intact FN (~220 kDa) quantified by densitometry. Control FN was incubated for 16hrs with non-conditioned media.

## **Cell Spreading Assay**

Polyacrylamide hydrogels were produced as previously described<sup>50</sup>. Briefly, acrylamide solution (Bio-Rad) was mixed with N-N'-methylene-bis-acrylamide solutions (BioRad) and then polymerized between a glutaraldehyde-activated glass surface and hydrophobic coverslip. Polymerized substrates were then activated for protein conjugation with the heterobifunctional crosslinker Sulfo-SANPAH at 0.5 mg/mL (Pierce Chemical Co.) under UV exposure for 15 min. After wash with HEPES buffer, then functionalized with Fibronectin. Gels were determined by atomic force microscopy to have elastic moduli of ~120 kPa. Functionalized gels were washed with PBS, and ES2 shSCRM or shDDR2 were plated. Live cells were imaged on a Nikon Ti-E microscope with a humidity and temperature controlled incubation chamber (LiveCell). Data were collected by 3x3 tiling of 10X regions of view. Time-lapse imaging was performed with 6 hour duration and 20-minute frame intervals. Image analysis was performed using Matlab (The Mathworks, Natick MA) and Image J. Cell area was computed for each cell in each field of view using custom software to detect cell boundaries. Data was plotted using R graphing library<sup>51</sup>.

## **Spheroid-induced mesothelial clearance assay**

Mesothelial cells were cultured on 6-well plastic plates (Techno Plastic Products) and used in the clearance assay once a confluent monolayer was formed (approximately 72 hours). Mesothelial cells were labeled 18 hours prior with CMFDA-green (Molecular Probes), washed with PBS and incubated with fresh culture medium until use. Spheroids were prepared 18 hours in advance. Cells were labeled with CMTPX-red (Molecular

Probes), washed with PBS, dissociated by trypsinization and resuspended in culture medium. Labeled cells were then counted and plated at 200 cells/well in ultra-low attachment multiwell plates (Corning) with 10ug/mL of soluble bovine fibronectin for increased cohesion. Spheroids were placed onto the monolayer of mesothelial cells at the microscope and images captured at 0, 1, and 7 hours. Normalized clearance value is determined by measuring the total mesothelial cell area cleared by the spheroid in ImageJ, and normalizing to the size of the spheroid at time 0.

### **Survival analysis**

For the survival analysis, the Tothill database was accessed<sup>39</sup>. Raw expression mRNA values for DDR2 and overall survival was used as an endpoint. Samples were dichotomized into two groups after determining the optimal cutoff level for gene expression. Survival curves were calculated using the Kaplan–Meier method, and statistical significance was assessed using the log-rank test to determine if there was a statistically significant association between DDR2 expression and overall survival.

### **Orthotopic Model of Ovarian Cancer**

All procedures involving animals and their care were performed in accordance with the guidelines of the American Association for Accreditation for Laboratory Animal Care and the U.S. Public Health Service Policy on Human Care and Use of Laboratory Animals. All animal studies were also approved and supervised by the Washington University

Institutional Animal Care and Use Committee in accordance with the Animal Welfare Act, the Guide for the Care and Use of Laboratory Animals and NIH guidelines (Protocol 20140178).

For genetic studies, A2780 shSCRM or shDDR2 were injected intraperitoneally (i.p.) with  $7.5 \times 10^6$  cells in 0.5 ml of PBS into female 6- to 8- week old ( $n=8$  per group) Balb/c nude (Taconic). ES2 shSCRM or shDDR2 cells were injected intraperitoneally (i.p.) with  $10 \times 10^6$  cells in 0.5 ml of PBS into female 6- to 8- week old ( $n=8$  per group) NU/NU nude (Charles River) mice. Mice were monitored for adverse events and sacrificed with CO<sub>2</sub> exposure and cervical dislocation at 14 days (A2780 model) and 28 days (ES2 model) after i.p. injection. At the completion of each experiment, aggregate tumor weight, location, and number of tumor nodules were recorded for each group.

### **Statistical Analysis**

Statistical analysis was performed using Prism software (GraphPad). Two-tailed unpaired Student's *t* test was performed to analyze statistical differences between groups. *P* values < 0.05 were considered statistically significant.

## Figures

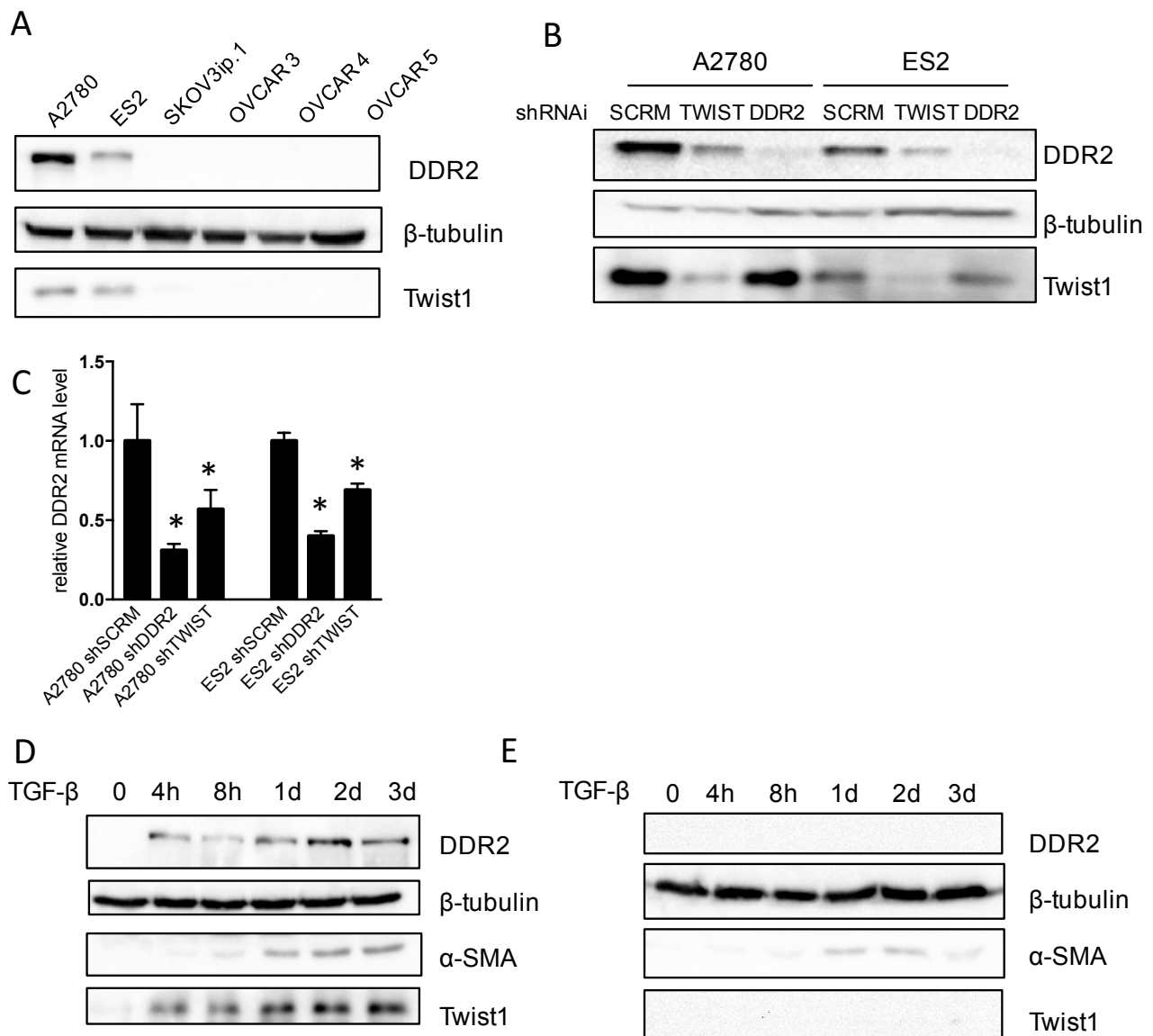


### Figure 3.1: TWIST1 regulates DDR2 expression in Ovarian Cancer Cells

(A) Western blot analysis of DDR2 and Twist1 protein expression in established ovarian cancer cell lines

(B) A2780 or ES2 ovarian cancer cell lines were infected with lentivirus expressing the indicated shRNAi. Western blotting performed using the indicated antibodies.

(C) Q-PCR analysis of mRNA isolated from A2780 or ES2 cells shRNA-depleted of DDR2, TWIST1 or transduced with scrambled control (SCR). Three replicates of each gene were done for each experiment. Data are representative of two independent experiments. \* $p < 0.05$  versus shSCR control, Student's t test.

(D) Western blot of indicated proteins from whole cell lysates of OVCAR3 cells treated with 2ng/mL TGF-β to biochemically induce EMT for indicated times.

(E) Western blot of indicated proteins from whole cell lysates of OVCAR3 shTwist1 cells treated with 2ng/mL TGF-B to biochemically induce EMT for indicated times.

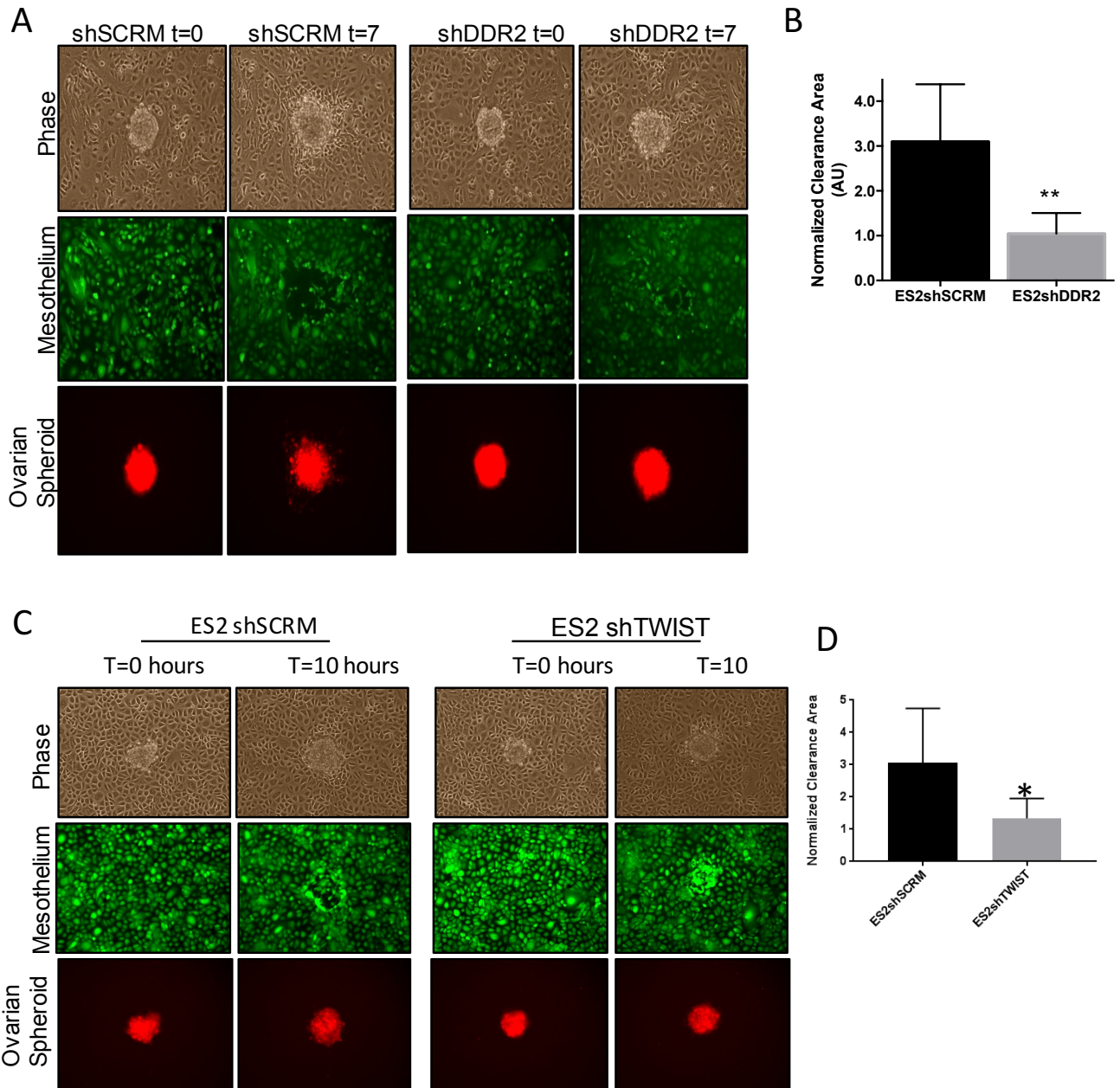


**Figure 3.2: DDR2 promotes mesothelial cell clearance**

(A) ES2 ovarian cancer spheroids expressing SCRMs or DDR2 shRNAi labeled with CMTCX dye (red) were added to a confluent monolayer of primary mesothelial cells that were labeled with CMFDA dye (green) and monitored over 7 hours. Images show representative mesothelial clearance and 0 and 7 hours.

(B) Quantification of experiment in (A). >5 spheroids averaged per condition. Error bars denote SEM. \*\* $p < 0.01$ , Student's t test.

(C) ES2 ovarian cancer spheroids expressing SCRMs or TWIST1 shRNAi labeled with CMTCX dye (red) were added to a confluent monolayer of primary mesothelial cells that were labeled with CMFDA dye (green) and monitored over 7 hours. Images show representative mesothelial clearance and 0 and 10 hours.

(D) Quantification of experiment in (C). >5 spheroids averaged per condition. Error bars denote SEM. \*\*P<0.05, Student's t test.

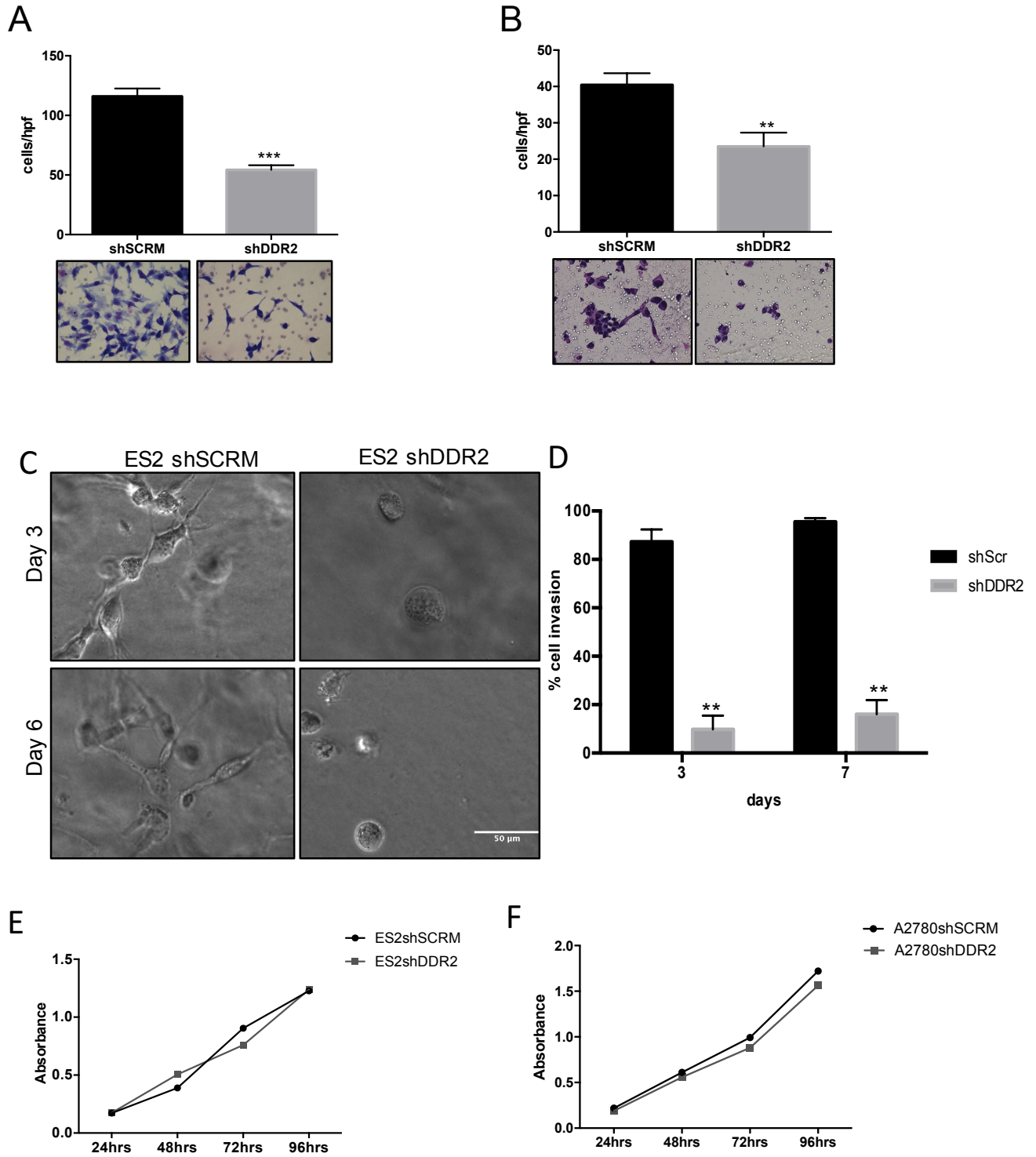


**Figure 3.3: DDR2 contributes to invasion and migration of ovarian cancer cells but does not influence proliferation.**

(A-B) Matrigel invasion assays. A. ES2 and B. A2780 cells were depleted of DDR2 or control (SCRM) and added to Matrigel coated Boyden chambers (8um pore size). Representative images and quantification plotted as number of cells invading through to

lower surface per high powered field (hpf). Means and s.d. are shown for 3 individual chambers per group, 4 hpf per chamber. Unpaired t-test, \*\* $p < 0.01$ , \*\*\* $p < 0.001$ .

(C) Collagen I invasion assays of ES2 shDDR2 or control (shSCRM) cells.

Representative photographs taken at day 3 and day 6.

(D) Quantification of collagen invasion. 20 cells per well, 3 wells per condition quantified. Mean and s.d. are shown, unpaired t-test \*\* $p < 0.01$

(E-F) Cellular proliferation curves for (E) ES2 and (F) A2780 shSCRM and shDDR2 cells measured by XTT assay.

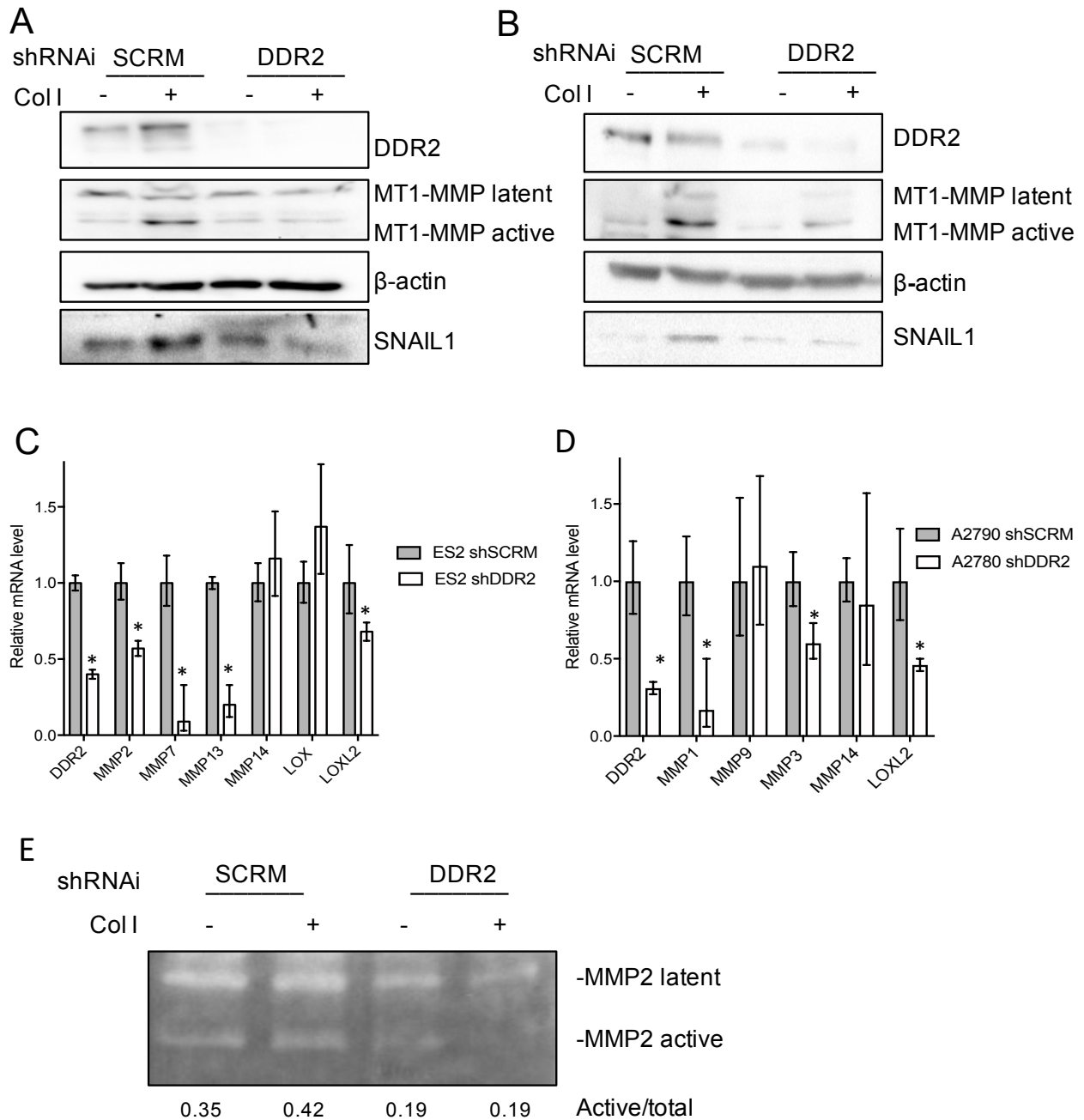


**Figure 3.4: DDR2 stabilizes SNAIL1 and regulates expression and activity of matrix remodeling enzymes**

(A-B) A. ES2 or B. A2780 cells depleted of DDR2 or control (SCRM) were added to collagen I coated (+) or uncoated (-) plates for 6 hours. Western blotting with the indicated antibodies was performed on cell extract.

(C-D) Q-PCR analysis of mRNA isolated from C. ES2 or D. A2780 shRNA-depleted of DDR2 or transduced with scrambled control (SCRM). Three replicates of each gene were done for each experiment. Data are representative of two independent experiments. \* $p < 0.05$  student's t test

(E) Gelatin zymography was conducted on the supernatants from ES2 cells depleted of DDR2 or control (SCRM) that had been plated on collagen I coated (+) or uncoated (-) plates for 6 hours.

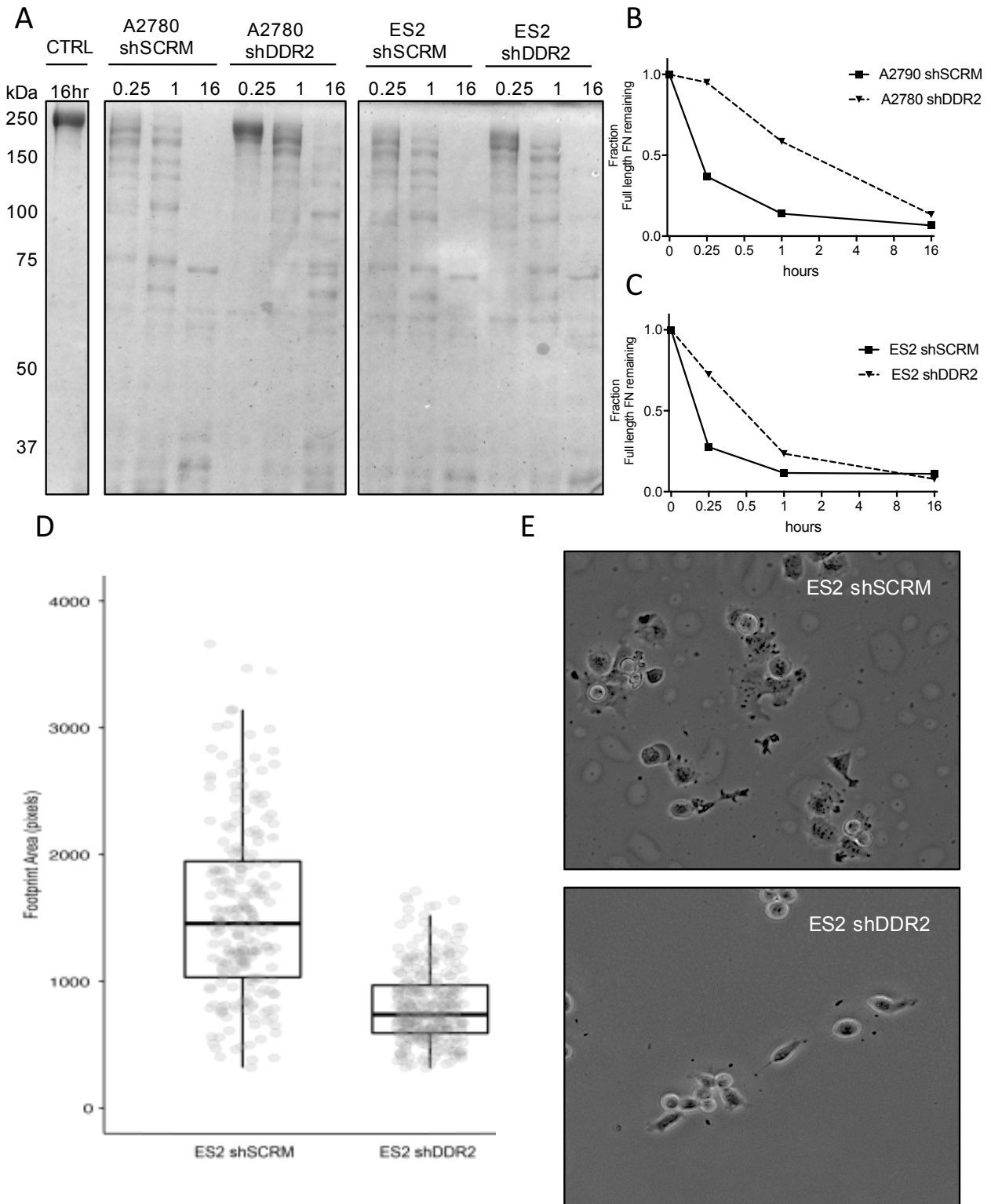


**Figure 3.5: DDR2 contributes to fibronectin cleavage by ovarian cancer cells and promotes ovarian cancer cell spreading on fibronectin**

(A) ES2 or A2780 shRNAi-depleted of DDR2 or transduced with scrambled control (SCRM) were cultured for 6 hours under serum free conditions on 2mg/mL of collagen I,

and cell free media was incubated with recombinant human fibronectin (FN). Extent of cleavage was measured at time intervals of 0.25, 1, and 16 hours by SDS Page followed by coomassie staining.

(B-C) Quantification of cleavage of intact FN by B. A2780 or C. ES2 plotted as a fraction of remaining intact FN as compared to control. Amount of remaining intact FN (~220 kDa) quantified by densitometry. Data are representative of 2 independent experiments

(D) Quantification of cell area when plated on fibronectin coated hydrogels for 3 hrs. Dots represent individual cell areas, with box plot overlay depicting the median and interquartile ranges of area spread.

(E) Representative images of ES2 shSCRM or shDDR2 cells plated on fibronectin coated hydrogels.

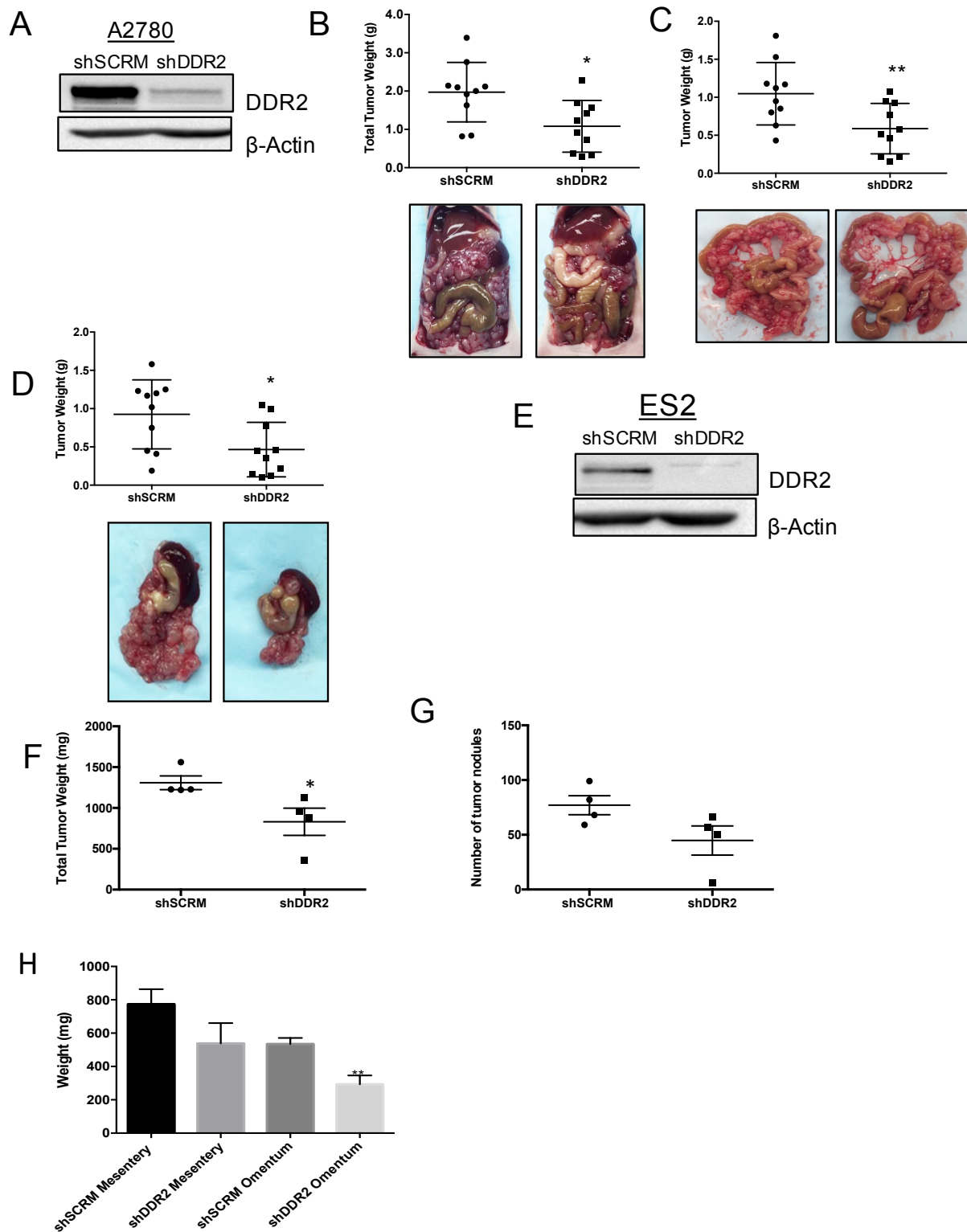


**Figure 3.6: DDR2 is critical for ovarian cancer metastasis *in vivo***

(A) A2780 cells stably expressing shRNA targeting sequence for scramble control (shSCRM) or DDR2 (shDDR2). Beta-Actin was used as a protein loading control.

(B-D). Representative images and quantification of Balb/c Nu mice injected IP with  $7.5 \times 10^6$  A2780 shSCRM or shDDR2 cells. Tumor burden was assessed at 14 days post injection in the B. entire peritoneal cavity C. Mesentery only D. Omentum only. N=10 mice per group. Means and s.d. Unpaired t-test, \*P<0.05, \*\*P≤0.01

(E) ES2 cells stably expressing shRNA targeting sequence for scramble control (shSCRM) or DDR2 (shDDR2). Beta-Actin was used as a protein loading control.

(F-H) Quantification of Nu/Nu mice injected IP with  $10 \times 10^6$  ES2 shSCRM or shDDR2 cells. Tumor burden was assessed at 14 days post injection by measuring F. total tumor burden G. number of tumor nodules H. Tumor burden in the mesentery or omentum only. N=4 mice per group. Means and s.d. Unpaired t-test, \*P<0.05, \*\*P≤0.01

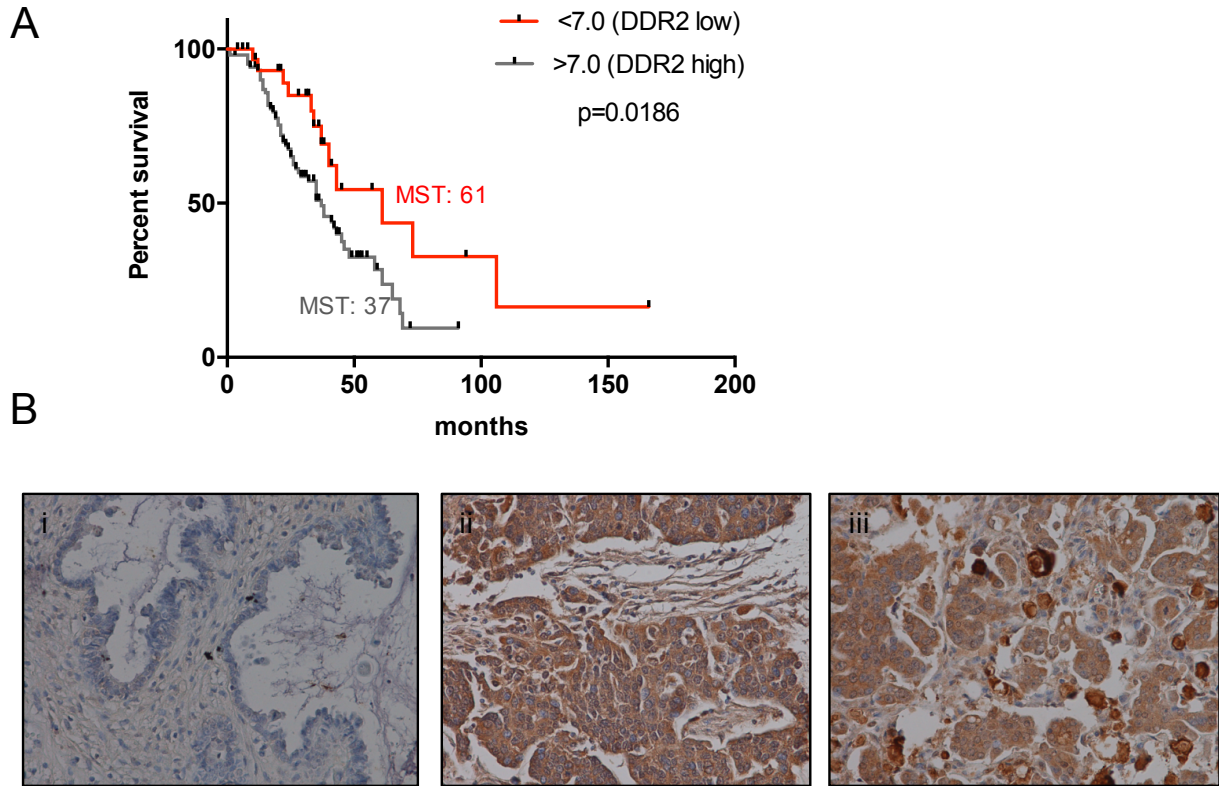


**Figure 3.7: DDR2 is expressed in human ovarian carcinomas and is an indicator of poor prognosis**

(A) Overall survival of Advanced-stage III, IV serous ovarian cancers by Kaplan-Meier methods and log rank test. MST: Median survival time.

(B) Representative images of DDR2 immunohistochemical staining in i) early stage IA primary tumor ii) advanced stage IV primary tumor iii) mesenteric metastatic implants  
(C) Classification of immunohistochemical analysis of DDR2 staining in normal (benign) ovary, human primary ovarian tumors, and metastatic implants.

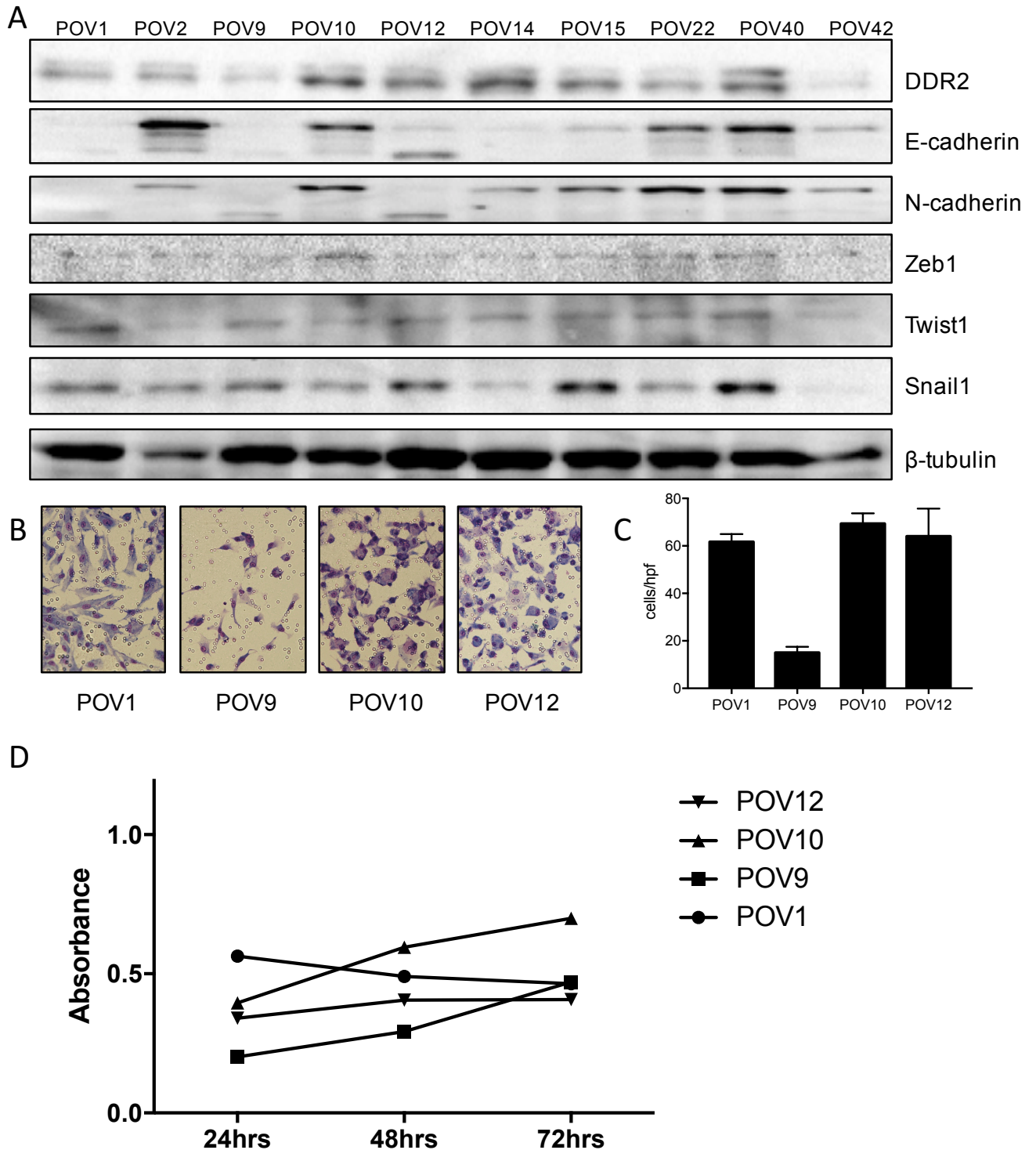


**Figure 3.8: DDR2 expression level is correlated with increased invasion in patient derived primary ovarian cancer cells**

(A) Western blot of patient derived primary ovarian tumor (POV) cells for expression of indicated proteins.

(B-C) A subset of POV cells were added to Matrigel coated Boyden chambers to assay invasion. B. Representative images of inserts and C. quantification plotted as number

of cells invading through to lower surface per high powered field (hpf). Means and s.d. are shown for 3 individual chambers per group, 4 hpf per chamber.  
(D) POV cells were plated and proliferation was measured with an XTT assay at 24hr time intervals

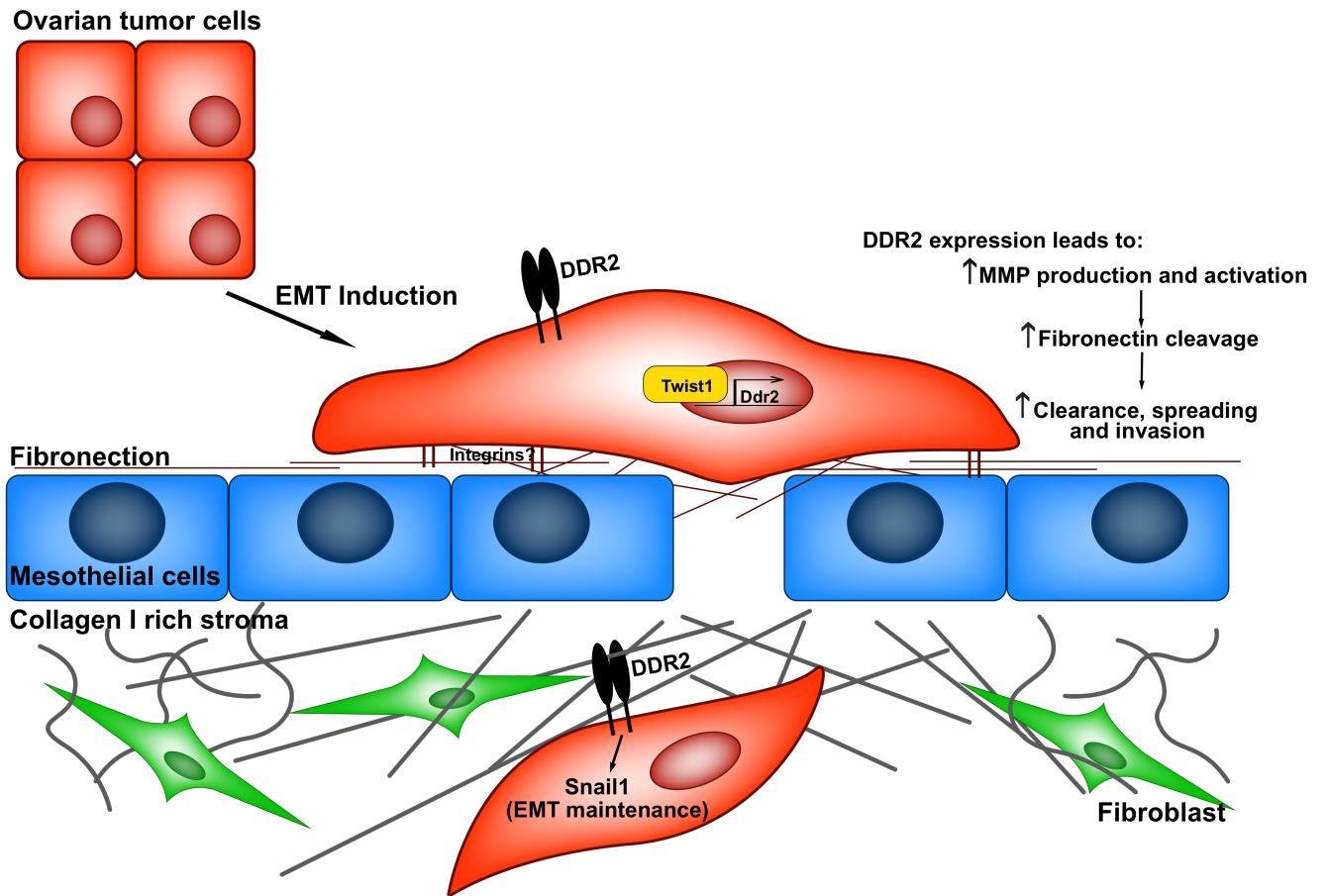


**Figure 3.9: Proposed role for DDR2 in ovarian cancer metastasis**

## References

1. Yeung, T.L., *et al.* Cellular and molecular processes in ovarian cancer metastasis. A Review in the Theme: Cell and Molecular Processes in Cancer Metastasis. *American journal of physiology. Cell physiology* **309**, C444-456 (2015).
2. Iwanicki, M.P., *et al.* Ovarian cancer spheroids use myosin-generated force to clear the mesothelium. *Cancer Discov* **1**, 144-157 (2011).
3. Kenny, H.A., Kaur, S., Coussens, L.M. & Lengyel, E. The initial steps of ovarian cancer cell metastasis are mediated by MMP-2 cleavage of vitronectin and fibronectin. *The Journal of clinical investigation* **118**, 1367-1379 (2008).
4. Cho, A., Howell, V.M. & Colvin, E.K. The Extracellular Matrix in Epithelial Ovarian Cancer - A Piece of a Puzzle. *Frontiers in oncology* **5**, 245 (2015).
5. Davidowitz, R.A., *et al.* Mesenchymal gene program-expressing ovarian cancer spheroids exhibit enhanced mesothelial clearance. *The Journal of clinical investigation* **124**, 2611-2625 (2014).
6. Chen, D., *et al.* Effect of down-regulated transcriptional repressor ZEB1 on the epithelial-mesenchymal transition of ovarian cancer cells. *International journal of gynecological cancer : official journal of the International Gynecological Cancer Society* **23**, 1357-1366 (2013).
7. Terauchi, M., *et al.* Possible involvement of TWIST in enhanced peritoneal metastasis of epithelial ovarian carcinoma. *Clinical & experimental metastasis* **24**, 329-339 (2007).
8. Wang, Y.L., *et al.* Snail promotes epithelial-mesenchymal transition and invasiveness in human ovarian cancer cells. *International journal of clinical and experimental medicine* **8**, 7388-7393 (2015).
9. Bildsoe, H., *et al.* Transcriptional targets of TWIST1 in the cranial mesoderm regulate cell-matrix interactions and mesenchyme maintenance. *Developmental biology* **418**, 189-203 (2016).

10. Corsa, C.A., *et al.* The Action of Discoidin Domain Receptor 2 in Basal Tumor Cells and Stromal Cancer-Associated Fibroblasts Is Critical for Breast Cancer Metastasis. *Cell reports* **15**, 2510-2523 (2016).
11. Zhang, K., *et al.* The collagen receptor discoidin domain receptor 2 stabilizes SNAIL1 to facilitate breast cancer metastasis. *Nature cell biology* **15**, 677-687 (2013).
12. Ren, T., *et al.* Discoidin domain receptor 2 (DDR2) promotes breast cancer cell metastasis and the mechanism implicates epithelial-mesenchymal transition programme under hypoxia. *J Pathol* **234**, 526-537 (2014).
13. Yan, Z., *et al.* Discoidin domain receptor 2 facilitates prostate cancer bone metastasis via regulating parathyroid hormone-related protein. *Biochimica et biophysica acta* **1842**, 1350-1363 (2014).
14. Rodrigues, R., *et al.* Comparative genomic hybridization, BRAF, RAS, RET, and oligo-array analysis in aneuploid papillary thyroid carcinomas. *Oncol Rep* **18**, 917-926 (2007).
15. Chua, H.H., *et al.* Upregulation of discoidin domain receptor 2 in nasopharyngeal carcinoma. *Head & neck* **30**, 427-436 (2008).
16. Xie, B., *et al.* DDR2 facilitates hepatocellular carcinoma invasion and metastasis via activating ERK signaling and stabilizing SNAIL1. *Journal of experimental & clinical cancer research : CR* **34**, 101 (2015).
17. Hammerman PS, S.M., Ramos AH, *et al.* Mutations in the DDR2 Kinase Gene Identify a Novel Therapeutic Target in Squamous Cell Lung Cancer. *Cancer Discovery* **1**, 78-89 (2011).
18. Xu, J., *et al.* Overexpression of DDR2 contributes to cell invasion and migration in head and neck squamous cell carcinoma. *Cancer biology & therapy* **15**, 612-622 (2014).
19. Vogel, W., Gish, G.D., Alves, F. & Pawson, T. The discoidin domain receptor tyrosine kinases are activated by collagen. *Molecular cell* **1**, 13-23 (1997).

20. Shrivastava A, R.C., Campbell E, Kovac L, McGlynn M, Ryan TE, Davis S, Goldfarb MP, Glass DJ, Lemke G, Yancopoulos GD. An Orphan Receptor Tyrosine Kinase Family Whose Members Serve as Nonintegrin Collagen Receptors. *Mol. Cell* **1**, 25-34 (1997).
21. Nadiarnykh, O., LaComb, R.B., Brewer, M.A. & Campagnola, P.J. Alterations of the extracellular matrix in ovarian cancer studied by Second Harmonic Generation imaging microscopy. *BMC cancer* **10**, 94 (2010).
22. Borza, C.M. & Pozzi, A. Discoidin domain receptors in disease. *Matrix biology : journal of the International Society for Matrix Biology* **34**, 185-192 (2014).
23. Valiathan, R.R., Marco, M., Leitinger, B., Kleer, C.G. & Fridman, R. Discoidin domain receptor tyrosine kinases: new players in cancer progression. *Cancer metastasis reviews* **31**, 295-321 (2012).
24. Leitinger, B. Discoidin domain receptor functions in physiological and pathological conditions. *International review of cell and molecular biology* **310**, 39-87 (2014).
25. H Xu, D.B., F Chang, PH Huang, RW Farndale, B Leitinger. Discoidin Domain Receptors Promote  $\alpha 1\beta 1$ - and  $\alpha 2\beta 1$ - Integrin Mediated Cell Adhesion to Collagen by Enhancing Integrin Activation. *PLoS One* **7**, e52209 (2012).
26. Davidson, B., Trope, C.G. & Reich, R. Epithelial-mesenchymal transition in ovarian carcinoma. *Frontiers in oncology* **2**, 33 (2012).
27. Xu, J., Lamouille, S. & Derynck, R. TGF-beta-induced epithelial to mesenchymal transition. *Cell research* **19**, 156-172 (2009).
28. Davidowitz, R.A., Iwanicki, M.P. & Brugge, J.S. In vitro mesothelial clearance assay that models the early steps of ovarian cancer metastasis. *Journal of visualized experiments : JoVE* (2012).
29. Matsuo, N., et al. Twist expression promotes migration and invasion in hepatocellular carcinoma. *BMC cancer* **9**, 240 (2009).

30. Yang, Z., *et al.* Up-regulation of gastric cancer cell invasion by Twist is accompanied by N-cadherin and fibronectin expression. *Biochemical and biophysical research communications* **358**, 925-930 (2007).
31. Elias, M.C., *et al.* TWIST is expressed in human gliomas and promotes invasion. *Neoplasia* **7**, 824-837 (2005).
32. Wang, Y., Liu, J., Ying, X., Lin, P.C. & Zhou, B.P. Twist-mediated Epithelial-mesenchymal Transition Promotes Breast Tumor Cell Invasion via Inhibition of Hippo Pathway. *Scientific reports* **6**, 24606 (2016).
33. Son, H. & Moon, A. Epithelial-mesenchymal Transition and Cell Invasion. *Toxicological research* **26**, 245-252 (2010).
34. Egeblad, M. & Werb, Z. New functions for the matrix metalloproteinases in cancer progression. *Nature reviews. Cancer* **2**, 161-174 (2002).
35. Olaso, E., *et al.* Discoidin domain receptor 2 regulates fibroblast proliferation and migration through the extracellular matrix in association with transcriptional activation of matrix metalloproteinase-2. *The Journal of biological chemistry* **277**, 3606-3613 (2002).
36. Olaso, E., *et al.* DDR2 receptor promotes MMP-2-mediated proliferation and invasion by hepatic stellate cells. *The Journal of clinical investigation* **108**, 1369-1378 (2001).
37. Xu, L., *et al.* Activation of the discoidin domain receptor 2 induces expression of matrix metalloproteinase 13 associated with osteoarthritis in mice. *The Journal of biological chemistry* **280**, 548-555 (2005).
38. Zhang, X., Chen, C.T., Bhargava, M. & Torzilli, P.A. A Comparative Study of Fibronectin Cleavage by MMP-1, -3, -13, and -14. *Cartilage* **3**, 267-277 (2012).
39. Tothill, R.W., *et al.* Novel molecular subtypes of serous and endometrioid ovarian cancer linked to clinical outcome. *Clinical cancer research : an official journal of the American Association for Cancer Research* **14**, 5198-5208 (2008).

40. Fan, Y., *et al.* Prognostic significance of discoidin domain receptor 2 (DDR2) expression in ovarian cancer. *American journal of translational research* **8**, 2845-2850 (2016).
41. Pankov, R. & Yamada, K.M. Fibronectin at a glance. *Journal of cell science* **115**, 3861-3863 (2002).
42. Pradeep, S., *et al.* Hematogenous metastasis of ovarian cancer: rethinking mode of spread. *Cancer cell* **26**, 77-91 (2014).
43. Burleson, K.M., Boente, M.P., Pambuccian, S.E. & Skubitz, A.P. Disaggregation and invasion of ovarian carcinoma ascites spheroids. *Journal of translational medicine* **4**, 6 (2006).
44. Domcke, S., Sinha, R., Levine, D.A., Sander, C. & Schultz, N. Evaluating cell lines as tumour models by comparison of genomic profiles. *Nat Commun* **4**, 2126 (2013).
45. Coelho, N.M., *et al.* Discoidin Domain Receptor 1 Mediates Myosin-Dependent Collagen Contraction. *Cell reports* **18**, 1774-1790 (2017).
46. Kenny, H.A., *et al.* Organotypic models of metastasis: A three-dimensional culture mimicking the human peritoneum and omentum for the study of the early steps of ovarian cancer metastasis. *Cancer treatment and research* **149**, 335-351 (2009).
47. Yeh, J.E., Toniolo, P.A. & Frank, D.A. Targeting transcription factors: promising new strategies for cancer therapy. *Current opinion in oncology* **25**, 652-658 (2013).
48. Heinrich, M.C., *et al.* Inhibition of c-kit receptor tyrosine kinase activity by STI 571, a selective tyrosine kinase inhibitor. *Blood* **96**, 925-932 (2000).
49. Livak, K.J. & Schmittgen, T.D. Analysis of relative gene expression data using real-time quantitative PCR and the 2(-Delta Delta C(T)) Method. *Methods* **25**, 402-408 (2001).

50. Zhang, K., *et al.* Mechanical signals regulate and activate SNAIL1 protein to control the fibrogenic response of cancer-associated fibroblasts. *Journal of cell science* **129**, 1989-2002 (2016).
51. Team, R.C. R: A language and environment for statistical computing. R Foundation for Statistical Computing. (2013).

## **Chapter 4**

### **Kinase Independent Functions of Discoidin Domain Receptor 2**

## **Introduction**

The majority of cellular functions mediated by receptor tyrosine kinases (RTKs) can be attributed to their catalytic kinase activity. In response to their cognate ligands, RTKs catalyze the phosphorylation of select tyrosine residues in target proteins, and this modification is a pivotal component of cellular communication and signaling. The phosphorylated tyrosine residues within the RTK itself serve as docking sites for cytoplasmic signaling proteins containing Src homology-2 and protein tyrosine binding domains, which then assemble signaling complexes to activate a cascade of intracellular biochemical signals that define a response to a given external signal<sup>1</sup>. This signal transduction plays key roles in cellular processes such as growth, differentiation, metabolism, and motility<sup>2</sup>.

While this kinase dependent signaling by RTKs is undeniably important to the function and homeostasis of cells, an accumulating body of evidence suggests that a number of non-catalytic properties of RTKs are also essential for their function. These roles include acting as scaffolds for protein complexes, allosteric effects on other enzymes, and DNA binding<sup>3</sup>. For example, EGFR has been shown to interact with and stabilize the sodium/glucose cotransporter SGLT1. This stabilization occurs independent of EGFR kinase activity, promotes glucose uptake into cancer cells to maintain intracellular glucose levels<sup>4</sup>. Another example is in the case of the receptor ErbB4, where upon cleavage of its ectodomain, a C-terminal fragment translocates to the nucleus to affect the transcription of target genes. That C-terminal fragment of ErbB4 is able to activate transcription by associating with YAP2 transcription factor, and this occurs even when the fragment is lacking the kinase domain, suggesting this

function may be independent of kinase activity of ErbB4<sup>3,5</sup>. Within the DDR family, there is also evidence of kinase independent function. The C-terminus of DDR1 contains a PDZ-binding motif, which has been shown to interact with the cell polarity protein Par3/Par6 complex to decrease actomyosin contractility and support collective cell migration, independent of ligand induced stimulation<sup>6</sup>. Previous studies have illustrated that DDR2 plays a role in fibroblast migration independent of collagen binding<sup>7</sup>. Therefore, the possibility of non-catalytic function of a given RTK must be taken into consideration when evaluating its function. Evidence from these studies suggests the potential for kinase-independent functions within the DDR family of proteins.

The fibrillar collagen receptor DDR2 has been found to promote tumor cell invasion in 2D and 3D culture models<sup>8</sup> and metastasis *in vivo*<sup>9</sup>. While in 3D collagen cultures an abundance of ligand exists to stimulate kinase activity of the receptor, DDR2 expressing cells showed increased invasion through Matrigel-coated transwells. This is surprising, given that Matrigel, a basement membrane surrogate, is predominately composed of laminin, collagen IV, perlecan, and various growth factors<sup>10</sup>. As DDR2 only recognizes fibrillar collagens as ligand, these components are unable to directly drive signaling through the DDR2 receptor.

Additional evidence for kinase independent functions of DDR2 were observed when assessing cell spreading (Figure 3.5D-E). We found that DDR2 expressing ovarian cancer cells show increased adhesion and spreading to fibronectin coated hydrogels. In the absence of ligand, this suggests a that a non-kinase role of DDR2 could be promoting this increased ability of cells to spread. Taken together, these

findings led us to hypothesize that DDR2 may have functions independent of its kinase activity that promote adhesive and invasive behaviors of cancer cells,

## **Results**

### **DDR2 functions independent of kinase activity to promote Matrigel invasion**

To determine whether the ability of cancer cells to invade through basement membrane extract (Matrigel) was independent of kinase activity of DDR2 we employed an approach where DDR2 expression in cells was rescued with a single point mutant form of the receptor that renders it kinase deficient (DDR2<sup>K608E</sup>)<sup>11</sup>. We first confirmed that this point mutation did indeed prevent ligand induced activation of the receptor. We overexpressed a pCDNA WT DDR2 or DDR2<sup>K608E</sup> plasmid in HEK293 cells, followed by stimulation with 30ug/mL of soluble collagen for 4 hours (Figure 4.1A). Cells were then lysed, DDR2 immunoprecipitated, and western blotting was performed demonstrating that the DDR2<sup>K608E</sup> mutant was not activated in response to collagen stimulation. Both breast and ovarian cancer lines showed that DDR2 contributed to matrigel invasion (Figures 2.12D-E and 3.3A-B). Therefore, both a human breast (BT549) and ovarian (ES2) cancer cell line were depleted of DDR2 using lentiviral shRNA constructs targeting the 3'UTR of DDR2. The 3'UTR DDR2 shRNA allows for rescue expression of the protein since the hairpin will not target the exogenous copy of the protein. DDR2 expression was then rescued via lentiviral transduction with either wild type DDR2 or DDR2<sup>K608E</sup>. Western blot analysis indicated efficient knockdown of DDR2 and subsequent rescue with the kinase deficient receptor (Figure 4.1B and 4.1C). These cells were then plated on Matrigel-coated transwells and allowed to invade for 48hrs. in shRNAi-depleted BT549 cells with a kinase dead mutant (DDR2<sup>K608E</sup>). DDR2<sup>K608E</sup> expression rescued the invasive potential of the tumor cells through Matrigel (Figure 4.2A and 4.2B). We obtained similar results with the ES2 cell line, where again

DDR2<sup>K608E</sup> expression rescued the invasive potential of the tumor cells (Figure 4.2C and 4.2D). These results indicated that there is likely a non-ligand mediated function of DDR2 that is promoting invasion in this assay.

Further, being that the developed inhibitor of DDR2 (WRG-28) acts via the extracellular domain to inhibit DDR2 receptor binding and activation, we wanted to assess whether it was capable of inhibiting non-kinase functions of the receptor. Treatment with WRG-28 was still able to inhibit invasion of the BT549 DDR2<sup>K608E</sup> expressing cells (Figure 4.2A and 4.2B). This demonstrated that WRG-28, through its allosteric action upon the extracellular domain of DDR2, has the potential to inhibit both kinase-dependent and kinase-independent functions of the receptor.

### **Kinase driven DDR2 function predominates in 3D collagen**

We next wanted to determine the role of DDR2 kinase activity in a setting where an abundance of ligand is present. Given the dramatic phenotype attributed to the activity of DDR2 on cell invasion in 3D collagen (Figures 2.12A-B and 3.3C-D), we assessed the ability of DDR2<sup>K608E</sup> expressing cells to rescue the ability of cells to invade in that assay. In contrast to what was seen in Matrigel invasion assays, in 3D collagen invasion assays rescue of DDR2 expression with DDR2<sup>K608E</sup> in knockdown cells was unable to rescue invasion in either BT549 (Figure 4.3A) or ES2 (Figure 4.3B) cells, indicating that DDR2 kinase activity is important for driving 3D invasion through collagen

## **DDR2 enhances cell adhesion spreading independent of kinase activity**

DDR2 has previously been shown to promote cellular adhesion via activation of integrin activation<sup>12</sup>. While that study examined adhesion in the context of collagen ligand, we also documented increase in cell adhesion and spreading of DDR2 expressing cells on fibronectin (Figure 3.5D-E). Additionally, other groups have shown that DDR2 influences fibroblast spreading on both collagen and fibronectin coated surfaces<sup>7</sup>. Given that fibronectin does not serve as a cognate ligand for DDR2, we set out to determine whether DDR2 was functioning independent of its kinase activity to regulate this behavior. To do this, we performed time lapse imaging of cells as they adhered to and spread on polyacrylamide hydrogels coated with various substrates. In BT549 cells, we examined the ability to spread on both collagen I and fibronectin coated hydrogels (Figure 4.4A and 4.4B). At 2 hours shRNAi-depleted BT549 cells there was a dramatic reduction in cell spreading on either substrate, as compared to the shSCR control cells. Reintroduction of DDR2 expression with the DDR2<sup>K608E</sup> kinase dead mutant led to rescued ability of the cells to spread on both substrates, thus indicating that the enhancement in spreading by DDR2-expressing cells is not a function of kinase activity of the receptor, or presence of its ligand.

We next carried out similar experiments with ES2 cells. However, rather than varying the ligand present, we carried the experiment out for longer time points. As can be seen (Figure 4.5A and 4.5B), consistent with previous findings (Figure 3.5D-E) depletion of DDR2 in ES2 cells results in decreased spreading on fibronectin, and this decrease persists out to 6 hours. Similar to what was observed with BT549 cells,

rescue in the DDR2 depleted cells with the DDR2<sup>K608E</sup> kinase dead mutant resulted in an increase in cell spreading ability.

Additionally, we wanted to test the ability of WRG-28 to inhibit DDR2 enhanced spreading. When the ES2 shDDR2 rescue DDR2<sup>K608E</sup> cells were treated with WRG-28, the ability of cells to spread on fibronectin was diminished (Figure 4.5C). These results again illustrated that the inhibitor could display efficacy towards the kinase independent functions of the DDR2 receptor.

## **Co-Immunoprecipitation followed by Mass Spectrometry Profiling identifies**

### **Candidate DDR2 interacting proteins**

We have attributed a number of tumor cell phenotypes to DDR2, and identified some of these DDR2 driven behaviors as being independent of receptor kinase signaling. While a few identified pathways of DDR2 signaling, including stabilization of SNAIL1 and phosphorylation of SRC as a downstream effector<sup>8,13</sup>, have been delineated, there is relatively little known about downstream effectors of the receptor. Further, as these are among the first reports of kinase independent functions of the receptor, it is not known how these functions are being mediated. Therefore, we conducted a mass spectrometry proteomics screen in order to identify potential interacting partners of DDR2. The goal of this study was to identify candidate interacting partners of DDR2, to allow for assessment as to how the receptor could be working at a mechanistic level.

To conduct this screen, lentivirus was used to introduce a DDR2-Flag-His-His version of the receptor into BT549 cells. This served to both increase the DDR2 pool in the cell, as well as provide a tag for more efficient pull down. In one sample, cells were unstimulated, and in a second sample, cells were stimulated with collagen for 3 hours. Parental BT549 cells that did not contain the tagged receptor construct were used as a control sample. Prior to lysis, cells were treated with the membrane impermeable cross-linker, DTSSP. DTSSP is a reducible crosslinker, and therefore does not interfere with downstream proteomics analysis. The purpose of DTSSP was to capture cell surface interactions DDR2 might be making with other membrane proteins. Given that many cell surface interactions are driven by transmembrane contacts<sup>14</sup>, we wanted to ensure that these were not lost during cell lysis. After crosslinking, cells were lysed, and then immunoprecipitated using Flag-M2 agarose beads. A small amount of the immunoprecipitated sample was run on a Western blot to confirm quality of the sample (Figure 4.7). SRC was used as a positive control as it is known to interact and co-immunoprecipitate with DDR2<sup>15</sup>.

Mass spectrometry analysis of the co-immunoprecipitation samples revealed 87 identified proteins in the non-collagen stimulated sample, and 164 in the collagen stimulated sample. Results are listed in Tables 4.1 and 4.2.

## **Discussion**

Accumulating evidence shows that non-catalytic properties of RTKs also contribute to their functions<sup>3</sup>. We have found that DDR2 displays such kinase independent functions. We examined cancer cell lines in a number of assays, where we found that DDR2 kinase independent activity drives invasion through Matrigel, but not collagen I. Further, expression of the DDR2<sup>K608E</sup> kinase dead mutant rescued cells ability to adhere and spread on both fibronectin and collagen I coated hydrogels. Additionally, to identify potential DDR2 interacting partners that could be driving these kinase independent behaviors, we performed a co-immunoprecipitation experiment of DDR2 from BT549 breast cancer cells, followed by mass spectrometry proteomics identification of binding partners.

In regards to these presumed kinase independent functions of DDR2, although fibrillar collagen is not a predominant component of Matrigel, proteomic analysis of Matrigel have noted trace amounts of fibrillar collagen<sup>16</sup>. Therefore, although not abundant, it could still be possible that DDR2 is binding to this trace amount of collagen, although previous studies have shown Matrigel is not capable of stimulating DDR2 activation<sup>17</sup>. Additionally, given the cell spreading results where the matrix composition is controlled and there is clearly no ligand present, it appears that DDR2 exerts functions independent of kinase signaling. While there is clearly a kinase independent role to cell adhesion and spreading, how exactly DDR2 is mediating these behaviors on non-ligand substrate is unknown. Previous studies suggest that this could be occurring via an enhancement of integrin activation<sup>12</sup>. However, the mechanism by which DDR2

could be enhancing activation of integrins, and whether the same mechanism is responsible for DDR2 enhanced spreading on different substrates, is unknown.

While it is currently unknown which, or how many, of DDR2's pro-metastatic functions *in vivo* are dependent upon catalytic activity or not, the data herein confirm that an allosteric inhibition strategy (WRG-28) has the promise to disrupt such kinase independent functions, in contrast to canonical TKI strategies. If indeed these non-kinase roles of the receptor show significance in the setting of disease, this becomes an additional strength to a mechanism of inhibition such as that seen for WRG-28.

In our studies, re-expression of a kinase deficient DDR2 receptor in DDR2 knockdown cells was unable to rescue invasion through 3D collagen, indicating that in some contexts, signaling through DDR2 is critical to drive invasive behavior. The ability of DDR2 to stabilize SNAIL1 levels to sustain EMT has been shown to be dependent on the kinase activity of the receptor<sup>8</sup>. As EMT has been shown to be important for cancer cell invasion, it is possible that SNAIL1 stabilization may be one of the actions of DDR2 that is important for cell invasion through a 3D collagen matrix. Additionally, it is likely that there are other pertinent pathways activated downstream of DDR2 phosphorylation, and it would be of interest to uncover these downstream effectors.

*In vitro* we have identified phenotypes attributed to kinase independence. It will be important to determine if these cell based assays translate to significance in the *in vivo* setting. Given the results of the 3D collagen assay, it is possible that *in vivo* invasion through the collagen rich tumor microenvironment is predominately driven by kinase dependent actions of the DDR2 receptor. However, DDR2 appears to promote

invasion through basement membrane independent of kinase activity. It is possible that early stages of metastasis, such as breaching the basement membrane, may be achieved efficiently by the kinase deficient rescue *in vivo*. Whether or not alternative pathways exist to compensate and drive invasion through collagen in the setting of a kinase deficient DDR2 receptor *in vivo* remains uncertain. Therefore, in addition to end point metastasis, it will be important to examine local invasion at the primary site as well, to allow determination of the role DDR2 signaling is playing in an *in vivo* context.

Finally, our co-immunoprecipitation mass spectrometry screen uncovered a number of candidate proteins that could be interacting with DDR2 at the protein level. Among these putative interacting partners are other membrane receptors, proteins involved in force generation, and proteins involved in receptor trafficking. There are a number of interesting candidates, and follow up studies will be necessary to elucidate at a mechanistic level how DDR2 is exerting its pro-metastatic functions.

## **Materials and Methods**

### **Cell culture**

Ovarian ES2 cells were maintained in McCoy's 5A (modified) medium (Life Technologies) supplemented with 10% heat inactivated fetal bovine serum and 1% penicillin and streptomycin. HEK293 and HEK293T cells were from ATCC and maintained in DMEM + 10% heat inactivated fetal bovine serum and 1% penicillin and streptomycin.. BT549 cells were provided by J. Weber (Washington University in St. Louis, USA) and were maintained in DMEM + 10% heat inactivated fetal bovine serum and 1% penicillin and streptomycin..All cell lines were maintained at 37°C in a 5% CO<sub>2</sub> incubator. Production of lentiviruses and infection of target cells were described previously<sup>18</sup> . To make stable cell lines of BT549 and 4T1 cells selection was carried out in 3 µg/ml puromycin.

### **Plasmids, shRNAi lentiviruses**

pFLR DDR2-Flag-His-His was previously described<sup>8</sup>. For DDR2<sup>K608E</sup> plasmid, overlapping PCR was used to introduce the point mutation in DDR2 cDNA, and then subcloned into the pFLRu vector<sup>19</sup> with a YFP tag. All mutations and cloning were verified by sequencing. shRNAis were subcloned into the pFLRu vector. shRNAi target sequences are as follows: SCR control sequence 5'- CCTAAGGTTAAGTCGCCCTCGCTC-3', shDDR2 directed at the 3' UTR with sequence 5'- GCCCATGCCTATGCCACTCCAT-3' was used to allow for expression of rescue construct.

### **Invasion and Migration Assays**

Matrigel invasion assays were performed according to the manufacturer's protocol (Corning). Briefly, cells were serum starved for 24 hours and 25,000 cells were plated in media containing 1% FBS onto Matrigel coated boyden (8um pore size) chambers. Media containing 10% FBS and 5ug/mL fibronectin was placed in the lower chamber as chemoattractant. Invasion assays were stained and analyzed after 48 hours. Invaded cells were quantified by counting the number of invading cells per high powered field, 4 high powered fields per insert, and 3 inserts per condition were quantified.

For ES2 cells, collagen I invasion assays were performed where cells were mixed with 2mg/mL collagen and plated in 48 well format. After polymerization, media was added and cells were monitored for invasive branching over 7 days.

For BT549 cells,  $10^5$  cells were embedded in 20 $\mu$ l of type I collagen gel (2.0mg/mL) extracted from rat tail (BD Biosciences). After gelling, the plug was embedded in a cell-free collagen gel (2.0 mg/mL) within a 24-well plate. After allowing the surrounding collagen matrix to gel (1 h at 37°C), 0.5 mL of culture medium was added on the top of the gel and cultured for another 2 days. Invasion distance from the inner collagen plug into the outer collagen gel was quantified.

### **Cell Spreading Assay**

Polyacrylamide hydrogels were produced as previously described<sup>20</sup>. Briefly, acrylamide solution (Bio-Rad) was mixed with N-N'-methylene-bis-acrylamide solutions (BioRad)

and then polymerized between a glutaraldehyde-activated glass surface and hydrophobic coverslip. Polymerized substrates were then activated for protein conjugation with the

heterobifunctional crosslinker Sulfo-SANPAH at 0.5 mg/mL (Pierce Chemical Co.) under UV exposure for 15 min. After wash with HEPES buffer, then functionalized with Fibronectin. Gels were determined by atomic force microscopy to have elastic moduli of ~120 kPa. Functionalized gels were washed with PBS, and ES2 shSCRM or shDDR2 were plated. Live cells were imaged on a Nikon Ti-E microscope with a humidity and temperature controlled incubation chamber (LiveCell). Data were collected by 3x3 tiling of 10X regions of view. Time-lapse imaging was performed with 6 hour duration and 20-minute frame intervals. Image analysis was performed using Matlab (The Mathworks, Natick MA) and Image J. Cell area was computed for each cell in each field of view using custom software to detect cell boundaries. Data was plotted using R graphing library<sup>21</sup>.

### **Co-Immunoprecipitation/Mass Spectrometry proteomic analysis**

BT549 or BT549 DDR2-Flag-His-His cells were grown in DMEM + 10% FBS. One plate of BT549 DDR2-Flag-His-His cells was stimulated with 50 $\mu$ g/mL rat tail Collagen I in the media for 2 hours at 37°C. At that time, all samples were treated with DTSSP (Thermo Scientific) according to manufacturer's protocol. After quenching of the crosslinker, cells were lysed using co-immunoprecipitation buffer (1% NP-40, 50 mM NaCl, 50 mM tris-HCl, 5 mM EDTA, + protease inhibitors) for 30min on ice. 1mg of total protein pre-cleared for 1hr at 4°C with 15uL protein G agarose beads, and then incubated with 50uL Flag-M2 agarose beads (Sigma) overnight at 4°C. After washing the beads three times with co-IP buffer, the protein was eluted from the beads with SDS sample buffer. 10% of the eluent was used to assess quality of the immunoprecipitation by Western blot.

Samples were sent to MS Bioworks (Ann Arbor, MI) for proteomic analysis conducted using the following workflow:

### Sample Preparation

50% of each submitted sample was processed by SDS-PAGE using a 10% Bis-Tris NuPAGE gel (Invitrogen) with the MES buffer system, the gel was run approximately 2cm. The mobility region was excised into 10 equally sized bands. In-gel digestion with trypsin was performed on each band using a ProGest robot (DigiLab) with the following protocol: washed with 25mM ammonium bicarbonate followed by acetonitrile, reduced with 10mM dithiothreitol at 60°C followed by alkylation with 50mM iodoacetamide at RT, digested with trypsin (Promega) at 37°C for 4h, quenched with formic acid and the supernatant was analyzed directly without further processing.

### Mass Spectrometry

Half of each gel digest was analyzed by nano LC-MS/MS with a Waters NanoAcquity HPLC system interfaced to a ThermoFisher Q Exactive. Peptides were loaded on a trapping column and eluted over a 75µm analytical column at 350nL/min; both columns were packed with Luna C18 resin (Phenomenex). The mass spectrometer was operated in data-dependent mode, with the Orbitrap operating at 60,000 FWHM and 17,500 FWHM for MS and MS/MS respectively. The fifteen most abundant ions were selected for MS/MS.

### Data Processing

Data were searched using a local copy of Mascot with the following parameters:

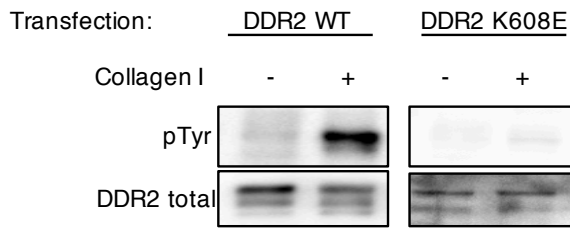
Enzyme: Trypsin/P Database: SwissProt Human (concatenated forward and reverse plus common contaminants). Fixed modification: Carbamidomethyl (C) Variable modifications: Oxidation (M), Acetyl (N-term), Pyro-Glu (N-term Q), Deamidation (N/Q) Mass values: Monoisotopic Peptide Mass Tolerance: 10 ppm Fragment Mass Tolerance: 0.02 Da Max Missed Cleavages: 2 Mascot DAT files were parsed into the Scaffold software for validation, filtering and to create a non- redundant list per sample. Data were filtered using at 1% protein and peptide FDR and requiring at least two unique peptides per protein.

Proteins were given a NSAF Calc, which contains the conversion to Spectral Abundance Factor (SAF) and subsequent Normalized Spectral Abundance Factor (NSAF). This was based on the equation:  $NSAF = (SpC/MW) / \sum (SpC/MW)N$  Where SpC = Spectral Counts, MW = Protein molecular weight in kDa, N = Total Number of Proteins

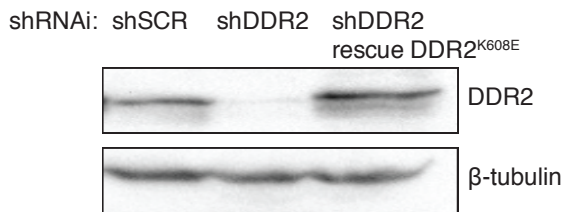
Proteins interactions identified were considered significant if 1. Protein had at least 5 SpC in the experimental sample. 2. Protein was not detected in the control sample OR 3. Protein was detected with a 4-fold or more increase based on dividing NSAF values

## Figures

A



B



C

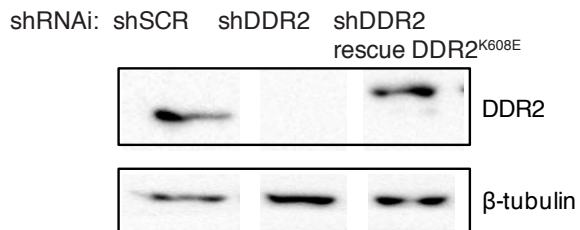


### Figure 4.1: Rescue of DDR2 expression with a kinase-dead DDR2 receptor

(A) HEK293 cells transfected with DDR2<sup>K608E</sup>-Myc were added to plates and stimulated with 30µg/mL collagen I for 4 hours in the presence of various concentrations of WRG-28. DDR2 was immunoprecipitated with Myc antibody and bound products western blotted with pTyr 4G10 or DDR2 antibodies

(B) BT459 cells depleted of DDR2 (shDDR2) were infected with lentivirus expressing a kinase dead DDR2 (DDR2<sup>K608E</sup>). Western blot analysis was performed to confirm re-expression of DDR2.

(C) ES2 cells depleted of DDR2 (shDDR2) were infected with lentivirus expressing a kinase dead DDR2 (DDR2<sup>K608E</sup>). Western blot analysis was performed to confirm re-expression of DDR2.

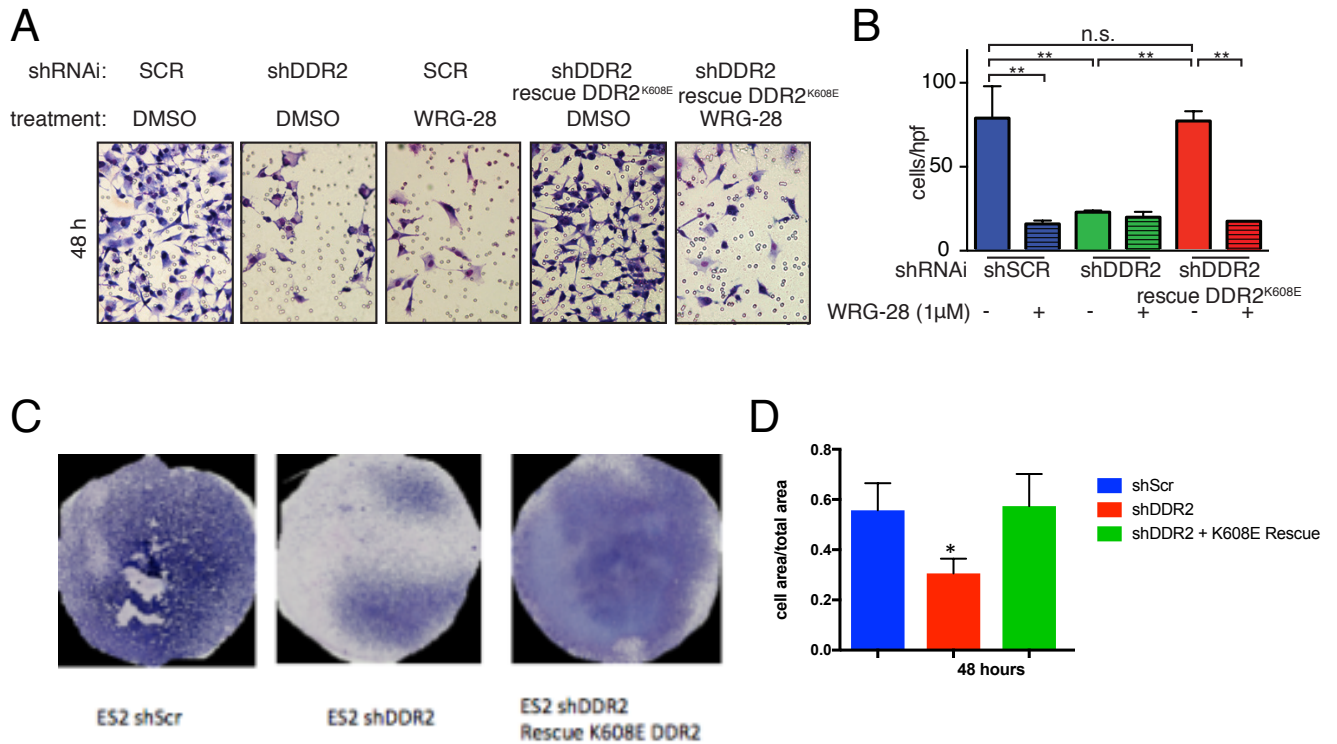


### Figure 4.2: DDR2 functions independent of its kinase activity to promote Matrigel invasion

(A) Matrigel invasion of BT549 cell lines treated with 1µM WRG-28 or control as compared to depleted of DDR2 or shRNAi depleted cells rescued with a kinase dead DDR2 (DDR2<sup>K608E</sup>) at 48 hours. Representative images of H&E stained inserts, 20x hpf.

(B) Quantification of experiment described in (A). BT549 shSCR (blue), shDDR2 (green), or shDDR2 rescued with DDR2<sup>K608E</sup> (red). Striped bars indicated WRG-28 treated cells (\*\*p<0.01, ANOVA, n=3 inserts per condition, 4hpf per insert. Experiment was performed 3 independent times with similar results.

(C) Matrigel invasion of ES2 cell lines treated comparing control SCR to depleted of DDR2 or shRNAi depleted cells rescued with a kinase dead DDR2 (DDR2<sup>K608E</sup>) at 48 hours. Representative images of entire H&E stained inserts.

(D) Quantification of experiment described in (C). ES2 shSCR (blue), shDDR2 (red), or shDDR2 rescued with DDR2<sup>K608E</sup> (green). (\*p<0.05, compared to control. ANOVA, n=3 inserts per condition, Matlab program used to quantify total area occupied by H&E stained cells as compared to total measured area of the insert)

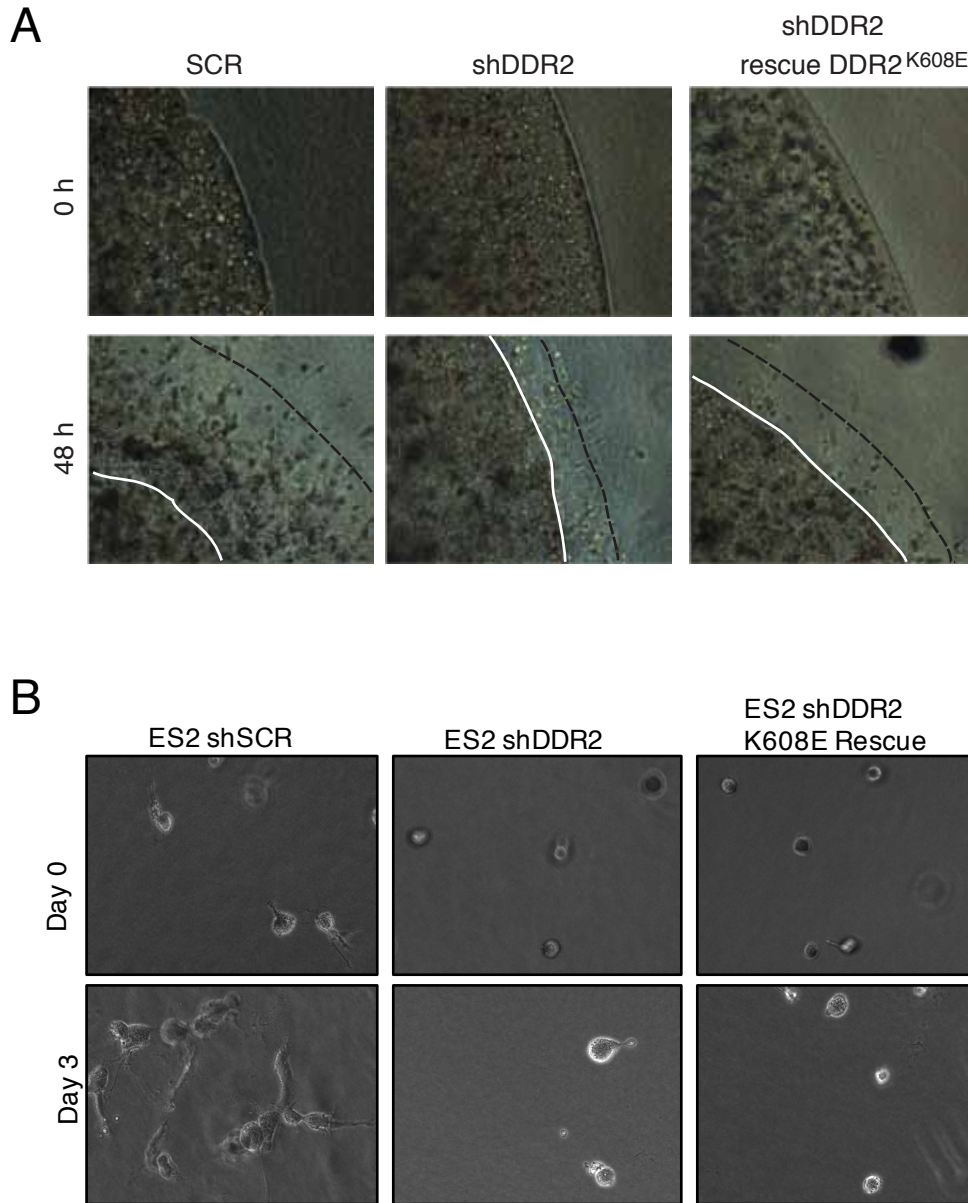


**Figure 4.3: DDR2 kinase activity predominates in 3D collagen invasion**

(A) Cell invasion in 3D collagen gels of control BT549 shSCR cells as compared to cells depleted of DDR2, or depleted cells rescued with a kinase dead DDR2 (DDR2<sup>K608E</sup>). Distance traveled relative to control cells was determined at 48hrs. Representative images shown. Solid white line delineates original cell boundary, dashed black line delineates invasive front.

(B) Collagen invasion of control ES2 shSCR cells as compared to cells depleted of DDR2, or depleted cells rescued with a kinase dead DDR2 (DDR2<sup>K608E</sup>) looking at single cell invasion through collagen I. Representative images shown.

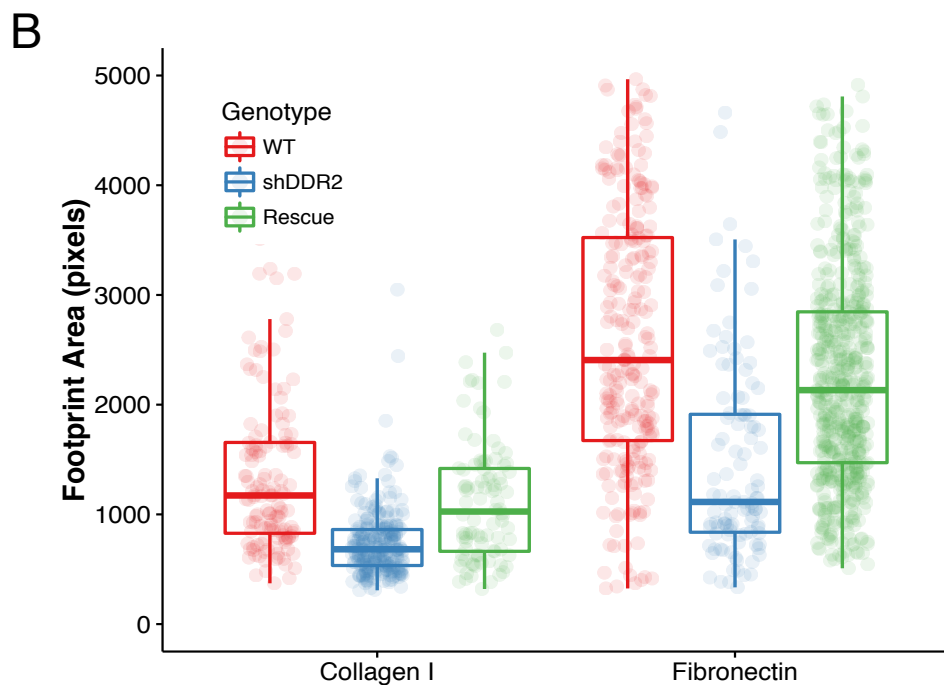
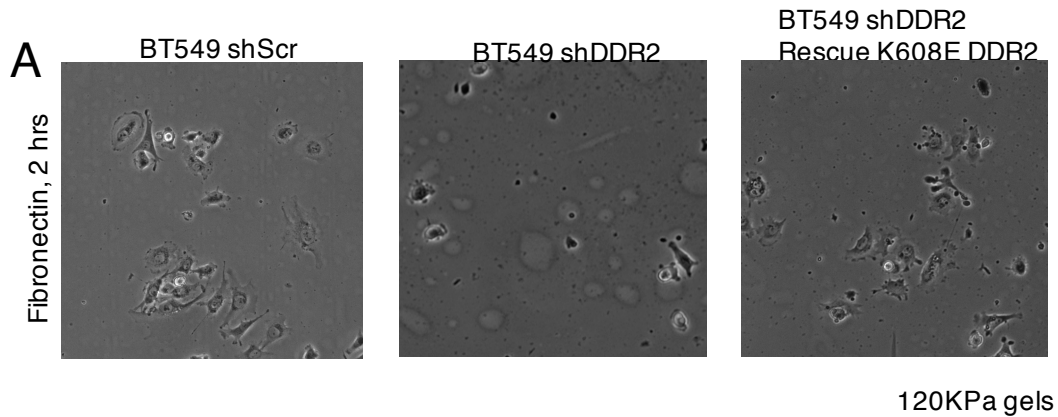


**Figure 4.4: DDR2 influences BT549 cell spreading on collagen I and fibronectin independent of kinase activity**

(A) Representative images of ES2 shSCR, shDDR2, or shDDR2 rescued with DDR2-K608E mutant cells plated on Fibronectin coated hydrogels after 2 hours.

(B) Quantification of cell area when plated on either collagen I or fibronectin coated hydrogels for 2hrs. Dots represent measure areas of individual cells, with box plot overlay depicting the median and interquartile ranges of area spread.

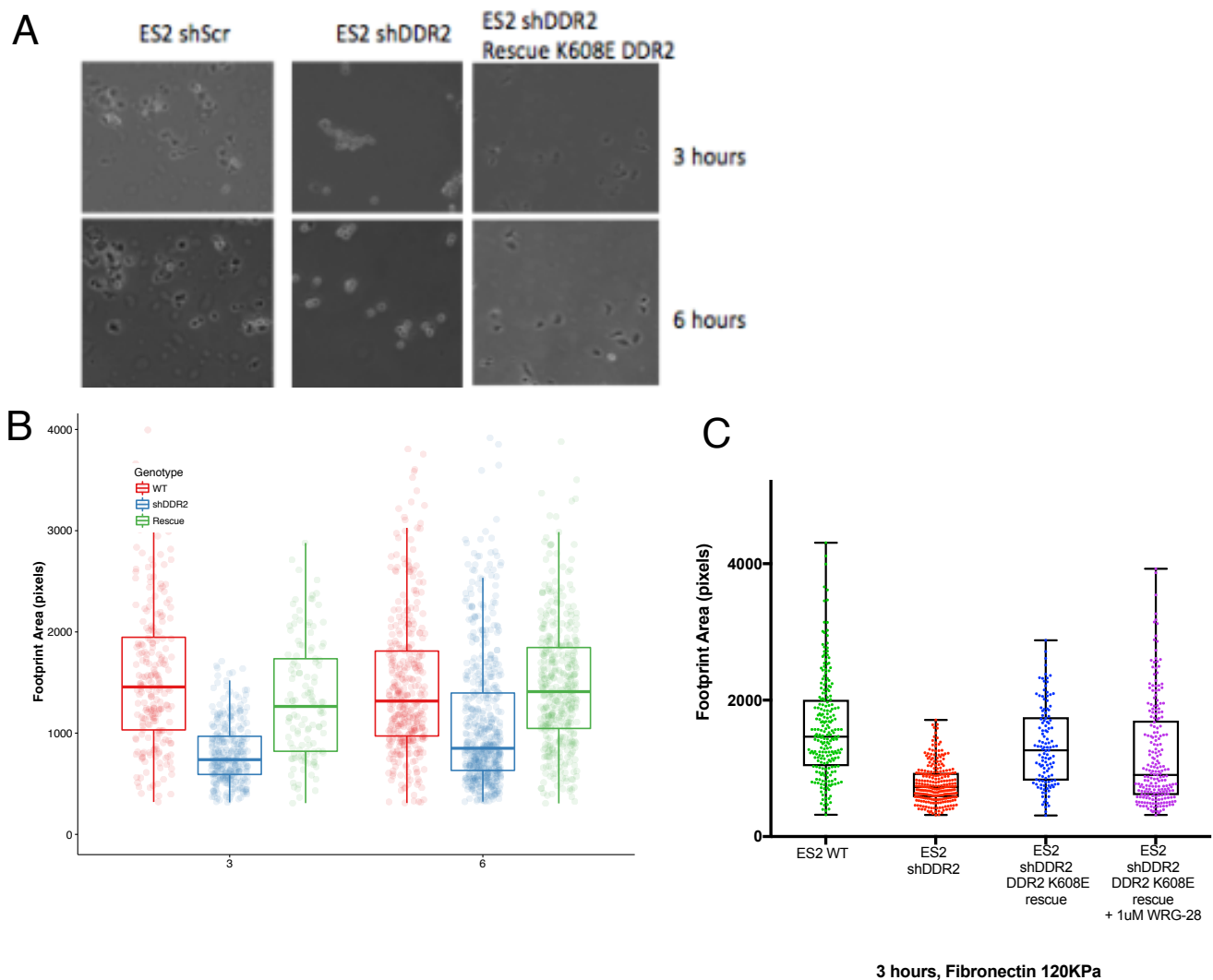


**Figure 4.5: DDR2 influences ES2 cell spreading on fibronectin independent of kinase activity and this is blocked by WRG-28**

(A) Representative images of ES2 shSCR, shDDR2, or shDDR2 rescued with DDR2-K608E mutant cells plated on fibronectin coated hydrogels after 3 and 6 hours.

(B) Quantification of cell area when plated on fibronectin coated hydrogels for at both 3 and 6hrs. Dots represent measure areas of individual cells, with box plot overlay depicting the median and interquartile ranges of area spread

(C) Quantification of cell area when plated on fibronectin coated hydrogels for 3hrs for ES2 shSCR, shDDR2, shDDR2 rescued with DDR2-K608E, and shDDR2 rescued with DDR2-K608E treated with 1uM WRG-28. Dots represent measure areas of individual cells, with box plot overlay depicting the median and interquartile ranges of area spread

**Table 1: Putative DDR2 interacting proteins in the absence of collagen ligand**

Identified Proteins	Control Spectral Counts	Collagen Unstimulated Sample Spectral Counts
Phospholipid phosphatase 3	0	5
Disintegrin and metalloproteinase domain-containing protein 12	0	5
Integrin alpha-6	0	5
Integrin alpha-3	0	5
E3 ubiquitin-protein ligase NEDD4	0	5
mRNA decay activator protein ZFP36L1	0	5
Receptor-type tyrosine-protein phosphatase S	0	5
Lysosomal-associated transmembrane protein 4B	0	5
Neuropathy target esterase	0	5
CD320 antigen	0	5
Acyl-CoA desaturase	0	6
Interferon-induced transmembrane protein 1	0	6
Non-receptor tyrosine-protein kinase TYK2	0	6
Hexokinase-2	0	6
Death-associated protein kinase 1	0	6
Guanine nucleotide-binding protein G(s) subunit alpha isoforms short	0	6
AMP deaminase 2	0	6
Ceramide glucosyltransferase	0	6
MICOS complex subunit MIC60	0	6
SWI/SNF complex subunit SMARCC2	0	6
Myeloid-associated differentiation marker	0	6
Hepatocyte growth factor receptor	0	7
Tumor necrosis factor receptor superfamily member 3	0	7
Pro-neuregulin-1, membrane-bound isoform	0	7
Desmoglein-2	0	7
Myotubularin-related protein 14	0	7
Transmembrane 9 superfamily member 2	0	7
Kinase D-interacting substrate of 220 kDa	0	7
H(+)/Cl(-) exchange transporter 7	0	8
Sorting nexin-17	0	8
Probable ATP-dependent RNA helicase DDX23	0	8
Low-density lipoprotein receptor-related protein 12	0	8
ATP-binding cassette sub-family D member 3	0	9
Histone-binding protein RBBP7	0	9
Myosin phosphatase Rho-interacting protein	0	9

Arrestin domain-containing protein 3	0	9
TGF-beta receptor type-2	0	10
Matrix metalloproteinase-14	0	10
NEDD4-like E3 ubiquitin-protein ligase WWP2	0	11
Guanine nucleotide-binding protein G(k) subunit alpha	0	11
Inactive tyrosine-protein kinase 7	0	11
CD166 antigen	0	11
Neurogenic locus notch homolog protein 2	0	12
Drebrin	0	12
Teneurin-2	0	12
Histone H2B type 1-J	0	13
Guanine nucleotide-binding protein G(l)/G(s)/G(t) subunit beta-1	0	13
Solute carrier family 12 member 2	0	14
Kin of IRRE-like protein 1	0	14
Guanine nucleotide-binding protein subunit beta-4	0	15
Forkhead box protein K1	0	16
E3 ubiquitin-protein ligase CHIP	0	17
Solute carrier family 12 member 4	0	17
Spectrin beta chain, non-erythrocytic 2	0	18
Dynactin subunit 1	0	18
Synaptotagmin-11	0	18
Myosin-14	0	37
Discoidin domain-containing receptor 2	0	237
Guanine nucleotide-binding protein G(i) subunit alpha-2	2	24
Microtubule-associated protein 2	2	23
Plasma membrane calcium-transporting ATPase 4	2	21
Gap junction alpha-1 protein	5	42
Pleckstrin homology-like domain family B member 2	2	16
Golgi apparatus protein 1	3	23
Structural maintenance of chromosomes protein 3	3	16
Thrombospondin-3	3	14
CD109 antigen	3	14
Unconventional myosin-Va	6	27
X-ray repair cross-complementing protein 6	2	9
Epidermal growth factor receptor	3	13
Hsp90 co-chaperone Cdc37	2	8
Cation-independent mannose-6-phosphate receptor	10	40
SCY1-like protein 2	5	19
Merlin	3	11
Ras-related protein Rab-7a	2	7
Low-density lipoprotein receptor-related protein 10	2	7
Transmembrane protein 59	2	7

A-kinase anchor protein 11	4	14
Protein prune homolog 2	8	28
Ephrin type-A receptor 2	14	47
Sodium/potassium-transporting ATPase subunit alpha-1	9	28
Coronin-1B	2	6
ATP-binding cassette sub-family E member 1	3	9
NEDD4 family-interacting protein 1	5	15
Replication factor C subunit 1	2	6
Ras GTPase-activating protein nGAP	2	6
Myoferlin	50	150

**Table 2: Putative DDR2 interacting proteins in the presence of collagen ligand**

<b>Identified Proteins</b>	<b>Control Spectral Counts</b>	<b>Collagen Stimulated Sample Spectral Counts</b>
Acyl-CoA desaturase	0	5
Gamma-glutamylcyclotransferase	0	5
Serpin B7	0	5
Long-chain-fatty-acid--CoA ligase 3	0	5
Immunoglobulin kappa variable 3-15	0	5
Immunoglobulin heavy variable 3-23	0	5
Hemopexin	0	5
Calpain-1 catalytic subunit	0	5
Neutrophil elastase	0	5
Prolactin-inducible protein	0	5
Histone H1.5	0	5
Zinc-alpha-2-glycoprotein	0	5
Kallikrein-7	0	5
Ras-related protein Rab-9A	0	5
H(+)/Cl(-) exchange transporter 7	0	5
Hexokinase-2	0	5
Neutrophil defensin 1	0	5
Trichohyalin	0	5
Lysosomal-associated transmembrane protein 4A	0	5
Sorting nexin-17	0	5
Sodium-coupled neutral amino acid transporter 2	0	5
Extracellular glycoprotein lacritin	0	5
Kallikrein-9	0	5
Low-density lipoprotein receptor-related protein 12	0	5
Unconventional myosin-I f	0	6
Syntaxin-6	0	6
Mammaglobin-B	0	6
Ig mu chain C region	0	6
Fibrinogen alpha chain	0	6
Glucosylceramidase	0	6
Annexin A4	0	6
Annexin A3	0	6
Tumor necrosis factor receptor superfamily member 1A	0	6
Integrin alpha-3	0	6
Bone morphogenetic protein receptor type-1A	0	6
Tumor necrosis factor receptor superfamily member 3	0	6
NADP-dependent malic enzyme	0	6

Bone morphogenetic protein receptor type-2	0	6
Receptor-type tyrosine-protein phosphatase kappa	0	6
E3 ubiquitin-protein ligase RNF149	0	6
Myotubularin-related protein 14	0	6
Phosphoglucomutase-2	0	6
Myeloid-associated differentiation marker	0	6
Transmembrane 9 superfamily member 2	0	6
Probable ATP-dependent RNA helicase DDX23	0	6
Teneurin-2	0	6
CDKN2A-interacting protein	0	6
Serpin B13	0	6
Immunoglobulin heavy variable 3-7	0	7
Creatine kinase U-type, mitochondrial	0	7
Annexin A8	0	7
Guanine nucleotide-binding protein subunit alpha-11	0	7
Guanine nucleotide-binding protein G(s) subunit alpha isoforms short	0	7
Neurogenic locus notch homolog protein 2	0	7
Kallikrein-6	0	7
Arrestin domain-containing protein 3	0	7
Tropomodulin-2	0	7
Probable ATP-dependent RNA helicase DDX41	0	7
Immunoglobulin lambda-like polypeptide 5	0	8
Thymidine phosphorylase	0	8
Leukocyte elastase inhibitor	0	8
TGF-beta receptor type-2	0	8
Sodium-dependent phosphate transporter 1	0	8
Cystatin-A	0	9
Immunoglobulin kappa variable 1-5	0	9
Ig kappa chain C region	0	9
Ig gamma-4 chain C region	0	9
ATP-binding cassette sub-family D member 3	0	9
Lipocalin-1	0	9
Serpin B5	0	9
Receptor-type tyrosine-protein phosphatase S	0	9
Guanine nucleotide-binding protein subunit beta-4	0	9
Kallikrein-13	0	9
Alpha-2-macroglobulin-like protein 1	0	10
Fibrinogen beta chain	0	10
Glutamine synthetase	0	10
Forkhead box protein K1	0	10
Ig alpha-1 chain C region	0	11
Myeloperoxidase	0	11

Cathepsin D	0	11
Insulin-degrading enzyme	0	11
Matrix metalloproteinase-14	0	11
Inactive tyrosine-protein kinase 7	0	11
Ceramide glucosyltransferase	0	11
Kin of IRRE-like protein 1	0	11
Solute carrier family 12 member 4	0	11
NEDD4-like E3 ubiquitin-protein ligase WWP2	0	13
Polymeric immunoglobulin receptor	0	13
Guanine nucleotide-binding protein G(l)/G(S)/G(T) subunit beta-1	0	13
Guanine nucleotide-binding protein G(k) subunit alpha	0	15
Synaptotagmin-11	0	15
Fibrinogen gamma chain	0	16
Drebrin	0	16
Ig gamma-1 chain C region	0	17
Cellular retinoic acid-binding protein 2	0	17
14-3-3 protein sigma	0	17
Ig gamma-3 chain C region	0	18
Protein S100-A7	0	20
Complement C4-A	0	21
Histone H2B type 1-J	0	22
Serotransferrin	0	29
Tropomyosin beta chain	0	35
Myosin-14	0	35
Serpin B4	0	44
Complement C3	0	54
Lactotransferrin	0	59
Discoidin domain-containing receptor 2	0	213
X-ray repair cross-complementing protein 6	2	24
Ankyrin	3	29
Guanine nucleotide-binding protein G(i) subunit alpha-2	2	18
Serpin B3	6	53
Gap junction alpha-1 protein	5	38
Merlin	3	22
Lysozyme C	5	36
Microtubule-associated protein 2	2	14
Ig gamma-2 chain C region	3	19
Glutathione S-transferase omega-1	2	12
FACT complex subunit SSRP1	3	18
Ras-related protein Rab-7a	2	11
EF-hand domain-containing protein D2	2	11
Coronin-1B	2	10
Plasma membrane calcium-transporting ATPase 4	2	10

Actin-related protein 2/3 complex subunit 3	4	20
NEDD4 family-interacting protein 1	5	24
Heat shock protein beta-1	3	14
Mitogen-activated protein kinase kinase kinase 7	5	22
Lamina-associated polypeptide 2, isoform alpha	3	13
LIM domain and actin-binding protein 1	4	17
Gelsolin	4	17
Twinfilin-2	2	8
Pleckstrin homology-like domain family B member 2	2	8
Immunoglobulin kappa variable 4-1	2	8
Golgi apparatus protein 1	3	12
Protein S100-A8	10	39
SCY1-like protein 2	5	19
Ephrin type-A receptor 2	14	52
Epidermal growth factor receptor	3	11
4F2 cell-surface antigen heavy chain	3	11
Plastin-3	3	11
Galectin-7	3	11
Protein-glutamine gamma-glutamyltransferase E	3	11
Fatty acid-binding protein, epidermal	6	22
Protein S100-A9	7	25
Sodium/potassium-transporting ATPase subunit alpha-1	9	32
Filaggrin	4	14
Proteasome subunit beta type-5	2	7
Ras-related protein Rab-8A	2	7
Sequestosome-1	2	7
Unconventional myosin-Va	6	21
Proteasome subunit alpha type-7	5	17
Tropomyosin alpha-1 chain	10	34
Transaldolase	3	10
CD109 antigen	3	10
26S protease regulatory subunit 7	6	20
Glutaminy-peptide cyclotransferase-like protein	4	13
Ras-related protein Rab-5C	2	6
ATP-binding cassette sub-family E member 1	3	9
Low-density lipoprotein receptor-related protein 10	2	6
Splicing factor 45	2	6
Neurabin-2	2	6
Transmembrane protein 59	2	6
Carnitine O-palmitoyltransferase 1, liver isoform	7	20
14-3-3 protein sigma	7	20
E3 ubiquitin-protein ligase Itchy homolog	7	20

## References

1. Paul, M.K. & Mukhopadhyay, A.K. Tyrosine kinase - Role and significance in Cancer. *Int J Med Sci* **1**, 101-115 (2004).
2. Lemmon, M.A. & Schlessinger, J. Cell signaling by receptor tyrosine kinases. *Cell* **141**, 1117-1134 (2010).
3. Rauch, J., Volinsky, N., Romano, D. & Kolch, W. The secret life of kinases: functions beyond catalysis. *Cell communication and signaling : CCS* **9**, 23 (2011).
4. Weihua, Z., *et al.* Survival of cancer cells is maintained by EGFR independent of its kinase activity. *Cancer Cell* **13**, 385-393 (2008).
5. Aqeilan, R.I., *et al.* WW domain-containing proteins, WWOX and YAP, compete for interaction with ErbB-4 and modulate its transcriptional function. *Cancer research* **65**, 6764-6772 (2005).
6. Hidalgo-Carcedo, C., *et al.* Collective cell migration requires suppression of actomyosin at cell-cell contacts mediated by DDR1 and the cell polarity regulators Par3 and Par6. *Nature cell biology* **13**, 49-58 (2011).
7. Herrera-Herrera, M.L. & Quezada-Calvillo, R. DDR2 plays a role in fibroblast migration independent of adhesion ligand and collagen activated DDR2 tyrosine kinase. *Biochemical and biophysical research communications* **429**, 39-44 (2012).
8. Zhang, K., *et al.* The collagen receptor discoidin domain receptor 2 stabilizes SNAIL1 to facilitate breast cancer metastasis. *Nature cell biology* **15**, 677-687 (2013).
9. Corsa, C.A., *et al.* The Action of Discoidin Domain Receptor 2 in Basal Tumor Cells and Stromal Cancer-Associated Fibroblasts Is Critical for Breast Cancer Metastasis. *Cell reports* **15**, 2510-2523 (2016).
10. Kleinman, H.K. & Martin, G.R. Matrigel: basement membrane matrix with biological activity. *Semin Cancer Biol* **15**, 378-386 (2005).

11. Labrador, J.P., *et al.* The collagen receptor DDR2 regulates proliferation and its elimination leads to dwarfism. *EMBO Rep* **2**, 446-452 (2001).
12. H Xu, D.B., F Chang, PH Huang, RW Farndale, B Leitinger. Discoidin Domain Receptors Promote  $\alpha$ 1 $\beta$ 1- and  $\alpha$ 2 $\beta$ 1- Integrin Mediated Cell Adhesion to Collagen by Enhancing Integrin Activation. *PLoS One* **7**, e52209 (2012).
13. Fu, H.L., *et al.* Discoidin domain receptors: unique receptor tyrosine kinases in collagen-mediated signaling. *The Journal of biological chemistry* **288**, 7430-7437 (2013).
14. Teese, M.G. & Langosch, D. Role of GxxxG Motifs in Transmembrane Domain Interactions. *Biochemistry* **54**, 5125-5135 (2015).
15. Ikeda, K., *et al.* Discoidin domain receptor 2 interacts with Src and Shc following its activation by type I collagen. *The Journal of biological chemistry* **277**, 19206-19212 (2002).
16. Hughes, C.S., Postovit, L.M. & Lajoie, G.A. Matrigel: a complex protein mixture required for optimal growth of cell culture. *Proteomics* **10**, 1886-1890 (2010).
17. Vogel, W., Gish, G.D., Alves, F. & Pawson, T. The discoidin domain receptor tyrosine kinases are activated by collagen. *Molecular cell* **1**, 13-23 (1997).
18. Zhang, K., *et al.* Lats2 kinase potentiates Snail1 activity by promoting nuclear retention upon phosphorylation. *The EMBO journal* **31**, 29-43 (2012).
19. Feng, Y., *et al.* A multifunctional lentiviral-based gene knockdown with concurrent rescue that controls for off-target effects of RNAi. *Genomics, proteomics & bioinformatics* **8**, 238-245 (2010).
20. Zhang, K., *et al.* Mechanical signals regulate and activate SNAIL1 protein to control the fibrogenic response of cancer-associated fibroblasts. *Journal of cell science* **129**, 1989-2002 (2016).
21. Team, R.C. R: A language and environment for statistical computing. R Foundation for Statistical Computing. (2013).

**Chapter 5**  
**Conclusions and Future Directions**

In summary, we have demonstrated that DDR2 was a candidate therapeutic target for breast cancer metastasis by temporally depleting *Ddr2* in early stage tumors in MMTV-PyMT mice. We developed small molecule inhibitors of DDR2 that target the extracellular domain of the receptor to inhibit ligand binding in a non-orthosteric manner. We were able to show that the developed inhibitor actively inhibits DDR2 activation and downstream signaling in response to collagen in both breast tumor cells and *in vivo*. We also elucidated a region at the interface of the two DDR2 extracellular domains that is important for receptor binding and activation. Furthermore, we have documented kinase independent functions of the DDR2 receptor, and identified putative interacting partners of the protein in breast cancer cells. The developed inhibitor is able to show efficacy towards kinase independent functions of the receptor, illustrating the potential advantage of such an inhibition strategy over traditional kinase inhibition. In ovarian cancer, we established DDR2 as critical for metastasis. Additionally, we detailed a pathway whereby DDR2 expression is regulated in invasive tumor cells. Upon induction of EMT, the EMT transcription factor TWIST1 drives the expression of DDR2, which in turn stabilizes the transcription factor SNAIL1 to sustain EMT. DDR2 in ovarian cells drives the cleavage and remodeling of fibronectin, which promotes mesothelial cell clearance by the cancer cell.

### **Small molecule targeting of DDR2**

DDR2 is a critical regulator of breast cancer metastasis, with pro-invasive roles in the tumor and stromal compartments. The work outlined here demonstrates the potential of DDR2 as a therapeutic target in the setting of metastasis. We have shown

that WRG-28, a non-orthosteric inhibitor that acts on the DDR2 extracellular domain, is effective in inhibiting the pro-metastatic functions of DDR2 both *in vitro*, and preliminarily *in vivo*. While this compound was efficacious as tested, further medicinal chemistry work will be necessary to optimize the compound for further development. Solubility of WRG-28 is sub-optimal, and addition of chemical moieties that enhance the aqueous solubility, or a formulation that does such, is needed. Furthermore, it will be important to conduct pharmacokinetic and pharmacodynamics studies to determine how the compound (or future derivatives) are metabolized, and how long they remain *in vivo* before being cleared. Such work will be necessary before this inhibitor can be tested in longer term models of metastasis.

It is important to note that in the therapeutic setting, a DDR2 inhibitor such as WRG-28 would not be useful as a single agent, as DDR2 does not have an appreciable effect on breast tumor proliferation. Therefore, it will be most efficacious in conjunction with other conventional chemotherapeutics that kill tumors or inhibit their growth. The subset of breast cancer patients that would most benefit from such a therapy remains a point of interest. Previous work has shown the important role DDR2 plays in the early stages of metastasis to facilitate collective migration away from the primary site<sup>1</sup>. Our work where DDR2 was temporally deleted in early stage tumors of MMTV-PyMT mice suggests that an ideal patient may be someone with early stage disease that is at risk for progressing to invasive disease. In such a case, DDR2 inhibition would be a preventative measure. However, many patients present with evidence of disseminated disease<sup>2</sup>. Data collected using late stage models of metastasis indicate that DDR2 inhibition may still be beneficial in later stage patients. When 4T1 cells depleted of

DDR2 were injected intravenously into mice, there was significantly less tumor burden in the lung than seen with 4T1 control cells, and treatment with WRG-28 showed a similar trend as the knockdown cells (Figure 2.17). This suggests that DDR2 plays a role in these later stages, and a DDR2 targeted therapy may be clinically useful even in this setting where tumor cells have disseminated.

### **Role of DDR2 in late breast metastasis**

We have shown that DDR2 depletion in 4T1 cells inhibits tumor seeding and colonization in the lungs following intravenous injection of these cells into the tail veins of BALB/cJ mice, and inhibition of control 4T1 cells with the DDR2 inhibitor WRG-28 shows a similar effect.

How exactly DDR2 is functioning to promote metastasis in these later stages is still unknown, and warrants further study. It is possible that similar to the pro-invasive phenotypes seen in the primary site<sup>1</sup>, DDR2 could be acting to promote invasion and migration into the lung parenchyma. In order to seed in the lung, tumor cells must extravasate from the vasculature. Whether DDR2 plays a specific role in tumor cell extravasation, distinct from its role in tumor migration, is unknown, and a possibility worth exploring. Additionally, DDR2 could be promoting survival in the circulation, increasing the number of cells available to seed in the lungs. DDR2 stabilizes SNAIL1 levels<sup>3</sup>, and SNAIL1 has been shown to promote tumor cell survival<sup>4</sup>. Whether DDR2 plays a role in cell survival dependent or independent of its stabilization of SNAIL1 remains unknown. Measuring levels of circulating tumor cells in the bloodstream of mice

after injection of wild type or DDR2 depleted cells would be one way to address this question.

Once in the lung parenchyma, there also remains the possibility that DDR2 could facilitate production and/or remodeling of ECM within the lung that influences colonization or growth. While we have not collected direct evidence in the setting of breast cancer, given the role of DDR2 in ovarian cells to cleave fibronectin and clear the mesothelial cell layer at secondary sites (Figures 3.5 and 3.2), it seems possible that this type of remodeling could be occurring in breast cancer secondary sites as well. In order to determine patient populations that could benefit from DDR2 inhibition, it will be important to fully elucidate the roles of the receptor at these late stages of metastasis.

Of note, given the stromal contribution of DDR2 in breast metastasis, we hypothesized that stromal DDR2 in the secondary site (i.e. lungs) may also be contributing to tumor cell seeding and metastasis. To test this possibility, we injected C57BL/6 mice that were either wild type or DDR2 ubiquitous null (DDR2<sup>-/-</sup>) intravenously via the tail vein with the highly metastatic PyMT-BO1 GFP/luc cell line<sup>5</sup>. Over the course of 8 days, tumor colonization and growth in the lung was assessed by bioluminescent imaging. It did not appear that stromal DDR2 contributed to growth or colonization by these tumor cells in this model (Figure 5.1). Therefore, this data suggests that while in the primary site stromal DDR2 plays a major role in contributing to metastasis, the effects of DDR2 in the later stages of breast cancer metastasis may be confined to the tumor cell itself.

## **Therapeutic targeting of DDR2 in other disease states**

DDR2 has gained significant attention as a therapeutic target in the treatment of lung cancer, where potential activating mutations in the Ddr2 gene have been documented<sup>6,7</sup>. While we have not tested WRG-28 in the setting of these specific point mutations, given the data collected showing that the inhibitor retains activity against activating “gatekeeper” mutations, it seems likely the compound would be efficacious in these settings as well. However, this will have to be addressed directly.

We have also demonstrated DDR2 as an important mediator of ovarian cancer metastasis. However, at this point, we have only addressed the importance of DDR2 in the tumor cell. It will be important to determine if DDR2 plays a role in the stromal compartment in this disease. As the metastatic course of ovarian cancer differs from breast, the stromal role of DDR2 in secondary sites that becomes of particular interest. Given that the majority of ovarian cancer cases present at advanced stage<sup>8</sup>, the stromal contribution becomes critical from a therapeutic standpoint, as intervention prior to tumor establishment at the metastatic site may not be possible in this patient population.

In addition to cancer, there other diseases where therapeutic targeting of DDR2 has shown promise. Including fibrosis and osteoarthritis (OA)<sup>9,10</sup>. In OA, DDR2 expression is increased in chondrocytes of OA patients and mouse models of OA<sup>11 12</sup>. Activation of DDR2 in chondrocytes leads to MMP13 upregulation, one of the major degradative enzymes of collagen II in the articular cartilage<sup>12</sup>. Overexpression of DDR2 alone in chondrocytes does not result in OA in normal mice, likely because normal articular chondrocytes are not directly exposed to collagen II<sup>13</sup>. However, injury

can expose chondrocytes to collagen II and the development of OA<sup>13</sup>. Genetically reducing DDR2 levels in mouse genetic models and injury models of OA attenuates OA progression<sup>14 15</sup>. Whether DDRs contributes to rheumatoid arthritis has not been experimentally tested but DDR2 is highly expressed in synovial fibroblasts from patients with RA<sup>16,17</sup>, and may act as one of the stimulators of the over-expression of MMP-1 in RA synovial fibroblasts<sup>18</sup>. A DDR2-CYR61-MMP1 signaling pathway has been proposed to contribute to RA pathogenesis<sup>17</sup>. Therefore, in the setting of arthritis, DDR2 may be a promising therapeutic target. Further, given that the OA is confined within a joint space, therapeutic targeting of DDR2 in this setting may be more practical, as patients may still benefit even in later stages of the disease; however, this notion must be tested.

Additionally, DDR2 has been shown to play a role in induction of fibrosis and angiogenesis in bleomycin induced lung fibrosis models<sup>19</sup>. When Ddr2 deficient mice were administered bleomycin, they showed a dramatic decrease in fibrosis and activation markers within the lung as compared to the wild type mice<sup>19</sup>. As a potential therapeutic for idiopathic pulmonary fibrosis, DDR2 may be promising. Indeed, it was shown that targeting DDR2 using siRNA beginning at the onset of bleomycin administration greatly reduced lung fibrosis. Some benefit was still seen when DDR2 siRNA administration begin at day 14 (of a 28-day model)<sup>19</sup>. However, given the irreversible loss of lung function that occurs with progression of this disease, it is likely there is some critical window after which DDR2 directed therapeutics may not be beneficial.

## **Identification of important regulatory regions in the DDR2 extracellular domain**

During our efforts to identify the potential binding site of WRG-28, we uncovered residues within the extracellular domain of DDR2 that are critical for the receptor function. Double mutants harboring F96A and T98A mutations were unable to bind to collagen *in vitro*, and did not activate in response to collagen in cells. These residues lie at the interface of the two extracellular domains. While such interdomain residues have been shown to be important in the function of other receptors<sup>20,21</sup>, how exactly they are mediating DDR2-collagen binding at a molecular level is unknown. Analysis of the extracellular domain *in vitro* shows that oligomers, which are present in the wild type protein, are notably absent in the DDR2<sup>F96A/T98A</sup> mutants (Figure 2.10E). We demonstrated that these oligomers bind to ligand with higher affinity than corresponding dimeric DDR2 ECD (Figure 2.8D). The functional dependence of these oligomers in DDR2 is unknown; however, the lack of binding of the DDR2<sup>F96A/T98A</sup> mutant would suggest that they are important. Work by others on DDR1 has shown that oligomerization of the ECD is critical for its function<sup>22</sup>. Some reports have suggested this clustering to be important for DDR2<sup>23</sup>, therefore will be important to determine the functional relevance of this oligomeric species.

It will also be important to make use of this DDR2<sup>F96A/T98A</sup> mutant in intact cells, to determine the impact on oligomerization of full length receptor. While such higher order clustering has been deemed important for DDR1 function<sup>24,25</sup>, its role in DDR2 has not been examined. We are currently using YFP-tagged version of the DDR2 receptor in live cells to answer this question. DDR2-YFP, DDR2<sup>W52A</sup>-YFP (collagen binding

mutant), and DDR2<sup>F96AT98A</sup>-YFP mutants are being expressed in cells depleted of DDR2, and receptor clustering in response to collagen I activation will be examined.

Additionally, the identification of these functionally important residues within the DDR2 extracellular domain opens the door to potential new therapeutic strategies. In addition to optimization of the already developed inhibitor WRG-28, rational based design of small molecules directed to this area of the protein could also be conducted. As this portion of the protein appears to be crucial for directing ligand binding, it would also be a possibility to develop antibodies directed to this region of the receptor as a potential therapeutic option.

### **Determining the molecular basis for DDR2 inhibition by WRG-28**

Computational modeling suggests that an interface region between the two DDR2 extracellular domains could be serving as the binding site for WRG-28 (Figure 2.9). Mutations within those residues lead to a receptor that is unable to bind collagen (DDR2<sup>F96AT98A</sup>) providing data on the critical nature of this region for proper receptor function, which could correlate to the ability of WRG-28 to mediate its effects. While DDR1 is not inhibited by WRG-28, when DDR1 residues in this region are replaced with the corresponding DDR2 residues (DDR1<sup>L96F/A98T</sup>), it becomes amenable to inhibition by WRG-28 (Figure 2.10). While this points to the importance of this region for the inhibitory ability of WRG-28, in the absence of structural data, it is impossible to know the molecular basis of binding and recognition for this inhibitor with DDR2. Further, given the data suggesting that the compound may be acting to disrupt clustering of the extracellular domain (Figure 2.8), it is possible that the binding site could be a

composite site formed by two or more interacting protomers. While a crystal structure may elucidate interactions of WRG-28 with DDR2, dimers were not seen in the crystal structure of the DS domain of DDR2 in complex with collagen peptide<sup>26</sup>, and only a suggestion of dimer was observed when the extracellular domain of DDR1 was crystallized<sup>27</sup>. Therefore if a composite site is needed for WRG-28 recognition, it may not be truly reflected in a crystal structure. Given that dimers and oligomers of the extracellular domain form in solution, an NMR solution based structure may be a more optimal approach to elucidate the molecular basis of interactions for DDR2 and WRG-28.

### **Establishing DDR2 as a critical regulator of metastasis in ovarian cancer**

Using cell based assays *in vitro*, and xenograft *in vivo* models, we show that DDR2 in ovarian cancer cells promotes metastasis. We establish this role using human derived ovarian cancer cell lines, which is important to predict clinical relevance. However, one shortcoming of this approach is that it necessitates use of immunocompromised mice for *in vivo* experiments. While there is one mouse derived ovarian cancer line available (ID8 cells, C57BL/6 derived) for use in syngeneic models, the metastatic burden in this particular cell line is low, and it lacks mutations characteristic of high grade serous carcinoma. Recently, derivatives of this cell line were engineered to delete either p53 (Trp53<sup>-/-</sup>) or p53 and Brca2 (Trp53<sup>-/-</sup>;Brca2<sup>-/-</sup>), more closely mimicking the human disease<sup>28</sup>, and inducing a more aggressive metastatic phenotype. We have obtained these lines and confirmed that they express high levels of DDR2. Knockdown of DDR2 in these cell lines and subsequent

transplantation will allow for the assessment of the contribution of DDR2 to metastasis in a syngeneic model of ovarian cancer metastasis.

Additionally, there is currently no data regarding the potential importance of DDR2 within the ovarian stromal environment. Ovarian metastases contain high levels of collagen I deposition, and given the importance of DDR2 in the breast tumor stroma, it remains possible that DDR2 plays a role in the ovarian stroma as well. Using the ID8 p53<sup>-/-</sup> or ID8 p53<sup>-/-</sup>;Brca2<sup>-/-</sup> lines transplanted into either wild type C57BL/6 or DDR2<sup>-/-</sup> C57BL/6 mice will allow us to assess the stromal contribution of DDR2 in ovarian cancer.

While the data demonstrates that DDR2 is important for ovarian cancer metastasis, whether DDR2 is a viable therapeutic target in this cancer remains of question. Notably, the majority of ovarian cancer patients present with late stage disease, where metastatic foci are already present. In the context of our studies, most assays were representing cellular events that occur early in the ovarian metastatic cascade. Whether DDR2 plays a role once metastatic lesions are present is unknown, and more sophisticated genetic approaches that allow for temporal deletion of the receptor will be required to answer this question.

### **Regulation of DDR2 expression**

In normal tissues, DDR2 is primarily a mesenchymal gene, while DDR1 is expressed in epithelial tissues<sup>10</sup>. It has previously been shown that under conditions of forced EMT, cancer cells will switch from expression of the epithelial DDR1, to expression of DDR2<sup>29</sup>. The molecular basis of this switch during cancer EMT was

unknown. Recently, it was reported that Ddr2 was a transcriptional target of TWIST1 in the developing cranial mesoderm<sup>30</sup>, leading us to hypothesize that TWIST1 may be inducing DDR2 after EMT induction in cancer cells. Using ovarian cancer cells, we demonstrated that in cells that display a mesenchymal phenotype and express biochemical markers of EMT, TWIST1 also drives DDR2 expression (Figure 3.1A and B). Additionally, TWIST1 is required to induce DDR2 expression in TGF-B induced EMT (Figure 3.1D and E). Whether or not this dependency is present for other methods of EMT induction is unknown, and warrants further study. While TWIST drives DDR2 expression in ovarian cancer, it will be important to determine if this same mode of regulation is consistent in other cancers where EMT has been shown to be important for metastasis. Furthermore, the molecular basis for the concurrent downregulation of DDR1 in cells undergoing EMT<sup>29</sup> is unknown.

It has long been speculated that upon reaching a metastatic site, a cancer cell that has undergone EMT must go through MET to become epithelial in nature and begin proliferation to form a metastatic foci, and recent data supports this notion<sup>31</sup>. DDR1, the epithelial expressed member of the DDR family, has also been shown to be important in ovarian cancer metastasis<sup>32,33</sup>. An interesting possibility is that upon undergoing MET, metastatic cells once again express DDR1, which drives cellular processes favorable for the newly seeded cells. Determining whether this switching occurs and what its potential contribution is to metastasis is of particular interest. Furthermore, determining the molecular mediators of this reverse switch will be important to more fully understand the regulation of these receptors in ovarian cancer, and may be applicable to other cancers as well.

## **Kinase independent functions of DDR2**

DDR2 is a member of the receptor tyrosine kinase family. As an RTK many pro-metastatic functions of DDR2 are dependent on its kinase activity. These include its ability to stabilize the EMT transcription factor SNAIL1<sup>3</sup>, and phosphorylation of Src as downstream effector<sup>34</sup>. However, it is not uncommon for RTKs to function independent of signaling to drive various cellular processes. Indeed, we uncovered a number of cellular phenotypes driven by DDR2 that are rescued by expression of a kinase dead (DDR2<sup>K608E</sup>) version of the receptor (Figures 4.2, 4.4, and 4.5). In addition to documenting this effect in cell culture, it will be important to determine whether these kinase independent roles of the receptor contribute to metastasis *in vivo*. Given the dramatic reduction in metastasis when DDR2 is knocked down in the 4T1-BALB/c transplant model<sup>3</sup>, this metastasis model would be ideal to evaluate these functions. Rescue of DDR2 knockdown with either wild type or a kinase deficient DDR2 receptor followed by transplantation and evaluation of metastasis should be conducted, in order to begin to determine if these non-signaling functions of the receptor contribute to metastasis.

Additionally, a mass spectrometry proteomics screen was conducted to identify potential interacting partners of DDR2, in order to shed light on how the receptor may be working independent of its kinase function at a mechanistic level. In addition to potentially identifying kinase independent functions of the receptor, these putative interacting partners may also help to shed light on various DDR2 signaling pathways in cells, as there is relatively little known about downstream kinase function of the receptor. While there is much work to be done to validate these candidate proteins and

determine if their interaction with DDR2 is functional, here I highlight some of the potentially interesting candidate proteins.

### **Receptors with Pro-Invasive Associations**

Putative interacting partner: PTK7

We have confirmed that Tyrosine-protein kinase-like 7 (PTK7) interacts with DDR2 at a protein level in breast cancer cells (Figure 5.2B). It is highly expressed in human BT549 breast cancer cell lines, and the expression level of the full length protein does not change with DDR2 knockdown or overexpression (Figure 5.2A). In a fibrosarcoma cell line, PTK7 was found to direct cancer cell motility and metastasis<sup>35</sup>. In cancer, PTK7 functionality is selectively regulated by MMP-14 and ADAMs. While the full length PTK7 receptor is anti-migratory, upon cleavage a soluble N-terminal fragment is shed, and intracellular C-terminal fragment is cleaved at the membrane by gamma-secretase to release a cytoplasmic tail fragment that can transport to the nucleus. This cleavage allows for the regulation of multiple genes and signaling pathways in cancer cells<sup>36</sup>. Interestingly, MMP-14 was also identified as a putative DDR2 interacting protein in the co-immunoprecipitation screen. While DDR2 has previously been shown to increase the levels and activity of MMP-14<sup>3,37</sup>, this is the first indication of a potential interaction at a protein level. It will be interesting to determine whether the DDR2/PTK7 interaction is of functional consequence. One possibility that by scaffolding both proteins, DDR2 brings PTK7 and MMP-14 into proximity to allow for the cleavage of PTK7 that is required for its pro-invasive functions. Future studies examining the levels of PTK7 cleavage products in the presence or absence of DDR2

will help further elucidate the function of this interaction. Alternatively, it is possible that soluble PTK7 could influence the ability of DDR2 to phosphorylate in response to collagen. Such a mechanism has been seen for DDR1, where in the presence of Wnt-5a protein the receptor is greatly enhanced in its ability to respond to collagen stimulation<sup>38</sup>. Additionally, PTK7 plays a crucial role in planar cell polarity as a regulator of Wnt signaling<sup>39</sup>, and planar cell polarity is important for collective cell migration. Recent work in our lab has illustrated that DDR2 in basal epithelial cells regulates collective invasion of breast tumor organoids<sup>1</sup>. It would be interesting to determine if an interplay between DDR2 and PTK7 could be mediating this role of DDR2 in collective invasion.

Putative interacting partner: CD109 antigen

Recently, CD109 was identified as a pro-metastatic factor in an *in vivo* screen of lung cancer metastasis<sup>40</sup>. While knockdown of CD109 dramatically reduced lung metastasis in that study, the mechanistic basis for this reduction is still unclear. Whether or not CD109 interaction with DDR2 plays a role in its pro-metastatic function is of interest. We have shown that knockdown of DDR2 in BT549 cells does not influence levels of CD109, and are now in the process of evaluating the reciprocal relationship. CD109 has been reported to interact with the EGF receptor and enhance its response to EGF stimulation<sup>41</sup>. Future studies should look at whether the presence of CD109 plays a role in attenuating the ability of DDR2 to respond to collagen.

## DDR2 and Mechanical Forces

Putative interacting partners: Myosin-14 (non-muscle IIc), unconventional myosin Va, unconventional myosin-I<sub>f</sub>

Cells interact with the surrounding ECM in several ways. Cell-matrix interactions are mediated by receptors, the most common of which are the matrix binding integrin receptors that bind multiple ECM components. Focal adhesions (FA) are formed in the areas where ECM-cell contacts are made, and important biochemical signals are relayed by these adhesions<sup>42</sup>. For FAs to stabilize and connect to the actin cytoskeleton, they undergo a process of maturation. During this process, myosin II- contractility is increased, providing a contractile force along actin filaments that provides the cellular tension necessary for FA maturation<sup>43</sup>. It has been reported that DDR2 promotes focal adhesion formation by interacting with non-muscle myosin IIA via the juxtamembrane 2 region of DDR2<sup>44</sup>. Additionally, DDR1 has been shown to interact with NMIIA to mediate cell motility<sup>45</sup> and collagen tractional remodeling<sup>24</sup>.

How DDR2 is interacting with non-muscle myosin to potentiate cell adhesion and contractility, and what consequences this has in the context of tumors is an active area of investigation. Myosin-generated force is utilized by ovarian cancer spheroids to promote mesothelial cell clearance and allow the tumor cell clusters to access the sub-mesothelial microenvironment<sup>46</sup>. We have demonstrated that DDR2 promotes mesothelial cell clearance by tumor spheroids (Figure 3.2A-B). Therefore, mesothelial clearance by ovarian tumor spheroids could be an interesting context in which to examine the role DDR2 plays in myosin mediated force generation.

## DDR2 Receptor Trafficking

Putative interacting partners: Rab5c, Rab-8a, Rab7a and Rab9a, sorting nexin 17

We identified a number of proteins involved in endosomal transport: Rab5c (early endosome), Rab-8a (post-Golgi to membrane), Rab7a and Rab9a (late endosome)

Receptors that rapidly recycle back to the plasma membrane (such as transferrin receptor), release ligand in the early endosome, whereas receptors such as EGFR remain ligand bound and active even at the low pH of later endosomes<sup>47</sup>. While some receptors maintain signaling within the endosome, some signaling requires receptor endocytosis or occurs exclusively on endosomal membranes. It has been shown that DDR1 undergoes cytoplasmic internalization and incorporation into the early endosome, at time scales much faster than receptor activation (5 minutes for endocytosis, versus 60-90 minutes for maximal activation)<sup>25</sup>. How this endocytosis interplays with receptor activation and signaling is unknown. There have not been studies addressing endocytic trafficking of DDR2.

Additionally, sorting nexin 17 (SNX17) was found to associate with DDR2. Members of the SNX family form retromer complexes that are recruited to Rab7-positive late endosomes and rescue cargo receptors from degradative pathways<sup>47</sup>. SNX17 has been previously shown to bind  $\beta$ 1 integrin tails in endosomes to stabilize the protein and recycle it back to the cell surface to be reused<sup>48</sup>.

Whether DDR2 is being endosomally trafficked, and how that may play a role in signaling by the receptor is a potential area of future study, especially given the delayed kinetics of activation for the DDR2 receptor. Given that a phosphorylation specific

DDR2 antibody (DDR2 p-Tyr740) is now available, it would be interesting to conduct co-localization with various markers (membrane, early endosome, late endosome, nucleus) by immunofluorescence after ligand stimulation to determine in which cellular compartments active DDR2 receptor is found.

Recently published work assessing DDR2 in mesenchymal stem cells suggest an upregulation of phosphorylated DDR2 receptor within the nucleus of stimulated cells, suggesting that activation induces DDR2 localization in the nucleus<sup>49</sup>. The functional relevance of that nuclear pool is unknown. The nuclear fractions of RTKs have been reported to interact with promoters of target genes and function as transcription factors<sup>50</sup> or serve as coregulators of transcription<sup>51</sup>. Therefore, the trafficking of DDR2 and potential translocation into the nucleus warrants further investigation to determine if it produces a relevant biologic activity, or if it is merely a housekeeping mechanism of degradation.

### **Transcriptional Regulation by DDR2**

Putative interacting partner: Notch2

When the Notch receptor is activated, this leads to the proteolytic cleavage of the receptor and release of the Notch intracellular domain (ICD). This Notch ICD translocates to the nucleus to interact with C promoter-binding factor 1 and initiate transcription of Notch target genes, many of which are transcription factors.<sup>52</sup> DDR1 has been reported to bind to the Notch1 receptor, and activation of DDR1 with collagen led to induced activation of Notch and subsequent downstream signaling, and increased active form of Notch1 in the nuclear fraction<sup>53</sup>. A number of reports correlate DDR2

expression to changes in transcription level of various proteins<sup>1,49,54</sup>. In addition to regulation of the SNAIL1 transcription factor, potential signaling through cross-activation of Notch could be a mediator in the transcriptional activation of various proteins by DDR2.

### **Matrix interacting proteins**

Putative interacting proteins: Integrin  $\alpha$ 3, Integrin  $\alpha$ 6

In both breast and ovarian cells, DDR2 was found to promote enhanced adhesion and spreading to fibronectin—a matrix protein that does not serve as a binding ligand of DDR2 (Figures 4.4 and 4.5). How exactly DDR2 is mediating this enhancement is still an unanswered question. One possibility is cross talk or enhancement of direct matrix binding proteins. Among the proteins to co-immunoprecipitate with DDR2 were: Integrin  $\alpha$ 3, the alpha subunit that combines with  $\beta$ -1 integrin to form a receptor for fibronectin and laminin; and Integrin  $\alpha$ 6, the alpha subunit that combines with  $\beta$ -1 integrin to form a receptor for laminin. There are numerous possibilities as to how DDR2 could be interacting with these proteins. It should first be evaluated whether DDR2 is directly interacting with these proteins, or whether they are co-immunoprecipitating as part of a complex formed within focal adhesion. It has previously been shown that DDR2 can enhance the activation of  $\alpha$ 1 $\beta$ 1 and  $\alpha$ 2 $\beta$ 1 to promote adhesion<sup>55</sup>, however a mechanistic basis for this activation is unknown.

## Figures

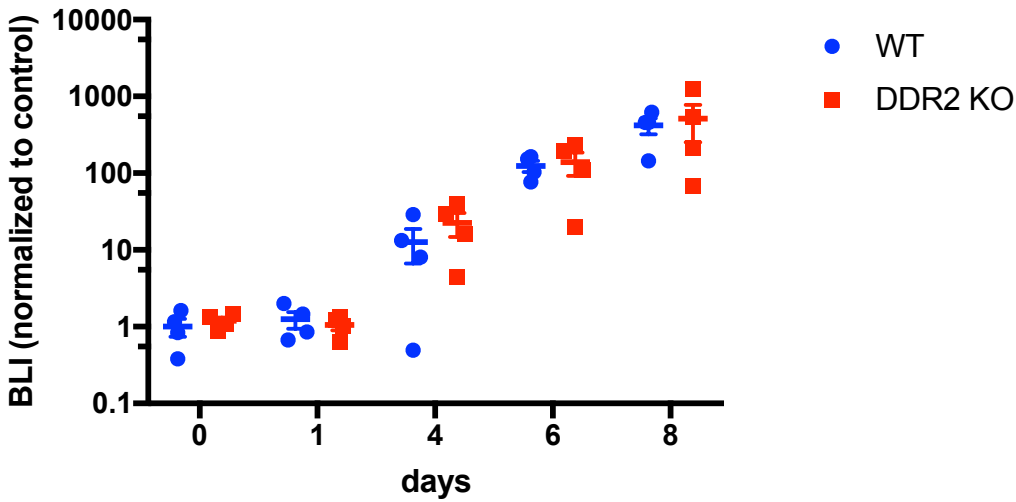


### Figure 5.1: Role of stromal DDR2 in secondary site growth and colonization

To model the later stages of metastasis, C57BL/6 wild type or DDR2<sup>-/-</sup> mice were injected via tail vein with the syngeneic BO1-GFP/luc breast cancer cell line, and growth and colonization in the lungs assessed over 8 days.

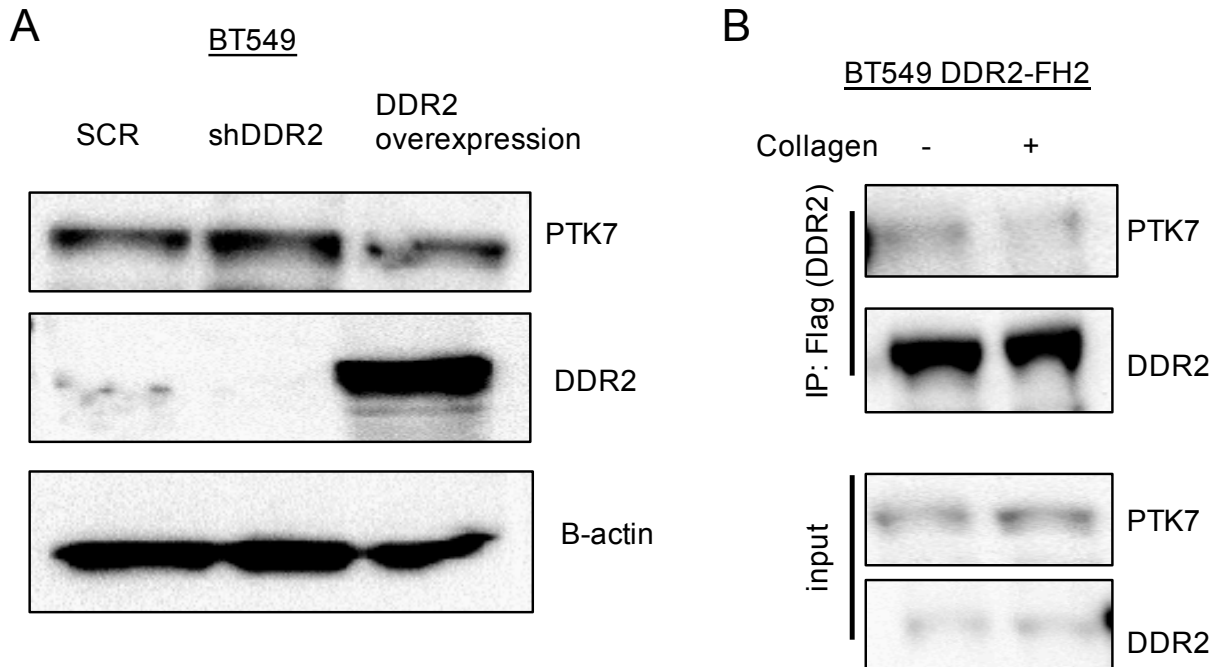


**Figure 5.2: PTK7 co-immunoprecipitation validation**

(A) Expression of PTK7 in control BT549 shSCR, BT549 shRNA depleted of DDR2, or BT549 DDR2 overexpressing cells, showing no overall changes in amount of full length PTK7.

(B) Confirmation that PTK7 co-immunoprecipitates with DDR2 in BT549 cells expressing a DDR2-Flag-His-His protein

## References

1. Corsa, C.A., *et al.* The Action of Discoidin Domain Receptor 2 in Basal Tumor Cells and Stromal Cancer-Associated Fibroblasts Is Critical for Breast Cancer Metastasis. *Cell reports* **15**, 2510-2523 (2016).
2. Banys, M., Krawczyk, N. & Fehm, T. The role and clinical relevance of disseminated tumor cells in breast cancer. *Cancers (Basel)* **6**, 143-152 (2014).
3. Zhang, K., *et al.* The collagen receptor discoidin domain receptor 2 stabilizes SNAIL1 to facilitate breast cancer metastasis. *Nature cell biology* **15**, 677-687 (2013).
4. Wu, Y. & Zhou, B.P. Snail: More than EMT. *Cell adhesion & migration* **4**, 199-203 (2010).
5. Su, X., *et al.* Antagonizing Integrin beta3 Increases Immunosuppression in Cancer. *Cancer research* **76**, 3484-3495 (2016).
6. Hammerman PS, S.M., Ramos AH, *et al.* Mutations in the DDR2 Kinase Gene Identify a Novel Therapeutic Target in Squamous Cell Lung Cancer. *Cancer Discovery* **1**, 78-89 (2011).
7. Valiathan, R.R., Marco, M., Leitinger, B., Kleer, C.G. & Fridman, R. Discoidin domain receptor tyrosine kinases: new players in cancer progression. *Cancer metastasis reviews* **31**, 295-321 (2012).
8. Masoumi Moghaddam, S., Amini, A., Morris, D.L. & Pourgholami, M.H. Significance of vascular endothelial growth factor in growth and peritoneal dissemination of ovarian cancer. *Cancer metastasis reviews* **31**, 143-162 (2012).
9. Borza, C.M. & Pozzi, A. Discoidin domain receptors in disease. *Matrix biology : journal of the International Society for Matrix Biology* **34**, 185-192 (2014).
10. Leitinger, B. Discoidin domain receptor functions in physiological and pathological conditions. *International review of cell and molecular biology* **310**, 39-87 (2014).

11. Xu, L., *et al.* Activation of the discoidin domain receptor 2 induces expression of matrix metalloproteinase 13 associated with osteoarthritis in mice. *The Journal of biological chemistry* **280**, 548-555 (2005).
12. Xu, L., *et al.* Increased expression of the collagen receptor discoidin domain receptor 2 in articular cartilage as a key event in the pathogenesis of osteoarthritis. *Arthritis and rheumatism* **56**, 2663-2673 (2007).
13. Xu, L., *et al.* Intact pericellular matrix of articular cartilage is required for unactivated discoidin domain receptor 2 in the mouse model. *The American journal of pathology* **179**, 1338-1346 (2011).
14. Xu, L., *et al.* Attenuation of osteoarthritis progression by reduction of discoidin domain receptor 2 in mice. *Arthritis and rheumatism* **62**, 2736-2744 (2010).
15. Salazar, A., Polur, I., Servais, J.M., Li, Y. & Xu, L. Delayed progression of condylar cartilage degeneration, by reduction of the discoidin domain receptor 2, in the temporomandibular joints of osteoarthritic mouse models. *Journal of oral pathology & medicine : official publication of the International Association of Oral Pathologists and the American Academy of Oral Pathology* **43**, 317-321 (2014).
16. Su, J., *et al.* Discoidin domain receptor 2 is associated with the increased expression of matrix metalloproteinase-13 in synovial fibroblasts of rheumatoid arthritis. *Molecular and cellular biochemistry* **330**, 141-152 (2009).
17. Huang, T.L., *et al.* DDR2-CYR61-MMP1 Signaling Pathway Promotes Bone Erosion in Rheumatoid Arthritis Through Regulating Migration and Invasion of Fibroblast-Like Synoviocytes. *Journal of bone and mineral research : the official journal of the American Society for Bone and Mineral Research* **32**, 407-418 (2017).
18. Wang, J., *et al.* Functional analysis of discoidin domain receptor 2 in synovial fibroblasts in rheumatoid arthritis. *J Autoimmun* **19**, 161-168 (2002).
19. Zhao, H., *et al.* Targeting of Discoidin Domain Receptor 2 (DDR2) Prevents Myofibroblast Activation and Neovessel Formation During Pulmonary Fibrosis. *Molecular therapy : the journal of the American Society of Gene Therapy* (2016).
20. Cho, H.S. & Leahy, D.J. Structure of the extracellular region of HER3 reveals an interdomain tether. *Science* **297**, 1330-1333 (2002).

21. Verstraete, K. & Savvides, S.N. Extracellular assembly and activation principles of oncogenic class III receptor tyrosine kinases. *Nature reviews. Cancer* **12**, 753-766 (2012).
22. Yeung, D., Chmielewski, D., Mihai, C. & Agarwal, G. Oligomerization of DDR1 ECD affects receptor-ligand binding. *J Struct Biol* **183**, 495-500 (2013).
23. Agarwal, G., Kovac, L., Radziejewski, C. & Samuelsson, S.J. Binding of discoidin domain receptor 2 to collagen I: an atomic force microscopy investigation. *Biochemistry* **41**, 11091-11098 (2002).
24. Coelho, N.M., *et al.* Discoidin Domain Receptor 1 Mediates Myosin-Dependent Collagen Contraction. *Cell reports* **18**, 1774-1790 (2017).
25. Mihai, C., Chotani, M., Elton, T.S. & Agarwal, G. Mapping of DDR1 distribution and oligomerization on the cell surface by FRET microscopy. *Journal of molecular biology* **385**, 432-445 (2009).
26. Carafoli, F., *et al.* Crystallographic insight into collagen recognition by discoidin domain receptor 2. *Structure* **17**, 1573-1581 (2009).
27. Carafoli, F., *et al.* Structure of the discoidin domain receptor 1 extracellular region bound to an inhibitory Fab fragment reveals features important for signaling. *Structure* **20**, 688-697 (2012).
28. Walton, J., *et al.* CRISPR/Cas9-Mediated Trp53 and Brca2 Knockout to Generate Improved Murine Models of Ovarian High-Grade Serous Carcinoma. *Cancer research* **76**, 6118-6129 (2016).
29. Maeyama, M., *et al.* Switching in discoid domain receptor expressions in SLUG-induced epithelial-mesenchymal transition. *Cancer* **113**, 2823-2831 (2008).
30. Bildsoe, H., *et al.* Transcriptional targets of TWIST1 in the cranial mesoderm regulate cell-matrix interactions and mesenchyme maintenance. *Developmental biology* **418**, 189-203 (2016).
31. Beerling, E., *et al.* Plasticity between Epithelial and Mesenchymal States Unlinks EMT from Metastasis-Enhancing Stem Cell Capacity. *Cell reports* **14**, 2281-2288 (2016).

32. Quan, J., Yahata, T., Adachi, S., Yoshihara, K. & Tanaka, K. Identification of receptor tyrosine kinase, discoidin domain receptor 1 (DDR1), as a potential biomarker for serous ovarian cancer. *Int J Mol Sci* **12**, 971-982 (2011).
33. Heinzelmann-Schwarz, V.A., *et al.* Overexpression of the cell adhesion molecules DDR1, Claudin 3, and Ep-CAM in metaplastic ovarian epithelium and ovarian cancer. *Clinical cancer research : an official journal of the American Association for Cancer Research* **10**, 4427-4436 (2004).
34. Fu, H.L., *et al.* Discoidin domain receptors: unique receptor tyrosine kinases in collagen-mediated signaling. *The Journal of biological chemistry* **288**, 7430-7437 (2013).
35. Golubkov, V.S., *et al.* Protein-tyrosine pseudokinase 7 (PTK7) directs cancer cell motility and metastasis. *The Journal of biological chemistry* **289**, 24238-24249 (2014).
36. Golubkov, V.S. & Strongin, A.Y. Downstream signaling and genome-wide regulatory effects of PTK7 pseudokinase and its proteolytic fragments in cancer cells. *Cell communication and signaling : CCS* **12**, 15 (2014).
37. Majkowska, I., Shitomi, Y., Ito, N., Gray, N.S. & Itoh, Y. Discoidin domain receptor 2 mediates collagen-induced activation of membrane-type 1 matrix metalloproteinase in human fibroblasts. *The Journal of biological chemistry* **292**, 6633-6643 (2017).
38. Jonsson, M. & Andersson, T. Repression of Wnt-5a impairs DDR1 phosphorylation and modifies adhesion and migration of mammary cells. *Journal of cell science* **114**, 2043-2053 (2001).
39. Berger, H., Wodarz, A. & Borchers, A. PTK7 Faces the Wnt in Development and Disease. *Front Cell Dev Biol* **5**, 31 (2017).
40. Chuang, C.H., *et al.* Molecular definition of a metastatic lung cancer state reveals a targetable CD109-Janus kinase-Stat axis. *Nat Med* **23**, 291-300 (2017).
41. Zhang, J.M., *et al.* CD109 attenuates TGF-beta1 signaling and enhances EGF signaling in SK-MG-1 human glioblastoma cells. *Biochemical and biophysical research communications* **459**, 252-258 (2015).

42. Baker, E.L. & Zaman, M.H. The biomechanical integrin. *J Biomech* **43**, 38-44 (2010).
43. Kuo, J.C. Mechanotransduction at focal adhesions: integrating cytoskeletal mechanics in migrating cells. *J Cell Mol Med* **17**, 704-712 (2013).
44. Eunae You, S.P., Daehwan Kim, Jangho Jung, Panseon Ko, Chan-Mi Park and Sangmyung Rhee. Role of the intracellular juxtamembrane domain of discoidin domain receptor 2 in focal adhesion formation. *Animal Cells Syst (Seoul)* **18**, 372-379 (2014).
45. Huang, Y., Arora, P., McCulloch, C.A. & Vogel, W.F. The collagen receptor DDR1 regulates cell spreading and motility by associating with myosin IIA. *Journal of cell science* **122**, 1637-1646 (2009).
46. Iwanicki, M.P., *et al.* Ovarian cancer spheroids use myosin-generated force to clear the mesothelium. *Cancer Discov* **1**, 144-157 (2011).
47. Elkin, S.R., Lakoduk, A.M. & Schmid, S.L. Endocytic pathways and endosomal trafficking: a primer. *Wien Med Wochenschr* **166**, 196-204 (2016).
48. Bottcher, R.T., *et al.* Sorting nexin 17 prevents lysosomal degradation of beta1 integrins by binding to the beta1-integrin tail. *Nature cell biology* **14**, 584-592 (2012).
49. Gonzalez, M.E., *et al.* Mesenchymal Stem Cell-Induced DDR2 Mediates Stromal-Breast Cancer Interactions and Metastasis Growth. *Cell reports* **18**, 1215-1228 (2017).
50. Lin, S.Y., *et al.* Nuclear localization of EGF receptor and its potential new role as a transcription factor. *Nature cell biology* **3**, 802-808 (2001).
51. Carpenter, G. & Liao, H.J. Receptor tyrosine kinases in the nucleus. *Cold Spring Harb Perspect Biol* **5**, a008979 (2013).
52. Andersson, E.R., Sandberg, R. & Lendahl, U. Notch signaling: simplicity in design, versatility in function. *Development* **138**, 3593-3612 (2011).

53. Kim, H.G., Hwang, S.Y., Aaronson, S.A., Mandinova, A. & Lee, S.W. DDR1 receptor tyrosine kinase promotes prosurvival pathway through Notch1 activation. *The Journal of biological chemistry* **286**, 17672-17681 (2011).
54. Zhang, S., *et al.* A host deficiency of discoidin domain receptor 2 (DDR2) inhibits both tumour angiogenesis and metastasis. *J Pathol* **232**, 436-448 (2014).
55. H Xu, D.B., F Chang, PH Huang, RW Farndale, B Leitinger. Discoidin Domain Receptors Promote  $\alpha$ 1b1- and  $\alpha$ 2b1- Integrin Mediated Cell Adhesion to Collagen by Enhancing Integrin Activation. *PLoS One* **7**, e52209 (2012).